
Electronic Thesis and Dissertation Repository

7-28-2015 12:00 AM

An Approach to Developing a Spatio-Temporal Composite Measure of Climate Change-Related Human Health Impacts in Urban Environments

Mohammad Amin Owrangi
The University of Western Ontario

Supervisor

Professor Slobodan Simonovic

The University of Western Ontario Joint Supervisor

Professor Robert Lannigan

The University of Western Ontario

Graduate Program in Civil and Environmental Engineering

A thesis submitted in partial fulfillment of the requirements for the degree in Doctor of Philosophy

© Mohammad Amin Owrangi 2015

Follow this and additional works at: <https://ir.lib.uwo.ca/etd>



Part of the [Civil and Environmental Engineering Commons](#)

Recommended Citation

Owrangi, Mohammad Amin, "An Approach to Developing a Spatio-Temporal Composite Measure of Climate Change-Related Human Health Impacts in Urban Environments" (2015). *Electronic Thesis and Dissertation Repository*. 2998.

<https://ir.lib.uwo.ca/etd/2998>

This Dissertation/Thesis is brought to you for free and open access by Scholarship@Western. It has been accepted for inclusion in Electronic Thesis and Dissertation Repository by an authorized administrator of Scholarship@Western. For more information, please contact wlsadmin@uwo.ca.

AN APPROACH TO DEVELOPING A SPATIO-TEMPORAL COMPOSITE
MEASURE OF CLIMATE CHANGE-RELATED HUMAN HEALTH IMPACTS IN
URBAN ENVIRONMENTS

(Thesis format: Monograph)

by

Mohammad Amin Owrangi

Graduate Program in
Civil and Environmental Engineering

A thesis submitted in partial fulfillment
of the requirements for the degree of
Doctor of Philosophy

The School of Graduate and Postdoctoral Studies
The University of Western Ontario
London, Ontario, Canada

© Mohammad Amin Owrangi 2015

Abstract

Introduction:

Rapid population growth along with an increase in the frequency and intensity of climate change-related impacts in coastal urban environments emphasize the need for the development of new tools to help disaster planners and policy makers select and prioritize mitigation and adaptation measures. Using the concept of the resilience of a community, which is a measure of how rapidly the community can recover to its previous level of functionality following a disruptive event is still a relatively new concept for many engineers, planners and policy makers, but is becoming recognized as an increasingly important and some would argue, essential component for the development and subsequent assessment of adaptation plans being considered for communities at risk of climate change-related events. The holistic approach which is the cornerstone of resilience is designed to integrate physical, economic, health, social and organizational impacts of climate change in urban environments. This research presents a methodology for the development of a quantitative spatial and temporal composite measure for assessing climate change-related health impacts in urban environments.

Methods:

The proposed method is capable of considering spatial and temporal data from multiple inputs, relating to both physical and social parameters. This approach uses inputs such as the total population density and densities of various demographics, burden of diseases conditions, flood inundation mapping, and land use change for both historical and current conditions. The research has demonstrated that the methodology presented generates sufficiently accurate information to be useful for planning adaptive strategies. To assemble all inputs into a single measure of health impacts, a weighting system was assigned to apply various priorities to the spatio-temporal data sources. Weights may be varied to assess how they impact the final results. Finally, using spatio-temporal extrapolation methods the future behavior of the same key spatial variables can be projected.

Although this method was developed for application to any coastal mega-city, this thesis demonstrates the results obtained for Metro Vancouver, British Columbia, Canada. The data

was collected for the years 1981, 1986, 1991, 1996, 2001, 2006 and 2011, as information was readily available for these years. Fine resolution spatial data for these years was used in order to give a dynamic simulation of possible health impacts for future projections. Linear and auto-regressive spatio-temporal extrapolations were used for projecting a 2050's Metro Vancouver health impact map (HIM).

Conclusion:

Results of this work show that the approach provides a more fully integrated view of the resilience of the city which incorporates aspects of population health. The approach would be useful in the development of more targeted adaptation and risk reduction strategies at a local level. In addition, this methodology can be used to generate inputs for further resilience simulations. The overall value of this approach is that it allows for a more integrated assessment of the city vulnerability and could lead to more effective adaptive strategies.

Keywords: climate change; human health; sea level rise; flooding; spatio-temporal modeling

To my family

Acknowledgments

First, I would like to thank my supervisor, Dr. Slobodan Simonovic for giving me the opportunity to be part of his research group, for his guidance, enthusiasm, and everlasting support. He was not only a great supervisor to me, but also a mentor who inspired and challenged me by sharing his research insight and passion throughout this research project. I owe him many thanks for his constructive criticism during my time in his lab.

I would also like to express my deepest appreciation to my co-supervisors Dr. Robert Lannigan for believing in me and for his invaluable guidance and support. His insightful suggestions and advice provided me with new ideas and directions for my research.

I would also like to thank coastal cities at risk team: Dr. Gordon McBean, Dr. Hassan Virji, Dr. Jim Davies, Mrs. Deborah Harford, Dr. Carrie Mitchell, Mrs Linda Mortsch, Dr. Paul Whitfield, and Dr. Brent Doberstein. Thanks to Mrs. Christine Homut from map and data center, UWO and Dr. Ali Baligh Jahromi, Department of Earth and Space Science, York University who were always helping me with GIS and remote sensing related issues and data collection.

Some of the knowledge I gained during the last four years will eventually be outdated and replaced, but the memories of happiness and solicitude which I shared with my FIDS colleagues – will not. They will stay with me for life. Thank you, Leanna, Angela, Vladimir, Abhishek, Sohom, Andre, Roshan, Sarah, Jordan, Patrick, Nick, Bogdan, Dejan, Stuart, Arunkumar and Benyou.

A very special thank you to my parents, Zahra and Daryoosh, my wife Razieh, and my brothers, Amir and Ehsan for their true love, patience and support. Thank you for all of your support and encouragement through my PhD studies.

I also would like to acknowledge the financial support made available by the International Development Research Center (IDRC) together with the Canadian Institutes of Health Research (CIHR), the Natural Sciences and Engineering Research Council of Canada (NSERC) and the Social Sciences and Humanities Research Council of Canada (SSHRC).

Table of Contents

Abstract	i
Acknowledgments	iii
List of figures	ix
List of tables	xiii
List of Appendices	xiv
List of Acronyms	xv
Chapter 1	1
1. Introduction.....	1
1.1 Climate change	1
1.1.1 Flood	5
1.1.2 Sea Level rise	8
1.2 Urbanization (coastal mega-cities).....	10
1.2.1 Land-use change	12
1.3 Climate Change as a Human Health Risk	14
1.4 Coastal mega-cities	17
1.5 Spatio-temporal modeling for assessing climate change impact on human health in coastal mega-cities	18
1.6 Research Questions	19
1.7 Objectives of the Study	20
1.8 Outline of the thesis.....	21
Chapter 2	23
2. Literature review	23
2.1 Introduction.....	23
2.2 Climate change and cities.....	23
2.3 Assessments of climate change impacts on flooding and sea level rise.....	27

2. 3.1 Floods	27
2. 3.2 Sea level rise and coastal inundation	37
2.4 Land use-based assessment in natural hazard management	41
2.5 Climate change impacts on human health	46
2.5.1 Communicable diseases	50
2.5.2 Non-communicable diseases	53
2.5.3 Injuries	54
2.6 Contributions of the research	55
Chapter 3	60
3. Methods	60
3.1 Spatial data sources	68
3.1.1 Geodatabase	68
3.1.2 Remote sensing data	70
3.2 Remote sensing	71
3.2.1 Land-use change	72
3.2.2 Flood inundation map	77
3.3 Assessing potential human health impacts in urban environment	81
3.3.1 Years of Life Lost due to premature mortality (YLL)	82
3.3.2 Years Lived With Disability (YLD)	82
3.3.3 Disability-Adjusted Life Year (DALY)	83
3.4 Development of a composite measure for estimation of climate change-related human health impacts	84
3.5 Spatio-temporal interpolation and extrapolation	88
3.5.1 Kriging spatial interpolation	89
3.5.2 Spatio-temporal auto regressive extrapolation model	94
Chapter 4	98

4. Case study	98
4.1 Study area	99
4.2 Land-use	102
4.3 Sea level rise and flood history	103
Chapter 5	106
5. Results.....	106
5.1 Land-use change and vegetation analysis	107
5.2 Flood inundation map.....	114
5.3 Climate change impact on human health	119
5.3.1 Burden of disease	119
5.3.2 Disability Adjusted Life Years (DALYs) calculation for Metro Vancouver .	122
5.3.3 Demographic assessment	125
5.4 Mapping climate change-related health risks for an integrated city resilience model	130
5.4.1 Nonphysical health impact map (NPHIM)	130
5.4.2 Integration of physical and nonphysical impacts of climate change on human health	133
5.4.3 Health impact map (HIM).....	134
Chapter 6	150
6. Conclusions.....	150
6.1 Lessons learned in the shift from qualitative to quantitative climate change-related health impact assessment for city resilience studies	150
6.2 Types of spatio-temporal data required for quantitative assessment	152
6.3 Use of the final outcomes of this approach in the comparison of short and long term climate change adaptation policies.....	156
6.4 Recommendations and future works.....	156

References	159
Appendices	180
Curriculum Vitae	264

List of figures

Figure 1 Annual global observed mean temperatures (black dots) and overall decadal trend, along with trend lines calculated from the last 150, 100, 50, and 25 years (top).	3
Figure 2 Trend of annual land precipitation amounts for 1901 to 2005 (top, % change per century) and 1979-2005 (bottom, % change per decade) Source: Parry, 2007.	4
Figure 3 Causes of extreme floods since 1985 (Source: NASA supported Dartmouth Flood Observatory).....	6
Figure 4 Climate, just as anthropogenic or natural variability, affects both climatic and human-related drivers. Risk on coastal systems is the outcome of integrating drivers' associated hazards, exposure, and vulnerability (Source: Wong et al., 2014).	8
Figure 5 The estimated increase in height (m) that flood protection structures would need to be raised in the 2081–2100 period to preserve the same frequency of exceedances that was experienced for the 1986–2005 period, shown for 182 tide gauge locations and assuming regionally varying relative sea level rise projections under an Representative Concentration Pathway 4.5 (RCP4.5) scenario (Source: Hunter et al., 2012).	10
Figure 6 presents the link between population growth, land-use change and global warming.	11
Figure 7 Land-use transitions (DeFries et al., 2004)	14
Figure 8 Pathways by which climate change affects human health, including local modulating influences and resulting consequences (Source: McMichael, et al., 2006).	16
Figure 9 World population trends—urban and rural breakdown (Source: OECD 2008).	25
Figure 10 Global need for coastal flood protection and large scale examples (Source: Temmeran et al., 2013).	34
Figure 11 Modeled elevation of Mean High Water according to NOAA's VDatum (Source: Strauss et al., 2012).....	39
Figure 12 Census county equivalents) living on land less than 1 m above local Mean High Water high tide lines (Source: Strauss et al., 2012).....	40
Figure 13 Sea level rise estimates by Sandwell (2011).	41
Figure 14 Spatial distribution of the existing mega-cities of the world and their population development since 1975 (Source: UNDP, 2009).	45

Figure 15 The incidence of infectious disease outbreaks following flooding in relation to time (Source: Brown and Murray, 2013).	52
Figure 16 System performance and system resilience (after Simonovic and Peck, 2013).	63
Figure 17 Illustration of the methodology for generating a human health impact map.	65
Figure 18 Presentation of the development of the health impact map method.	67
Figure 19 Presentation of the use of remote sensing for developing physical health impact map.....	72
Figure 20 Presentation of the extraction of NDVI from the satellite images.	73
Figure 21 Geometric correction.	74
Figure 22 The application of ground control points for geometric correction in the ENVI environment.	75
Figure 23 The production of MVC according to the Maximum NDVI Value (Source: www.vito-eodata.be).	76
Figure 24 Schematic difference between hydraulic simulation and DEM-based flood inundation maps (Source: Manfreda et al., 2011).	79
Figure 25 The method adopted for creating the composite flood map.	80
Figure 26 Calculating the difference squared between the paired locations (Source: Esri, 2015).	92
Figure 27 Empirical semivariogram graph example (Source: Esri 2015).	93
Figure 28 Queen neighbours, which are defined as the 8 cells adjacent to each grid cell.	95
Figure 29 Neighbours addressed for models 1, 2 and 3 (Source: de Espindolaa, 2014).	96
Figure 30 Metro Vancouver in the province of British Columbia in Canada.	100
Figure 31 Population growth in Metro Vancouver.	102
Figure 32 Timeline of sea level rise storm surge and flash flooding events that affected Metro Vancouver between 1962 and 2012 (Forseth, 2012).	104
Figure 33 Historic vulnerability with flooding in Ladner as far back as 1895.	105
Figure 34 Proposed zones for detailed discussion of the results.	107
Figure 35 Vegetation condition for Metro Vancouver for the years 1984, 1991, 1995, 2000, 2005 and 2012 (Source: Owrangi et al., 2014).	110
Figure 36 The vegetation condition for Metro Vancouver for 1984.	111
Figure 37 The vegetation condition for Metro Vancouver for 2012.	112

Figure 38 Vegetation trend between 1984 and 2012, Metro Vancouver (Source: Owrangi et al., 2014).	113
Figure 39 Shuttle Radar Topography Mission (SRTM) from USGS with a resolution of 90 m ² for Metro Vancouver.	115
Figure 40 Canadian Digital Elevation Model (CDEM) from Natural Resources Canada with a resolution of 25 m ² for Metro Vancouver.	116
Figure 41 Inundation map using modified topographic index map for Metro Vancouver based on the Canadian Digital Elevation Model (CDEM).	118
Figure 42 Inundation map using modified topographic index map for Metro Vancouver based on the SRTM inundation map.	119
Figure 43 Calculated normalized densities of communicable diseases for Metro Vancouver for 2011 (number of communicable diseases per square kilometer).	123
Figure 44 Calculated normalized densities of non-communicable diseases for Metro Vancouver for 2011 (number of non-communicable diseases per square kilometer).	124
Figure 45 Calculated normalized densities of injuries for Metro Vancouver for 2011 (number of injuries per square kilometer).	125
Figure 46 Calculated normalized population density for Metro Vancouver for 2011 (population per square kilometer).	126
Figure 47 Calculated normalized senior population density for Metro Vancouver for 2011 (number of seniors per square kilometer).	128
Figure 48 Calculated normalized children population density for Metro Vancouver for 2011 (number of children per square kilometer).	129
Figure 49 Nonphysical health impact map (NPHIM) generated for Metro Vancouver for 2011.....	131
Figure 50 Population change for major municipalities in Metro Vancouver from 1981 to 2014.....	132
Figure 51 Comparison of nonphysical health impact map generated for Metro Vancouver between the years 1981 and 2011.	133
Figure 52 Human health impact map generated for Metro Vancouver for 1981.....	135
Figure 53 Human health impact map generated for Metro Vancouver for 2011.....	136
Figure 54 Human health impact map generated for Metro Vancouver for 2050 using linear spatio-temporal extrapolation.	137

Figure 55 Human health impact map generated for Metro Vancouver for 2050 using auto regressive spatio-temporal extrapolation.	138
Figure 56 Comparison of the human health impact map between 1981 and 2011.	139
Figure 57 Comparison of the human health impact map between 2011 and 2050.	139
Figure 58 Comparison between linear spatio-temporal extrapolation (left) and auto regressive spatio-temporal extrapolation (right) for Metro Vancouver.	140
Figure 59 Comparison between linear spatio-temporal extrapolation (left) and auto regressive spatio-temporal extrapolation (right) for the cities of Vancouver, North Vancouver, West Vancouver and Burnaby.	141
Figure 60 Comparison between linear spatio-temporal extrapolation (left) and auto regressive spatio-temporal extrapolation (right) for the Cities of Richmond and Delta.	141
Figure 61 Comparison between linear spatio-temporal extrapolation (left) and auto regressive spatio-temporal extrapolation (right) for the Cities of Surrey, Longley, Pitt Meadows, Burnaby, and Maple Ridge.	142
Figure 62 Healthcare facilities, major roads and highways overlaid onto the health impact map for 2011.	143
Figure 63 Building footprints and health impact map for 2011.	144
Figure 64 Elementary Schools, High Schools (secondary schools), Universities, Colleges and the health impact map for 2011.	145
Figure 65 Hydrographic structures and health impact map for 2011.	146
Figure 66 Parks & Recreation regions and health impact map for 2011.	147
Figure 67 Water pipelines and power transmission and health impact map for 2011.	148

List of tables

Table 1 Inland floods versus coastal floods.	7
Table 2 Flood types.	29
Table 3 Flood disasters by continent 1993-2002, (EM-DAT, 2011).	47
Table 4 Metro Vancouver municipalities.	100
Table 5 Comparison of different types of DALYs for seven major municipalities in Metro Vancouver based on 2011 population census data.	121

List of Appendices

Appendix A Python code for flood inundation mapping	180
Appendix B DALY calculation	187
Appendix C Developed maps for different physical and nonphysical variables of the composite health impacts measure for Metro Vancouver	192
Appendix D Detailed information how to access shapefile boundaries for Metro Vancouver	254
Appendix E Access to the satellite images used in this study	257
Appendix F <i>spautolm</i> Spatial conditional autoregression modeling code	258

List of Acronyms

- ASTER Advanced Spaceborne Thermal Emission and Reflection Radiometer
- AR Auto Regressive
- CCFVI Coastal City Flood Vulnerability Index
- CCOG Canadian Council on Geomatics
- CDRCs Chronic Disease and Related Conditions
- CRED Centre for Research on the Epidemiology of Disasters
- DALY Disability Adjusted Life Year
- DEM Digital Elevation Maps
- EEA European Environmental Agency
- ESRI Environmental Systems Research Institute
- GDP Gross Domestic Product
- GHG Green House Gasses
- GIS Geographic Information System
- GMSLR Global Mean Sea Level Rise
- GRASS Geographic Resources Analysis Support System
- HIM Health Impact Map
- IPCC Intergovernmental Panel on Climate Change
- MVC Maximum-Value Composite
- NDVI Normalized Difference Vegetation Index
- NIR Near Infrared
- NOAA- AVHRR National Oceanic and Atmospheric Administration-Advanced Very High Resolution Radiometer
- NPHIM Non-Physical Health Impact Map
- PIEVC Public Infrastructure Engineering Vulnerability Committee
- POES Polar Orbiting Environmental Satellites
- RCP Representative Concentration Pathways
- RDBM Relational DataBase Models
- SLR Sea Level Rise

- SPOT Satellite Pour l'Observation de la Terre
- SQL Structured Query Language
- SRTM Shuttle Radar Topography Mission
- STDRM Space-time Dynamic Resilience Measure
- TIm Modified Topographic Index
- UNDP United Nations Development Programme
- USGS United States Geological Survey
- VIS Visible
- WHO World Health Organization
- YLD Years Lived With Disability
- YLL Years of Life Lost due to premature mortality

Chapter 1

1. Introduction

This document describes a new research approach to quantify the potential climate change-related health impacts on coastal mega-cities. The integrated approach offers an improved understanding of a variety of ongoing and potential future climate change-related impacts to human health and life in coastal mega-cities.

This particular section contains a discussion of climate change impacts with emphasis on the human health sector. An introduction to the physical impacts of climate change (floods and sea level rise), urbanization (land use change), and nonphysical impacts (social, economic, and health) of climate change is provided. Following, the major research objectives of this work are presented.

1.1 Climate change

One of the most thought provoking impacts on human life is that of weather and climate. Climate has both contributed to and limited human activities in terms of the availability of resources such as food production, water, and overall health and wellbeing. The climate system consists of five major components: the atmosphere, the cryosphere (ice, glaciers, and permafrost), the hydrosphere (water bodies), the biosphere (living beings) and land surface (Parry, 2007), and climate impinges upon and sustains the interactions between these components. The atmosphere is perhaps the most complex, dynamic and unstable component in the climate system. Concentrations of greenhouse gases such as carbon dioxide (CO₂), methane (CH₄), water vapor and nitrous oxide (N₂O) can directly change the energy balance of the climate system, especially when the dynamism of these elements is factored in with radiation levels, atmospheric aerosol concentrations and the variables of land cover.

Concentration of greenhouse gases in the atmosphere can vary over time as a result of different processes such as the release of carbon dioxide from decomposing plant matter, or

anthropogenic modifications. Climate affects communities in many ways, and climate change and variability are significant factors for community development. Over the past century (1906-2005), global average surface temperature has increased by 0.74 ± 0.18 °C (Parry, 2007). Based on observations of global air and ocean temperatures and changes in snow/ice extent and sea level, the Intergovernmental Panel on Climate Change (IPCC) has determined that it is 'unequivocal' that the climate system has warmed (Parry, 2007).

Figure 1 shows the observed trend in global mean temperature for 1850-2005. The bottom figures show the troposphere (right figure, 10km above surface) for the period 1979-2005, in °C per decade. Regional warming has been observed at the surface (left figure). The temperature is rising and an increasing rate of temperature change can also be observed. The trends of temperature increases per decade in Figure 1 are subtracted using different time periods ranging from the past 150 to the past 25 years. It is clear that the temperature rise has become more and more severe during the recent years with a change of 0.177 °C per decade over the last 25 years. As the temperature increases, sea level is expected to increase both because of contributions from glacier ice melt and thermal expansion of the oceans.

Figure 2 presents the observed trend of precipitation changes, for the period 1901-2005 (top, per century) and 1979-2005 (bottom, per decade). Increasing annual precipitation is observed in some regions although decreasing amounts can be noticed for other areas. These trends are attributable to changes in the hydrologic cycle, since higher temperatures lead to increased evaporation and concentration of atmospheric water vapor (King, 2012). In southern Canada, some studies suggest that precipitation amounts have increased by 12% during the 20th century (Zhang et al., 2000; Min et al., 2011). As emissions increase and surface temperatures continue to rise, studies suggest that there will be changes in the rate of extreme precipitation events, in terms of their duration, intensity and frequency (Allan and Soden, 2008; World Bank, 2009; Pall et al., 2011).

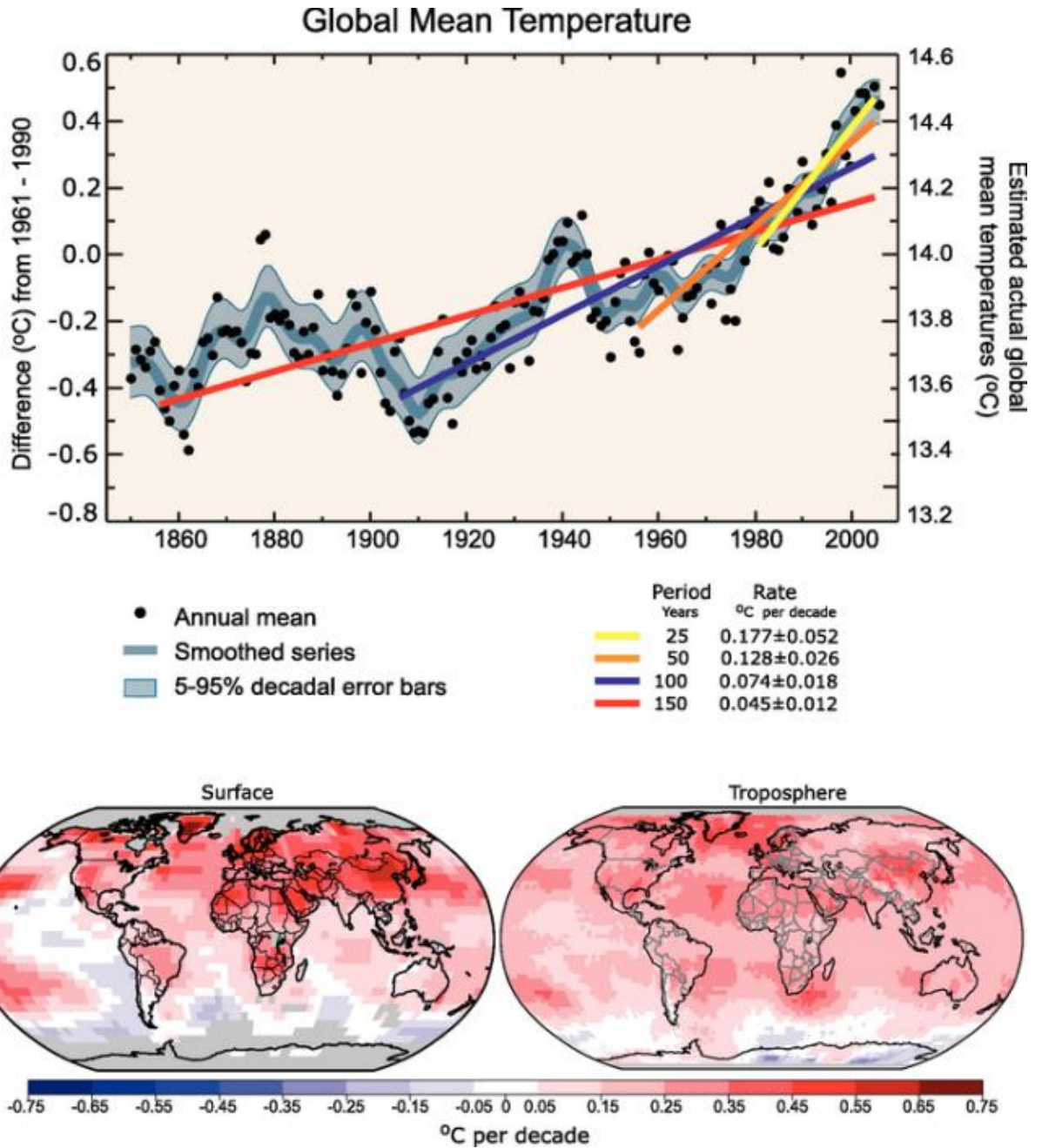


Figure 1 Annual global observed mean temperatures (black dots) and overall decadal trend, along with trend lines calculated from the last 150, 100, 50, and 25 years (top).

Below are the patterns in surface temperature change (°C per decade) from 1979-2005 at the surface (right) and the upper troposphere (left). Source: Parry, 2007.

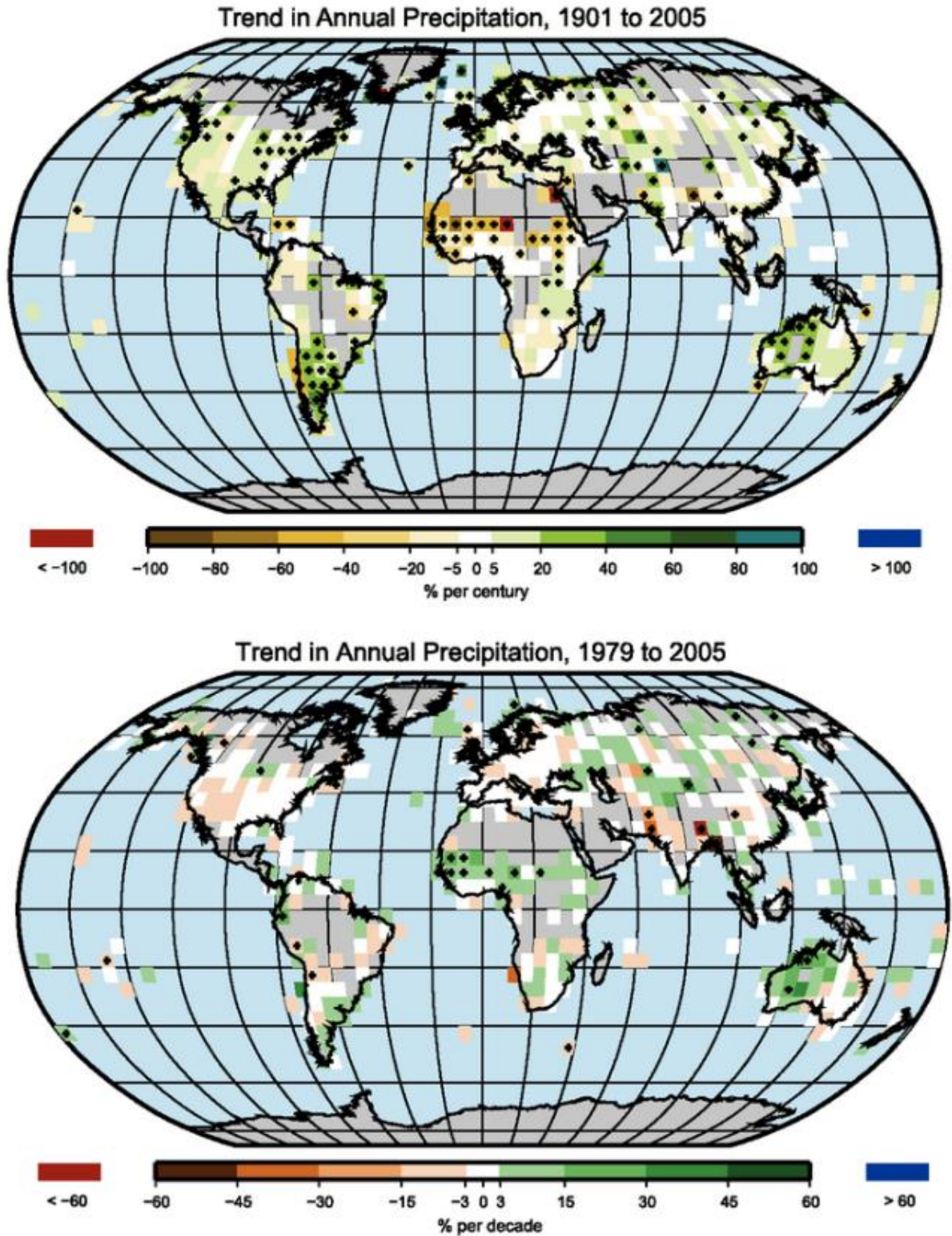


Figure 2 Trend of annual land precipitation amounts for 1901 to 2005 (top, % change per century) and 1979-2005 (bottom, % change per decade) Source: Parry, 2007.

Hydrologic impact assessments of climate change have shown that changing precipitation patterns have the potential to alter stream flows (Jiang et al., 2008; Eum et al., 2010). Changes in the hydrologic variability can affect the quantity, quality, and timing of available water along with the ecological sustainability and agricultural production (World Bank, 2009). Changing stream flows have major implications for water resources infrastructure in terms of hydroelectric production, flood protection and reservoir storage. Consequently, it is becoming increasingly essential in water resources management to further understand and predict changes in extreme precipitation and stream flow, to help in effective management of extreme flooding and droughts. Because precipitation is variable in time and space, quantification of such changes at a global level presents several challenges. The net change in global temperatures as a result of both natural causes and anthropogenic activities is leading to changes in precipitation and humidity, decreasing snow and ice cover, increasing sea levels and overall changes in ocean circulation patterns.

The catastrophic events that will displace populations have two different drivers: (1) climate-related processes such as sea-level rise, desertification, salinization of agricultural land, and growing water scarcity; and (2) climate hazard events such as flooding, storms, and glacial lake outburst floods (Simonovic, 2011). It is essential to note that non-climate elements and drivers, such as general population growth, government policy and community-level resilience to natural disasters, are also of major importance.

1.1.1 Flood

A flood refers to a situation where water accumulates in places that are not usually submerged. The leading cause of inland floods is heavy rainfall, but they can also be generated as a result of melting snow and dam break flows. Intense precipitation may also cause standing water to accumulate in urban areas as the capacity of drainage is exceeded. Inland floods are classically categorized as either flash floods or slow-rising riverine floods (UN/ISDR, 2004). Flash floods are associated mostly with intense precipitation over a short period of time that rapidly overwhelms the drainage capacity of small river basins. Flash floods are the most deadly due to a quick increase in water levels with only a short time for

people to be warned and to seek shelters. By contrast, slow-rising river floods are less deadly but often carry a higher risk for increased, longer term, morbidity. Slow-rising floods are often the consequence of river-level increases due to longer periods of rainfall in larger river basins (UN/ISDR, 2004). Figure 3 shows the spatial distribution of ‘extreme’ floods since 1985.

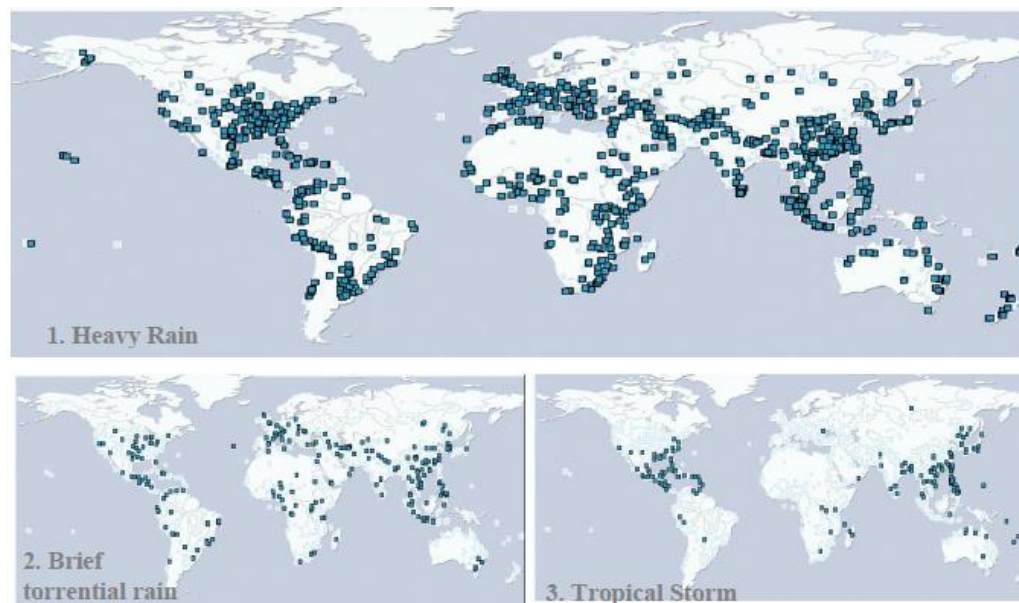


Figure 3 Causes of extreme floods since 1985 (Source: NASA supported Dartmouth Flood Observatory).

The other category of flood is coastal. Floods along the shoreline are primarily caused by tidal waves and tsunamis (such as the 2004 tsunami in the Indian Ocean and the 2011 tsunami in Japan). Researchers argue that the locations most vulnerable to sea-level change include the coastal strips of South and South-east Asia, as well as the urbanized coastal lowlands around the African continent (Nicholls et al., 1999). All of these have a high concentration of relatively unprotected people living in low-lying coastal locations.

Table 1 gives a summary of the leading causes of floods. It is important to note that floods may result from a mixture of causes, such as the big storm-related coastal flood that hit the east of the UK and the Netherlands in January 1953, which was combined with inland flooding due to heavy precipitation (UN/ISDR, 2004).

Table 1 Inland floods versus coastal floods.

Flood type	Flood subtype	Cause
Inland floods	Flash floods	High rainfall
	Slow-onset	Melting of ice
	riverine floods	Dam break
		Urban drain flood
Coastal floods	Tsunami	Wave extremes
	Tidal waves	Earthquakes
	Storm surges	Cyclones
		Breaching of sea defenses

Variations in climate and climate change are another major cause of significant trends in the occurrence of flooding over time. However, explanations and interpretations of these variations have not produced convincing evidence as of yet on the character of these impacts. At a global scale, the warming of the atmosphere will increase its capacity to hold water, and will also accelerate many of the processes involved in the redistribution of moisture (Simonovic, 2012). This implies that flood-generating processes linked to the warming of the atmosphere are likely to increase. Warming also alters many other aspects of the global water cycle, leading to increased evaporation, changing frequency and intensity of precipitation and changing processes relating to surface water storage, such as snowpack generation, snowmelt, river ice breakup, and glacial melt. Many of these processes are active contributors to the generation of floods (Simonovic, 2012).

1.1.2 Sea Level rise

Coastal systems can be broken down into natural and human systems (Figure 4). The natural systems include different coastal features and ecosystems such as rocky coasts, beaches, barriers, sand dunes, lagoons, deltas, river mouths, wetlands, and coral reefs (Wong et al., 2014). These components help define the seaward and landward boundaries of the coast. In spite of providing a wide variety of regulating, provisioning, supporting, and cultural facilities (Mooney, 2005), they have been changed and heavily influenced by human activities, with climate variation constituting only one among many pressures these systems are facing. The human systems include the built environment (e.g., settlements, water, drainage, transportation infrastructure and networks), human activities (e.g., tourism, aquaculture, fisheries), as well as formal and informal institutions that organize human activities (e.g., policies, laws, customs, norms, and culture). The human and natural systems form a closely coupled socio-ecological system (Berkes and Folke, 1998; Hopkins et al., 2012).

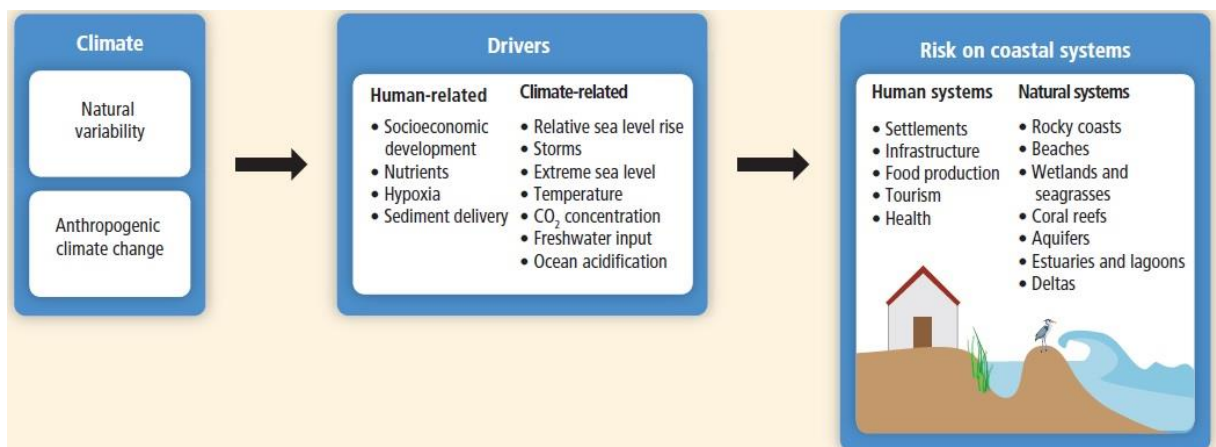


Figure 4 Climate, just as anthropogenic or natural variability, affects both climatic and human-related drivers. Risk on coastal systems is the outcome of integrating drivers' associated hazards, exposure, and vulnerability (Source: Wong et al., 2014).

Population density in coastal regions and islands is around three times higher than the global average (Simonovic, 2011). Currently, more than 160 million people live less than 1 meter above sea level and this allows even a small sea level rise to have catastrophic impacts. Such populations are likely to be badly impacted by storm surges, coastal erosion and flooding, loss of coastal wetlands, groundwater contamination, and other issues. It is very likely that

global mean sea level rose at a mean rate of 1.7 [1.5 to 1.9] mm yr⁻¹ between 1900 and 2010 and at a rate 3.2 [2.8 to 3.6] mm yr⁻¹ from 1993 to 2010 (IPCC, 2013a). Ocean thermal expansion and melting of glaciers have been the main contributors, accounting for more than 80% of the global mean sea level rise (GMSLR) over the latter period (IPCC, 2013a). Future rates of GMSLR during the 21st century are projected to go beyond the observed rate for the period 1971–2010 of 2.0 [1.7 to 2.3] mm yr⁻¹ for all representative concentration pathways (RCP) scenarios (IPCC, 2013b). Sea level rise has thus been 80% faster than projected by models (Rahmstorf et al., 2007). Future sea level rise is highly uncertain and the main reason for the uncertainty is in the response of the major ice sheets of Greenland and Antarctica (Simonovic, 2011). Sea level will continue to increase for many centuries after global temperatures stabilize, since it takes a significant amount of time for the oceans and ice sheets to fully respond to a warmer climate. The future estimates highlight that it is likely to raise sea level by several meters in the coming centuries, leading to the loss of many major coastal cities.

Sea level rise has already affected many parts of coastal cities. Climate change does not force sea levels to increase at the same rate everywhere. Rather, there are spatial variations of sea level rise superimposed on a global average rise. These variations are forced by dynamic processes, arising from circulation, variations in temperature and/or salinity, and by static equilibrium processes, arising from mass redistributions changing gravity and the Earth's rotation and shape. Extrapolations from data herein range from 20 to 29 cm (Sallenger et al., 2012). Sea level rise superimposed on storm surge, wave run-up and set-up will increase the vulnerability of coastal cities to flooding, and the vulnerability of beaches and coastal wetlands to deterioration (Sallenger et al., 2012).

Assuming that sea level extremes follow a simple extreme value distribution like a Gumbel distribution, and accounting for the uncertainty in projections of future sea level rise, Hunter (2012) has industrialized a technique for estimating a sea level allowance, that is, the minimum height that structures would need to be raised in a future period so that the number of exceedances of that height remains the same as under present climate conditions (Figure 5) (Wong et al., 2014). Such an allowance can be factored into adaptive responses to rising sea levels. It should be noted, however, that extreme sea level distributions might not follow a

simple Gumbel distribution (e.g., Tebaldi et al., 2012) due to different factors manipulating extreme levels that may not be accounted for by tide gauges (e.g., Hoeke et al., 2013).

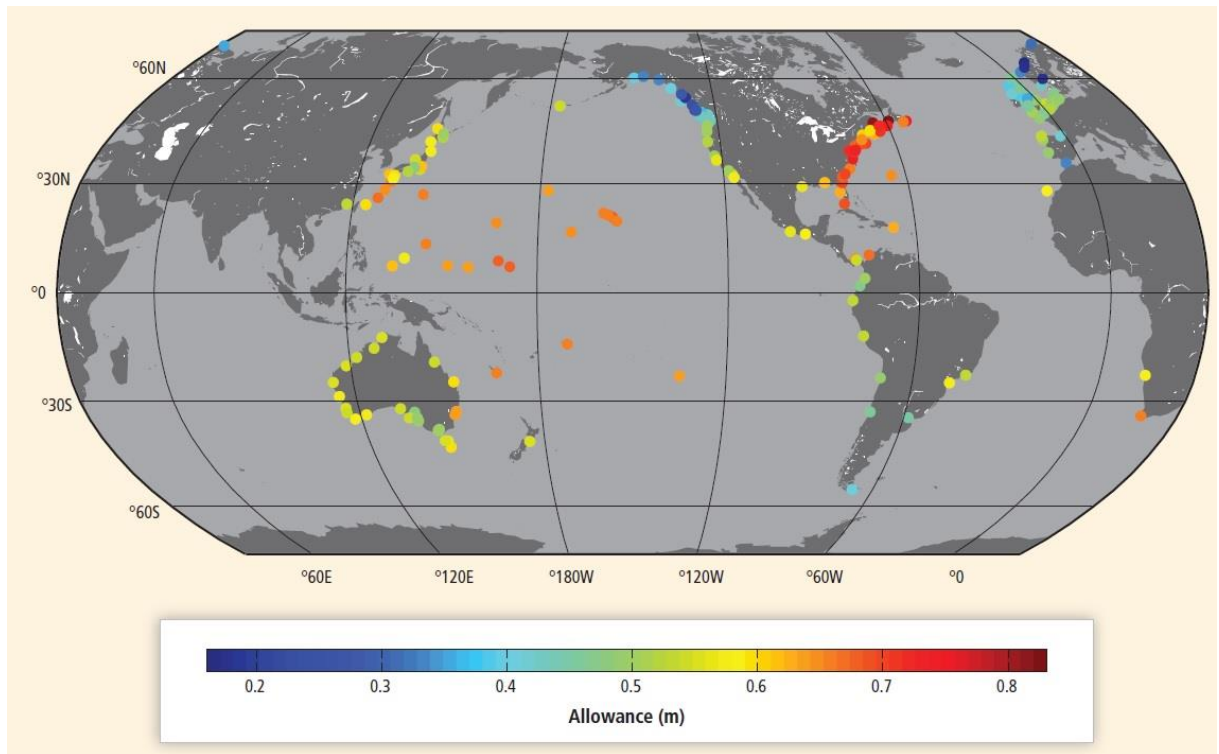


Figure 5 The estimated increase in height (m) that flood protection structures would need to be raised in the 2081–2100 period to preserve the same frequency of exceedances that was experienced for the 1986–2005 period, shown for 182 tide gauge locations and assuming regionally varying relative sea level rise projections under an Representative Concentration Pathway 4.5 (RCP4.5) scenario (Source: Hunter et al., 2012).

1.2 Urbanization (coastal mega-cities)

The Population Division of the Department of Economic and Social Affairs of the United Nations Secretariat (2009) reports that the world population of 6.8 billion in 2009, is likely to reach 9 billion in 2050. Most of these additional 2.2 billion people projected by 2050 will be concentrated in developing countries, whose population is projected to increase from 5.6 billion in 2009 to 7.9 billion in 2050 (Simonovic, 2011). On the other hand, the population of more developed countries is estimated to change only slightly, from 1.23 billion in 2009 to

1.28 billion in 2050. A large proportion of the population of the developing countries is still quite young, with 49% of people under the age of 24. Access to family planning is the most important factor in controlling population growth, particularly in the least developed countries. If fertility were to continue constant at the levels of 2005–2010, the population of the developing countries would increase up to 9.8 billion in 2050, instead of the 7.9 billion projected by assuming some level of fertility decline. Without further reductions in fertility, the world population could rise to nearly twice its current expectations (UN, 2013).

Negative impacts of catastrophic events are directly linked to population trends and changes. Larger numbers of people correlate with larger exposure and higher risk from hazards. Population and climate change are closely connected – most of the increase in greenhouse gases in the atmosphere can be attributed to anthropogenic activities. Figure 6 presents how population growth contributes to global warming. Increase in food production and changes in land use resulting from increasing urbanization are the two major consequences of population growth. Both activities lead to significant releases of greenhouse gases. Therefore, population growth has a direct impact on global warming because it results in increased greenhouse gas emissions.



Figure 6 presents the link between population growth, land-use change and global warming.

Many low-lying coastal and river delta mega-cities are already stressed as a result of rapid population growth and various issues relating to economic, social, health and cultural problems. These cities are now becoming increasingly vulnerable to climate change, particularly as a result of more frequent extreme weather events such as heat waves, heavy rainfall and high winds. In addition, the threats of rising sea levels (Arkema et al., 2013) as well as more intense storm surges make coastal cities more vulnerable to adverse conditions with which human populations need to cope. A combination of mitigation measures and

adaptation strategies will hopefully increase resilience and decrease cities' vulnerability to these events. Coastal mega-cities are extremely complex environments in which a large number of factors can impact individual and population health. An increasing burden of disease in urban environments presents a major challenge as coping with the consequences of poor health diverts resources that could be put to other uses and increases the overall vulnerability of a population. Climate change is a factor that decision-making bodies need take into consideration in order to ensure ongoing urban health, well-being and sustainability.

1.2.1 Land-use change

Climate-related migrations will add another layer of complexity to the issues of climate change adaptation, disaster management and urban development planning. One of the points made by the Intergovernmental Panel on Climate Change (Parry, 2007) is that the chief particular impact of climate change could be on human migration with millions of people migrating as a result of shoreline coastal flooding, erosion, agricultural disruption, etc. Since then, several forecasters have tried to estimate future flows of climate migrants (sometimes called "climate refugees") and the most commonly stated estimate is 200 million by 2050 (IOM, 2008).

Land-use changes typically involve conversion of natural landscapes for human use, and have changed a large percentage of the planet's land surface. Deforestation, expansion of built environments, intensification of farmland production, and the damming or diversion of watercourses for energy or irrigation are human actions which are changing the world's land-use in essentially irreversible ways (DeFries et al., 2004). Built environments, in particular, increase the vulnerability to extreme events such as heavy rainfall because they reduce the absorptive capacity of the land.

Figure 7 shows transitions in land-use activities that may be experienced within a given region over time. As with demographic and economic transitions, societies appear also to follow a classification of different land-use managements: from pre-settlement natural vegetation to boundary clearing, then to subsistence agriculture and small-scale farms, and as a final point to intensive agriculture, urban areas and protected recreational lands (Foley et

al., 2005). Different parts of the world are in different transition phases, based on their social and economic conditions and ecological environment. Land-use practices vary across the world; the ultimate outcome is however mostly the same: the acquisition of natural resources for direct human needs comes at the cost of disrupting environmental conditions and ecosystem cycles. According to the fourth assessment report by the Intergovernmental Panel on Climate Change (Parry, 2007), one of the effects of climate change is an increase in the magnitude and frequency of extreme hydrologic events. A number of studies in the Canadian context concur with the findings of IPCC (2007). In particular, a study completed by Environment Canada (Cheng, 2007) on four selected river basins in Ontario using a modeling exercise indicates that the impacts of future climate change on the frequency and magnitude of precipitation, stream flow and associated flood risks will increase in that part of Canada. Increasing magnitudes and frequencies of extreme hydrologic events, in combination with rapid urbanization and land-use change, make it more likely that catastrophic events such as the 2013 Calgary flood will happen again. The impact of these events on physical infrastructure, personal property, and socioeconomic activities has significant short- and long-term consequences for these communities. The physical, mental and spiritual well-being of the population living in such communities is not exempt and needs to be considered in any future mitigation and adaptation measures.

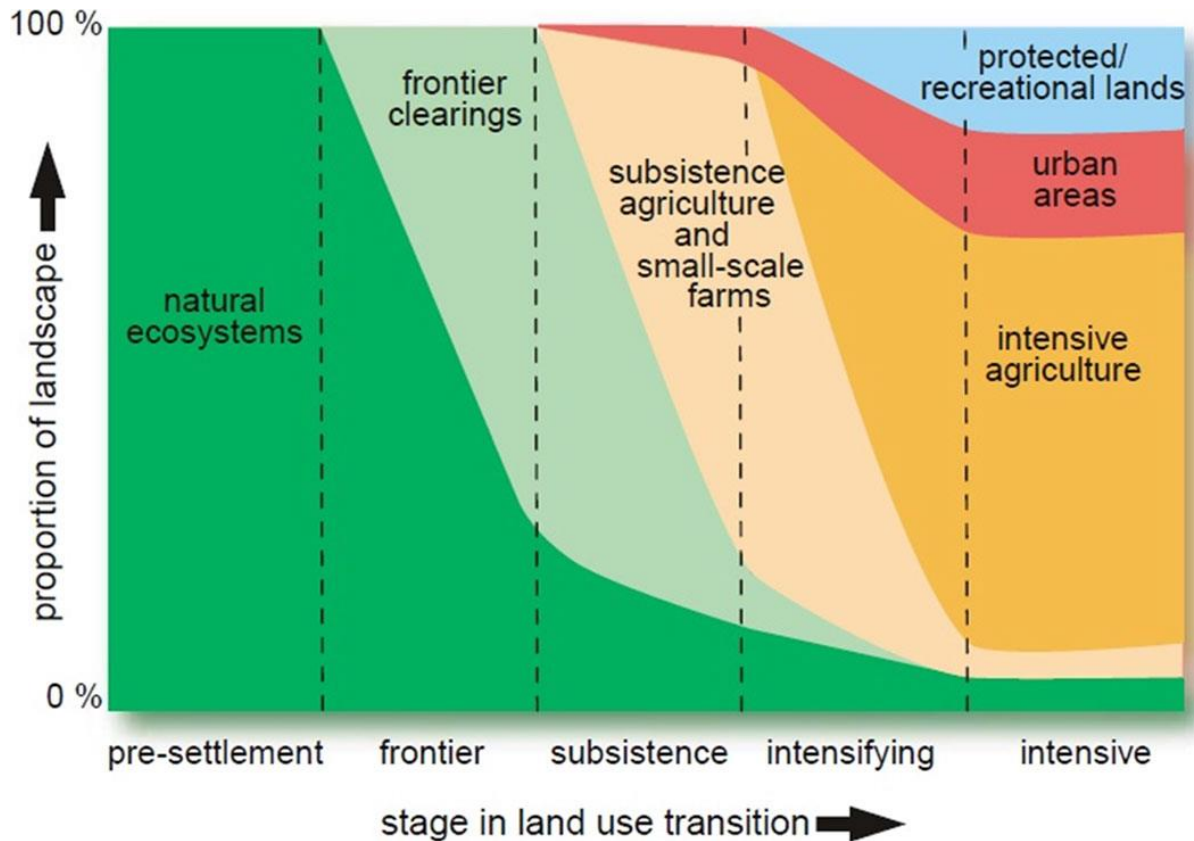


Figure 7 Land-use transitions (DeFries et al., 2004)

1.3 Climate Change as a Human Health Risk

There was little indication that climate change resulted in impacts to human health in 2001 when the Intergovernmental Panel on Climate Change's third assessment report was published (McCarthy et al., 2001). By 2007, the IPCC announced with confidence that "climate change currently contributes to the global burden of disease and premature deaths" (Parry et al., 2007). In some nations, public health representatives are aware of the growing human health risks associated with climate change. In 2008, a survey of Ministries of Health in the British Commonwealth found that of the 31 health ministries, all were concerned about climate change's existing or future public health impacts, mainly on children, the elderly and those in poverty, as a result of sea level rise, flooding, changes in temperature and precipitation, and food insecurity (Commonwealth Health Minister's Update, 2009). A 2008 survey of public health department directors in the United States found that almost 70%

believed that their county or city would experience severe negative health impacts related to climate change over the next two decades (Maibach et al., 2008).

Global climate affects human health in very complex ways and on different temporal and special scales. Correspondingly, the health impacts of future changes would vary spatially as a function both of environment and topography and of the vulnerability of the local population (McMichael et al., 2003). These impacts would be both negative and positive (even though expert scientific reviews anticipate mainly negative). The main categories of health impact of climate change are shown in Figure 8. As mentioned in the figure, environmental effects can be classified in 4 different groups: Extreme weather events (in terms of severity, frequency, and geography), effects on ecosystems (land and sea), sea level rise (salination of coastal land and freshwater; storm surges) and environmental degradation (e.g. land, coastal ecosystems and fisheries). Environmental effects are the consequences of the changes in mean climatic conditions and variability, including temperature, precipitation, humidity, and wind pattern. These environmental effects will lead to different types of health consequences including physical stress (e.g. deaths, illness, injury/death from floods, extreme heat, storms, cyclones and bushfires, leading to more deaths), microbial proliferation (e.g. food poisoning and unsafe drinking water), changes in vector-pathogen-host relations and in infection and disease geography, loss of livelihood, displacement, mental health, infectious diseases, malnutrition and physical risks.

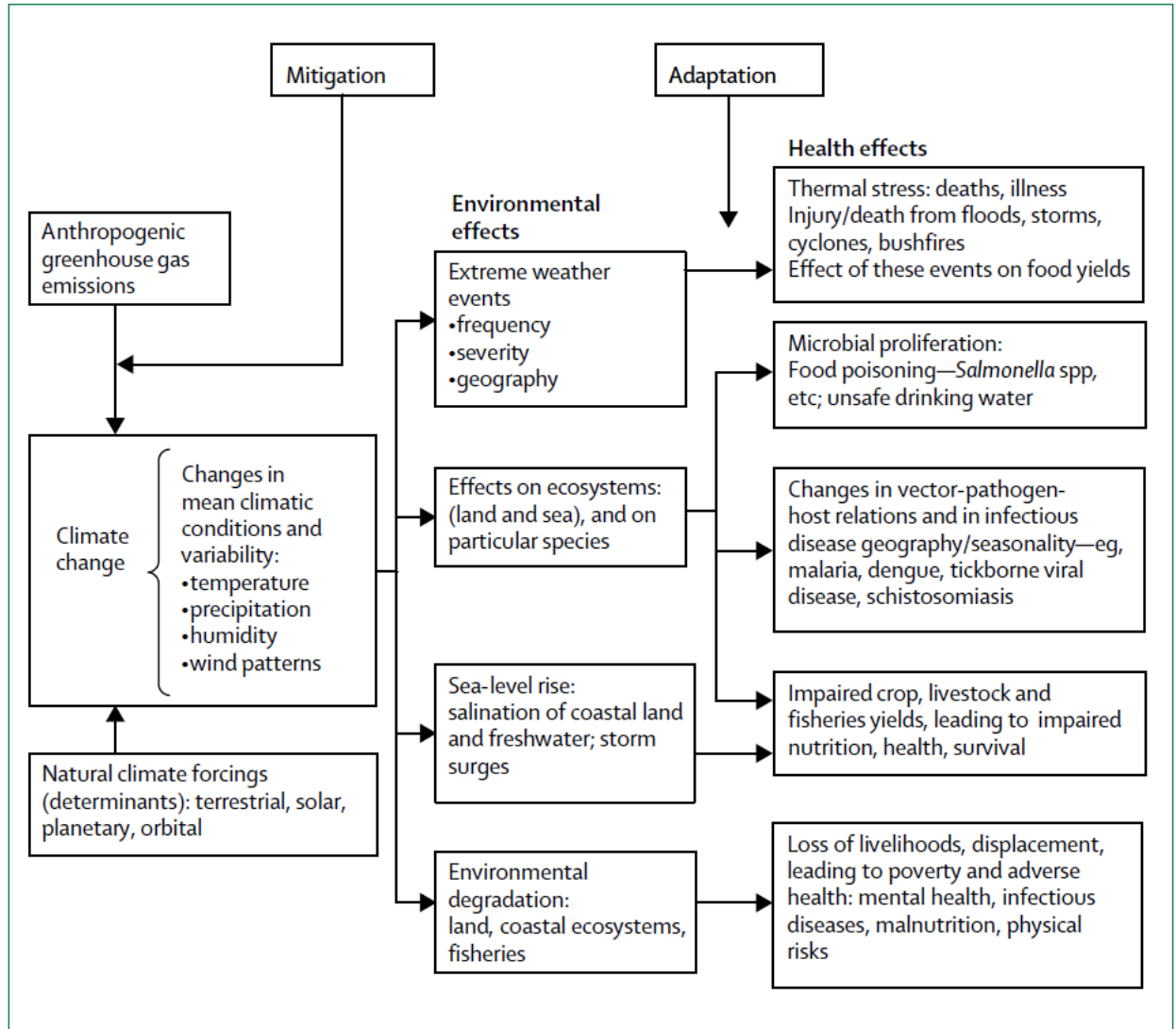


Figure 8 Pathways by which climate change affects human health, including local modulating influences and resulting consequences (Source: McMichael, et al., 2006).

Changes in exposure to weather extremes (heatwaves); increases in other extreme weather events (floods, droughts, storm-surges); and increased production of certain air pollutants and aeroallergens (spores and molds) have more direct impacts on health. In countries with a high level of winter mortality, like the United Kingdom, health improvements may be more apparent than the detrimental impacts (Malakooti, M.A. et al., 1998). The level of change in the intensity, frequency and location of extreme weather events due to climate change remains uncertain. Climate change will likely affect the transmission of many infectious

diseases (especially water, food and vector-borne diseases) and could also impact regional food productivity (especially cereal grains) through less direct mechanisms (McMichael et al., 2003). In the longer term and with substantial difference between populations as a function of geography and vulnerability, these indirect impacts are likely to have bigger magnitude than the more direct ones (Mouchet, J. et al., 1998).

Floods are high-impact events that overwhelm human resilience, physical infrastructure, and social organization. Between 1992 and 2011, there were 2257 reported disasters including extreme temperature, droughts, floods, forest/scrub fires, cyclones, and windstorms. The most repeated natural weather related extreme was flooding (43%), affecting over 1.2 billion people and killing almost 100,000 people (EM-DAT, 2011). Floods result from the interaction of rainfall, sea level, surface run-off, wind, evaporation, and local topography. In inland regions, flood regimens fluctuate significantly and are subject to catchment size, topography, and climate (Poff, 2002). Water management practices, intensified land-use, urbanization, and forestry practices can noticeably change the risks of floods (Mudelsee et al., 2003). In high-income countries, the trend for people to move to coastal regions, river deltas and coral atolls, means that many settlements and a considerable proportion of arable land are at increasing risk from flooding due to increasing sea levels (Pilkey and Cooper, 2004). Some health consequences arise during or immediately following flooding (such as injuries and communicable diseases) (Stachel et al., 2002), while others, for example malnutrition (Del Ninno and Lundberg, 2005) and mental health disorders (Reacher et al., 2004) occur later. Extreme rainfall also enables the entry of human sewage and animal wastes into channels and drinking water supplies, increasing the potential for water-borne diseases (Singh et al., 2001).

1.4 Coastal mega-cities

Mega-cities are the largest class of urban agglomerations; these attract significant attention because of their large populations, geographical complexity and their economic, socio-cultural, environmental and political influence. There are a large number of coastal mega-cities that are low lying and located in coastal and river delta regions. Many of these mega-

cities are already stressed by rapid population growth and economic, social, health and cultural difficulties, and are now becoming increasingly vulnerable to climate change impacts, which in turn lead to an increased risk of disasters. An OECD report that ranks cities (Nichols et al., 2007a) in terms of population and other exposures lists Tokyo, New York, Shanghai, Miami, and Bangkok among the top ten delta cities whose population is presently at risk to sea level rise. The IPCC (Nichols et al., 2007b) concludes: “The impact of climate change on coasts is exacerbated by increasing human-induced pressures;” and “Adaptation for the coasts of developing countries will be more challenging than for coasts of developed countries, due to constraints on adaptive capacity.”

Metro Vancouver is the coastal city in Canada that is most at risk from sea-level rise in combination with other climate change-related exposure threats. In the OECD report, Vancouver is rated 16th for exposed assets, with USD \$55 billion at risk, and 32nd in terms of population at risk, with 320,000 people exposed. Vancouver’s coastal infrastructure at risk includes highways, sewer systems, waste treatment facilities, shipping and ferry terminals, and Vancouver’s International Airport. A one-meter rise in sea level would inundate more than 4600 ha of farmland and more than 15,000 ha of industrial and residential urban areas (Yin, 2001). Approximately 220,000 people live near or below sea level in the Vancouver suburbs of Richmond and Delta, which are protected by 127 km of dykes that were not built to accommodate sea-level rise (Walker and Sydneysmith, 2007).

1.5 Spatio-temporal modeling for assessing climate change impact on human health in coastal mega-cities

Due to the increase in data sets that are both spatially and temporally indexed, spatio-temporal modeling has received increased attention in the last few years, particularly in relation to the measurement or estimation of the resilience of a particular community. Spatio-temporal datasets contain information that is collected across time as well as space. Data analysis has to take into account the spatial dependence and the observations at each data point over time form a time series. Both temporal and spatial correlations should be considered.

Climate change is a dynamic process and quantifying the risks associated with it is a complex process. A model that attempts to factor in changes over time is far more likely to correspond to real-world conditions than one that is temporally static. Spatio-temporal models enable researchers to take more information into account and permit a more substantial scrutiny of the availability and accuracy of data. Simply put, approaching data along multiple vectors of inquiry will expand our knowledge of processes.

A spatio-temporal modelling approach is used to model the health impacts of climate change in large coastal cities and to inform urban stakeholders and governments about the state of human health. The models can assist in the identification of vulnerable regions in the city. Using these models, policy makers can explore how susceptible the city is in the face of flooding events, sea level rise and storm surges, either alone or in combination. Spatio-temporal modeling can assist engineers with interpolation and extrapolation assessment problems. By using spatio-temporal interpolation like Kriging, it is possible to amass and refine the available data sets. The interpolation procedure is an important task to change the resolutions of spatial data to an appropriate scale before any spatio-temporal extrapolation can be carried out. Then, by using spatio-temporal extrapolation (e.g. an autoregressive model), data can be projected and extrapolated to determine the spatial climate change-related health impact for the future and show how it is changing with time.

1.6 Research Questions

To deal with the scientific assessment of climate change impacts on human health in coastal mega-cities, this work adopts an approach that, like integrated assessments, focuses on a variety of spatio-temporal data. The impacts affecting most of urban areas include population growth, the effects of climatic change (e.g. floods, sea level rise, etc.) and changes in land-use patterns. This assessment involves the use of mapping techniques with Geographic Information Systems (GIS) and Remote Sensing tools. The methodology developed in this research is designed to provide support for improving health resilience in coastal mega-cities through spatio-temporal modelling.

The spatio-temporal composite measure is designed to address three important questions:

1. How to shift from a traditional qualitative climate change-related health impact assessment to a more spatio-temporal quantitative assessment?
2. What types of spatio-temporal data are essential for this complex quantitative approach and how can the integration process be formalized? The answer to this question can help in the prioritization of different data sources and allow for the use of a variety of sources with various units and resolutions in a single measure of health impact.
3. How would results from this approach offer practical help to engineers, health professionals, and policy makers for different short- and long-term adaptation policies?

1.7 Objectives of the Study

The following are the objectives of the study:

- To develop a useful and rapid tool for a preliminary delineation of flooding areas in ungauged basins and in areas where expensive and time-consuming hydrological-hydraulic simulations are inadvisable because of lack of access to the available data, questionable accuracy of the data and/or lack of knowledge of the process.
- To assess land-use change in coastal mega-cities using remote sensing techniques.
- To develop a spatio-temporal composite human health measure that could be used in the development of both short and long-term adaptation policies for coastal mega-cities.

- To develop a climate change-related health impact map for adaptation planning, using the new composite human health measure, flood inundation map, and land-use change map.
- Development of future climate change-related human health impact maps that incorporate both physical and sociological parameters using Spatio-Temporal Autoregressive (STAR) Models.

1. 8 Outline of the thesis

The Thesis consists of six chapters. The chapters are structured in the following way:

Chapter 1 presents a brief introduction to the research area and the objectives of the work presented in the thesis.

Chapter 2 reviews literature related to climate change impact assessments on hydrometeorological extremes including floods and sea level rise, as well as remote sensing and land-use change studies, climate change impact on human health studies and risk assessments, and contributions of the work presented.

Chapter 3 gives a description of the development of a spatio-temporal approach for assessing climate change impacts on human health in coastal mega-cities. This includes a description of how different elements of the measure have been, and in the future could be, deployed. The chapter also describes the application of land-use change analysis, flood inundation map development, potential human health impacts assessment, integration and weighting systems, and finally spatio-temporal interpolation and extrapolation procedures.

Chapter 4 presents the study area. The focus of this chapter is on the climate, land-use, sea level rise, and flooding in Metro Vancouver.

Chapter 5 is the results section. First this chapter contains a survey of data requirements and sources and assesses the accuracy of the data. Land-use change analysis (vegetation trend) is presented next taking into consideration remote sensing techniques. The third part of this

chapter details the development of a flood inundation map for Metro Vancouver using open source spatial software. Following, a nonphysical health impact map using various sources of data including burden-of-diseases and census data is developed. The final section in this chapter contains some conclusions concerning the mapping of health impacts in the urban littoral in general and in Metro Vancouver in particular. This section first explains how we dealt with different input units and resolutions. Putting together all our findings from the assortment of spatio-temporal models, we produce this document's final health-impact map.

Chapter 6 presents the summary and conclusions of the study. This chapter also provides suggestions for future work.

Chapter 2

2. Literature review

2.1 Introduction

Climate change is one of the greatest environmental, economic and social pressures challenging the planet. As understood in recent decades, climate change implies an increase in rainfall variability (factored as a global average), which could lead to even more frequent and severe natural disasters including floods (Genovese, 2006). The objectives of studying climate change impact on human health in coastal cities are described in chapter 1. In this chapter, the following related problems which have direct impact on human health in urban environments are explored in greater detail through a review of existing literature.

1. Climate change impacts assessment at hydrometeorological extremes including floods and sea level rise.
2. Land-use change analysis in urban areas using remote sensing tools.
3. Hydrometeorological extremes and urbanization (the effects of this combination) on human health are presented.
4. Finally, the findings of this review are summarized and research objectives to be addressed in this thesis are defined.

2.2 Climate change and cities

Urban environments have a significant contribution on the acceleration of climate change-related impacts in several ways, and they are also quite vulnerable to these impacts. The impacts of climate change have a direct effect on public health in urban environments. In this section, potential climate change-related impacts as a consequence of population growth and urbanization of coastal cities are presented.

In recent years, the scientific consensus is approaching near certainty that the planet's climate is warming, as described in the IPCC's assessment reports (IPCC, 2007; IPCC, 2013).

Unfortunately, the trend in global emissions of greenhouse gases is likely to continue (IPCC, 2013). The increased atmospheric concentration of greenhouse gases will lead to extensive environmental and human impacts, including economic costs, and this will be increasingly obvious across different regions of the globe, in the oceans as well as inland. Coastal megacities are poised, if not for disaster, then at least for significant negative impacts.

Human activities are increasingly altering the Earth's climate. Climate change effects are combining with natural influences that have been present throughout Earth's history. Scientific evidence strongly indicates that natural influences are unable to explain the rapid increase in global near-surface temperatures observed during the second half of the 20th century (Houghton et al., 2001). Consequently, IPCC's Fifth Assessment Report (2013), states that it is a scientific consensus that the climate is changing and the main cause of this change is human activity. The immediate causes of this change are emissions of greenhouse gases from agriculture, energy production and consumption, transport and ecological processes (McBean, 2014).

Climate change due to human activity is expected to continue in the coming decades (IPCC, 2013) with significant effects on human society and the environment. The magnitude of the impacts highly depends on the rate of future temperature increase and the consequences of climate change include an increased risk of floods and droughts, sea level rise, human health threats, and damage to economic sectors such as forestry, agriculture, tourism and the insurance industry (IPCC, 2013).

Around 50% of the world's population live in cities, and this proportion has an increasing trend, with the urban population proportion projected to reach 60% by 2030 (OECD, 2008; Fig. 9). Additionally, the majority of urban population growth in this period is likely to occur in developing countries. The population growth in developing countries is projected to be approximately double that of developed countries in the 2005– 2030 period. Cities also contribute a large proportion of the national gross domestic product (GDP) as they are the central hub for economic activity of all countries, in particular in the developed world but more and more so in developing countries as well (Dodman et al. 2012). Cities are tasked with providing not only jobs but also important cultural, social, and environmental services

(OECD, 2008), and these complex environments are made even more so as a result of population concentration, which can increase vulnerability in urban areas.

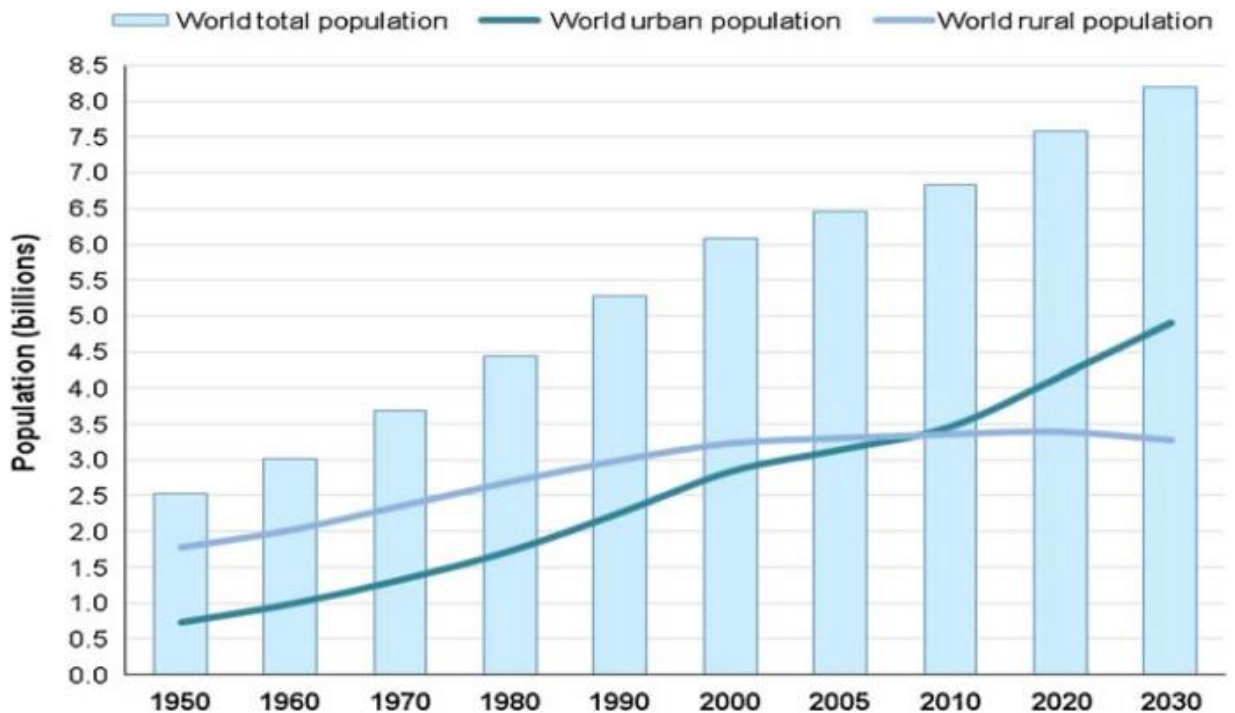


Figure 9 World population trends—urban and rural breakdown (Source: OECD 2008).

The relationship between cities and climate change invokes both vulnerability and responsibility (Lankao, 2007). Metropolitan centers are home to a large percentage of the world's population, physical infrastructure, and economic activity that are highly vulnerable to the risk of floods, sea level rise, landslides, heat waves, storms, droughts and other climate-related extremes.

The U.S. National Assessment of Climate Variability and Change (Rosenzweig and Solecki, 2011) and other early reports mentioned that accelerated sea level rise and intensified coastal flooding as a result of climate change are a critical concern for coastal cities all around the world.

In Europe economic losses due to climate change have increased substantially over the past 20 years to an average of EUR 10 billion in the 1990s. Four of the five years with the highest economic losses have occurred since 1997 to 2001 (EEA, 2004). A study by the European

Environmental Agency (EEA, 2004) summarizes the consensus within the European research community. It clearly states that there is growing evidence that changes in frequency and extent of climate extremes are likely to be caused by a shift in the mean climate to more extreme conditions, with more frequent and stronger deviations from this mean.

The European Union has gone on record enumerating climate change as a key priority. Considerable reductions in emissions of greenhouse gases will be needed to enable Europe to meet its short-term emission goals and thus to assist it in moving on to medium-term adaptation measures to manage the damaging impacts of climate (Genovese, 2006).

Similarly, a number of studies in the Canadian context concur with the findings of IPCC (2007). Particularly, a study completed by Environment Canada (Cheng, 2007) on four selected river basins in Ontario, indicates that the impacts of future climate change on the frequency and magnitude of precipitation, stream flow, and associated flooding risks will increase in that part of Canada.

The most common climate change-related hazard in Canada is flooding. There have been more flood disasters in Canada's history than disasters attributed to any other hazard. Flood disasters have injured more people and caused more damage to property and infrastructure than any other kind of disaster (PSC, 2014). In the last decade, the total flood-related damages exceeded 10 billion dollars (MMM, 2014). The 2014 floods across the prairies and the 2013 floods in the Greater Toronto Area and southern Alberta illustrate both the scale of the hazard and how widespread the threat is in Canada. Flood risk in cities is a particular concern. Local floods caused by extreme rainfall events are happening increasingly often in urban areas, to the point that periodic urban flooding is becoming a "new normal" in Canada (Davison, 2013).

Sea level rise as a result of climate change is projected to affect coastal areas, including river deltas in Canada (BC Flood Safety Section, 2014). In Vancouver, the provincial government has lately released a policy directing local planners to consider the ramifications of 1.2 meters of sea level rise by 2100 (BC Ministry of Environment, 2011). Climate change-related hazards have caused municipalities in the region to implement modifications to existing development plans that will mitigate flood and sea level rise risks.

There is a significant amount of research dealing with the potential climate change-related impacts on human health in urban environments. More recently, an important research question is how to quantify these impacts in a generic way to assess human health in coastal cities.

2. 3 Assessments of climate change impacts on flooding and sea level rise

Climate change impacts temperature, precipitation, air pressure, wind direction, wind speed, and many other variables. Temperature and precipitation affect hydrologic cycles (climate modeling), changes in hydrologic cycle affect runoff (hydrologic modeling), and changes in hydrologic cycle result in flooding, sea level rise, etc. (hydraulic modeling). Risk analyses should take into consideration all of these effects, for example in the calculation of the expected annual flood loss. This section focuses on studies relating to climate change impacts on the rate and frequency of flooding and sea level rise.

2. 3.1 Floods

Flooding is the most common natural disaster at the global level. Each year, more deaths are caused by flooding than by any other climate related-hazard (Vanneuville, 2011). A significant amount of research is done to assess climate change impacts on the frequency and magnitude of floods all over the world.

There are several different types of floods (Table 2). The following three definitions are perhaps the most common definitions used by researchers in North America and Europe.

- 1- 'A flood is a relatively high flow which overtaxes the natural channel provided for the runoff' (Chow, 1956).
- 2- 'Extremely high flows or levels of rivers, whereby water inundates flood plains or terrains outside of the water-confined major river channel. Floods also occur when water level of lakes, ponds, reservoirs, aquifers and estuaries exceed some critical values and

inundate the adjacent land, or when the sea surges on coastal lands much above the average sea level' (Yeveyevich, 1983).

- 3- 'A flood is a body of water which rises to over flow land which is not normally submerged' (Ward, 1978).

Chow (1956) defines floods in relation to inland, riverine flooding. However, Yeveyevich (1983) provides a more detailed definition that recognizes the fact that floods can occur inland in a number of ways other than riverine flooding. Ward (1978) offers one of the most economically worded definitions. None of these definitions insists that a flood must be a purely 'natural' phenomenon, even though natural processes almost unaffected by human activities certainly do cause floods. For example, the sudden releases of water from glacial lakes that cause floods in Kashmir, Argentina, and other glaciated regions happen almost completely naturally (Parker, 2000).

Table 2 Flood types.

Agent	Examples and details
Rainfall	Slow-onset or flash flood Riverine or non-riverine Convectonal/frontal/orographic Torrential rainfall floods
Snowmelt	Riverine Overland flow
Coastal/sea/tidal floods	Storm surge (tropical or temperate induced) Ocean swell floods Tsunamis (included by geological process) Percolation floods
Ice melt	Glacial meltwater (rise in air temperature) Glacial meltwater (geothermal heat source) Spate floods
Flooding during freeze-up	Riverine
Flood by ice breakup	Riverine (also called ice jam floods)
Mud floods	Floods with high sediment content
Dam	Dam-break flood Dam overtopping
Sewer/urban drain flood	Storm discharge to sewers and drains exceeds capacity
Combined events	Example includes: riverine/tidal flooding; rain on snow floods

Note: Types of floods are not essentially mutually exclusive. For example, convectonal rainfall may generate flashfloods and frontal rainfall may be influenced by topography creating orographic rainfall floods (Source:

Parker, 2000)

Milly et al. (2002) report that the occurrence of large floods (exceeding 1/100 year levels) increased during the 20th century for big rivers in high latitude areas of North America and Eurasia. However there was no indication of a rising trend in floods of a lesser magnitude. Frei (2003) reports that in Europe, there appears to have been an increase in the number of high-magnitude flood events over the last decade, however it is hard to prove this statistically because only a small number of actual events are being considered.

It is important to consider that flood dynamics have multiple drivers and this makes it difficult to attribute a causal link between flood trends and climate change. Changes in land cover and urbanization impact the water absorption characteristics of land surfaces, typically increasing runoff rates and thus exacerbating flooding from high rainfall. Loss of wetlands that can act as a buffer against tidal floods may heighten coastal flood risk. Although these changes happen at a local scale, they can combine to form cumulative trends in land-use change that are associated with continent- and ocean-basin-wide trends in flooding. Human vulnerability to flood events is also affected by other agents of change, including population growth and settlement patterns.

Spatial and temporal analyses are required to assess the flooding in the region. One component of this variation is simply the year-to-year change in the occurrence of floods caused by climate variability. The other element is long-term change associated with substantial shifts in flood trends over several decades. It is important to consider the evidence for current global flood trends and to address the possibility that the increase in flooding is due to anthropogenic forcing related to the increase in atmospheric greenhouse gas levels.

Although the current information on flood trends may not be reliable, global trends in sea level and temperature now offer robust indications of a climate change signal that is becoming increasingly clear despite random natural variations. The direction of international scientific opinion has changed conclusively to the viewpoint that a process of anthropogenically-forced climate change is currently exceeding the normal background climatic variability. The fifth Assessment Report (AR5) of the IPCC proposes a series of modeling methodologies to evaluate how climatic parameters are likely to change in the future, and the report sketches a variety of possible impacts that may result from these changes. The size of change depends partially on whether society succeeds in reducing

greenhouse gas emissions. Even with strenuous efforts in climate change mitigation, some climate impacts are unavoidable (Few and Ahern, 2004). Over the next 100 years, yearly average near-surface temperatures across the globe are predicted to rise by between 1.4°C and 5.8°C. Greater than 1°C and less than 6°C is of course a wide variation, but even a single degree increase is likely to significantly increase the number of floods in some areas due to the associated impacts this could have on the hydrologic cycle. There are a great deal of potential impacts to consider including sea level rise, seasonal precipitation fluctuations, new and unpredictable patterns of wind storms (Houghton et al., 2001; McCarthy et al., 2001).

It is not yet clear whether a climate change signal can be identified in present-day global flooding statistics. Warming of the climate in the next 100 years is in any case highly likely, and warming is extensively projected to lead to changes in rainfall and flood risk nearly everywhere. The key problem is locating exactly where water levels will increase or decrease. Results from a series of climate models analyzed by Arnell (2004) point to reduced annual runoff from precipitation in ‘much of Europe, southern Africa, the Middle East, North America and most of South America’ and increased annual runoff in ‘high latitude North America and Siberia, parts of arid Saharan Africa and Australia, eastern Africa, and south and east Asia’. Clearly this is a wide swath of territory and almost certainly these impacts will be felt both on the coast and in the inland areas. Rising trends may be particularly apparent in areas of oceanic climate, monsoon regions and zones where precipitation strongly correlates with tropical cyclones (Hunt, 2002). Seasonality of rainfall can be masked by annual totals, and the most useful information includes seasonal temperature breakdowns. Predictions by Palmer and Rälsänen (2002) for northern Europe, for example, recommend that high rainfall winters will become 3-5 times more frequent.

The link between increased rainfall and flooding is highly complex because the flood outcome will depend also on adjacent and imbricated river basins and flow regime characteristics. Despite this, some authors have clearly addressed future potential flood risk (King et al., 2012). If the correlation between rainfall and flooding is strong, predictions from GCMs indicate that flooding will increase in South Asia, which is at present the world’s most flood-prone region.

The work by Palmer and Rälsänen (2002) predicts an increase of 3-7 times in the probability of high monsoon precipitation in the next 100 years, generating increases in the peak discharges of the region's main rivers. Mudelsee et al. (2003), and Christensen and Christensen (2003), predict a higher frequency of flooding in the summer in Europe. A recent report from the Foresight Future Flooding project pictures a two- to four fold increase in inland flood risk throughout the UK by the 2080s (Evans, 2004).

The study by Mirza (2002) also recommends that the predicted discharge from the Brahmaputra River is unusually sensitive to mean temperature rise, and inferences can be drawn for future flooding in famously low-lying Bangladesh. Due to the complexity of hydro-meteorological processes and future uncertainties over greenhouse gas emissions, vigorous estimates (including well-defended and specific projections) remain to be made about the scale of potential flooding impacts in particular geographical locations remain to be made. The analytical picture is similarly obscured by the potential effect of other environmental variables that may intensify climate-induced changes, such as deforestation and mangrove clearance, land-use changes, construction of coastal defenses and river channel engineering (Bronstert, 2003). For extreme events of low probability and high consequence the tasks for quantification and prediction are particularly great (Goodess et al., 2001).

In another study, Hallegatte et. al, (2013) has investigated potential future flood losses in major coastal cities. They provide a quantification of present and future flood damages/losses in the 136 of the world's largest coastal cities. Based on a controlled register of assumptions relating to possible human adaptations and deploying a new database of urban protection, they account for existing and future flood defenses with atypical specificity. Global flood losses in 2005 were assessed at approximately US\$6 billion per year. Using that baseline Hallegatte's team projected flood losses of US\$52 billion by 2050. This is a linear projection based on the period from 2005 to 2012. Things could get much worse; the unacceptably high US\$1 trillion or more is not an impossible scenario if the existing protection infrastructure is not upgraded (Hallegatte et. al, 2013).

As Milly et al. (2002) state changes in the global water cycle as a result of climate change are likely to result in an increased risk of riverine flooding from overtopped catchments. This

might impact several phases of a river basin's flood regime, including changes in magnitude, frequency, timing, temporal duration and spatial extent of floods (Mirza, 2002). There would be also changes in the timing of peak flows and the coincidence of peaks from different streams of large river basins. Moving from such comprehensive statements to forecasts for specific rivers has an added challenge arising from the use of coarse spatial resolution in global climate models (with grid sizes of hundreds of kilometers) (Hunt, 2002). Grid sizes of 10 km² or so may be needed to generate an accurate simulation of precipitation and river flows, and the inherent infrequency of extreme flood events makes prediction of their impacts even more challenging (Bronstert, 2003; Palmer, 2002).

Balica et al., (2012) have developed a flood vulnerability index for coastal cities for use in assessment of climate change impacts. This is an important partial response to an essential need to develop methodologies and tools to assess this vulnerability. This study focuses on developing a Coastal City Flood Vulnerability Index (CCFVI) based on potential exposure, vulnerability and resilience to coastal flooding. Nine different coastal mega-cities across the world with different potential exposures were chosen for this study. By considering three systems' components (hydro-geological, socio-economic and politico-administrative), the index seeks to demonstrate which cities are most vulnerable to coastal flooding. The index assigns either a 0 or a 1 to indicate low or high coastal flood vulnerability, which inherently has a certain amount of imprecision, but the application of a go/no-go profile lends itself well to computer digitization. This index provides a sense of which cities are in need of further, more detailed investigation to develop future adaptation policies.

The prevention of urban flooding has become an important task in many parts of the world. Kulkarni et al. (2014) have developed an integrated flood assessment model (IFAM) for coastal urban flood simulation. This web-based GIS has been implemented to create spatial datasets for the study area considered. The IFAM covers a 1-D finite element based channel flow model based on diffusion wave approximations, mass balance based 1-D overland flow model, and a continuity equation based quasi 2-D raster flood inundation model. They implemented the application for two coastal urban watersheds in India. Their study demonstrates the efficiency of the flood simulation tool in a web GIS environment that can help data access and visualization of the GIS datasets and simulation results.

In another recent study, Temmeran et al. (2013) summarize the current information and future scenarios that may result from coastal flooding events, determining some of the potential effects these events may have on coastal communities. Latest examples include the flooding caused by Cyclone Nargis in 2008 in southern Myanmar, Hurricane Katrina in 2005 in New Orleans, Hurricane Sandy in 2012 in New York, and Typhoon Haiyan in 2013 in the central Philippines. These types of flood disasters are mainly caused by storm surges that can increase the local sea level by up to two meters when combined with severe wind.

Coastal flood risk is expected to increase over the coming decades due to global and regional changes. These risks include increasing storm intensity, accelerating sea level rise and land subsidence. At the same time, the coastal population is growing. It is obvious that humans and the sea are on a collision course. At present there are 40 million people and around 3000 billion USD worth of assets that are located in flood prone coastal cities. These numbers are projected to increase to 150 million people and 35000 billion USD by 2070. Figure 10 presents an overview of the high-risk coastal cities all over the world (Temmeran et al., 2013).



Figure 10 Global need for coastal flood protection and large scale examples (Source: Temmeran et al., 2013).

Direct impact to human life is not the target of this study. Jakob et al. (2014) determined that even in the absence of a long-term increase in extreme weather events, flood risk will

increase as real estate and agricultural development on the floodplain continues. Cunderlik and Ouarda (2009) have stated that spring snowmelt has been occurring significantly earlier in the southern part of Canada and 20% of the stations studied showed significant adverse trends in the scale of snowmelt floods over the last three decades. The trend is significant enough that it would likely not be significantly mitigated by the inclusion of data from the last two winters in eastern Canada, which have been colder than average.

The Public Infrastructure Engineering Vulnerability Committee (PIEVC) established by Engineers Canada conducted an assessment seven years ago concerning the vulnerability of Canadian public infrastructure to changing climatic conditions (Eum et al., 2010). Their conclusion was simple: failures of public infrastructure across Canada will become more common as a result of climate change-related impacts.

An example of a major flood event that has significantly affected municipalities is the Red River flood of the spring of 1997. The Red River crosses the international border between the U.S. and Canada, and following the 1997 flood event, both nations have conducted a comprehensive set of investigations. Akter and Simonovic (2005) used a fuzzy set approach to multi-objective selection of flood protection measures in the Red River basin, Manitoba, Canada. The methodology that they derived involves integration of the preferences of a large number of stakeholders with the use of a fuzzy predictable value. Simonovic and Ahmad (2007) present a novel technique for spatial flood risk assessment using a fuzzy set approach. Three fuzzy risk parameters of reliability, resilience and robustness were developed using fuzzy sets for flood risk mapping.

Another Canadian study (Peck et al., 2011) has focused on climate change and flood risk to municipal infrastructures in general and to the city of London in particular. The study provides a new approach to integrating climate change into flood risk analysis and combines elements of probabilistic and fuzzy set approaches. The recommendations of the study could be implemented as part of an overall municipal climate change adaptation policy (Peck et al., 2011).

Flood events are an important challenge for the Fraser Valley, British Columbia, Canada, a portion of which surrounds Metro Vancouver. Mountainous topography is the most salient

feature affecting the hydrology of British Columbia. Related flood characteristics include deep and uneven snow accumulation, highly variable precipitation and vegetation, glaciation, deltas, flood plains, canyons, alluvial fans, debris torrents, and debris cones. Rivers of central British Columbia and of the south coastal lowlands have numerous small reservoirs for local water supply and irrigation, but these rarely have significant impacts on flood.

Most streams in the province are subject to high flows during the spring freshet, and all rivers are affected during and after snow melt. Peak discharges are a function of snowpack capacity and of weather conditions during the melt period. Peak flows are typically as late as June and July. A 1948 flood in the Fraser and Columbia River basins was characteristic of a large event of its type (Jakob et al., 2014). The mountain snowpack continued to accumulate up until May because of cool weather and the sudden onset of hot weather of two weeks duration made for high snowmelt rates and swelled many rivers up to record flood conditions.

Coastal and near-coastal areas of British Columbia, including Vancouver, are subject to annual snowmelt peaks, but can also demonstrate irregular flood peaks resulting from frontal rainstorms. When frontal rains of moderate intensity but long duration precipitate on a shallow snowpack, both rainfall and snowmelt contribute to the flood. A flood in November 1978 in the Kitimat-Terrace area of west central British Columbia was the result of a typical frontal rainstorm. Approximately 400 mm of warm rain drizzled onto shallow snowpack over a three-day period that year. The meteorological developments leading to this flood are described by Schaefer (1979). Some watersheds on the east side of the Coast Mountains have been affected by the same type of event, due to the carry-over of intense storms across the mountains. These events produce the rarest and highest floods. A record-breaking surge in December of 1980 on the Tulameen and Coldwater rivers illustrates some of the highly variable weather anomalies that can occur in mountain climates, and the impact of extreme weather events on steeply angled riverine systems (Septer, 2007). As discussed in detail in the next section, Vancouver is also subject to the threat of rising water from the seas. Down from the mountains, in and up from the sea: Vancouver is faced with flooding threats from both directions (Septer, 2007).

The Canadian and international flood events and studies presented in this section show the importance of considering the impacts of increased frequencies and magnitudes of floods as a result of climate change across the globe. The occurrence of flooding on the west coast of Canada is illustrated by a number of studies relating to British Columbia and Vancouver in particular. Vancouver is also subject to flooding by coastal inundation. As such, it is essential to consider flooding as one of the climate change-related hazards that can impact human health in urban environments.

2. 3.2 Sea level rise and coastal inundation

Sea level rise is a long-term problem. Is it possible to develop infrastructure in time to counter the major threats associated with sea level rise? In ocean environments, inundation can result from a number of compounding effects including sea level rise, lunar (tidal) effects, storm surges, and so on. In addition to peak level effects there are also slow corrosive effects such as the erosion of both hardened human structures and also of soft, resilient ecosystems. It is possible for several of these effects to combine in the “perfect” storm that could cause significant damage (Agam, 2014).

Sea level rise is one of the most important factors in climate change risk for coastal cities, given the increasing concentration of urban populations within low-elevation zones near the coast (McGranahan et al., 2007). The most recent IPCC assessments for global mean sea level rise are between 26 and 98 cm by 2100, which is significantly higher than the 18 to 59 cm originally estimated in the 4th Assessment Report (IPCC, 2007; IPCC, 2013). Sea level rise, which is linked to coastal and estuarine degradations (erosion, compromised original vegetation, and so on), in aggregation with storm surges, could have extensive effects on populations, coastal vegetation and ecosystems, property, and the economy (Pavri, 2010; Hanson et al., 2011). Low-lying areas in coastal cities such as New York, Boston, Lagos, Bangkok, Mombasa, Manila, or Mumbai are at a proportionally higher risk of flooding (Adelekan, 2010; Owrangi et al., 2015). Structures on infilled soils in the lowlands of Lagos and Mumbai are more susceptible to the risk of flooding than comparable structures built on consolidated native materials (Revi et al., 2014). Coastal cities as economically diverse as

Vancouver, Bangkok, Manila, and Dhaka have sites at risk from both riverine and coastal storm surges (Rosenzweig et al., 2011; Owrangi et al., 2014).

Hanson et al. (2011) estimated the change in flash flooding events by the 2070s in coastal cities. They found that with a 50 cm rise in sea level, the population at risk could be vulnerable at more than three times current levels however asset exposure is expected to increase by more than 10 times. The top 20 cities identified for both asset and population exposure to coastal flooding in both the current and 2070 rankings are distributed across low, middle, and high income nations (Revi et al., 2014) and in particular in Asian deltaic regions. Revi et al. (2014) found that cities at risk include Mumbai, Guangzhou, Shanghai, Miami, Ho Chi Minh, Kolkata, New York, Osaka-Kobe, Alexandria, Tokyo, Tianjin, Bangkok, Dhaka, and Hai Phong. Using asset exposure as the metric, cities in high-income nations and in China figure prominently: Miami, New York City, Tokyo, and New Orleans as well as Guangzhou, Shanghai, and Tianjin (Revi et al., 2014). Comprehensive site studies can describe the local level of risk from sea level rise and other factors such as groundwater withdrawal, harbor development, dredging and erosion, subsidence and other factors.

The IPCC outlines rates of sea level rise using diverse modeling tools. These models are process based and the following processes are considered by the IPCC in their calculation (Church et al., 2013):

- Thermal Expansion of oceans
- Glaciers melting
- Greenland ice sheet change
- Antarctic ice sheet change
- Land water storage
- Antarctic ice sheet rapid dynamics

Shepard et al., (2012) studied about how to quantify the effects of sea level rise on storm surge risk for the southern shores of Long Island, New York, United States. They applied GIS-based approach to quantify potential changes in storm surges as a result of sea level rise.

This method combines community vulnerability and hazards exposure to spatially characterize existing and future risks using available spatial data. The outcomes of this study show that sea level rise will potentially create risk where it was not before. They find that even 0.5 meter of predicted sea level rise by 2080 massively increases the numbers of impacted people (47% increase) and property loss (73% increase) by storm surge.

Strauss et al. (2012) considered 1 meter of sea level rise for most of the coastal cities in the United States. By using high resolution national elevation dataset using VDatum (VDatum is a newly available tidal model covering the contiguous US and is designed to vertically transform geospatial data between a variety of tidal and ellipsoidal vertical datums), together with Census data from the 2010, housing, low-lying coastal land, and population comparative to sea level rise, ranging from ~0 to 3 meter in elevation are quantified. The resulting map of mean high water according to NOAA's VDatum is presented in Figure 11 and Census county equivalents living on land less than 1 meter presented in figure 12.

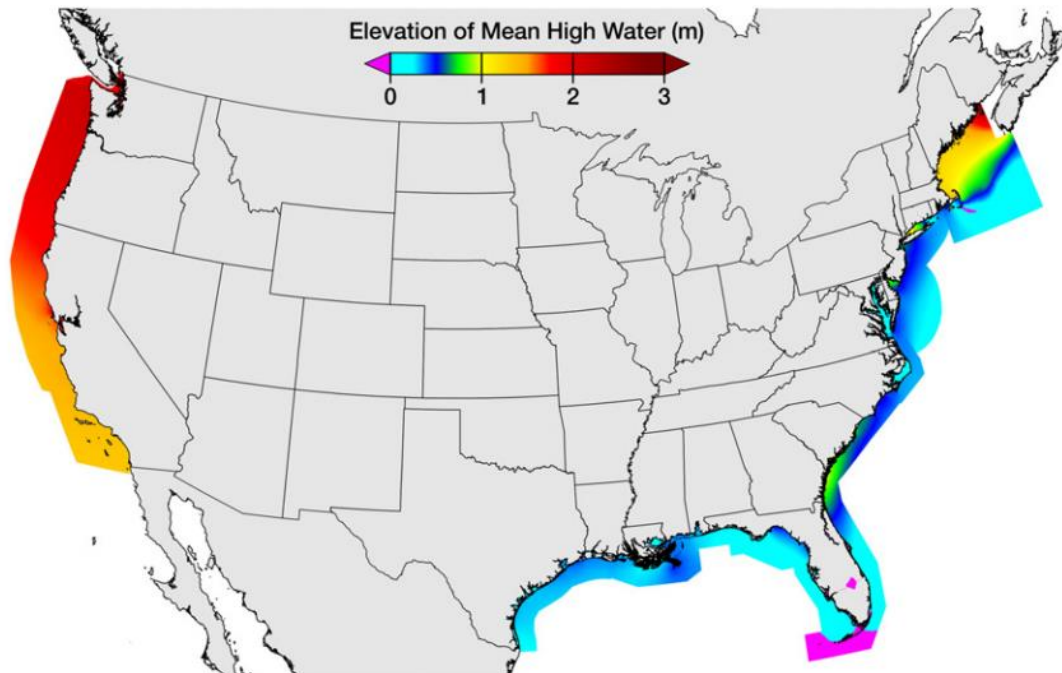


**Figure 11 Modeled elevation of Mean High Water according to NOAA's VDatum
(Source: Strauss et al., 2012)**

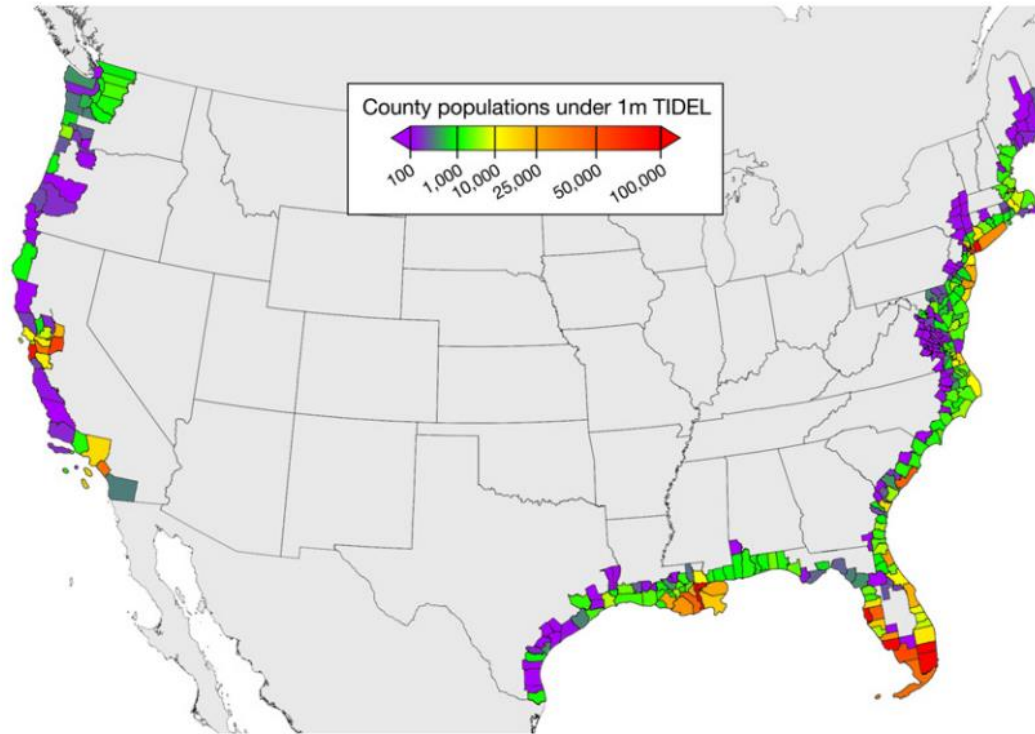


Figure 12 Population living on coastal area with less than 1 m above local Mean High Water high tide lines (Source: Strauss et al., 2012)

A 2011 study by Ausenco Sandwell for the Government of B.C made an attempt to select a realistic sea level rise estimate path. The study recommended to the government of British Columbia (B.C.) to plan for a sea level rise of 50 centimeters by the year 2050, 1.0 meter by the year 2100 and 2.0 meters by the year 2200 (Sandwell, 2011). Figure 13 shows the recommended design curve for sea level rise.

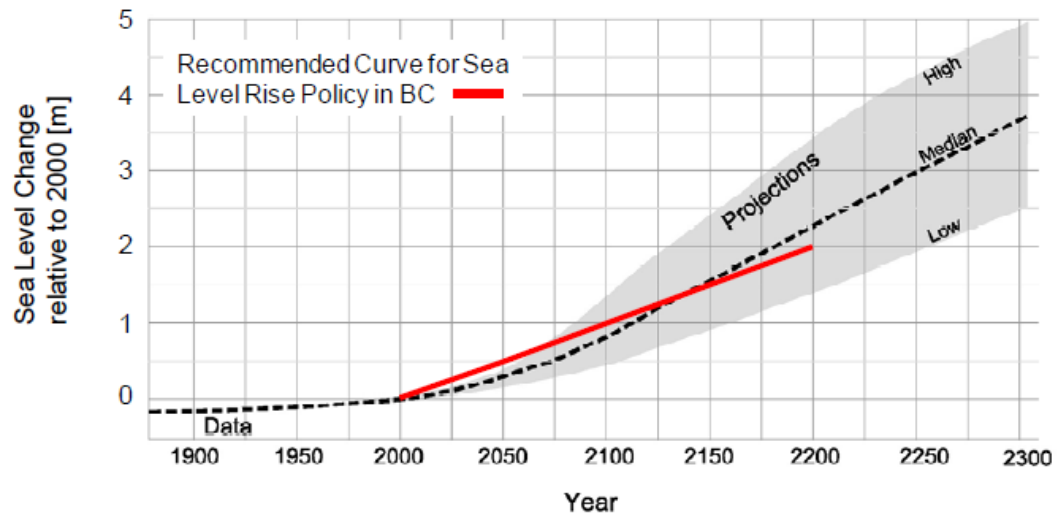


Figure 13 Sea level rise estimates by Sandwell (2011).

Globally, all the projections show that sea level rise is occurring as a result of climate change. There is no specific literature that quantifies sea level rise impacts on human health in coastal cities. Therefore, this phenomenon should be considered alongside riverine flooding as major hydro-meteorological impacts of climate change on human health in coastal cities.

2.4 Land use-based assessment in natural hazard management

Over the past decades, immigration from rural regions to urban areas has been an unvarying global trend. The land-use change related to urban development affects flooding in various ways. Activities including land surface grading, removal of vegetation and soil and the building of drainage networks all contribute to increased runoff to streams from rainfall and snowmelt. Consequently, the peak flow, volume, and frequency of floods change and increase in nearby streams. The limited capacity of stream channels to convey floodwaters is the consequence of urban development. Vegetation cover and bare soil regions are removed or covered for infrastructure development in most cities. Therefore, some of the infrastructure, including roads and buildings constructed in flood-prone areas, are exposed to

the increased flood hazards to which their construction helped contribute. Information about areas exposed to flood risk and how stream flows are affected by land-use can help communities decrease their current and future vulnerability to floods (Konrad and Booth, 2002).

Urbanization of floodplains is an ongoing problem, and a great deal more of ongoing city development occurs at elevations that are only slightly higher than the floodplain and therefore still quite close to high water levels. Historically, proximity to water has meant proximity to trade. This interface between human use of rivers and floodplain development is a recipe for disaster. Once a flood occurs, damage and will occur along vectors of human habitation and low-lying real estate commitment. As urban areas grow and land-use changes, both demographically and geographically, the flood risks increase, partially as a result of urbanization itself which alters local hydrologic characteristics (Montz, 2000).

In undeveloped regions such as grasslands and forests, rainfall and snowmelt accumulate and are stored on vegetation, in surface depressions, or in the soil column, and when the storage capacity of the soil is full, runoff flows gradually over soil as surface flow (Genovese, 2006). In urban areas, by contrast, infrastructure such as buildings, roads and parking lots cover much of the land surface, reducing the capacity of the land to store rainfall and snowmelt (Konrad, 2003). Building of roads and buildings has often involved the removal of vegetation, topsoil, and depressions from the land surface. By spreading the impermeable surfaces of modern life widely across ecosystems, permeable soil is lost or taken out of commission. The vital dispersal of rainwater through the natural infiltration and storage mechanisms and percolation of runoff into the groundwater is compromised. This consequently results in the acceleration of runoff and an overall volume increase. It is important for downstream populations to understand the science of this and to be concerned with policy decisions that will affect their property and lives.

Change along rivers, floodplains and stream channels may alter the capacity of a channel to convey water and can increase the height of the water surface (Konrad, 2003). Bridges and other forms of hardened infrastructure reduce the natural load capacity of the river and provide obstructions upon which debris can accumulate. Development inescapably imposes on river flow and characteristics. Parker (2000) points out that “once floodplains become

urbanized, there follows an almost inevitable demand from the local community for flood protection’.

A multi-disciplinary approach, with input and expertise from various fields for environmental risk management necessities, provides the best long-term solution to foreseeable problems and is most likely to underwrite the success of the venture because the entire community of experts and stakeholders are involved. A wide range of data is required for such an analysis, and can be spatial/temporal, simple/complex, or quantitative/qualitative in nature. Considering a wide range of inputs from all concerned stakeholders will ensure the process of environmental risk analysis is successful.

The spatio-temporal environmental risk analysis procedure involves preparation, processing and use of the information, and presentation of the information in different methods, for example proportional or relative risk analysis, health impact analysis, land-use change analysis, etc. There is a need to deploy and analyze a huge volume of spatio-temporal environmental hazard and exposure data in a reasonably accurate way. Geographical Information Systems (GIS) and remote sensing based software applications using a selection of modeling techniques serve as dominant tools for effective environmental risk assessment and management (Raheja, 2003).

Shalaby et al. (2007) present a study about the use of GIS and remote sensing for mapping and monitoring land cover and land-use changes in the Northwestern coastal zone of Egypt. In this study, spatial analysis including maximum likelihood supervised classification and post-classification change detection techniques were applied to Landsat images, to map land cover changes in the Northwestern coast of Egypt. Ground truth information collected during field trips conducted for the same period of time and land cover maps from before the study period were used to evaluate the accuracy of the classification results. An administered classification was applied individually on the six reflective bands for the images with the aid of ground truth data. Using additional data, visual analysis and expert knowledge of the area through GIS further refined the classification results. Changes among different land cover classes were evaluated. Results indicated that during the study period, very severe land cover

changes took place in the region because of agricultural and tourist development projects and such changes lead to vegetation degradation and water logging in part of the study area.

Nirupama and Simonovic (2007) studied about increasing of the flood risk due to urbanization. They also mentioned that the concern among the policy makers who deal with emergency preparedness and natural disaster management is that urbanization is increasing the risk from river flooding in urban areas. This study concerns such a risk for the City of London, Ontario, Canada. They prepared databases using remote sensing satellite images (Landsat between 1974 and 2000) on land use classification and this information was integrated with meteorological and hydrological data records. It has been shown that there has been a significantly higher risk from floods due to heavy urbanization in London and in the Upper Thames River watershed, where the City of London is located.

Taubenböck et al. (2012) also studied land use changes as a result of urbanization in mega-cities using satellite images. Until 1975 there were just three mega-cities in the world (Tokyo, New York, and Mexico City) and today there are 27 cities with populations of more than 10 million (Figure 14). This research presents an application-oriented method using multi-temporal remotely sensed data to monitor the spatio-temporal dynamics of the world's urban giants. Pixel-based classification image analysis techniques are applied to Landsat and TerraSAR-X data in order to define urbanized areas at different points in time. Then by applying post-classification change detection on urban footprint levels at roughly decadal intervals, almost 40 years of urbanization are monitored. The generated urban footprint results show accuracies greater than 80%, which is promising for future applications in fields such as risk management, urban planning, or population assessment.

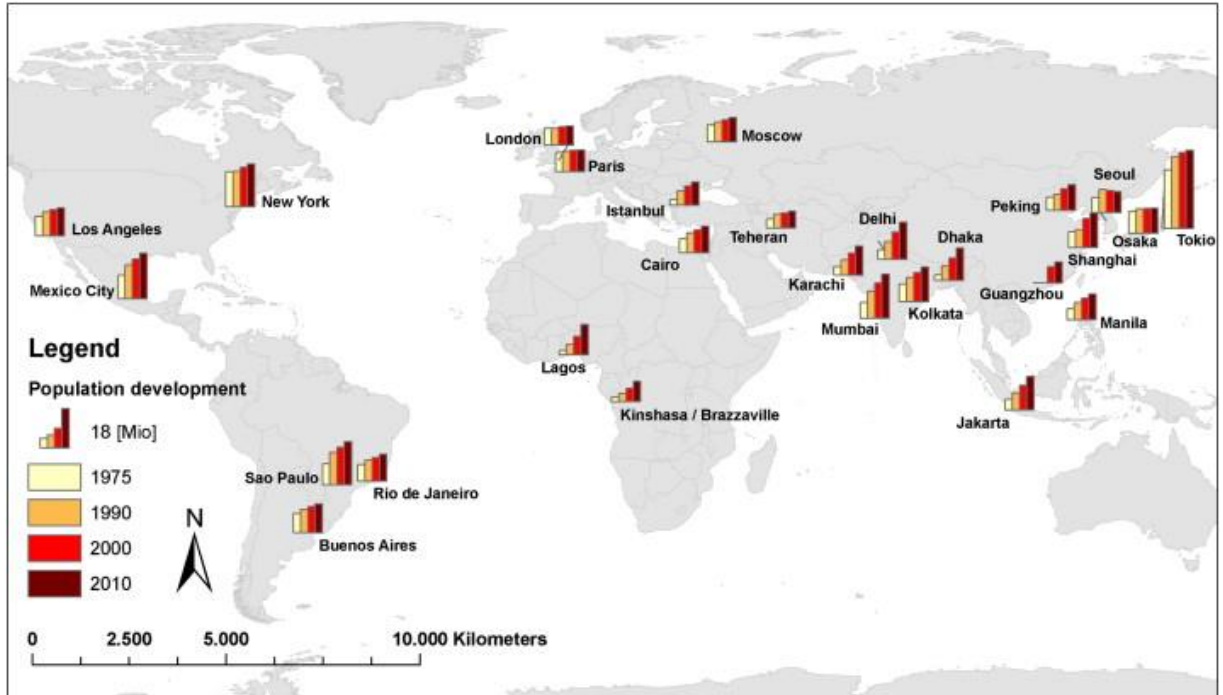


Figure 14 Spatial distribution of the existing mega-cities of the world and their population development since 1975 (Source: UNDP, 2009).

GIS is a systematic means of geographically referencing a number of “layers” of spatial data to facilitate the quantification, overlaying, and synthesis of information in order to orient decisions. Such applications can be used for a range of environmental risk analysis purposes. These applications can vary from change of database systems for simple to complex GIS layers overlays, to complex regional decision-making systems for studying the impact of natural extremes on the artificial and natural environment, including properties, infrastructure, human beings, vegetation and ecology (Genovese, 2006).

These tools and systems can correspondingly be connected with other linked systems, providing online and real-time input data feeds or communication systems, to allow nonstop monitoring of environmental risks in an integrated way (Raheja, 2003). Different types of floods have the highest rate of potential damage of all natural disasters globally and as a result, the highest number of people is affected. It is likely that the number of people and the amount of property affected from flooding are increasing dramatically. Society should move away from the current standard of post-disaster response and instead work to prevent floods by developing adaptation plans to break the current event-disaster cycle. There is an

overwhelming need for decision makers to adopt approaches for flood disaster mitigation and management (ISDR, 2005).

2.5 Climate change impacts on human health

The Centre for Research on the Epidemiology of Disasters (CRED) (EM-DAT, 2010) continues to build a global database on extreme impacts. CRED classifies an event as a disaster if at least one of the following has happened:

- a) 10 or more people killed;
- b) 100 or more people reported affected;
- c) A call for international assistance;
- d) And/or a declaration of a state of emergency.

Based on CRED collected disaster data, floods come second only to drought in causing direct mortality, and account for more than half of all people affected by any type of natural disaster. Since people affected are those requiring immediate assistance during a period of emergency, the availability of basic survival essentials such as food, water, shelter, sanitation and medical assistance provide a measure to assess the scale of health impacts associated with flooding (IFRC, 2003).

Despite their limitations, disaster statistics offer a sense of the variability in flood risk to human populations. Table 3 presents flood disaster statistics for different continents using the EM-DAT data from CRED. From the table, it is clear that flood disasters and their mortality impacts are heavily skewed toward Asia, where there are high population concentrations in floodplains of major rivers, such as the Ganges-Brahmaputra (located in Bengal, India, and Bangladesh) (Few et al., 2004).

Table 3 Flood disasters by continent 1993-2002, (EM-DAT, 2010).

Continent	Reported disasters	People reported killed	People reported affected
Africa	238	9,642	19,939
Americas	239	35,236	9,730
Asia	385	47,009	1,364,957
Europe	187	1,654	6,700
Oceania	26	20	147

Source: EM-DAT, CRED, University of Louvain, Belgium

The second warmest year on record was in 2010. Globally-averaged total land precipitation in 2010 was also the highest on record. It was 52 mm above the 1961–1990 average of 1,033 mm, and there was extensive flooding in Europe, Australia, and many parts of Asia (WMO, 2011). The year 2010 is considered the worst year for floods in three decades. Extreme weather disturbances have been identified as the key culprit in crop supply shortfalls across a range of commodities, including corn, coffee, rice, wheat, and sugar. In 2010, agricultural prices increased consequent upon a series of crop failures in major crop-producing regions. The effects of flooding on health can be considered as either immediate (occurring during or immediately after the flooding event) or delayed (Hunter, 2003). Immediate health impacts include injuries and communicable diseases or exposure to toxic pollutants, and long term impacts include malnutrition and mental health disorders (McMichael et al., 2006).

Natural disasters and catastrophic events caused by extreme weather are a major cause of mortality and morbidity worldwide (IFRC, 2001). Short and long-term averages and variability of weather conditions are influencing these impacts (Kovats, et al., 1999).

Extreme weather events considered for monitoring and estimating disease burden include the following (McMichael et al., 2006):

- Coastal flooding, driven by sea level rise
- Inland flooding and mudslides caused by increased frequency of extreme precipitation.

Because of a deficiency of quantitative data, climate change effects on the following impacts of natural disasters cannot be calculated. Nevertheless, the total effect of such longer-term procedure may very well be greater than from the severe effects (McMichael et al., 2003):

- Longer term health impacts resulting from population displacement

- Consequences of damage to health systems
- Effects of wind storms
- Effects of melting snow and glaciers on floods and landslides
- Infectious disease outbreaks and mental problems due to emergency situations.

Natural disasters are determined by the rate of extreme precipitation over a limited time and the average amount of precipitation at the local level. Their severity is also calibrated to the geographical and topographical distribution of population as well as social characteristics of vulnerability, together with the quality of housing. Traditional systems of tsunami warning in coastal cities appear to have been generally lost, and implementing up-to-date early warning systems could reduce the impacts of low-probability high-impact coastal events (Kundzewicz and Kaczmarek, 2000). Kundzewicz and Kaczmarek (2000) also calculated the changes in the frequency of extreme events under various climate scenarios for each cell of the global climate model grid. Using spatial software like GIS, this was overlaid upon a map of global population distribution. This allowed the calculation of an exposure in each region. In contrast to the other health impacts considered in the WHO (2011) assessment, natural disaster-caused health impacts do not refer to a specific disease, with a related burden calculated by WHO. It is essential to estimate the impacts attributable to these extreme climate events by first calculating and archiving baseline climate conditions. Relative risk estimates for future scenarios can then be applied to these numbers.

Injury and morbidity numbers are based on the EM-DAT database (EM-DAT, 2010), which archives events that have resulted in at least one of the following:

- >10 people killed,
- >200 injured,
- A call for international assistance.

This is the most comprehensive data compilation accessible at the global scale, and yet it is likely subject to significant under-reporting, so estimates are expected to be conservative. EM-DAT estimates numbers of people killed, injured and affected. For this calculation and

assessment only the numbers of people killed are used as the EM-DAT group considers injury numbers for floods to be undependable. The assessment is therefore unlikely to fully characterize the health impacts of flooding (McMichael et al., 2003). The annual frequency of death attributable to such disasters under baseline climate environments is projected by the researchers using 20-year averages for each region.

Baseline frequency rates change over time, according to vulnerability. Some factors such as improved flood defenses (occasionally societies become wealthier and can devote resources to this) actually decrease vulnerability, while others follow the more usual trend of increasing vulnerability as population grows and storm surges become more frequent (McMichael et al., 2006). Changes to the database are of course made on an ongoing basis to account for these effects (where resources allow this). Nicholls' model (Nicholls et al., 1999) integrates coastal flooding defenses and population distribution.

The numbers of people affected and killed in coastal floods are very large, but this includes a low disease burden in terms of people immediately injured and killed (McMichael et al., 2006). Impacts of inland floods are projected to rise by a comparable order of size and usually cause a greater severe disease burden. In contrast to most other impacts, the increase in risks (inland versus coastal) is comparable in both developed and developing areas. Assessments are subject to uncertainty around the expected efficiency of adaptation measures and the calculable relationships between the frequency of flooding, changes in precipitation, and related health impacts.

The direct impacts of variability and climate change on the North American region include floods, hurricanes, heat stress, injury and mortality due to convective storms, tornadoes and ice storms (McMichael et al., 2003). Floods are the most frequent of all types of natural hazards in the United States and Canada, and an important cause of death from natural disasters. The mean annual loss is estimated to be 147 deaths (Patz, 2000). In 1997, the Red River flood in Canada displaced more than 25000 people (Simonovic, 2011). The urban areas of south-eastern Ontario and Quebec could be affected very negatively by warmer temperatures as indicated in climate-modeling studies (Kalkstein and Smoyer, 1992). On the other hand, warmer winters could result in a smaller number of cold-related deaths. A number of vector-borne diseases are widespread in North America (McMichael et al., 2003).

The World Health Organization declared the United States free of malaria in 1970, although in Canada the disease was gone at the end of the nineteenth century (McMichael et al., 2006). Lyme disease is the most public vector-borne condition in the United States with around 10,000 cases being reported in 1994. Also in Canada, the tick vector disease has been detected in number of cases (Morshed et al., 2012). It is likely that, with climate change, Lyme disease and Rocky Mountain spotted fever will migrate in to Canada (McMichael et al., 2003).

Based on WHO classification, there are three broad categories of diseases:

- Communicable diseases,
- Non-communicable diseases
- Injuries

For reviewing the literature about the potential climate change-related impacts on human health, it is easier to focus on these major categories separately. Although data is available for specific diseases within each category, and these vary depending on the geographic location, using the data that is “rolled up” into communicable, non-communicable and injuries provides a practical way of looking at the burden of disease of a population and helps direct efforts to identify adaptation and mitigation strategies specific to each major component of the burden of disease.

2.5.1 Communicable diseases

Floods are related to an increased risk of water- and vector-borne diseases (WHO, 2011). The World Health Organization (WHO) has noted that after floods, the risk of communicable disease transmission increases when infrastructure is seriously impacted, populations are displaced, and water supply systems are damaged leading to the contamination of drinking water (WHO, 2011; Watson et al., 2007). In general, diseases resulting from water contamination include cholera, hepatitis A and E, leptospirosis, parasitic diseases, rotavirus, diarrheal disease, shigellosis and typhoid fever (Ligon, 2006). Particular water-borne diseases connected to floods include wound dermatitis, conjunctivitis and ear, nose and throat

infections (WHO, 2011). The risk of infectious diseases increases as a result of flooding through the contamination of freshwater resources with high pathogen concentrations (Bezirtzoglou et al., 2009). Additionally, floods create conditions contributing to outbreaks of vector borne infectious diseases particularly those due to mosquitos, as heavy rains leave small stagnant water ponds which serve as insect breeding sites. Floods may also drive rodents to high ground, which may carry ectoparasites (eg. fleas) or endemic pathogens (eg. *Leptospira*) that may then have a greater opportunity to move to human hosts as mixing of human and rodent populations increases (Bezirtzoglou et al., 2009).

Floods can increase the rate of vector-borne diseases through an increase in the amount and extent of vector habitats. Overflow of rivers or stagnant water caused by intense rainfall can act as breeding sites for mosquitoes, and consequently increase the potential for exposure of the disaster-affected population and rescue teams. These diseases may include dengue, malaria and West Nile fever and are dependent on the geographic location of the flooding event in terms of which vector borne diseases are endemic in the region. Most often flooding flushes out mosquito-breeding areas, but these areas come back when the waters move away and the start of a malaria epidemic can take up to 6-8 weeks to occur (WHO, 2014).

Brown and Murray (2013) studied the relationship between infectious diseases and flooding in Europe. Their research was a systematic literature review and summary of possible public health interventions. They noted that many infectious diseases are sensitive to climatic changes; in general and to flooding in particular. The authors reviewed relevant publications from 2004 to 2012, scanning databases including Medline, Scopus, PubMed, Cochrane Library, and Evidence Aid. Their results indicated that water-borne, rodent-borne, and vector-borne diseases can be correlated with flooding in Europe, although at a lower rate than in comparison with developing countries (Figure 15).

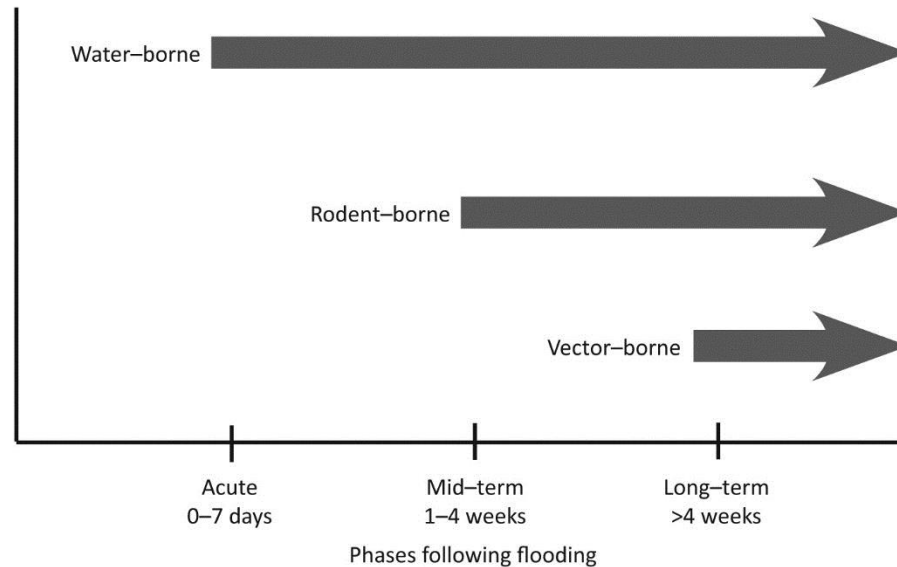


Figure 15 The incidence of infectious disease outbreaks following flooding in relation to time (Source: Brown and Murray, 2013).

The literature review by Ivers (2006) focuses on some of the potential infectious disease consequences of disastrous natural phenomena and severe weather, with a specific emphasis on infections related to floods and the destruction of infrastructure. The findings show that the risk of infectious diseases after flood-related natural disasters is often specific to the event itself and is dependent on a number of factors, including the endemicity of specific pathogens in the affected area before the disaster, the category of disaster, the availability of shelter, the impact of the disaster on water and sanitation systems, the congregating of displaced persons, the functionality of the surviving public health infrastructure, the availability of healthcare services, and the rapidity, extent, and sustainability of the response after the disaster. In conclusion Ivers' team mention that weather or flood-related natural disasters could be correlated with an increased risk of respiratory, diarrheal, soft tissue, and vector-borne infectious diseases amongst both survivors and responders.

2.5.2 Non-communicable diseases

The long-term impact of floods on morbidity and mortality is complex and not well understood (Alderman et al., 2012). Health impacts such as mortality may be attributed to floods directly, or with moderate directness such as occurs with increases in diarrheal deaths in low-income countries (Ramin and McMichael, 2009; Schwartz et al., 2006) and these are mostly related to the early period of the event itself and the periods shortly after the event (days to a few weeks), or these impacts might work indirectly on health and wellbeing in the longer term (months to years), by exacerbating poverty, impairing food and economic systems, and causing malnutrition. It is being increasingly recognized that in developed systems where there are significant populations that require ongoing access to life support services, end stage renal disease, cancer management etc floods may disrupt access to these services. In affected populations in the first year following a flood, the mortality rate may continue to increase by up to 50% (Fundter et al., 2008), as confirmed with the 47% increase in percentage of deaths in the first year after Hurricane Katrina (1317 deaths per month versus 924 per month comparative to a four year baseline) (Stephens et al., 2007). A study of the impact of floods on health in China has shown that two years after the flood the mortality and years of potential life lost for five leading causes of death were significantly higher in groups exposed to floods (Li et al., 2007).

In 2008, 63 percent of all deaths in the world were from non-communicable diseases (36 out of 57 million people) such as cancer, cardiovascular disease, chronic lung diseases and diabetes (Friel et al., 2011; WHO, 2011). Low income and medium income countries have experienced 80% of all non-communicable disease-attributable deaths, and this trend is estimated to continue (Friel et al., 2011; WHO, 2011). Chronic disease and related conditions (CDRCs) can get worse as a result of different extremes, increasing a person's exposure to adverse health outcomes following a flood (Sharma et al., 2008).

A variety of studies in the United States suggest that CDRCs represent a large proportion of flood-related hospitalizations, particularly amongst seniors. In the immediate post-flood period this burden has been found to increase non-fatal injuries (Diaz, 2003; Sharma et al., 2008). Investigation data from New Orleans taken two months after Hurricanes Katrina and Rita showed that of 21,673 health care calls, nearly 60% were for illness, 24.3% of these for

CDRCs (Sharma et al., 2008). The main barrier to continuity of care for chronic conditions during the disaster was the inability to maintain a stable medication uptake, with insufficient data and financial constraints as contributing factors (Arrieta et al., 2009).

In the Japanese flood of 2006, individuals who were older than 75 years of age and those receiving long-term care services were more likely to have their medications interrupted due to floods (Tomio et al., 2010). No similar surveillance data appear to have been collected in low-income countries, however, with low-income countries carrying the largest burden of chronic disease generally, the impacts of flooding on non-communicable diseases can be well imagined.

One of the least studied categories of non-communicable diseases are those related to mental health of populations in the aftermath of major flooding events. A number of categories of mental illness such as depression and Post Traumatic Stress Disorder (PTSD) are included in the non-communicable disease category and as such provide some measure of the burden of mental health disorders in a community.

2.5.3 Injuries

Exacerbation of chronic illness and nonfatal injuries are the leading causes of morbidity among affected residents and relief workers immediately following floods (Diaz, 2003; Sullivent et al. 2006). Injuries can happen before, during and after the flood, and during the clean-up phase (Abaya et al., 2009). Cuts, falls, being struck by falling debris or objects moving quickly in flood water, and being bitten or stung are the most common reasons for flood-inflicted nonfatal injuries (Abaya et al., 2009; Ahern et al., 2005; Diaz, 2003; Sullivent et al., 2006).

In Hurricane Hugo (USA, 1989) almost 90% of over 2000 patients treated in emergency departments were hospitalized for injuries, resembling the pattern observed in previous US hurricanes such as Hurricane Andrew in 1992 and Hurricane Opal in 1995 (Diaz, 2003). Surveillance conducted post-Hurricane Katrina/Rita in Greater New Orleans recorded over 7500 nonfatal injuries among residents and relief workers. In both groups young to middle

aged males were most at risk, partly due to the fact that they were the ones most actively participating in the relief and clean-up efforts (Sullivent et al., 2006). While patterns of injuries varied between residents and relief workers, in both groups, most of the injuries occurred during the clean-up phase with cuts representing the leading mechanism of injury (27% and 19% respectively; Sullivent et al., 2006). Sullivent et al., (2006) found that a greater number of residents compared to rescue workers were injured during the repopulation period, primarily due to falls (23% versus 10%) and motor vehicle crashes (9% versus 4%).

2.6 Contributions of the research

Climate change-related impacts are affecting human health in coastal mega-cities. Climate change impacts (e.g. floods, sea level rise, etc.) can combine with population growth and land-use change patterns to affect people living in coastal mega-cities. In this study, a generic approach is developed to assess spatio-temporal climate change impacts on human health in coastal mega-cities. This task relies on an improved understanding of mapping techniques deploying Geographic Information Systems (GIS) and Remote Sensing tools. The development of a health impact map for coastal mega-cities requires a significant amount of spatial data including physical data related to climate change impacts and nonphysical data such as census data (total, seniors and children populations). The methodology presented in this research is designed to provide support for improving health resilience in coastal mega-cities through development of a spatio-temporal climate change-related health impact measure. Emphasis is placed on explicit assessment of the key aspects of climate change impacts on human health in coastal mega-cities, including:

1. Flood inundation-mapping
2. Land-use change analysis
3. Nonphysical spatial data analysis
4. Data integration and
5. Application of spatio- temporal extrapolation

Flood inundation-mapping

Developing a significantly high-resolution flood inundation map for mega-cities requires a correspondingly significant amount of accurate data. Municipalities are faced with challenges relating to the development of hydrologic and hydraulic models in order to generate accurate flood inundation data. One of the contributions of this research is the use of the Digital Elevation Maps (DEM) and Geographic Resources Analysis Support System (GRASS) software as a useful and rapid tool for a preliminary delineation of flood prone areas in ungauged basins and in areas where expensive and time-consuming hydrological-hydraulic simulations are not possible because of lack of access to available data, inaccurate data and lack of knowledge of the hydrologic/hydraulic processes involved.

Land-use data analysis

Due to rapid urbanization and changing climatic conditions, cities will be exposed to increasing risks in the future. It is important to accurately assess these risks in order to make informed decisions about how to manage infrastructure and development. Various components of land-use such as changes in vegetation cover should be studied in order to understand and process land use change and the associated change in vulnerability. Vegetation condition change is typically analyzed using the normalized difference vegetation index (NDVI), which tracks changes using remotely sensed images from satellite sensors, for example Satellite Pour l'Observation de la Terre (SPOT) and National Oceanic and Atmospheric Administration-Advanced Very High Resolution Radiometer (NOAA-AVHRR)).

Nonphysical spatial data analysis

For human health related data input, this research mainly focuses on the development of a useful and quantifiable nonphysical spatial data input. The data inputs require two important characteristics: (1) they should be quantifiable and (2) they should be available in spatial format. Boundary conditions are established and data pertaining to the health and population

of various demographics are used to get a baseline. Total population, senior population, children population and “burden of disease” measured in Disability Adjusted Life Years (DALY’s) have been used in order to establish the city’s baseline state. As mentioned earlier, the World Health Organization (WHO) publishes tables of DALY’s related to country-wide estimates of various diseases that are tallied as both individual diseases but are further “rolled up” into three major categories, namely, communicable, non-communicable and injuries. They are published as DALY’s per 100,000 persons. DALY’s are also given in an age-standardized format, removing the need to have age stratified population figures for each city.

To begin to develop a composite human health input, a baseline estimate of the burden of disease in each of the three major categories (communicable, non-communicable and injuries) is required. The DALY data is directly linked to population numbers and although the quality of census data varies from country to country, it is a useful starting point. Census data is also available in a spatially relevant format in many countries. Both population numbers and their distribution within a city are often available over time and using this method an estimate of the burden of disease for each of the aforementioned categories can be calculated. The WHO data is based on countrywide estimates of disease burden but these can reasonably be applied because urban populations now comprise 50% or more of the population. In addition, if necessary, the burden of a particular category of disease could be modified for any particular city if it is known that there are areas within the city that have a higher prevalence of a particular disease than the country average. Although the estimate of the burden of disease is highly dependent on the availability and accuracy of census data, it nevertheless provides a useable input and a dynamic component for the burden of disease. Most resilience models require this dynamic component.

Data integration

Human health and well-being of a population is a component of the overall resilience of a city. The burden of disease is only one such component but it is important because during the recovery phase of the community, following a climate related event such a flood, resources

will need to be available to cope with this eventuality. Developing a more integrated set of inputs that incorporate health, economic, social vulnerability and physical infrastructure is the major focus of this research. The output from the human health aspect is in the form of maps that help identify parts of the city where health and well-being of the population are impacted disproportionately by flooding events. Such maps could help focus urban planners on where adaptation and mitigation strategies would have the greatest impact on human health prior to the event. Having these measures already in place would increase the overall resiliency of the city, allowing a more speedy resumption of functionality in the event of a climate change-related flooding event. This approach has not been applied before in coastal mega-cities. The integration of a variety of different sources of input data (land-use change, flood extent maps, burden of disease, census data, etc.) with different units and resolutions poses a unique challenge in the synthesis of this research. A weighting system has been utilized to integrate these different data sources. This weighting system provides an opportunity to produce a comprehensive risk map that reflects priorities and concerns in specific locations as well as across an entire city. The final results are a set of health impact maps, which have been generated using spatio-temporal data and statistical techniques in order to estimate future potential health risks in Metro Vancouver.

Application of spatio- temporal extrapolation

One of the key contributions of this research is the application of spatio-temporal models to extrapolate information relating to future health impacts, which can be displayed using a map. Physical and nonphysical spatial data can be integrated based on this proposed methodology for different coastal mega-cities. Following this, two different spatio-temporal extrapolation models (1) linear spatio-temporal and (2) spatio-temporal auto regressive, are applied to generate a future health impact map.

Chapter 3

3. Methods

Coastal mega-cities are exposed to sea level rise and flooding as a result of climate change. Vulnerability of coastal mega-cities increases when climate change-related disasters combine with rapid population growth. Such cities require plans for mitigation and adaptation to these increasing risks. A variety of potential mitigation protocols and adaptation procedures/schedules should be considered, taking advantage of the latest data and interpretive techniques. Policy makers can in turn take advantage of the latest science and technology to guide the decision making process. Resilience is a new concept for many engineers, planners and policy makers, but it is essential for assessment of potential adaptation plans. There is currently no widely adopted procedure to quantify resilience, which makes it difficult to compare estimates across different cities since such estimates have typically been based on qualitative data.

For building a holistic quantitative resilience framework, huge sources of accurate spatio-temporal data are required. The resilience model is required to integrate physical, economic, health, social and organizational impacts of climate change into a holistic quantitative approach. This research presents a methodology for providing spatial and temporal information on climate change-related health impacts. The problem necessitates integration of the available information relating to the spatial distribution of climate change impacts on human health in urban environments. In the process, a time series of maps will be assembled to represent visually the changing conditions and impacts. Essential steps include spatial data collection, definition of potential physical and nonphysical inputs and application of appropriate techniques for spatio-temporal interpolation and extrapolation of the collected data.

The exposure and vulnerability of an urban environment to climate extremes is temporally and spatially variable and dependent on a number of factors. Most of these factors are related to baseline conditions: the overall health of the population, the local economy, social infrastructure, environmental conditions, geography, demographics, cultural values, institutional organization and governance. The United Nations Development Programme

(UNDP) and World Health Organization (WHO) are involved in a series of projects that aim to increase public health resilience through the development, preparation, and the use of warning systems (WHO 2011). For example, one project uses a meteorological-based decision-support system to warn the public about oncoming heat waves in China (Chalabi and Kovats, 2014).

The key objective of this research is to develop procedures to assess climate-related impacts on human health in coastal mega-cities using spatio-temporal data. The resulting outcomes can assist in the reduction of uncertainty and streamline the decision-making process related to the development and implementation of urban health policies that will address major public health challenges triggered by the changing climate. This assessment can be provided for each city using generally available estimates which can then be modified and refined using specific local knowledge and data. The final product can be used as (1) input for the resilience model and (2) for the development of stand-alone health impact maps. Both of these can help provide direction to planners and policy makers in terms of what mitigation and adaptation strategies will provide the greatest benefit for the community.

City resilience simulation modeling (Simonovic and Peck, 2013) has been adopted as a tool that facilitates the integration of various impacts of climate-related disasters and allows for a quantitative comparison of different climate change adaptation options. There are many definitions of resilience and the common elements of these definitions include: (1) minimization of losses, damages and community disruption; (2) maximization of the ability and capacity to adapt and adjust when there are shocks to systems; (3) returning systems to a functioning state as quickly as possible; (4) recognition that resilient systems are dynamic in time and space; and (5) acknowledgements that post-shock functioning levels may not be the same as pre-shock levels.

For the purposes of resilience in coastal mega-cities, there is a sustainable network of physical (constructed and natural) systems and human communities (social and institutional) that possess the capacity to survive, cope, recover, learn and transform from catastrophic events by: (1) reducing failure probabilities; (2) reducing failure consequences (for example material damage); (3) reducing time to recovery; and (4) creating opportunity for development and innovation from adverse impacts. Numerous institutions, organizations, and

elements in the urban environment contribute to community resilience, for example water and power lifelines, acute-care hospitals, and organizations that have the responsibility for emergency management. Improving the resilience of lifelines is important for overall community resilience. For example, hospital functionality is crucial for community resilience in a flood situation in order to provide emergency care for injured victims.

The resilience quantification framework has two qualities: inherent (functions well during non-flooding periods); and adaptive (flexibility in response during flood events) and can be applied to the physical environment (built and natural), social systems, governance network (institutions and organizations), and economic systems (metabolic flows). The space-time dynamic resilience measure (STDRM) of Simonovic and Peck (2013) is designed to capture these relationships between the main components of resilience.

STDRM is based on two basic concepts: the level of system performance and adaptive capacity. Together, these concepts define resilience. The level of system performance integrates various impacts (i) of flood on a community. The following impacts (units of resilience(ρ^i)) can be considered: physical, health, economic, social and organizational. The general measure of risk, however, is not limited to consideration of only these aforementioned impacts. Measure of system performance $P^i(t,s)$ for each impact (i) is expressed in the impact units (physical impact may include for example length [km] of road being inundated; health impact may be measured using an integral index like disability adjusted life year (DALY); and so on). This approach is based on the notion that an impact, $P^i(t,s)$, which is spatially and temporally variable, defines a particular resilience component of a community, as shown in Figure 16, adapted from Simonovic and Peck (2013). The area between the initial performance line $P_0^i(t,s)$ and performance line $P^i(t,s)$ represents the loss of system resilience, and the area under the performance line $P^i(t,s)$ represents the system resilience ($\rho^i(t,s)$). In Figure 16, t_0 denotes the beginning of the flood event, t_1 the end, and t_r the end of the flood recovery period.

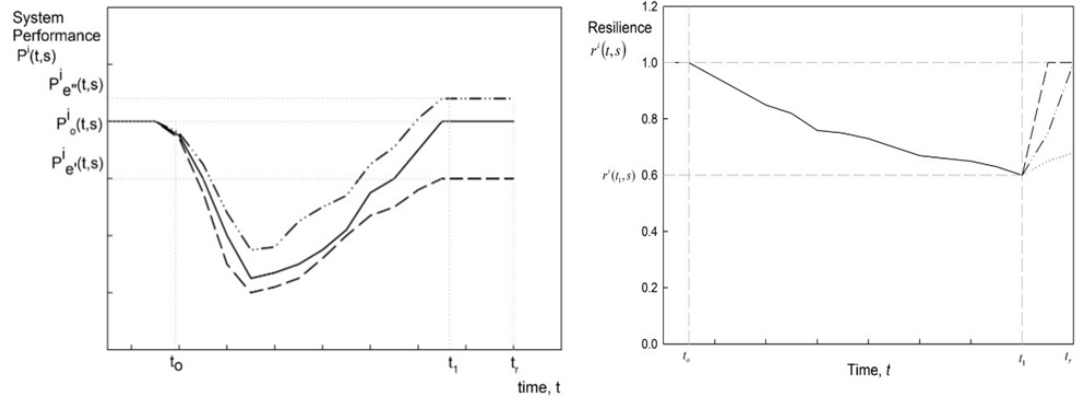


Figure 16 System performance and system resilience (after Simonovic and Peck, 2013).

In mathematical form the loss of resilience for impact (i) represents the area under the performance graph between the beginning of the system disruption event at time (t_0) and the end of the disruption recovery process at time (t_r). Changes in system performance can be represented mathematically as:

$$\rho^i(t, s) = \int_{t_0}^t [P_0^i - P^i(\tau, s)] d\tau \quad (1)$$

where $t \in [t_0, t_r]$.

When performance does not deteriorate due to disruption, $P_o^i(t, s) = P^i(t, s)$ the loss of resilience is 0 (i.e. the system is in the same state as at the beginning of disruption). When all system performance is lost, $P^i(t, s) = 0$, the loss of resilience is at the maximum value. The system resilience, $r^i(t, s)$ is calculated as follows:

$$r^i(t, s) = 1 - \left(\frac{\rho^i(t, s)}{P_0^i \times (t - t_0)} \right) \quad (2)$$

As illustrated in Figure 16, the performance of a system which is subject to a flood (disaster event) drops below the initial value and time is required to recover the loss of system performance. Disturbance to a system causes a drop in system resilience from value of 1 at t_0 to some value $r^i(t_1, s)$ at time t_1 , see Figure 16 (right). Recovery usually requires more time than the duration of the disturbance itself. Ideally the resilience value should return to a

value of 1 at the end of the recovery period, t_r (dashed line in Figure 16 (right)); and the faster the recovery, the better. The integral STDRM (over all impacts (i)) is calculated using:

$$R(t, s) = \left\{ \prod_{i=1}^M r^i(t, s) \right\}^{\frac{1}{M}} \quad (3)$$

where, M is the total number of impacts.

Also in this research, risk is defined as the exposure of the various segments of the population to three different health impacts (communicable and non-communicable diseases, and injuries) of inundation caused by climate change-related riverine flooding and sea level rise. The main objective of the work presented in this thesis includes development of an approach for addressing health impacts of climate change-related disasters. Health impacts, as presented above are one dimension (i) of the complex city resilience. The approach presented here used to generate maps showing the health impacts of climate change-related flooding and sea level rise in coastal mega-cities. The methodology and its application: (1) provide for a major shift in natural disaster management from risk to resilience, from static risk to dynamic spatial resilience, from single impact risk to integrated resilience measures; (2) illustrate how the available data and tools can provide for an effective implementation of the proposed approach; and (3) offer for the first time an integrated climate change-related health impact assessment for the coastal mega-cities.

Coastal mega-cities are very complex environments that are vulnerable to several of the negative impacts associated with climate change. In urban environments, a large number of factors impact human health. The methodology presented here uses an interdisciplinary approach to identify, assess and communicate climate change-related health impacts in coastal mega-cities (Figure 17). Climate change may result in significant alterations to the frequency and intensity of different climate related hazards. Impact on human health in urban environments is an important concern in much of the climate change-related research (McMichael et al., 2006). There are both physical and nonphysical elements which play a key role in impacting human health in urban areas. The best way to assess this impact is to build a climate change-related composite human health measure based on available spatial and temporal data. There are a variety of physical elements that can affect

hydrometeorological extremes in urban environments; three essential ones that ought to be considered are land-use change, flood inundation map, and topography. Nonphysical elements also affect public health conditions in urban environments. Social conditions including total, senior and children's population densities, as well as different categories of disease (communicable, non-communicable, injuries) are the essential nonphysical health inputs that should be considered in the assessment of climate change-related health impacts.

The main objective of this methodology is to develop an integrated measure of human health and map its value in time and space. The output of this mapping exercise provides an integrated view of population health that can be used in development of targeted and adaptive strategies to reduce local-level health risks in coastal mega-cities. This research demonstrates how composite health impact can be interpreted as a stand-alone product or utilized as an input for comprehensive resilience modeling.

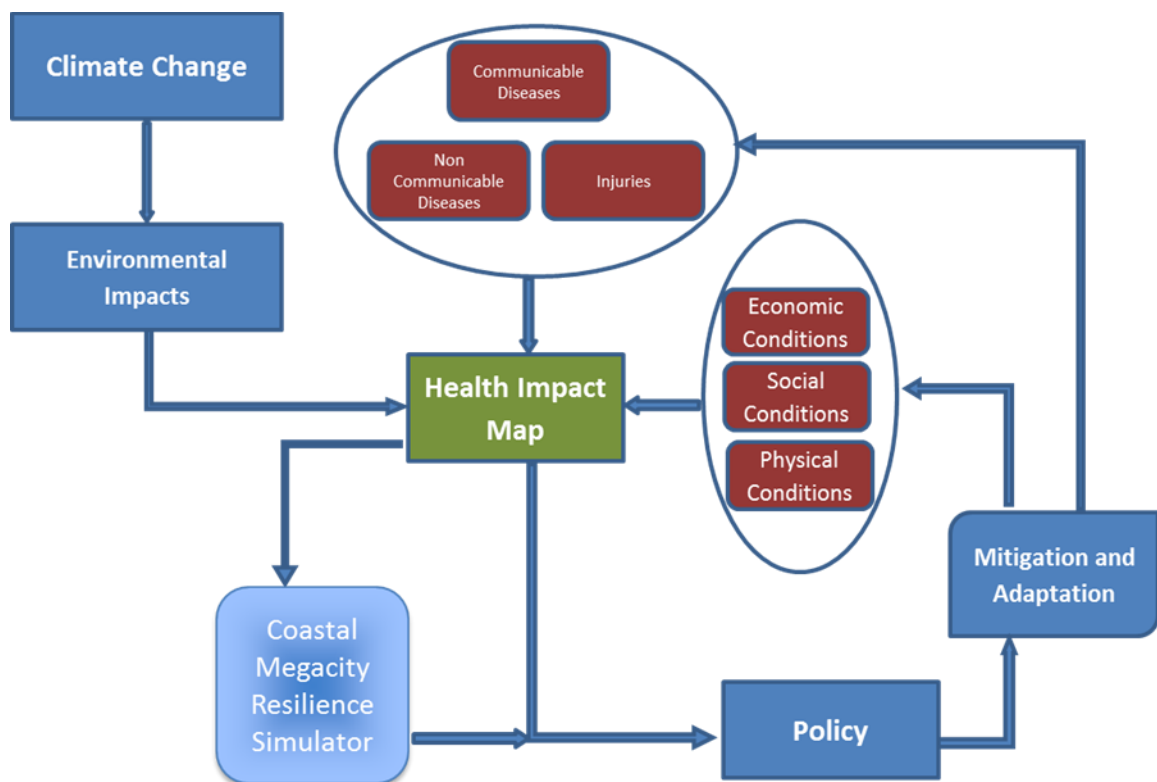


Figure 17 Illustration of the methodology for generating a human health impact map.

Physical vulnerability and risk assessment of climate change-related impacts on human health for urban areas is a complex procedure. The best way to decrease the uncertainty sources in risk assessment is to consider a variety of available data inputs. Consideration of nonphysical inputs is an essential task. As shown in Equation 4, the physical inputs include land-use, flood inundation mapping, and topography, while the nonphysical inputs include total population density, population densities of seniors and children, and different categories relating to the burden of disease. The unique aspect about this research is that the assessment procedure is dynamic and time plays an important role for future risk extrapolation.

$$\text{HIM} = f_t (\text{land-use, flood inundation map, topography, social conditions, burden of disease}) \quad (4)$$

where HIM is health impact map and f_t represent the functionality of time in this assessment. Figure 18 shows the expanded presentation of the methodology for assessment of the potential health impacts resulting from climate change in coastal mega-cities based on both physical and nonphysical spatial data inputs. Remote sensing is an essential tool for detailed spatio-temporal risk assessment. By using different sources of satellite images, analysis of the land-use change in different cities all over the world is possible. In addition, remotely sensed digital elevation maps (DEM) can help in the rapid development of flood inundation maps in different municipalities. Integration of these two potential physical health impact (flood inundation maps and land use change analysis) outcomes using the geographic information system (GIS) will help improve the accuracy of the final health impact assessment. For special assessment of nonphysical health impacts, two sources of social conditions and burden of disease data are vital. By spatially assessing both nonphysical and physical health impact conditions and applying the required interpolation, normalization and standardization techniques, production of a final health impact map is possible.

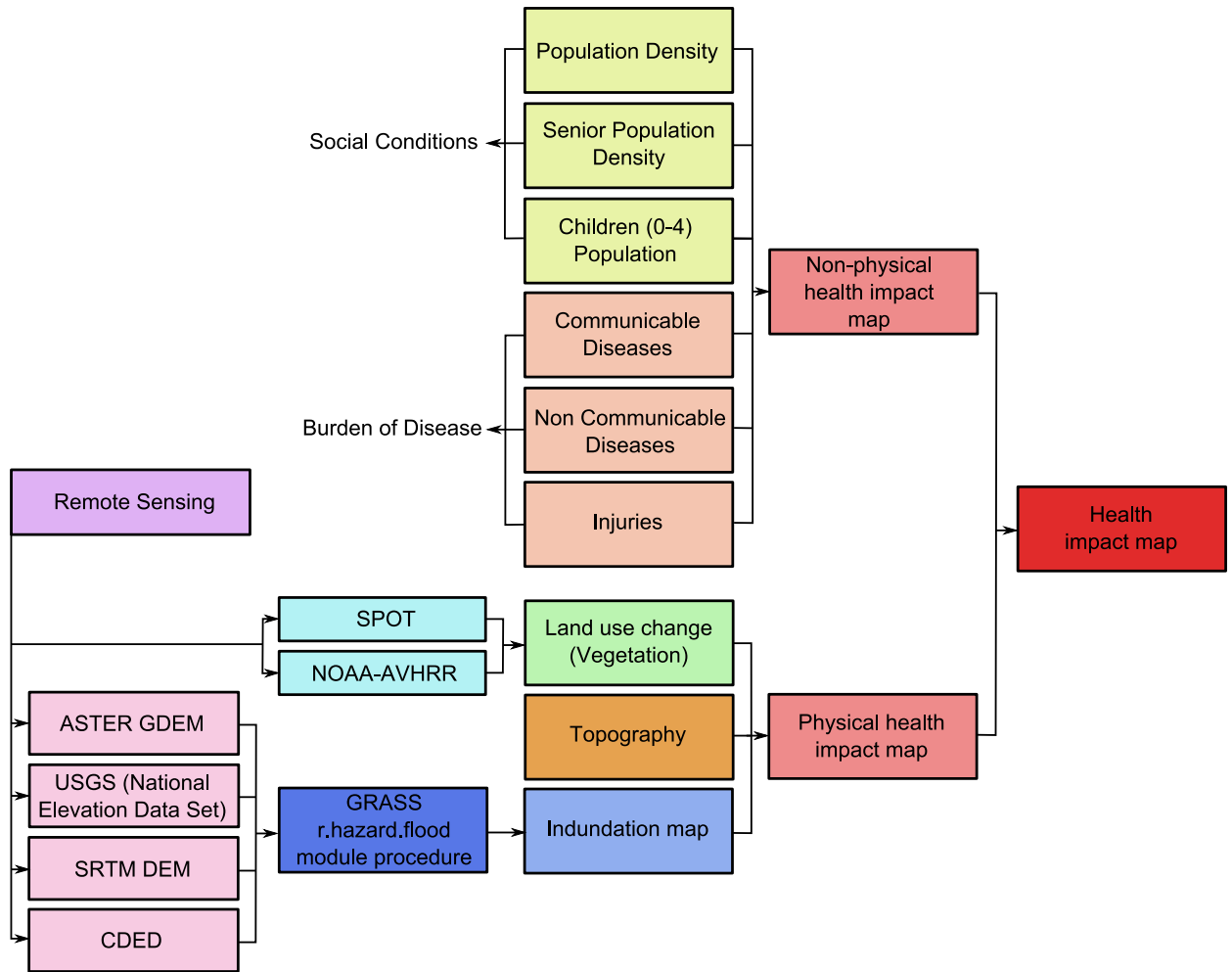


Figure 18 Presentation of the development of the health impact map method.

The remainder of this chapter provides details about the calculations and procedures associated with this methodology. Section 3.1 contains a description of different types of spatial data and their sources. Section 3.2 describes land-use change analysis (vegetation trend) using remote sensing techniques over the period of available satellite images. Also, a rapid tool for the preliminary delineation of flood inundation zones in ungauged basins is presented in this section. Section 3.3 follows, describing the assessment of potential human health impacts. In Section 3.4, the integration and weighting systems of different physical and nonphysical elements is presented. Finally in Section 3.5, the extrapolation procedure for production of a health impact map is presented.

3.1 Spatial data sources

The analysis of climate change-related health impacts in coastal mega-cities requires significant amounts of accurate spatial data. There are different types of spatial data available, each with different characteristics. This section addresses some practical concerns of the methodology. Budget, location and accessibility issues in relation to information sources are considered. Mega-cities are typically run by different municipalities, each with different rules and priorities; this presents a challenge where municipalities have different restrictions on sharing data.

For this research, spatial data is collected from different sources. Spatial databases are designed to store and manage data related to geometric features that are explicitly defined in geometric space. Geometric features are mostly stored in vector format, lines or polygons, can also can be in the form of other complex structures, such as 3D objects or networks. Different formats that are used to store spatial data related geographic locations include: shapefile, raster image, geodatabase, tabular data, and coverage (ESRI, 2014).

3.1.1 Geodatabase

A geodatabase is a database designed to query, store, and manipulate spatial and geographic data. This format created by Environmental Systems Research Institute (ESRI) is designed to apply all features of relational database models (RDBM). It stores geographic information and data using a Database Management System (DBMS), and it is a collection of geographic datasets of several types held in a particular file system folder (ESRI, 2014). It's goal is to create access to the group of datasets through a database management system using Structured Query Language (SQL). In general a geodatabase contains three key dataset types:

- Feature Classes
- Raster Datasets
- Tables

Datasets are designed mechanisms to manage geographic information. Feature classes present tables with shape files that contain line, point, or polygon geometries for geographic features. Each row in the table presents a distinct feature. Attribute tables are in different

formats such as dBase files, DBMS, Microsoft Access Tables, or Excel Spreadsheets. These are arranged in rows, each containing the same attributes or fields.

The raster data model uses a grid to cover the space and the value of each pixel in the grid to match to the characteristic of the physical feature at the pixel location. The pixel is the smallest unit in the grid and a grid is a matrix of pixels. Raster data could come from sources such as satellite imagery, digital pictures, aerial photographs, and scanned maps.

Raster data may be:

- Continuous data, as in rainfall maps, DEMs, or pollutant concentration maps;
- Discrete data or categorical data, as in land-use maps or soils maps;
- Satellite images or digital pictures, which are typically used as base maps for registration or digitization.

The main types of data likely to result in raster analyses are the discrete data and continuous data which establish the majority of raster data. In many ways, raster data match vector data in GIS applications, so the integration of both raster and vector data has become a common feature in a GIS projects.

One of the most important spatial datasets needed for developing flood inundation maps in different urban areas is a high-resolution digital elevation map (DEM). There are different potential DEM sources available free of charge for researchers with different resolutions that are accessible through the following links:

ASTER (Advanced Spaceborne Thermal Emission and Reflection Radiometer) is a Japanese sensor which is one of five on board the Terra satellite launched into Earth orbit by NASA in 1999. The instrument has been gathering data since February 2000. ASTER 30 m resolution DEM data download page is through NASA (<http://reverb.echo.nasa.gov/reverb/> Last Accessed Nov 2014). Registration needed in order to download the data.

Another potential source for downloading ASTER DEM files is from United States Geological Survey (USGS, formerly simply Geological Survey) website (<http://earthexplorer.usgs.gov/> Last Access Jan 2015).

The Shuttle Radar Topography Mission (SRTM) is an international investigation exertion that found digital elevation models on a near-global scale from 56° S to 60° N to produce the most complete high-resolution digital topographic database of Earth prior to the announcement of the ASTER GDEM in 2009 (Nikolakopoulos et al., 2006). Data is not available at a horizontal resolution of 30 m within Canada (it is only available in the United States). The data that is available is the SRTM3 (3 arc-seconds or 90m) and SRTM30 (30 arc-seconds or 900m). All of these datasets can be found at the USGS website (http://dds.cr.usgs.gov/srtm/version2_1/ Last Access Feb 2015)

GeoBase is a federal, provincial and territorial government initiative that is supervised by the Canadian Council on Geomatics (CCOG). It was established to ensure that all researchers would have access to the most up-to-date database of geospatial data for Canada. Through the GeoBase (<http://www.geobase.ca/> Last Access Dec 2014) website, users with an interest attention in geomatics have access to quality geospatial data at no cost and with unrestricted use.

3.1.2 Remote sensing data

In order to analyze land-use, there are different potential sources of satellite raw images that can be used to extract different land features. Vegetation is one of the most important elements of land-use to be analyzed in urban environments. Mega-cities tend to be very large so it is hard to find one satellite image that covers an entire metropolitan area. A satellite must be selected that can scan an entire city in one image. The following are two potential satellite data sources that provide free images for scientific research and have been used in this study.

- The AVHRR is a broad-band, five channel scanner, detecting in the visible, near-infrared, and thermal infrared portions of the electromagnetic spectrum. Since 1978 this sensor has been carried on the NOAA's Polar Orbiting Environmental Satellites (POES), and acquires and archives the 1km² resolution AVHRR raw images globally. AVHRR data can access through the following website:

http://www.class.ncdc.noaa.gov/saa/products/search?datatype_family=AVHRR (Last Access Mar 2014)

- The SPOT VEGETATION program is the result of space collaboration between several European partners: Belgium, France, Italy, Sweden and the European Commission. In 1998, it was added to the program that had been founded by Belgium, France and Sweden in 1978. It includes two observation instruments in orbit, VEGETATION 1 and VEGETATION 2, plus ground infrastructures. SPOT 4 launched on 24 March 1998 and the first of the two instruments launched at that time. The second is onboard SPOT 5, which was positioned into orbit on 4 May 2002. These images can be accessed through the following link:
<http://www.spot-vegetation.com/> (Last Access Dec 2014)

3.2 Remote sensing

Remotely sensed data can be utilized to develop a visual representation of potential impacts including flood inundation maps and land-use changes in an efficient and effective way. In this thesis, techniques are presented for flood mapping using remotely sensed DEM data and for land-use change analysis using vegetation index. Figure 19 contains a schematic showing what remotely sensed data can be used in development of physical health impact maps. For analysis of the land-use changes in different cities, several sources for DEM's, NOAA-AVHRR and SPOT satellite images are available. These data are used to analyze the amount of vegetation cover and to develop flood inundation maps in urban areas. In the following section different sources of freely accessible DEM files and open source spatial tools are presented for developing inundation maps for different locations all over the world.

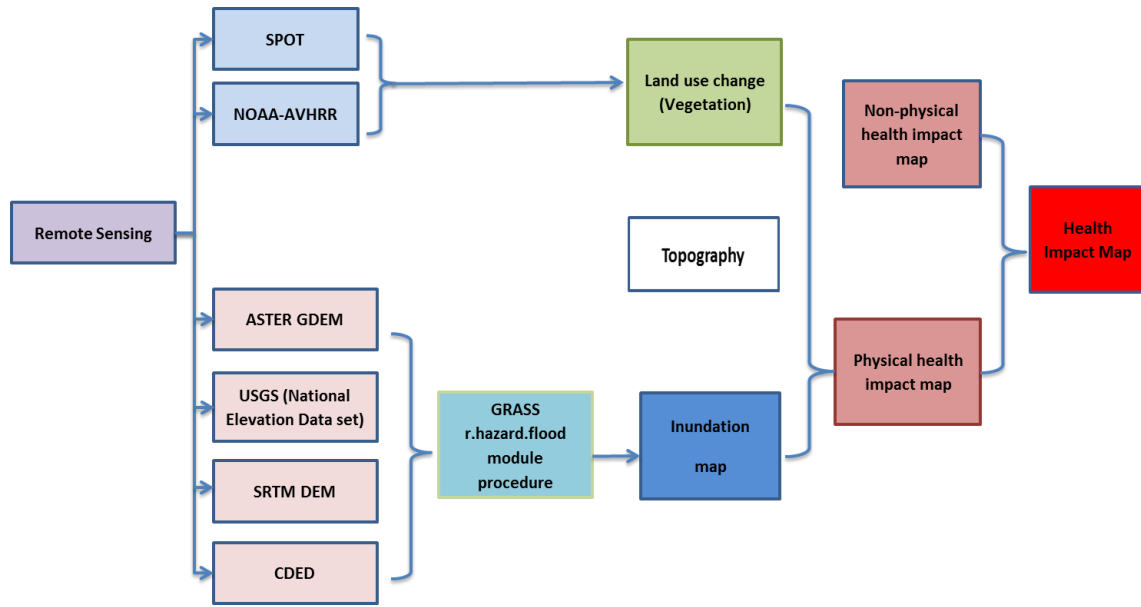


Figure 19 Presentation of the use of remote sensing for developing physical health impact map.

3.2.1 Land-use change

Local governments have many land-use management policies for increasing community resilience: critical and public facilities policies, development regulations, building standards, planning processes, land and property acquisition, and public information. Land-use planning and management leads to communities where people and property are kept out of the areas exposed to hazards, where development is designed to be resilient to natural forces, and where the mitigative capacity of natural environmental systems is not diminished. In many countries, land-use planning and management is not governed by the federal or state policies. These levels of government seem unwilling to take a role in land-use management, often communicate conflicting signals to local governments about exposure to hazards, and typically advocate measures to reduce risk (Simonovic, 2012). One of the key factors in land-use management is the analyses of land use change over the time.

The surface of the earth has been significantly changed by human activities. This has had an impact on local and regional river regimes. These changes are either direct, by manipulation of water resources, or indirect, through the effects of forest clearance and agriculture. Parker (2000) estimates that 20% of the earth's land area has been severely reformed by human

activities. Some of these modifications have increased the flood hazard. Elimination of the natural vegetation tends to reduce evapotranspiration losses and exposes the soil surface to the full kinetic energy of the falling rain causing breakup of the soil crumbs, clogging of pores in the soil, reductions in infiltration capacity, and in some cases, formation of impermeable patches (Simonovic, 2012).

Making both quantitative and visual comparisons of land-use changes and vegetation trends in municipal regions has allowed researchers to generate more useful and reliable results for predicting future flood scenarios. For prediction of land-use changes in coastal cities located in river deltas, more efficient study methods are required to reduce the processing time associated with conventional methods. Currently, remote sensing is one of the most advanced tools for analyzing land-use change and its relationship to flood magnitudes.

Land-use can both positively and negatively impact the climate change-related flood regime in urban areas. Therefore a land-use change analysis is essential when developing climate change strategies (Green, 2014). Flooding tends to be a corollary of vegetation loss. In this section, a methodology is presented for analysis of vegetation conditions in urban environments using satellite images. Normalized difference vegetation index (NDVI) is an index for assessing the vegetation conditions in different locations. Figure 20 presents the essential steps for NDVI extraction using different raw images of the two sensors of AVHRR and SPOT-VGT.

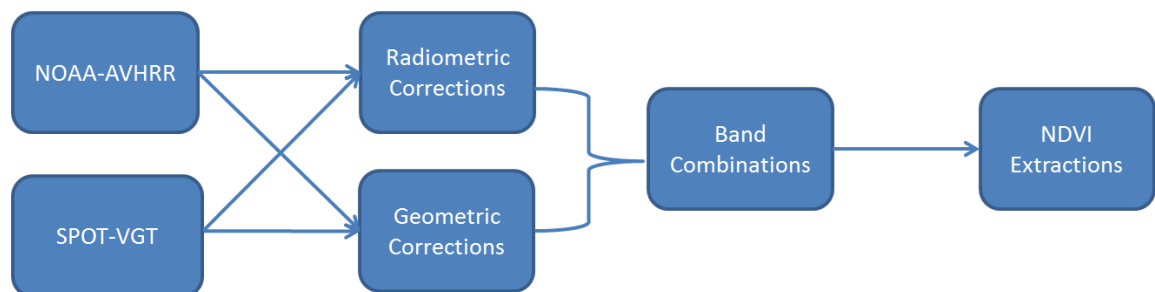


Figure 20 Presentation of the extraction of NDVI from the satellite images.

Both radiometric and geometric corrections are needed to apply raw, remotely sensed data before any further index calculation. Radiometric correction refers to the procedure that corrects and calibrates deviations in remotely sensed data values which are the result of specific distortions due to atmospheric effects or instrumentation errors (ESRI, 2015). Coefficients are needed for each image depending on the location of the case study, time of the image, and the sensor. Geometric correction refers to the correction of errors in remotely sensed data, including instrumentation errors (e.g. caused by satellites or aircraft not staying at a constant altitude or by sensors divergent from the primary focus plane). Ground control points can help mitigate these kinds of errors. By comparing ground control points on accurate basemaps, exact locations and appropriate pixel values can be calculated (Figure 21). Figure 22 demonstrates the application of ground control points for geometric correction in the ENVI (Exelis Visual Information Solutions) environment.

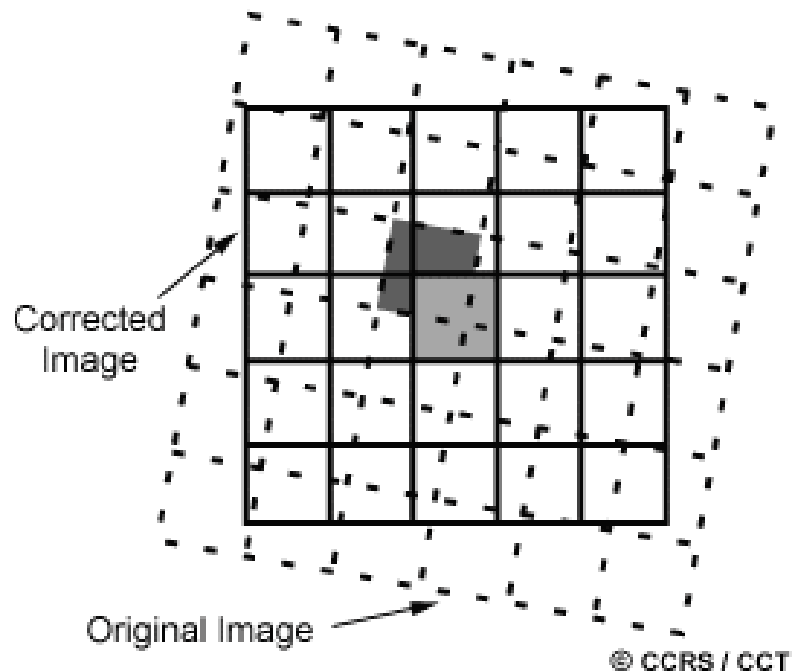


Figure 21 Geometric correction.

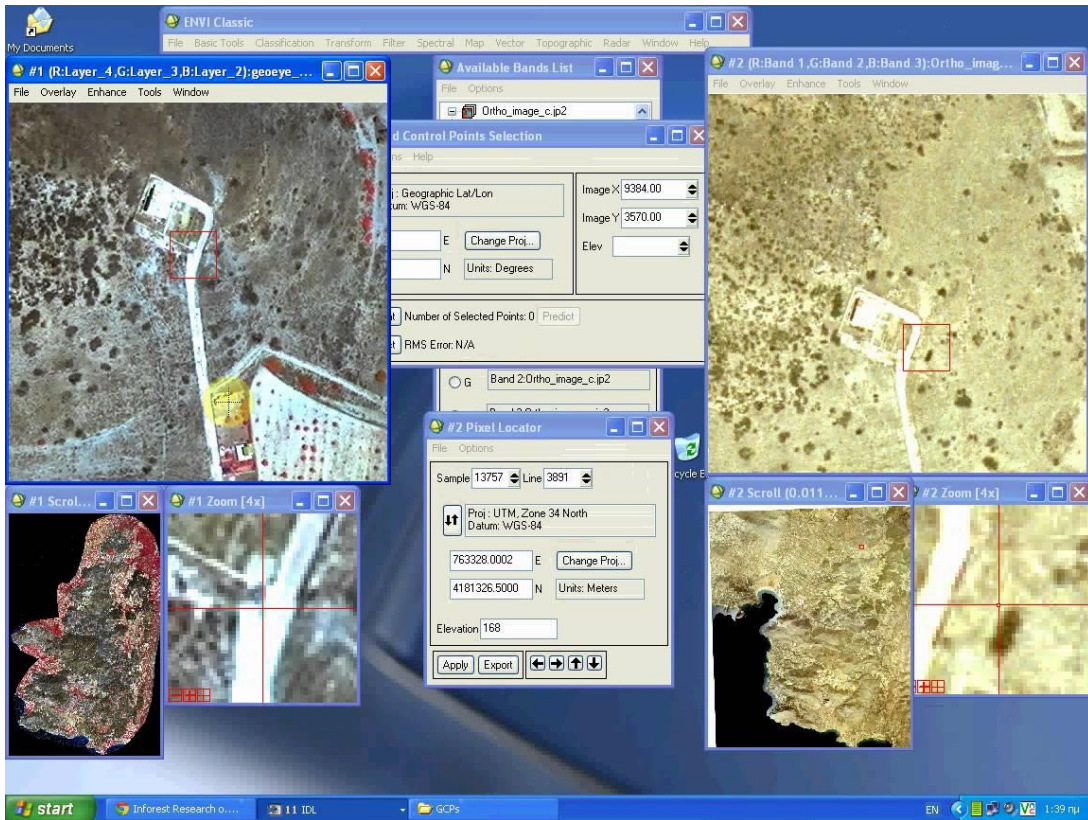


Figure 22 The application of ground control points for geometric correction in the ENVI environment.

NDVI is based on the fact that healthy vegetation has a low reflectance in the visible portion of the electromagnetic spectrum due to chlorophyll absorption and other pigments, and a high reflectance in the near infrared (NIR) because of internal reflectance by mesophyll spongy tissue of a green leaf (Campbell, 2002). NDVI can be calculated through the band combination using pixel's reflectance values of red (visible) band and the NIR band of a satellite sensor as:

$$\text{NDVI} = (\text{NIR} - \text{VIS}) / (\text{NIR} + \text{VIS}) \quad (5)$$

where VIS and NIR stand for the spectral reflectance (μm or micrometer) measurements acquired in the visible (red) and near-infrared regions. NDVI values range from -1 to +1. Because of the high reflectance in the NIR portion of the electromagnetic spectrum, healthy vegetation is represented by high NDVI values (between 0.05 and 1). Conversely, non-vegetated surfaces (such as water bodies) yield a negative NDVI value. Bare soil areas have NDVI values which are closest to 0 due to the high reflectance in both the visible and NIR

portions of the electromagnetic spectrum (Lillesand and Kiefer, 1994).

NOAA-AVHRR is available for all over the world from 1978, and SOPT-VGT is available globally from 1998. There are also different remote sensing software packages for image processing. ENVI is one of them. The maximum-value composite (MVC) procedure is applied for these satellite images after geometric and radiometric corrections are made.

The MVC is an approach in satellite imaging that can be applied for vegetation studies (Figure 23). First, a series of multi-temporal and geo-referenced satellite data are processed into NDVI images, then on a pixel-by-pixel basis, each highest NDVI value is retained for each pixel location. After all pixels have been assessed, the result is known as an MVC image (Holben, 1986).

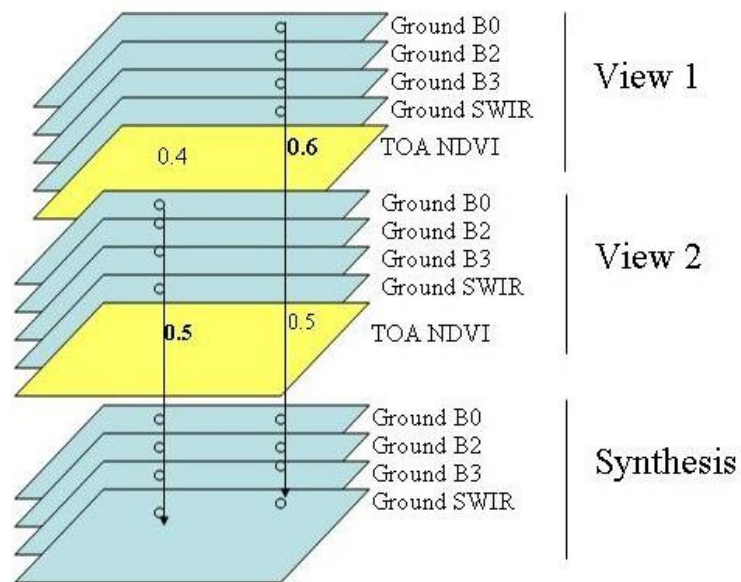


Figure 23 The production of MVC according to the Maximum NDVI Value (Source: www.vito-eodata.be).

The MVC procedure as described by Holben (1986) is applicable to merge NDVI values over the course of 10 days. The resulting surface reflectance value for each pixel corresponds to the date with the maximum NDVI value in a 10-day period. MVC for the synthesis of daily

NDVI values was found to be a reliable way for sensing changes in vegetation cover (Lanfredi et al., 2003).

Typical NDVI values range between 0.1 and 0.8 for vegetated areas, with a higher (composite) NDVI value corresponding to denser, greener vegetation. The temporal evolution of NDVI values is considered to be an effective way to analyze the impact of (1) natural seasonal variations, (2) extreme climatic events and (3) human activities on ecosystems (Telesca and Lasaponara, 2006). The temporal evolution of NDVI values for the period 1982–present is a great opportunity that gives municipalities a chance to overview their land-use over time and to inspect vegetation conditions in different locations of their metropolitan areas.

3. 2.2 Flood inundation map

Flooding is one of the most significant natural risks and it is a key element required for calculation of potential physical health impacts. Flood impact is a concern that affects urban communities in a number of ways, depending on the geographic location of the community as well as its social and economic structure (Degiorgis et al., 2012). The most efficient and effective way to assess flooding is through development of a flood inundation map.

Maps presenting flood hazards, flood-prone areas and associated spatial information are essential mechanisms for an effective approach to Integrated Flood Management (IFM) (Kang et al., 2013). This is especially important when discussing spatial issues including land-use planning in the context of flood management (WMO, 2011). Comprehensive practical approaches for calculating and mapping flood prone areas and flood risks are accessible in situations wherever data is available (Kang et al., 2013).

Flood inundation maps are developed through modelling techniques which apply hydrologic and hydraulic processes. The modeling procedure typically starts with collection of historical data relating to past flood events. This helps determine potentially hazardous reaches and river sections and provides a means to validate the model. The next step is development of a hydrologic model which converts rainfall to runoff by taking into consideration factors such

as permeability, time of concentration and antecedent soil moisture. The hydrologic analysis is used to determine peak flow discharges. Next, a hydraulic model is used to estimate water levels along the channel. Hydrologic modelling of flood events requires a discharge time series as well as information about the river channel geometry and relevant characteristics including surface roughness and boundary conditions (Degiorgis et al., 2012). Cities are faced with the challenge of incorporating various sources of data (that are inaccessible to the general public) into the development of up to date flood risk maps. Therefore it is essential to develop a useful tool for preliminary delineation of flood extents in urban areas.

Another potential approach for developing flood inundation maps is to focus only on the topography of the region using accurate high-resolution DEM files. A number of environmental disciplines are interested in the development of DEMs. Thus, the availability of new technologies like remote sensing to measure surface elevation (e.g., SAR, GPS, SAR interferometry, radar and laser altimetry) has helped improve the application of DEM-based models. Furthermore, in the last few years the DEM-based automatic characterization and description of hydrological and morphological features (e.g. stream channels, drainage area, valley bottoms, and floodplain identification) has become a fairly standard practice for hydrologists and geomorphologists, substituting time-consuming manual procedures for hydraulic modeling (Manfreda et al., 2011; Nardi et al., 2006, 2008).

In this section, a possible approach by Degiorgis et al. (2012) is outlined for the identification of flood-prone areas and for the hazard grading of datasets from remotely sensed elevation. A number of DEM-derived quantitative features were selected like site elevation and distance from the potential source of flooding, local slope, contributing area, and surface concavity. Figure 24 schematizes the difference between hydraulic simulation and DEM-based flood inundation maps.

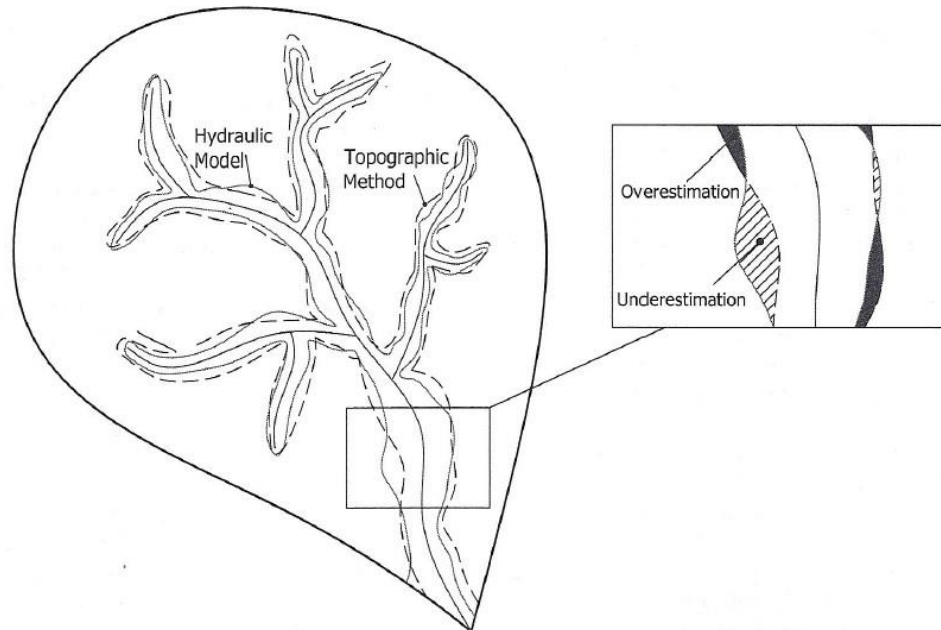


Figure 24 Schematic difference between hydraulic simulation and DEM-based flood inundation maps (Source: Manfreda et al., 2011).

The key objective of this research is to create an accessible and reliable flood inundation map for the development of a composite measure of climate change-related health impacts. For this case, a modified topographic index (TIm) plays an important role in development of a flood inundation map. TIm is a useful and rapid tool which is based on topography of the region and for the preliminary delineation of inundation areas in ungauged basins and areas where detailed hydrological- hydraulic simulation is not available. This efficient method could be very useful for other non-engineering applications including vulnerability analysis, emergency planning and evacuations. For generic planning this method is much faster compared to detailed hydraulic models but it requires to be calibrated using accurate local hydraulic models.

Four different sources of accurate publicly accessible DEM data sets are identified in Figure 19 for use in the development of a flood inundation map. Open source desktop GIS and Python command line utilities were used, including GRASS GIS and related add-on modules (GRASS, 2013a). The method adopted for creating the composite flood map is summarized diagrammatically in Figure 25. DEM files were clipped, transformed and rasterized to a spatial resolution of 25m² using Python command line utilities. The approach then examined

the utility of the modified topographic index (TIm), a technique established by Manfreda et al. (2011) and integrated into the GRASS *r.hazard.flood* add-on extension module. The module outlines the flood inundation area by calculating a TIm from a digital elevation model, and classifies those cells that are greater than a given threshold value when exposed to flooding. Therefore, the delineated flood-prone areas are the result of topographic parameters; the theory is that physical surface characteristics can reveal areas exposed to flood inundation. Land surface is shaped by hydrological processes, and the proposed methodology can help in the quantification of these processes. A full description of how to access the *r.hazard.flood* Python code is available in Appendix A.

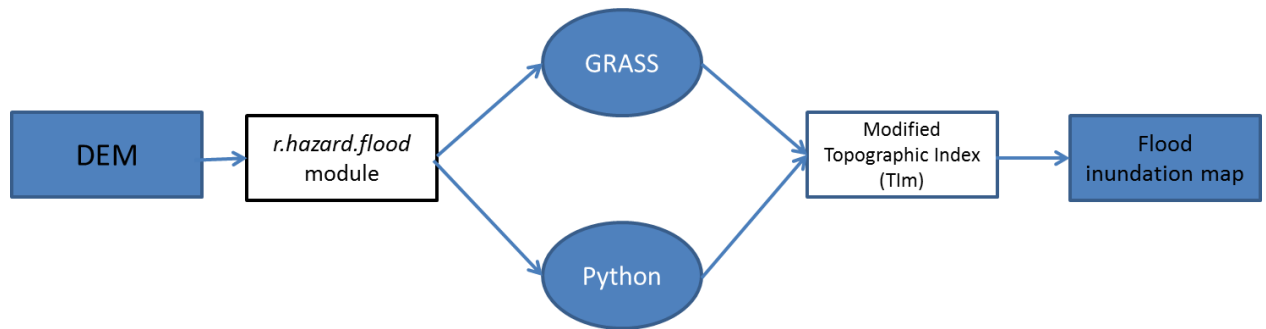


Figure 25 The method adopted for creating the composite flood map.

By comparing available hydraulic models in Amo River basin, Italy, Manfreda et al. (2008) has shown that the topographic index is a good indicator for the delineation of areas exposed to flood inundation. The capability of the approach has been improved through a modification of the topographic index (Manfreda et al., 2008). This new topographic index was calculated by changing the relative weight of the drained area a_d , with an exponent n . This index takes the following equation (Manfreda et al., 2011):

$$TIm = \log \left[\frac{a_d^n}{\tan(\beta)} \right] \quad (6)$$

where a_d^n is drained area per unit contour length (this value depends on the resolution of the DEM); and $\tan(\beta)$ is local gradient.

The *r.hazard.flood* add-on uses parts of the existing GRASS modules to derive TIm and determines a threshold value to generate a flood-inundation map; a_d from *r.watershed* (GRASS, 2013b), which is the drained area per unit of contour length; β from *r.slope.aspect* (GRASS, 2012) output as slope; and n is a function of DEM spatial resolution. The Python code that can be used in GRASS is available in Appendix A.

3.3 Assessing potential human health impacts in urban environment

An important aspect of the vulnerability of any city is human health. Trying to identify an appropriate composite health index for different coastal mega-cities, which will be sensitive to changes on the time scale of disasters, will be the major thrust of this health research. The index developed will act as the health component input to the model being developed to measure resilience, but in addition, the index can be used as a standalone measure to explore which adaptation measure might have the greatest impact during the course of a disaster.

Crude but robust measures such as life expectancy and infant mortality are readily available yet likely not sensitive enough for the purposes of this research. They may, however, prove useful as part of the composite index. A more substantial measure such as the burden of disease, using disability-adjusted life years (DALYs), would give a more complete assessment of public health and can be adapted to accommodate the spectrum of disease encountered in each region.

A composite health measure is proposed that can be applied for assessment of climate change-related health impacts in a variety of coastal mega-cities. The measure developed is based on a number of sources of information which are sensitive to changes in the timing and scale of disasters. Developing this composite health measure is the major research objective of this study.

3.3.1 Years of Life Lost due to premature mortality (YLL)

The YLL metric essentially corresponds to the number of deaths multiplied by the standard life expectancy at the age at which death occurs, and it can be rated according to social preferences. The basic formula for calculating the YLL (Equation 7) for a given cause, age or sex, is (Prüss-Üstün, 2003):

$$YLL = N \times L \quad (7)$$

where N is number of deaths and L is standard life expectancy at age of death (in years).

3.3.2 Years Lived With Disability (YLD)

There are at least two ways of measuring the aggregate time lived with a disability. One method is to take point prevalence measures of disability, adjusting for seasonal variation if present, and express them as an annual prevalence. The alternative is to measure the incidence of disabilities and the average duration of each disability. The product of the incidence and the duration will then provide an estimate of the total time lived with disability. This is the approach used for the DALY (Prüss-Üstün, 2003).

To estimate YLD (Equation 8) on a population basis, the number of disability cases is multiplied by the average duration of the disability and a weight factor that reflects the severity of the disease on a scale from 0 (perfect health) to 1 (dead). The basic formula (without applying social preferences) for one disabling event is:

$$YLD = I \times DW \times L \quad (8)$$

where I is the number of incident cases, DW is disability weight, and L is average duration of the case until remission or death (years).

3.3.3 Disability-Adjusted Life Year (DALY)

The disability-adjusted life year (DALY) is a measure that combines the number of years of healthy life lost due to premature mortality and disability. Traditional assessments of the number of healthy years lost have measured either the number of deaths due to disease, or the disease incidence, but not both, which makes it difficult to compare losses that occur at different ages, or from different causes of ill health. Summary measures of population health, such as the DALY, provide a framework for dealing with these questions. The DALY (Equation 9) measures health gaps as opposed to health expectancies. It measures the difference between a current situation and an ideal situation where everyone lives up to the age of the standard life expectation, and in ideal health. Based on life tables, the standard life expectancy at birth is set at 80 years for men and 82.5 for women. The DALY combines in one measure the time lived with disability and the time lost due to premature mortality (Prüss-Üstün, 2003):

$$\text{DALY} = \text{YLL} + \text{YLD} \quad (9)$$

For the baseline state, it is proposed that each city first divide the city territory into spatial units for which population data is available. The size of a spatial unit will, no doubt, vary from one city to another. It may be based on electoral districts or municipal boundaries etc. depending on how the population is counted and where the best estimates exist. For Metro Vancouver, for instance, there is good Statistics Canada census information based on a number of census tracts or dissemination areas. The population data does not need to be age stratified, total population will suffice. The next step is to convert the population data into a “health” index. A full description of how to access these tables is available in Appendix B.

3.4 Development of a composite measure for estimation of climate change-related human health impacts

Different coastal mega-cities have very different disease profiles, populations and availability of data to use in the development of a baseline state. This methodology is designed to be applied to any city. The comparison of methodology application between different cities can help to define better targeted adaptation policies. A common methodology, even though crude, is recommended to be used to provide a starting point. The inputs can be manipulated and refined as the resilience modeling outputs become available.

Human health impact is considered to be a function of physical factors, disease burden and social vulnerability data. All available data for each city are used as input into a computerized procedure for the computation of a composite human health measure. The results at different location are used to produce an impact map for each year. Additional years of historical data will provide improved opportunities for extrapolation of future health impacts, so putting time and effort into the collection of spatial data in each mega-city is an important and challenging task involved in this kind of spatio-temporal risk assessment.

The process adopted for this study can be sub-divided into four major steps: data collection, data transformation and normalization, data integration, and human health impact mapping.

Data collection. Topography of coastal mega-cities can be obtained from different sources as mentioned in Section 3.1. The social conditions are assessed using three variables: total population, population of people over age 65 and children under age 4. In Canada, this information can be collected from Statistics Canada and is based on census data (Statistics Canada, 2012). Children, Senior, and DALYs can all be based on census population data. The individual spatial data collected pertaining to the social conditions, burden of disease, and physical site conditions can be integrated using the GIS to generate the final human health impact map.

The burden of disease integrates communicable diseases, non-communicable diseases and injuries. WHO defines communicable diseases as: “Infectious diseases caused by pathogenic microorganisms, such as bacteria, viruses, parasites or fungi; the diseases can be spread, directly or indirectly, from one person to another” (WHO, 2008). Also, non-communicable

disease is a medical disorder or disease, which by definition is non-infectious and non-transmissible between people (Lim et al., 2010). The World Health Organization reports non-communicable diseases to be undoubtedly the primary cause of death in the world, representing over 60% of all deaths.

Data transformation and normalization. Raw data is first rescaled by using linear scale transformation methods and then normalized. A number of linear scale transformations exist in the literature (Massam, 1988). The two procedures used here are presented in Equations 10 and 11. For normalizing the data, each raw data point is divided by the maximum value for a given category according to:

$$x'_{ij} = \frac{x_{ij}}{x_j^{\max}} \quad (10)$$

or

$$x'_{ij} = 1 - \frac{x_{ij}}{x_j^{\max}} \quad (11)$$

where x'_{ij} is the normalized score for the i th category and the j th variable, x_{ij} is the variable value, and x_j^{\max} is the maximum value for the j th variable. The normalized data have a range from 0 to 1; the higher the value, the higher the risk. Equation 10 is used when the extent of risk is directly correlated with the variable value (i.e., total population, senior population, children population, communicable and non-communicable diseases, and injuries).

Since the risk of climate change-related hazards is higher where there are higher population densities, equation 10 is also used to normalize the population. Populations which are closer to the maximum population in small spatial regions (eg. dissemination areas) are associated with higher risk, since the normalized value is closer to 1. The same approach is used for other variables.

Equations 12, 13, and 14 are used in calculation of the normalized population (PopN), normalized senior population (SenN), and normalized children population (ChildN), respectively:

$$\text{PopN} = \frac{\text{Pop.}}{\text{Max Pop.}} \quad (12)$$

$$\text{SenN} = \frac{\text{Senior Pop.}}{\text{Max Senior Pop.}} \quad (13)$$

$$\text{ChildN} = \frac{\text{Child Pop.}}{\text{Max Child Pop.}} \quad (14)$$

where Pop is population (number of people) within the dissemination area, Max Pop is the number of people living in the most populated dissemination area of the entire city. Senior Pop is the number of people above 65 years old per dissemination area and Max Senior Pop is the number of seniors living in the dissemination area with the highest senior population in the city. Finally, Child Pop is the number of children (under 4 years old) in the dissemination area and Max Child Pop is the number of children living in the dissemination area with the most children in the entire metropolitan area.

Equations 15, 16, and 17 are used for calculation of normalized communicable (CatIN) and normalized non-communicable diseases (CatIIN), and normalized injuries (CatIIIN) based on the WHO's national DALY tables:

$$\text{CatIN} = \frac{\frac{\text{Pop}}{100,000} * \beta}{\text{Max}(\frac{\text{Pop}}{100,000} * \beta)} \quad (15)$$

$$\text{CatIIN} = \frac{\frac{\text{Pop}}{100,000} * \gamma}{\text{Max}(\frac{\text{Pop}}{100,000} * \gamma)} \quad (16)$$

$$\text{CatIIIN} = \frac{\frac{\text{Pop}}{100,000} * \lambda}{\text{Max}(\frac{\text{Pop}}{100,000} * \lambda)} \quad (17)$$

where Pop is the total number of people in the dissemination area and β is the communicable DALY rate for the country. γ is non-communicable DALY rate and λ is injury DALY rate (e.g. for Canada β is 601, γ is 920, and λ is 920).

If the measure is of the minimization type (i.e., the lower the value, the higher the risk, as in the case of ground elevation), Equation 11 is used in the normalization process. The normalized value of the ground elevation (DEM) is calculated according to Equation 18:

$$\text{DEM} = 1 - \frac{\text{Elevation}}{\text{Max Elevation}} \quad (18)$$

where Elevation is the elevation of each pixel (in meter), and Max Elevation is the highest elevation point in entire metropolitan area.

Data integration. The integration is performed on two levels. First, nonphysical health impacts are integrated into one map using Equations 12 to 17 which is then integrated with the map of physical health impacts. The following general equation (Equation 19) is used to integrate all the available data:

$$\text{HIM} = \alpha_1 (\sum_1^n W_i * \text{NP}_i) + \alpha_2 (\sum_1^m W_i * P_i) \quad (19)$$

where NP is the representation for nonphysical data, W_i is the weight of each variable considered, P_i is the available physical data, and α_1 and α_2 are weights associated with non-physical and physical data inputs, respectively. Introduction of a double weighting scheme allows for active participation of decision makers in the development of a human health impact map. Selection of different weights can be used to (a) represent different preferences of decision makers and (b) assess the impact of each weighting section on the final value of the human health impact.

By using the general integration format presented in Equation 19, health impact map developed for Metro Vancouver and it is a function of NDVI, FEM, DEM, and NPHIM (Equation 20). Therefore, a weighting system based on the governance priorities needs to be assigned.

$$\text{HIM} = 0.25(a_1 \text{NDVI} + a_2 \text{FEM} + a_3 \text{DEM} + a_4 \text{NPHIM}) \quad (20)$$

Where HIM is health impact map, NDVI is Normalized Difference Vegetation Index, FEM is flood inundation map, DEM is digital elevation map, and NPHIM is nonphysical health impact map.

Human health impact mapping. After transforming and normalizing all of available inputs, the weighting procedure can be easily implemented in the GIS environment before the integration. The resulting map provides an integrated view of population health for this region, information that may help in developing more targeted adaptation and risk reduction strategies at a local level. Empirical applications suggest that the weighting method is one of the most effective techniques for spatial decision making involving GIS based approaches (Malczewski et al., 1997).

3.5 Spatio-temporal interpolation and extrapolation

One of the key contributions of this research is in applying spatio-temporal models to extrapolate future health impacts which can be displayed visually using a map. This single outcome provides a useful tool for development of future adaptation and mitigation policies. By considering both physical and nonphysical spatial data, this methodology can provide a much more robust outcome for health impacts on different coastal mega-cities all over the world. Limitations in the availability of spatio-temporal data will, of course, reduce the quality of the outcome. Unfortunately there are different techniques and procedures for the collection spatial data all over the world. Even in one particular location, there are often significant changes in the resolution and quality of historical data in different years. As such, it is essential to apply spatial interpolation for the lower resolution data to ensure a consistent spatial resolution among all data points. Once all data are on the same scale, extrapolation of the results to represent future conditions is possible. In this section, kriging, which is a popular method for spatial interpolation, is presented. Following, a spatio-temporal Auto Regressive (AR) extrapolation scheme is presented.

3. 5.1 Kriging spatial interpolation

Interpolation is the process of estimating and valuing the unknown data values for a specific location using known data values from other locations. In many examples the assessment of continuous field data is preferred; however the only available data values are for the finite number of points. It therefore becomes essential to interpolate and estimate the values for the locations of interest.

Most interpolation methods can be divided into two types called global and local. Global interpolators use all of the existing data to deliver estimates for the points with unknown values; local interpolators use only the data in the neighborhood of the points being estimated. Global interpolation is often used to remove the effects of major trends before using local interpolators to analyze the residuals. Kriging technique is a specific type of local interpolation.

Kriging is a form of local interpolation using geostatistical methods, developed by French geostatistician Georges Matheron and the South African mining engineer D. G Krige (Krige, 1951). Kriging is a local, exact and stochastic method. It provides a number of advantages:

1. Given enough data, kriging creates better estimates than the other methods because the method considers the effects of random noise.
2. Kriging can provide an indication of the reliability of the estimates.

Kriging weights the surrounding measured values to derive a prediction for an unmeasured location. The general formula essentially uses a weighted sum of the data (Webster and Oliver 2007):

$$\hat{Z}(X_0) = \sum_{i=1}^N \lambda_i Z(x_i) \quad (21)$$

Where:

- $\hat{Z}(X_0)$ is the measured value at the i th location
- λ_i is an unknown weight for the measured value at the i th location; To certify the estimate is unbiased the weights are made to sum 1.

$$\sum_{i=1}^N \lambda_i = 1 \quad (22)$$

- x_i is the prediction location
- N is the number of measured values

And the expected error is $E [\hat{Z}(X_0) - Z(X_0)] = 0$. The estimation variance can be derived from Equation 23:

$$\text{var}\hat{Z}(X_0) = [E \{\hat{Z}(X_0) - Z(X_0)\}^2] = 2\sum_{i=1}^N \lambda_i \gamma(x_i, x_0) - \sum_{i=1}^N \sum_{j=1}^N \lambda_i \lambda_j \gamma(x_i, x_j) \quad (23)$$

where $\gamma(x_i, x_j)$ is a semivariance of Z between the data points x_i and x_j , and $\gamma(x_i, x_0)$ is the semivariance between the i th data point and the largest point x_0 . In the more general case Z may wanted to be estimated in a block B , which may be a line, area, or a volume subject to whether it is in one, two or three spatial dimensions.

In the kriging method, the weights are based on the distance between the measured points and the prediction location, and also on the overall spatial arrangement of the measured points. Quantification of the spatial autocorrelations is required. In ordinary kriging, the weight, λ_i , depends on a model fitted to the distance, to the prediction location, the measured points, and the spatial relationships between the measured values around the prediction location. This section discusses how the general kriging formula is used to create a prediction map.

There are two important tasks that need to be considered in making a prediction with the kriging interpolation method:

- Uncover the dependency rules.
- Make the prediction.

To understand these two tasks, kriging goes through a two-step process:

1. It creates variograms – In spatial statistics the hypothetical variogram is a function describing the degree of spatial dependence of a spatial random field or stochastic process). Variograms are defined as the variance of the difference between field values at two locations (and) across realizations of the field (Cressie, 1993) and covariance functions are used to evaluate the statistical dependence (spatial autocorrelation) from a model of the autocorrelation (fitting a model).
2. It calculates the unknown values (making a prediction).

Because of these two separate and different tasks it has been said that kriging uses the data twice: the first time to estimate the spatial autocorrelation of the data and the second to make the predictions (Cressie, 2011).

Spatial modeling or fitting a model is known as structural analysis, or variography. In spatial modeling of the structure of the measured points, you begin with a graph of the empirical semivariogram, computed with the following equation for all pairs of places parted by distance h (ESRI 2015):

$$\text{Semivariogram (distance}_h) = 0.5 * \text{average}\{(value_i - value_j)^2\} \quad (24)$$

The difference squared between the values of the paired locations should be calculated using this formula. The image below presents the pairing of one point (the red point) with all other measured locations and this process should be continued for each measured point.

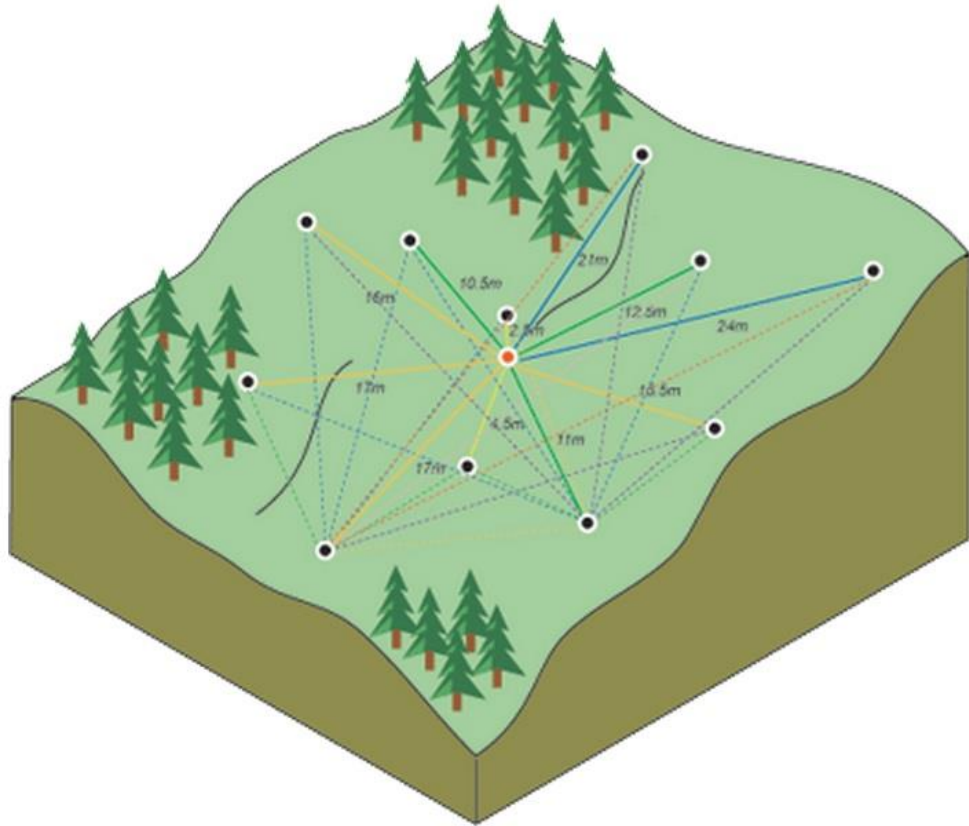


Figure 26 Calculating the difference squared between the paired locations (Source: Esri, 2015).

Each pair of locations has a unique distance, and there are often several pairs of points. It is unmanageable to plot all pairs quickly. Instead of plotting each individual pair, the pairs need to be grouped into lag bins. As an example, computation of the average semivariance for all pairs of points that is bigger than 40 meters but less than 50 meters is one lag bin. The empirical semivariogram is a graph of the distance (or lag) on the x-axis and the averaged semivariogram values on the y-axis (Figure 27).

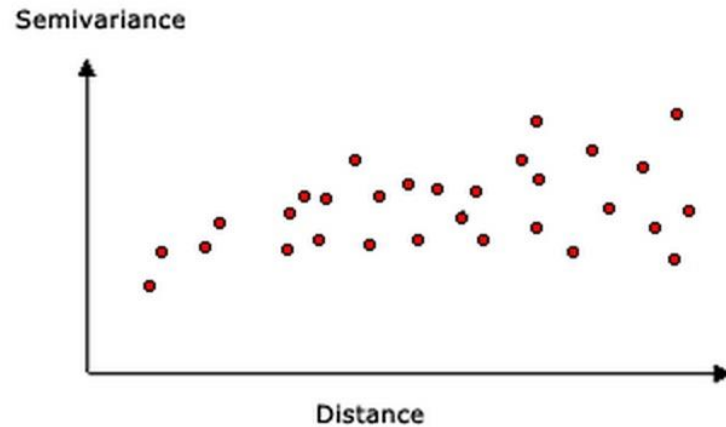


Figure 27 Empirical semivariogram graph example (Source: Esri 2015).

Spatial autocorrelation measures a simple principle of geography: things that are closer are more comparable than things farther apart. Accordingly, pairs of locations that are closer (far left on the x-axis of the semivariogram cloud) have more comparable values (low on the y-axis of the semivariogram cloud). As pairs of locations become farther away from each other they move to the right on the x-axis of the semivariogram cloud. The differences between the values should increase and so should their squared difference, causing them to move up on the y-axis of the semivariogram cloud (Oliver, 1990).

In different cities, for the composite spatio-temporal health impact assessment, various sources of spatial data need to be considered for increasing the accuracy of final results. Therefore applying such a spatial interpolation is a mandatory procedure that needs to be done before any integration of different spatial data.

When all the spatial data are in the same format and resolution, integration can be performed to generate the spatial climate change-related health impact assessment. This method needs to be applied for as many years as the historical spatial data is available. When there is a set of spatial health impact assessments for one specific city for different years (e.g. 1980 to 2010), then the extrapolation of a health impact map is possible based on different spatio-temporal methods. The next section presents a potential model that can be used for this extrapolation.

3.5.2 Spatio-temporal auto regressive extrapolation model

In this research, linear regression and auto regressive method is utilized for spatio-temporal extrapolation of the health impact maps to future time periods. This method is capable of being implemented on different spatial data in GIS and MATLAB (linear regression and AR toolbox) environment.

Regression modeling estimates a dependent variable with n observations $\mathbf{y} = (\mathbf{y}_1, \dots, \mathbf{y}_n)'$ to a set of p independent variables $x_j = (x_{1j}, \dots, x_{nj})'$ by a linear function (de Espindolaa, 2014),

$$y = \sum_{j=1}^N \beta_j x_j + e = X\beta + e \quad (25)$$

where X is the proposed matrix that has x_{ij} on row i and column j . The regression coefficient vector β is normally assessed by minimizing the residual sum of squares.

Auto regressive (AR) models (Cressie and Wikle, 2011) delineate the residual process $y - X\beta$ to follow an autoregressive procedure as follows:

$$y - X\beta = B(Y - X\beta) + v \quad (26)$$

which can be rewritten as

$$Y = X\beta + (1 - B)^{-1}v \quad (27)$$

where v follows a zero-mean normal distribution with covariance matrix $\sigma^2 I$ (i.e., is independent), and B defines which residuals are correlated, and to which degree (de Espindolaa, 2014). Usually, B is sparse, and $B_{ii} = \text{zero}$, and non-zero values (B_{ij}) happen only when Y_i and Y_j are neighbors and next to each other. Moreover, it is assumed that the non-zero values of B have a single value, which is the parameter that describes the degree of autocorrelation. This value will be called λ and for any non-zero B_{ij} cells i and j are neighbors and $B_{ij} = \lambda$. In order to define spatial neighbors, the queen neighbors method have been used which means the 8 cells adjacent (Figure 28) to each grid cell, or less in the case of missing valued (or masked) pixels or boundary cells in the neighborhood.

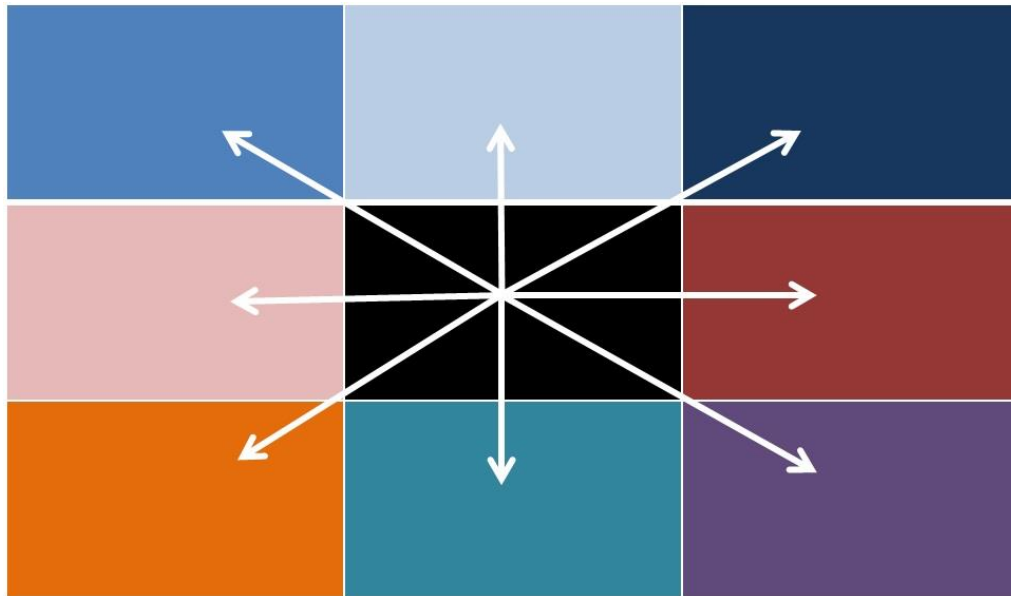


Figure 28 Queen neighbours, which are defined as the 8 cells adjacent to each grid cell.

The spatio-temporal regression model considers $Y[t] = (y_{1,t}, \dots, y_{n,t})$ as the observation in grid cell i and time step $t \in \{1, \dots, m\}$. As a first step from spatial AR models to spatio-temporal AR models, the spatial AR outcome of the residuals is calculated using a temporally lagged observation $y_{[t-1]}$, as in

$$y_{[t]} = X\beta + \gamma y_{[t-1]} + (I - B)^{-1}u, \quad t = 2, \dots, m \quad (28)$$

where B is spatial neighbors only and it called model 1.

The AR model (model 1) is then quantified for all time steps, but the B matrix not only addresses spatial neighbors $y_{i,t}$ and $y_{j,t}$ with $i \neq j$, but also the two temporal neighbors of $y_{i,t}$, $y_{i,t-1}$ and $y_{i,t+1}$ (de Espindolaa, 2014). An assumption here is that a single autocorrelation coefficient defines the correlation both in space and time and is called model 2.

The third model, extends model 2 with spatio-temporal neighbors, i.e. residuals $y_{i,t}$ and $y_{j,t+1}$ are linked when grid pixels i and j are neighbors. Once more, a single correlation coefficient

is fitted to define correlations among all (spatial, temporal, and spatio-temporal) neighbors. Figure 29 presents the different neighbors defined in models 1, 2 and 3.

Regressions can also be applied with the R function `spautolm` in R package `spdep` (Bivand et al., 2008), but before applying `spautolm`, generated health impacts maps need to be converted into matrices in MATLAB. This function provides maximum likelihood estimation of β and λ , but does not at the same time estimate λ , γ and β using maximum likelihood (Cressie and Wikle, 2011). One solution to this would be to describe neighbors in space and time, and use weighting factor to defines how neighboring in space relates to neighboring in time. The R function `spautolm` in R package `spdep` is presented in Appendix F.

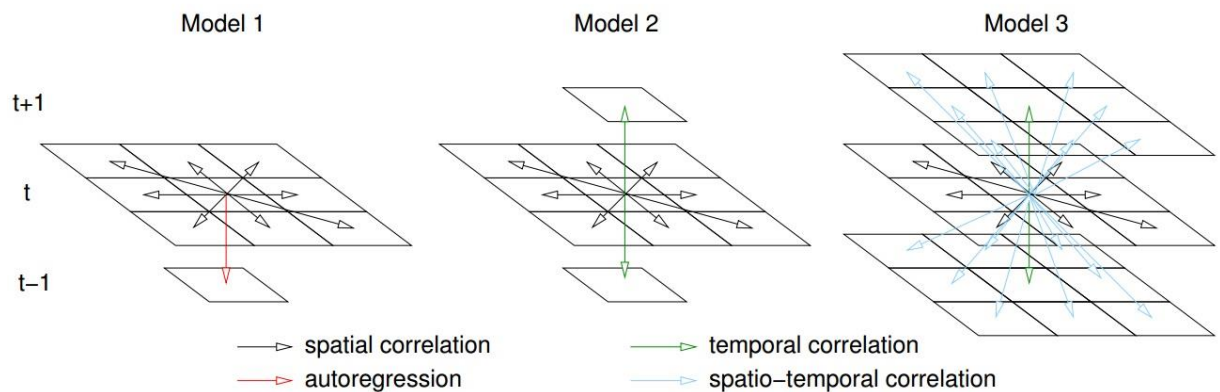


Figure 29 Neighbours addressed for models 1, 2 and 3 (Source: de Espindolaa, 2014).

Chapter 4

4. Case study

Over the 20th century the average global air temperatures has increased by 0.74°C, and the reality of climate change is now unquestionable. The average temperature in British Columbia, Canada, has increased by 1.1°C in 20th century and these temperature increases have been accompanied by changes in precipitation, and increases in the frequency and intensity of extremes events such as droughts, heavy precipitation events, tropical storms and heat waves (Fraser Basin Council, 2013).

Sea level rise is one of the key climate-related impacts that humans will have to adapt to. It occurs as a result of glacial melt associated increasing temperatures, and can also be attributed to thermal expansion of the oceans. Future sea level rise is dependent on a large number of elements and uncertainties, and is very difficult to forecast. The Intergovernmental Panel on Climate Change (IPCC) estimated in its 2013 assessment report that sea levels would increase by 18 to 59 cm by 2100. However, these estimates did not include the possibility of movement or calving of large ice sheets and very rapid warming trends have been observed in the Arctic in recent years. In 2010, the US National Research Council projected that sea level rise over the 21st century would be between 56 and 200cm.

River flooding is another significant climate-related impact. There is a clear relationship between climate change and the increased severity and frequency of flooding events globally. Changes in winter temperatures and precipitation amounts are altering the severity and timing of spring flooding, and increasing extreme precipitation events are linked to an increase in flooding (Fraser Basin Council, 2013). The impacts of sea level rise, storm surges and river flooding are not independent and they need to be considered together, and solutions should address all of these factors.

The province of British Columbia has a population of 4,400,057 and 80% of this population lives within 5 km of the coast (Agam, 2014). Most of the province's population lives in the Lower Mainland (also known as Metro Vancouver). Over 4,600 hectares of farmland and over 15,000 hectares of industrial and residential areas in the Lower Mainland are located within 1 m above sea level (The Arlington Group Planning and Architecture Inc., 2013).

4.1 Study area

The scope of the study area is Metro Vancouver, British Columbia, Canada (shown in Figure 30). Metro Vancouver has a moderate oceanic climate (Kottke et al., 2006). The summer months are typically dry, often resulting in moderate drought conditions, usually in July and August and the rest of the year is rainy, particularly between the months of October and March. The annual average temperature in Metro Vancouver is 11.0 °C which is amongst the warmest in Canada. Metro Vancouver is Canada's third rainiest city, receiving about 1457 mm of precipitation per year. By comparison in North Vancouver, a municipality on the north shore of Metro Vancouver, the amount of precipitation received almost doubles to 2477 mm per year as measured at the base of Grouse Mountain (Osborn, 2015).

Metro Vancouver is located in the Fraser River basin. The Fraser River is the longest river in British Columbia, rising at Fraser Pass near Mount Robson in the Rocky Mountains and flowing for 1,375 kilometers, into the Strait of Georgia at Metro Vancouver (Consultants, 2008). The Fraser River drains an area of 220,000 km² with an annual discharge of 112 km³ (3550 m³/s), and it discharges more than 20 million tons of sediment into the ocean annually (Cannings, 1996).

Metro Vancouver includes 21 municipalities (see Table 4, Figure 30), one Electoral Area and one Treaty First Nation that collaboratively plan for and deliver regional-scale services. Municipalities located along the coastline or the Fraser Delta may be vulnerable to sea level rise and flooding. Over the last several decades, Metro Vancouver has experienced a significant level of socioeconomic development. In that period, Metro Vancouver economic expansion has exceeded the federal average. As a consequence, according to census information (Statistics Canada, 2012), employment in Metro Vancouver reached 1.1 million in 2006, representing the fastest pace of job growth among Canada's three largest metropolitan areas. Rapid socioeconomic development has been shadowed by two parallel trends that directly affect local natural resources: considerable population growth and rapid urbanization. The population in Metro Vancouver has increased from 1,169,831 in 1981 to 2,476,328 in 2011, rising by over 100%, as shown in Figure 31 (Statistics Canada, 2012). The regional district has a land area of about 2,883km², with a population density of 856.2 people/km² (Statistics Canada 2012).

Table 4 Metro Vancouver municipalities.

Anmore	Coquitlam	Langley Township	New Westminister	Port Coquitlam	Tsawwassen
Belcarra	Delta	Lions Bay	North Vancouver City	Port Moody	Vancouver
Bowen Island	Electoral Area A	Maple Ridge	North Vancouver District	Richmond	West Vancouver
Burnaby	Langley City	Abbotsford park	Pitt Meadows	Surrey	White Rock

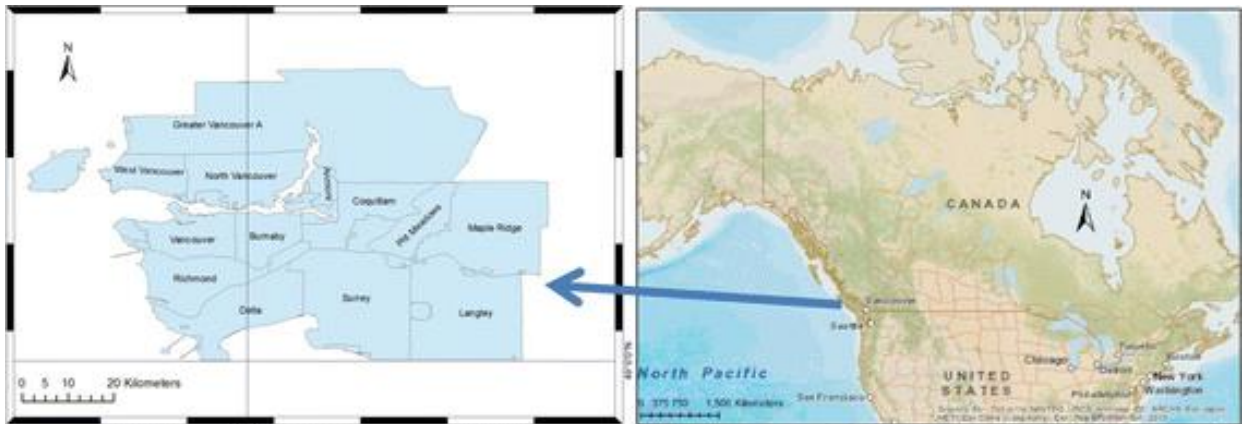


Figure 30 Metro Vancouver in the province of British Columbia in Canada.

The Fraser River is the largest river on the west coast of Canada, draining approximately one quarter of the area of British Columbia. Climate change has the potential to increase flooding

in the Fraser River which will directly impact some of the communities in Metro Vancouver (Owringi et al., 2014). The leading cause of inland floods is heavy rainfall, but floods can also result from snowmelt and dam-break flows. Intense precipitation may also cause standing water to accumulate in urban areas, as the capacity of drainage is exceeded (UN/ISDR, 2004).

Vancouver is exposed to multiple types of hydro-meteorological climate hazards including storm surges, tsunamis, sea-level rise, and coastal and riverine flooding. Urbanization and climate change will intensify the problems associated with these hazards in urban coastal mega-cities as the frequency and magnitude of events increases. Changes in the physical system have direct and indirect impacts on economic, social, health and organizational activities (Peck and Simonovic 2013). For instance, consider flood hazard. Riverine flooding directly affects water quality, which in turn may affect the health of a population and therefore impact the economy. Some areas within a city may experience greater impacts than others based on the magnitude of hazard (Peck and Simonovic, 2013).

In the OECD 2012 report on sustainable development challenges, Vancouver was rated 15th for exposed assets, with USD \$55 billion at risk, and the city rated 32nd in terms of population at risk, with 320,000 people exposed to the negative impacts of climate change. Vancouver's coastal infrastructure at risk includes highways, sewer systems, wastewater treatment facilities, shipping and ferry terminals, and Vancouver's international airport.

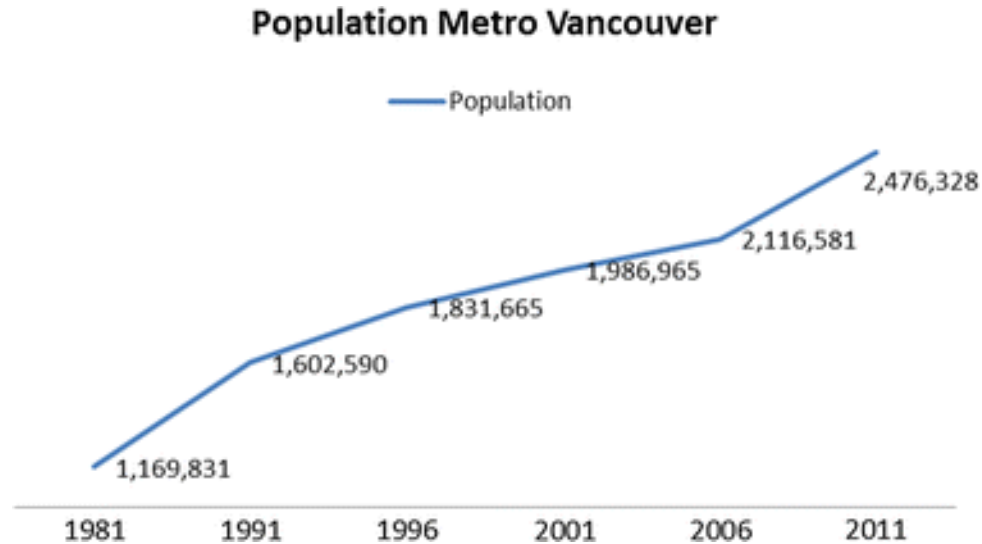


Figure 31 Population growth in Metro Vancouver.

4.2 Land-use

More than 50% of the world's population lives in urban areas (UNPD, 2009). In developed countries urbanization levels typically exceed 75%; in Canada around 80% of the population lives in urban regions (Statistics Canada, 2006).

Metro Vancouver is home to approximately 2.4 million people. The metropolitan region is located along the delta of one of Canada's largest rivers, the Fraser, and contains fertile agricultural land, forested mountains, and coastal shores with salmon, crab, and other fisheries. The region's main economic activities include: tourism, business services, agriculture, and manufacturing (BC Stats, 2010). The economy is mainly technical and other services, with the majority of business employment in the fields of public administration, private services, retail trade and construction (BC Stats, 2010). According to the literature Vancouver's consumption practices are characteristically first-world: urban, rapacious, and addicted to growth (Berelowitz, 2005; Rees, 2009). The majority (57%) of the region's population is between the ages of 25 and 64 years old with a labor force sharing rate of 67%. Within this age group 65% have some type of post-secondary education qualification (BC Stats, 2010).

Residential development occupies almost 15% of the metropolitan area and industrial, commercial and institutional uses occupy around 9% of the area. Roads and utility right-of-ways account for 8% of the area and 9% is unoccupied, meaning it is zoned for development but has not been developed to date. Around 60% of the area is protected in the “Green Zone” including: watersheds, agricultural land, natural and recreational areas (Vancouver, 2006).

There are three coastal mountain watersheds from which the region derives its drinking water supply and five wastewater treatment facilities. There are two municipal solid waste landfills (one of which is located 500 km outside the region) and an incinerator that works for a waste-to-energy facility supplying electricity back to BC Hydro which is the provincial electrical utility (GVTA, 2002). Regional transportation services include six subsidiary companies providing: 1) a regional elevated light-rapid rail system known as Sky Train, 2) a local car ferry, 3) an inter-regional commuter rail service, 4) Air Care vehicle emissions testing facilities, and 5) in-city bus and SeaBus service (GVTA, 2002).

4.3 Sea level rise and flood history

Vancouver’s history includes a number of disaster events that were caused by sea level rise, storm surges and flash flooding. The two most significant events of this type are the October 12th, 1962 landfall of Typhoon Freda and the February 4th, 2006 storm surge event that affected the Corporation of Delta. Figure 32 provides a timeline of historical extreme weather events in Metro Vancouver (Forseth, 2012).



Figure 32 Timeline of sea level rise storm surge and flash flooding events that affected Metro Vancouver between 1962 and 2012 (Forseth, 2012).

Using sea level measurements at the Point Atkinson tide gauge, the highest recorded levels are considered to be potential dates for sea level flooding. Based on the records, there were 7 sea level flooding events between 1960 and 2011. Three of these events caused major flooding and damage. Events on December 16th, 1982 and February 4th, 2006 both indicated damages of around \$2,000,000+ (in 2011 Canadian Dollars). The concurrence of the damage estimates shows that this may be a fair estimate of the current vulnerability of Metro Vancouver to sea level flooding.

Sea level flooding has affected many parts of Metro Vancouver in the past, including: the District and City of North Vancouver, the Corporation of Delta, the City of Vancouver, the District of West Vancouver, the City of Surrey, and the City of Richmond. The Corporation of Delta incurred the majority of the damages reported above and experienced flooding in 6 of the 7 events affecting Metro Vancouver as a result of its low elevation.

Subjective data helps put Metro Vancouver's vulnerability to sea level flooding into context. Figure 33 shows the vulnerability to flooding in Ladner as far back as 1895. Photographs of flooding in 1977 show the Kitsilano Pool inundated with sea water. Records of flooding in 1967 provide descriptions of flooding at Ambleside Beach, Water Street in Downtown Vancouver, and the effects on nearly every Metro Vancouver municipality exposed to the sea (Forseth, 2012).



Figure 33 Historic vulnerability with flooding in Ladner as far back as 1895 (Source: Forseth, 2012).

Chapter 5

5. Results

As described in the previous sections, this research aims to estimate the spatial distribution of climate change-related impacts on human health in an coastal urban environment and uses the information to develop a time series of maps that represent changing conditions and impacts. This chapter presents the outcomes from implementation of the methodology described previously to Metro Vancouver, British Columbia, Canada.

The size of Metro Vancouver is 2,877 square kilometers. This is a large area with remarkably variable terrain that boasts mountains, ocean and riverine shorelines. In order to consider such a wide-spread and variable terrain and its interface with complex river and ocean dynamics, the metropolitan area has been divided into six study zones as shown in Figure 34. This helps to assess the results for different approaches. For example: what is observed, why the generated results can help, what are the limitations associated with a particular approach, and how these results dovetail with the overall thesis goal.

Zone 1 refers to the sparsely populated region north and west of the city. Zone 2 refers to the most populated area of Metro Vancouver including the City of Vancouver, south part of North Vancouver and West Vancouver, and the north part of Richmond (which includes the airport). Zone 3 is the central part of the metropolitan area: Burnaby, the north part of Surrey, Coquitlam and the western portions of Pitt Meadows. Zone 4 includes newly developed portions of Maple Ridge, the east part of Pitt Meadows and the city of Langley. Zone 5 refers to the coastal and central part of Richmond and the corporation of Delta. Finally, zone 6 refers to the city of Surrey and its portion of the coast.

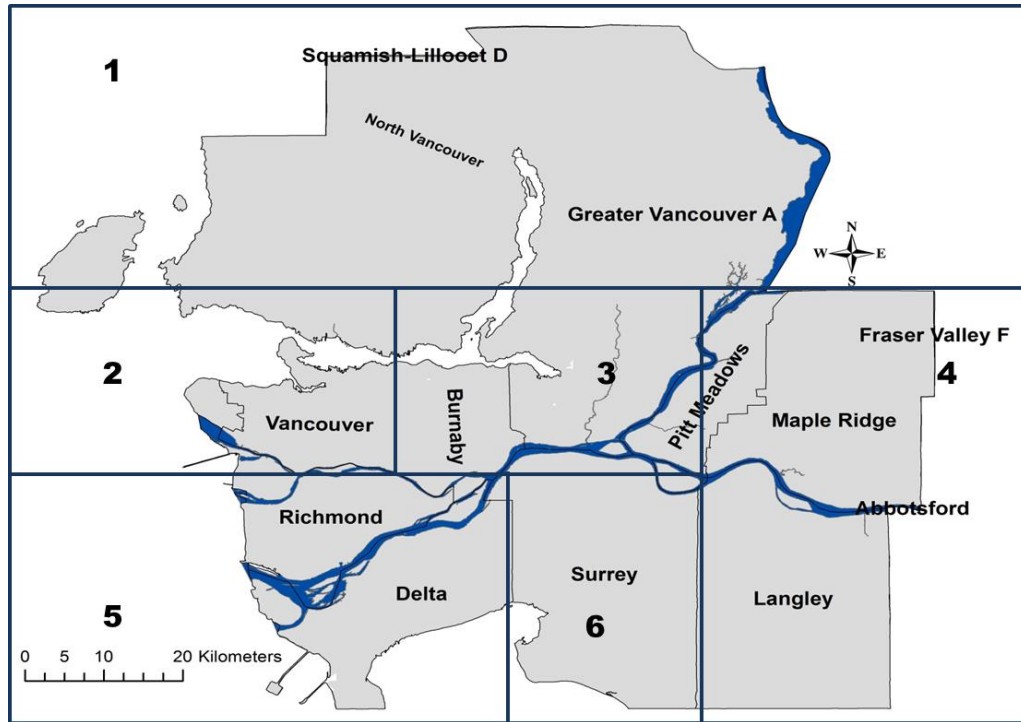


Figure 34 Proposed zones for detailed discussion of the results.

The rest of this chapter is organized as follows: The first section will present the results regarding land use change and vegetation analysis between 1984 and 2012; In section two the use of open source spatial software for developing a flood inundation map (in particular: GRASS) is described; In section three, results pertaining to different spatio-temporal variables involved in the nonphysical health impact map are presented. Section four describes the results of mapping climate change-related health risks for integrated city resilience modeling. The fifth section contains the results of the human health impact map extrapolation.

5.1 Land-use change and vegetation analysis

In order to study the land-use cover in Metro Vancouver, 10-day composite NDVI data are derived from the sensor VEGETATION on board the SPOT satellite platform which was assimilated from “Vlaamse Instelling Voor Technolo-gish Onderzoek” (SPOT-VGT 2011)

for 1998–2012. NOAA-AVHRR images have been used for 1984–1997. The SPOT-VGT S10 (10-day composite) NDVI composites have a spatial resolution of 1 km² and are derived from primary SPOT-VGT products; the composites were corrected for reflectance, scattering, water vapor, ozone and other gas absorption using the procedures described by Achard et al. (1994) and Duchemin (2000) in the ENVI environment. Appendix E provides more detail about how the remotely sensed data have been used in this study.

Using ENVI software, geometric corrections for all the images were performed in two stages using ephemeris data and ground control points. In the ground control point method, polynomial transformation was employed and root mean square (RMS) error values averaged around 0.8 pixels. The resulting images had a nominal spatial resolution of 1.1 km².

During each year of the study, images were collected from the same 10-day period for August, and the ones that had the least cloud contamination were selected to produce NDVI images. From these images, 10-day maximum NDVI monthly composites were subsequently generated. In order to validate SPOT-VGT maps, they were later compared to similar NOAA-AVHRR NDVI maps. After validating the NDVI images, min/max NDVI and long-term NDVI images were obtained based on maximum value composite (MVC) using ENVI software.

As previously mentioned, preprocessing was applied to the input data in order to obtain the 10-day NDVI images. Figure 35 shows the vegetation conditions in Metro Vancouver for the years 1984, 1991, 1995, 2000, 2005 and 2012 and Figure 36 and 37 present the vegetation condition for 1984 and 2012 separately. All the generated vegetation condition maps are available in Appendix C. NDVI varies between -1 and 1. A value closer to 1 represents a higher percentage of vegetation cover. A significant decrease in vegetation is visible in the central and eastern parts of the city in the last 28 years.

A vegetation condition analysis using remotely sensed data has not been previously applied to Metro Vancouver. Based on the obtained results there has been a significant change in land-use in the metropolitan area. Based on the zones defined in the first part of this chapter, it is clear there is no significant change in vegetation conditions in zone 1. This zone covers mainly the northern part of the city which is a sparsely populated residential area with

mountainous terrain. In zone 2 the land-use change is not that significant because the majority of Vancouver's population was already settled in the 80s and 90s. Most of the land-use change in this zone happened in the southern parts of North Vancouver and West Vancouver. In zones 3, 4, and 6, a higher rate of vegetation decrease is observed due to urbanization. For example in the city of Surrey there has been a significant change in land-use over the last 30 years and the population has increased notably. The population of Surrey has increased from 147,138 in 1981 to 468,251 in 2011. This population growth has severely influenced the vegetation cover of the region. Urbanization leads to increased impermeable ground cover (asphalt and concrete) which causes an increase in runoff and flooding, as we've often remarked in this document; climate change-related precipitation extremes amplify this problem. For zone 5, which includes mainly Richmond and Delta, the land-use change was not as drastic as in the eastern side of the metropolitan area but land-use management is still an essential issue in this zone.

Figure 38 shows vegetation trends between the years 1984 and 2012. From 1984 to 1997, NOAA-AVHRR images are used; from 1998 to 2012, SPOT-VGT sensor data. There are a few extreme drops in vegetation condition in the years 1991, 2002 and 2005 that are caused by cloud contamination of the images.

There are always limitations with any types of land-use change assessment. For this research there are two major limitations: Firstly, high resolution images were unavailable and secondly, there were no noise-free images from prior to 1984.

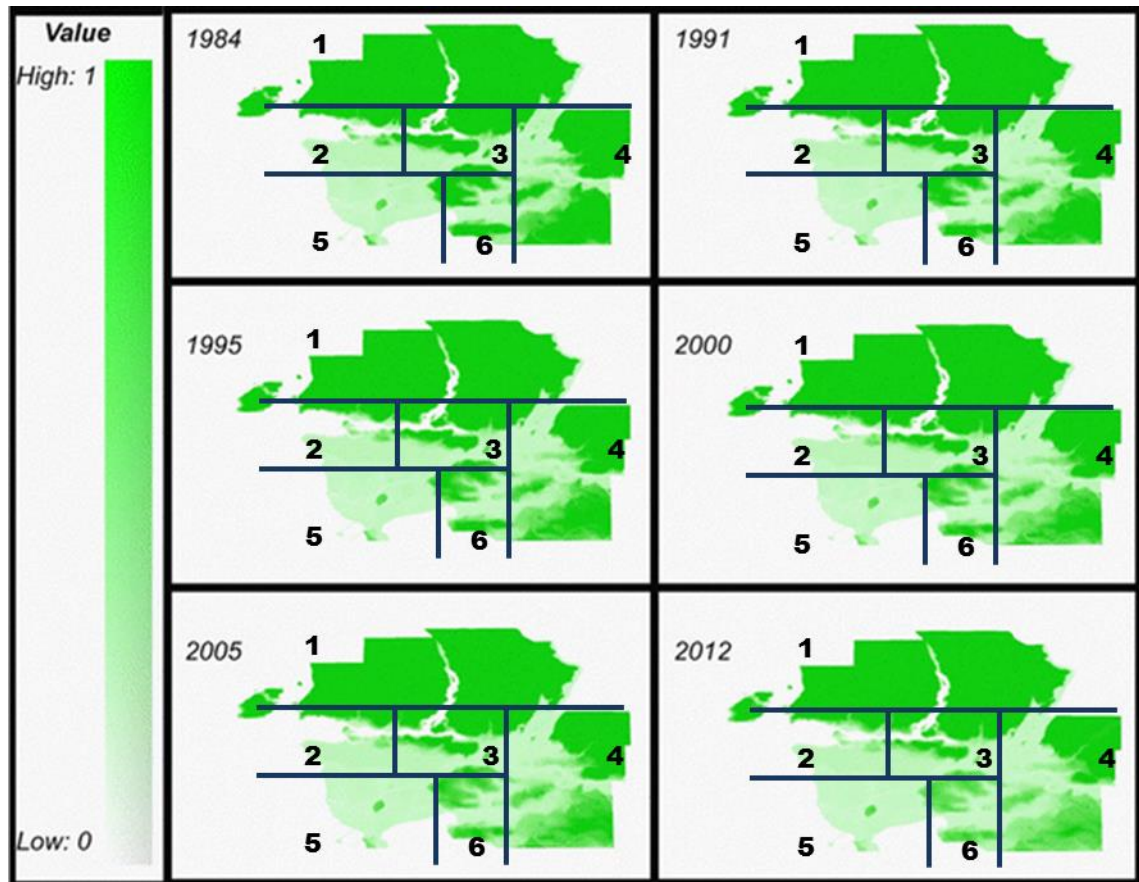


Figure 35 Vegetation condition for Metro Vancouver for the years 1984, 1991, 1995, 2000, 2005 and 2012 (Source: Owrangi et al., 2014).

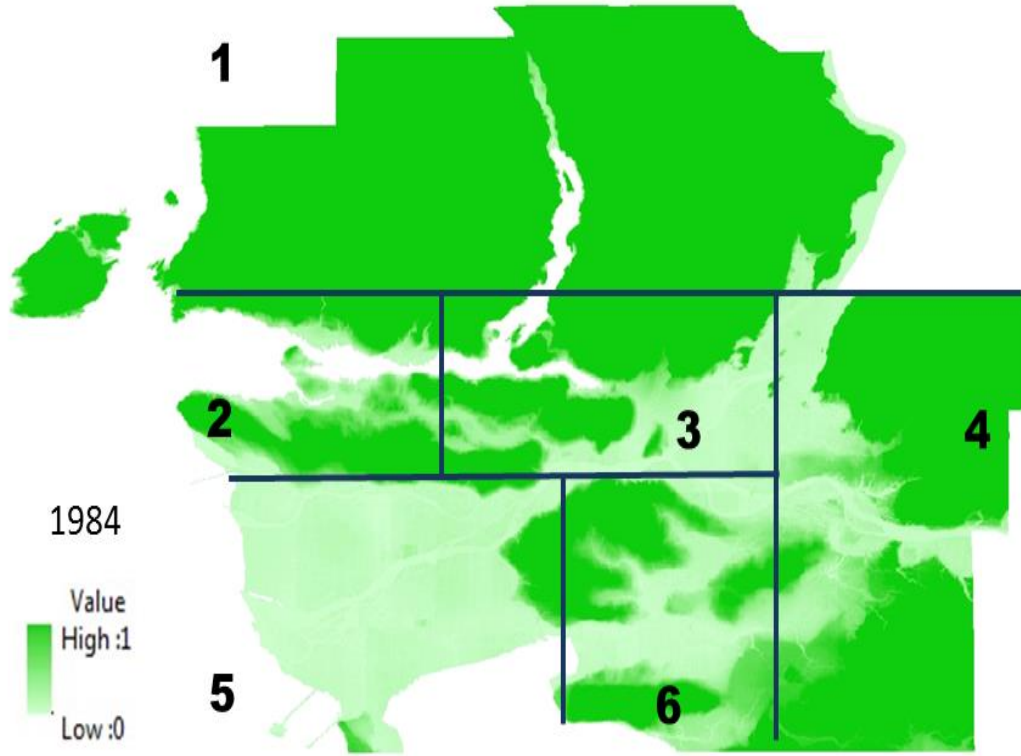


Figure 36 The vegetation condition for Metro Vancouver for 1984.

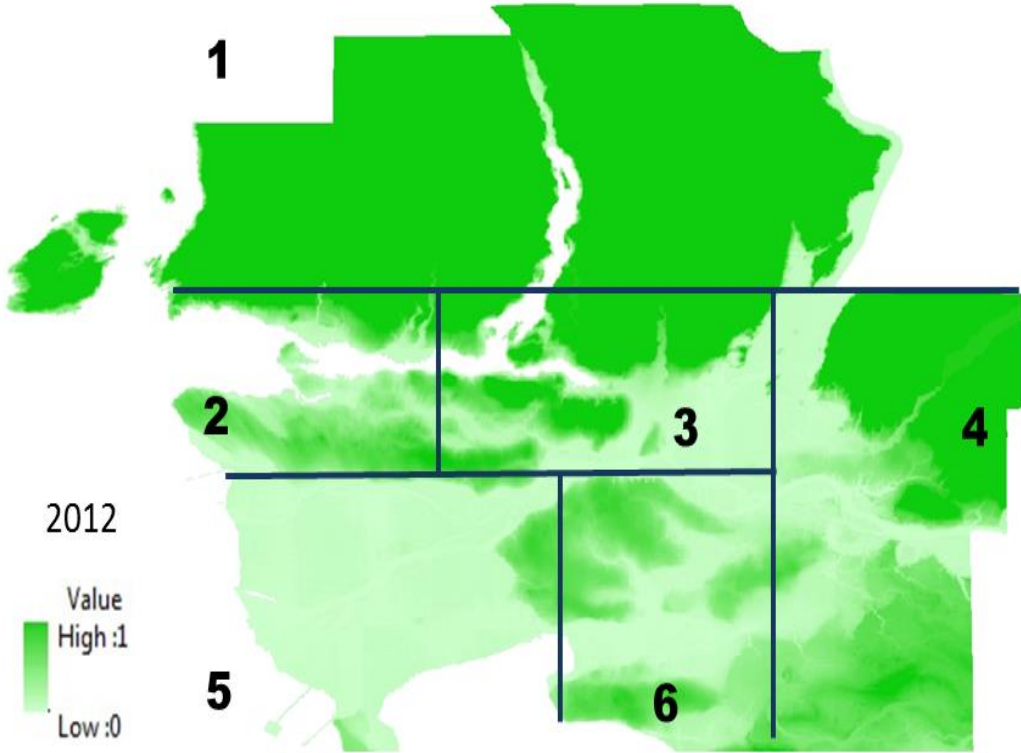


Figure 37 The vegetation condition for Metro Vancouver for 2012.

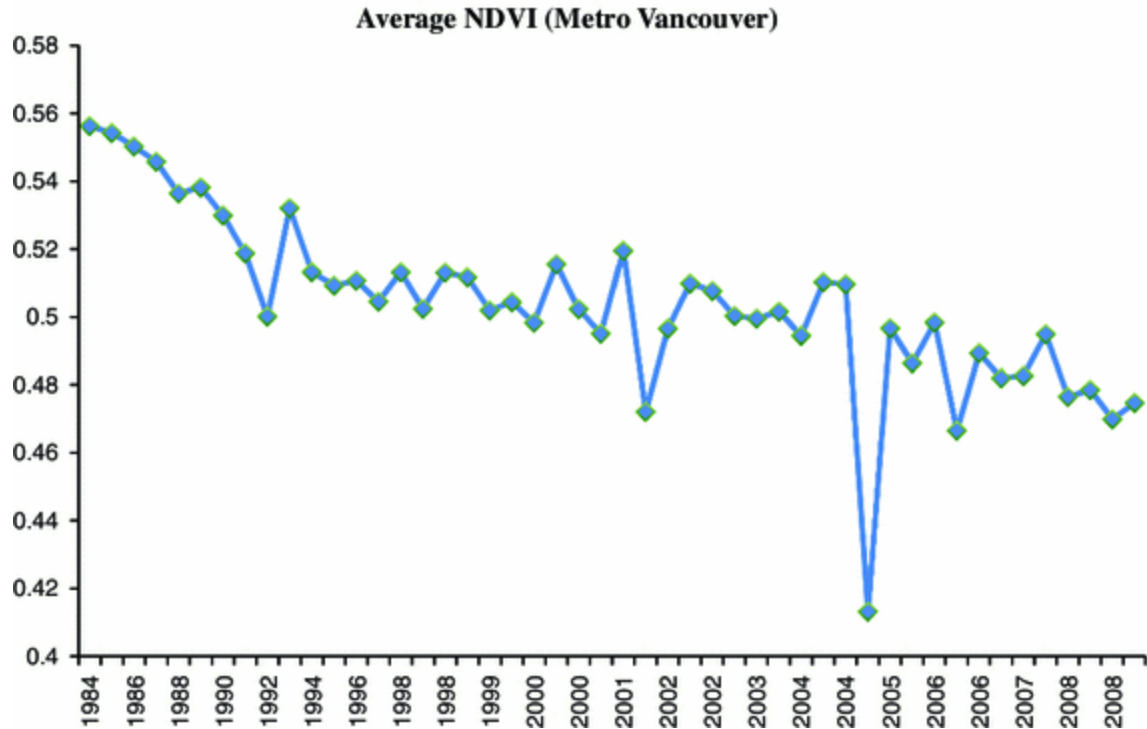


Figure 38 Vegetation trend between 1984 and 2012, Metro Vancouver (Source: Owrangi et al., 2014).

From a conservation point of view, urban planning is an essential aspect of urban development. In the Fraser River Delta where Metro Vancouver is located, severe land-use change has occurred over the last three decades. In this time, the central and southern parts of the city have become increasingly urbanized. The reduction in vegetation cover has the potential to increase river flows and the resultant flood damage. This results from an increase in the total impervious area; precipitation is no longer attenuated by vegetation or infiltrated so the time to peak flow is faster and the flows themselves are higher in the drainage channels. This de-vegetation as a result of urbanization is likely to be a continuing trend in the region and mainly zones 4 and 6.

The vegetation condition maps developed here play an important role in the final health impact assessment. By utilizing a set of temporal vegetation maps, it is possible to consider land-use change as one of the key physical elements for the proposed spatio-temporal health impact assessment.

5.2 Flood inundation map

Flooding is another essential factor that has been considered in the development of a climate change-related spatio-temporal health impact assessment. As such, developing a flood inundation map is an essential task.

Topography is fundamental to defining flow characteristics in hydrological processes. This concept is fundamental to understanding hydrologic and hydraulic dynamics within a catchment. The availability of technologies like remote sensing to measure surface elevation (e.g., SAR, ASTER, SAR interferometry, radar and laser altimetry) has improved the application of DEM-based models.

There are a variety of DEM sources, each with different spatial characteristics as described in the third chapter. There are a number of options for DEMs with an assortment of resolutions for the Metro Vancouver area. Development of a flood inundation map using DEMs and the open source software GRASS is explained in detail in chapter 3.2.2. This methodology has not been implemented in any Canadian city yet. The first step is to calculate the modified topographic index, using different available sources of DEMs. Two different sources of DEM data were selected: Shuttle Radar Topography Mission (SRTM) from the USGS with a resolution of 90 m² (Figure 39), and Canadian Digital Elevation Model (CDEM) from Natural Resources Canada with a resolution of 25 m² (Figure 40).

Metro Vancouver has high spatial climate variability due to its unique topography and proximity to the Pacific Ocean and the Fraser River. Metro Vancouver is also characterized by a wide range of land elevations due because it comprises both highly mountainous areas (eg. North Vancouver) and very low coastal delta regions (eg. Delta and Richmond).

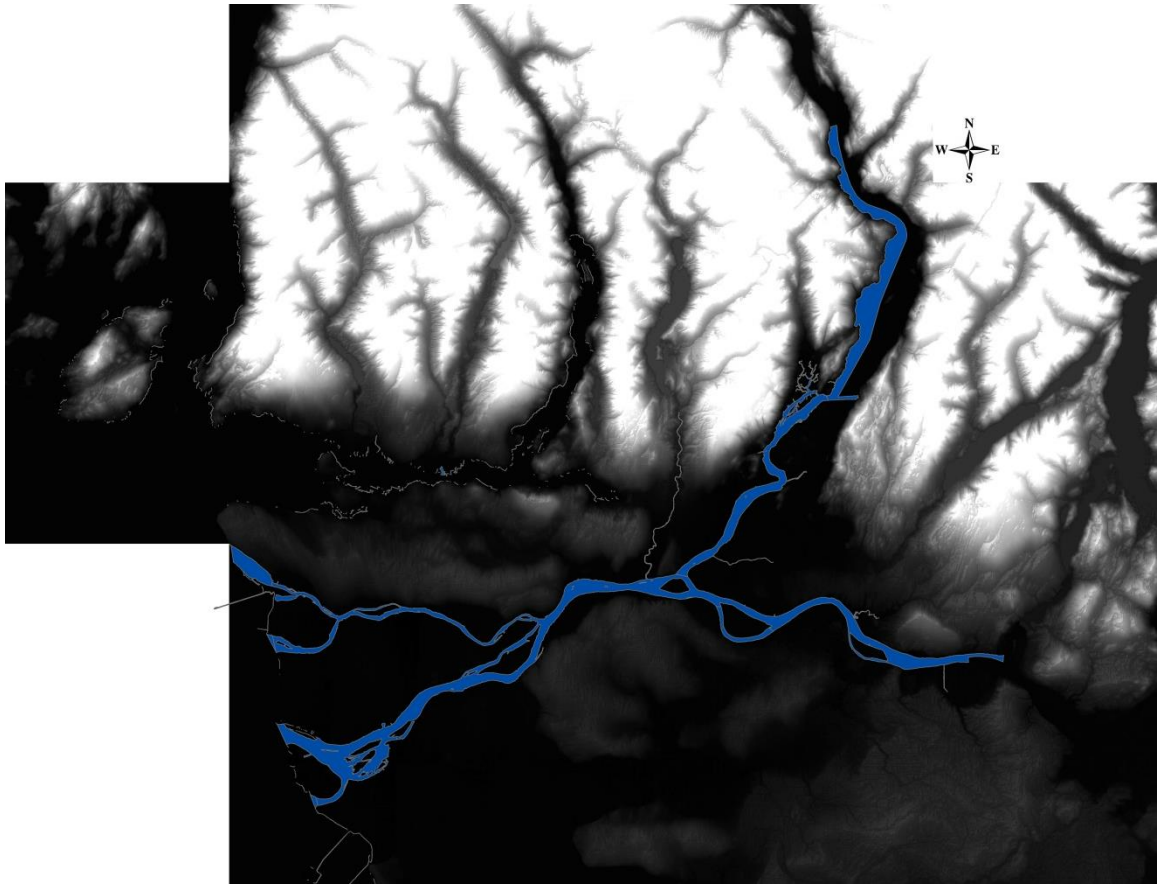


Figure 39 Shuttle Radar Topography Mission (SRTM) from USGS with a resolution of 90 m² for Metro Vancouver.

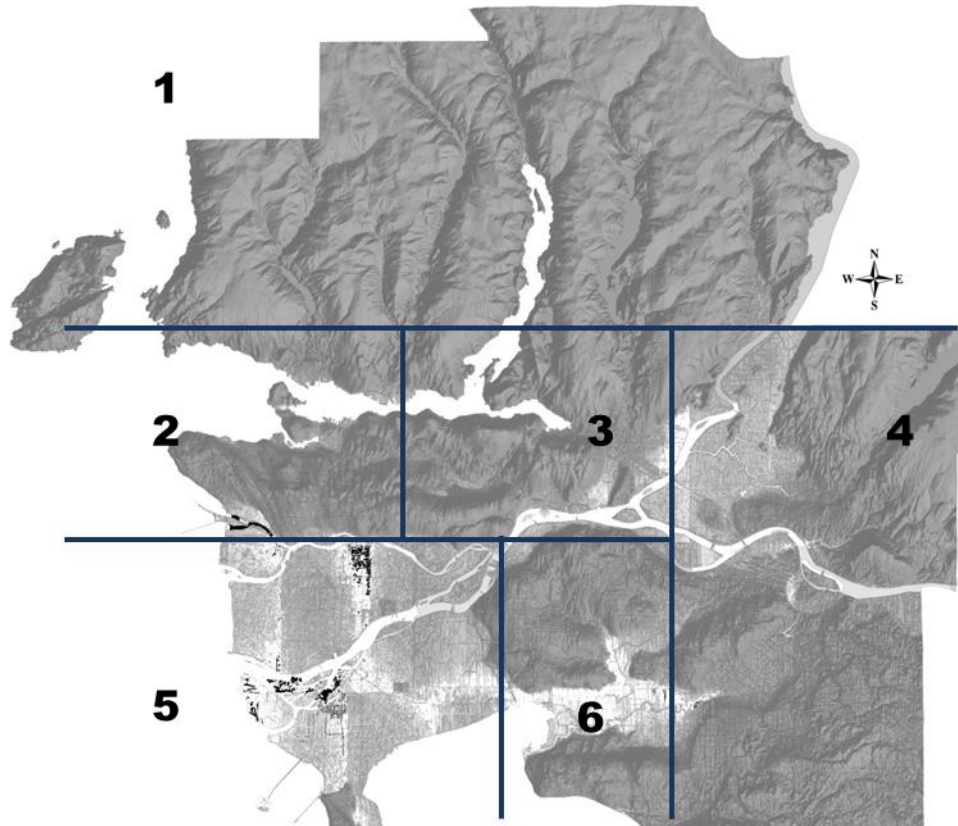


Figure 40 Canadian Digital Elevation Model (CDEM) from Natural Resources Canada with a resolution of 25 m² for Metro Vancouver.

The spatial distribution of the topographic index is highly correlated to the characteristic scale of the adopted DEM. This effect is examined by comparing the sensitivity of the calculated values using DEMs at different resolutions, starting from a DEM with a cell size of 25 m². The flow accumulation was computed using the multiple flow direction procedure suggested by Holmgren (1994), in which water flow is distributed to all neighboring cells with a lower elevation, using the slope in the direction of the neighboring cells as a weighting factor for comparative distribution of the water according to $\tan(\beta_i^h) / \sum \tan(\beta_i^h)$ where $0 < h < \infty$ (Manfreda et al. 2011). The value of h causes a gradual change from single directional flow (infinite; in practice values above 25) to multidirectional flow ($h = 1$) (Sorensen et al. 2006).

Similar to hydraulic simulation models which require high resolution topographical information, this approach also necessitates the use of high resolution DEMs because the modified topographic index is strongly influenced by the DEM resolution. The focus of this section is to develop a flood inundation map for Metro Vancouver. The highest resolution data for the region is the CDEM model (25m²).

The same procedure has been applied to SRTM data with a resolution of 90m². After developing TIm maps for both CDEM and SRTM elevation data, a GRASS add-on extension called *r.hazard.flood*, was used to develop inundation maps for both data sources with different resolutions for Metro Vancouver. Figure 41 presents the inundation map using CDEM data and Figure 42 presents an inundation map based on SRTM data. CDEM provides a better potential inundation map for Metro Vancouver because of the higher resolution in comparison to the SRTM, therefore the CDEM inundation output will be utilized in the final health impact map integration as a part of the physical health impact.

Based on the generated inundation map (deploying CDEM data), Zone 5 (Richmond, Delta and Vancouver International Airport, etc.) has the highest risk of flooding. This entire area is very flat and thus vulnerable to flooding. Zone 3 also has a high likelihood of flooding and for the same reason: it is located in a flat area that is dangerously proximate to the confluence of the Pitt and Fraser Rivers. In the central part of Surrey (zone 6) is a valley containing the Serpentine River and Nicomekl River. The area between these two rivers has a high chance of flooding as well. In zone 1 (North Vancouver and Vancouver proper), the chance of flooding is much lower than in zones 3, 4, 5, and 6. However, for some coastal zones in North Vancouver (mainly around Lynn Creek, Seymour River, and Capilano River) moderate flood risk remains so community planners should be vigilant.

This approach provides a quick rendering of the extent of flood inundation areas in the study region but is unable to calculate flow depth information. In the case of this spatio-temporal health impact assessment, a wide range of physical and nonphysical factors are used. This efficient spatial flood detection method provides an opportunity to consider the potential flood risk in the assessment of climate change-related health impacts.

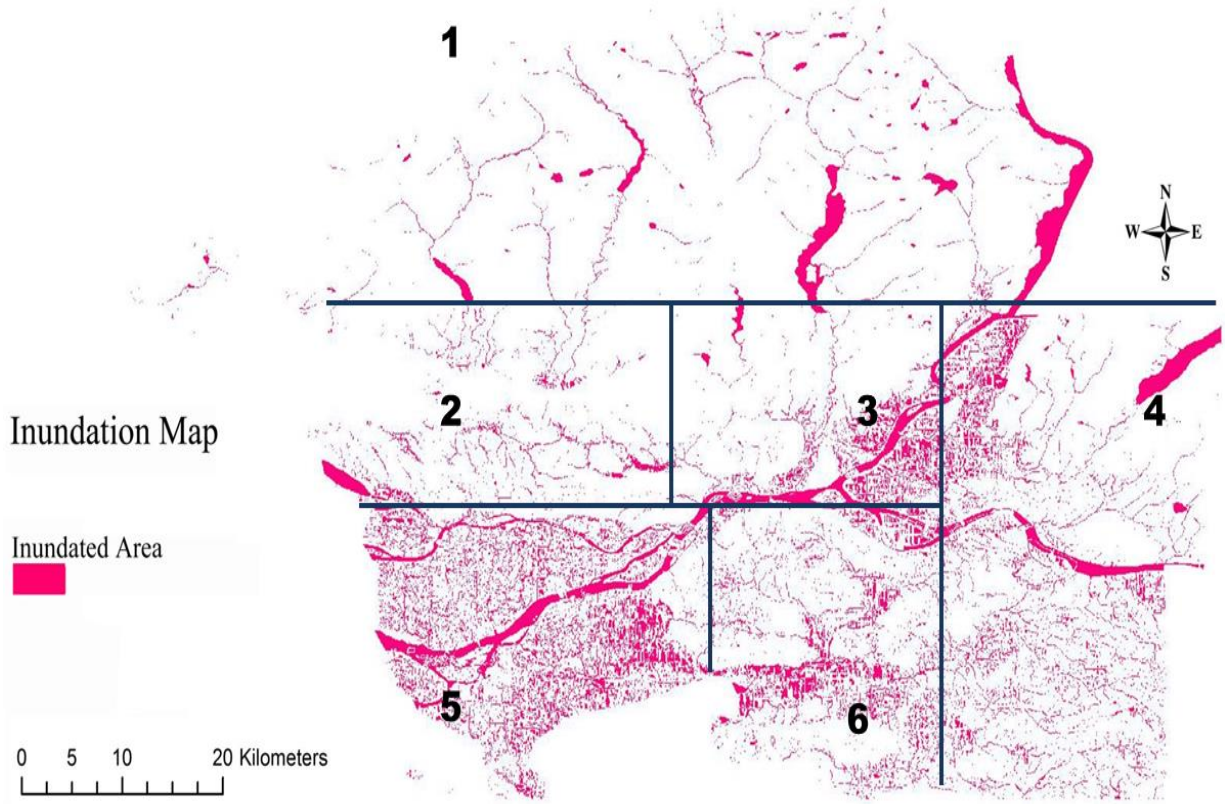


Figure 41 Inundation map using modified topographic index map for Metro Vancouver based on the Canadian Digital Elevation Model (CDEM).

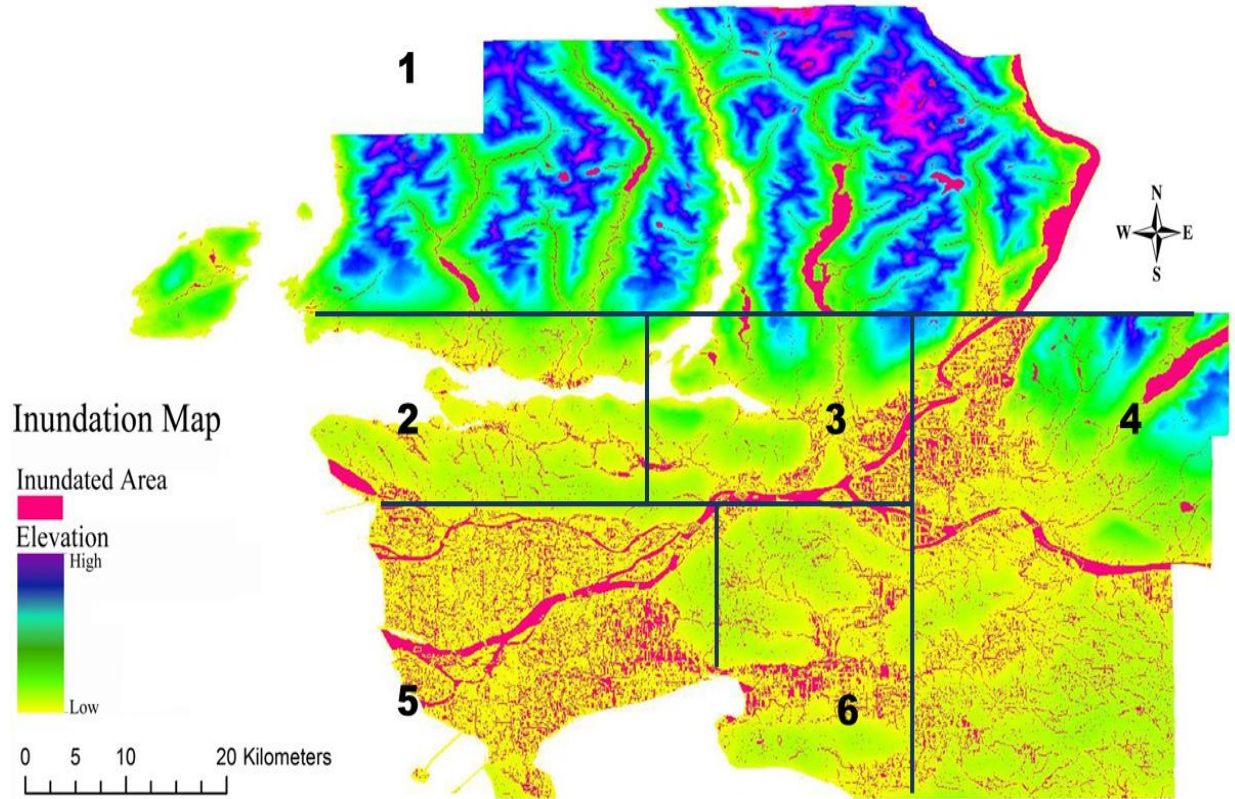


Figure 42 Inundation map using modified topographic index map for Metro Vancouver based on the SRTM inundation map.

5.3 Climate change impact on human health

5.3.1 Burden of disease

Major cities all around the world have different demographic characteristics. Based on the economic conditions of their country (developing or developed), each city will face different potential disease profiles as a result of climate changed related extremes. This section focus is on spatio-temporal health impact assessment for Metro Vancouver.

Section 3.3 describes the detailed calculation of DALYs. The DALY (Equation 9) measures health gaps as opposed to health expectancies. It measures the difference between a current situation and an ideal situation where everyone lives up to the age of the standard life expectation and in ideal health.

There are 165 different potential diseases named by the WHO age-standardized DALY table and they are classified into three broad categories: communicable diseases, non-communicable diseases, and injuries. Quantifying human health impacts caused by climate change is a complex task and there are huge sources of uncertainty involved with any kind of estimates. Therefore, researchers attempt to collect as much accurate data as they can to decrease the uncertainty. One of the most reliable strategies is to collect data in high resolution formats. For example population, senior population, and population of children are all important factors in assessment of human health impacts. Obtaining this information in accurate high resolution spatial formats gives researchers and policy makers a more focused vision concerning the resilience of their communities. Table 5 compares different types of DALYs for 7 major municipalities in Metro Vancouver based on 2011 population census data. Information relating to the occurrence of different types of DALYs can help city planners assess the potential health risks in different areas of the city. The quantification can help in various ways for example in comparison of health facilities across municipalities and the number of potential DALYs. Detailed assessments relating to the availability and accessibility of healthcare related facilities should take into consideration the potential demand that may be placed on them in the future as a result of climate change-related hazards.

Table 5 Comparison of different types of DALYs for seven major municipalities in Metro Vancouver based on 2011 population census data.

City	Population 2011	Communicable	Non-Communicable	Injuries	Total DALYS
Vancouver	603,503	3989	40766	3174	47929
North Vancouver	84,412	558	5718	444	6720
Coquitlam	126,456	836	8545	665	10046
New Westminster	65,976	436	4458	347	5241
Richmond	190,473	1259	12868	1002	15129
Delta	99,863	661	6755	526	7942
White Rock	19,339	126	1283	100	1508

Spatial decomposition of the mega-cities provides a significant advantage in development of resilience strategies because decision makers can better understand what areas are most vulnerable as a result of potential climate related hazards and how to prioritize investments in the city's health care system. As a result, this research has focused on the development of a methodology which can quantify climate change-related potential health impacts using high resolution spatial and temporal maps. Spatial population data based on dissemination and census tract areas have been collected for Metro Vancouver for the years 1981,1986,1991,1996, 2001, 2006, and 2011 and different population related elements have been calculated for the final health impact map.

5.3.2 Disability Adjusted Life Years (DALYs) calculation for Metro Vancouver

Canada is a high-income country, and infectious disease risk is generally considered low in high-income countries. This holds true for Canada. The highest infectious health risk is related to waterborne diseases as a result of drinking-water contamination. Experience has shown amongst higher income countries that in larger urban areas where water treatment and waste water infrastructures are well maintained and managed, the risk of waterborne infections remains low. Smaller communities with less well-developed infrastructure are at higher risk during extreme weather events, for example in the case of the Walkerton, Ontario incident (Schwartz and McConnell, 2009). Based on methodology in Section 3.3 and age standardized DALY tables by WHO, DALY have been calculated for the Metropolitan area based on three major categories which for the purpose of mapping exercises are sufficient. These categories are communicable diseases (601 DALYs per 100,000 population), non-communicable diseases (8,799 DALYs per 100,000 population) and injuries (920 DALYs per 100,000 population).

All three categories are considered and represented based on census tract and dissemination areas. Figure 43, 44, and 45 show these 3 categories for 2011. The same procedure has been applied to the other 6 years and the results can be seen in Appendix C.

Figure 43 presents a map of communicable diseases based on the national averages. As discussed in the methodology section, the number of DALYs is correlated with population; in this case the highest prevalence of communicable disease is in downtown Vancouver area (zone 2). For this calculation the calculated normalized densities of communicable diseases has been classified (number of instances per square kilometer) into 5 ranges as can be seen in the legend. The lowest rate of communicable diseases can be seen in zones 1 and 4. In Zone 3, 5, and 6 the occurrence of this category of disease is comparatively small.

Figure 44 shows that non-communicable diseases (number of non-communicable diseases per square kilometer) constitute a higher and more widespread burden than communicable diseases, which is to be expected. Many of these non-communicable diseases require ongoing support from health facilities e.g., dialysis, cancer care, etc. and during extreme weather-related events, accessibility of healthcare facilities is important to maintain public health.

Once the dynamic resilience model explained in Chapter 3 is in place, it will be possible to experiment with specific numbers of cases (for example, what will 5,000 cases of post-traumatic stress disorder (PTSD) in the non-communicable category and 50,000 cases of gastrointestinal infections (GI) in the communicable category, post flood event, do to the resilience of the city).

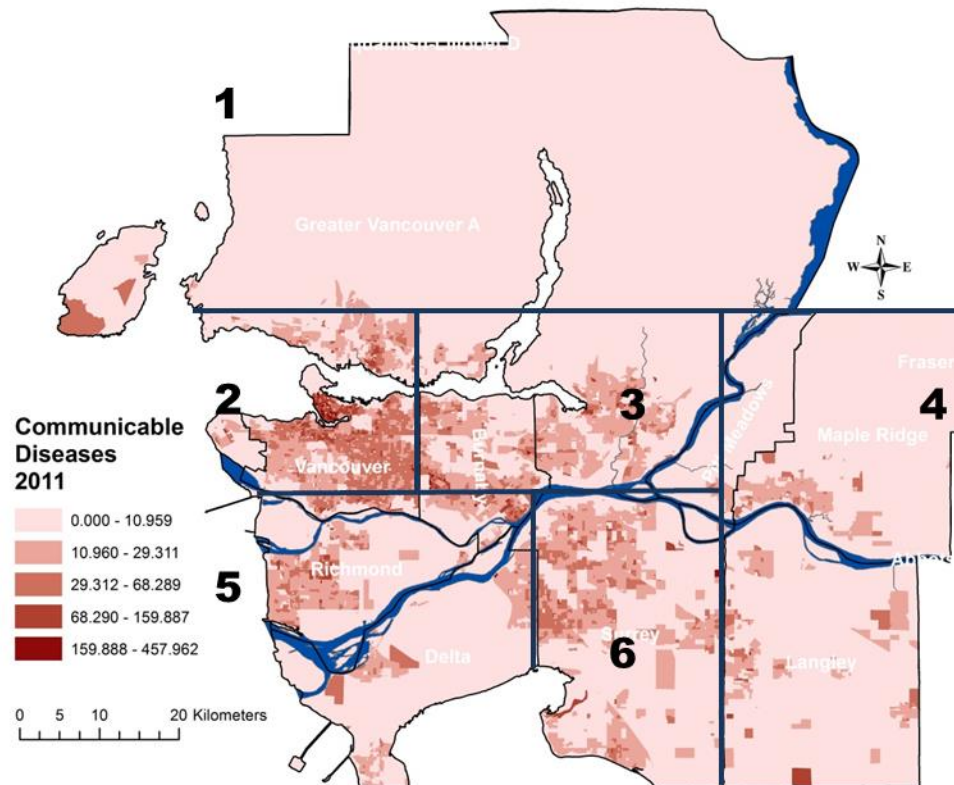


Figure 43 Calculated normalized densities of communicable diseases for Metro Vancouver for 2011 (number of communicable diseases per square kilometer).

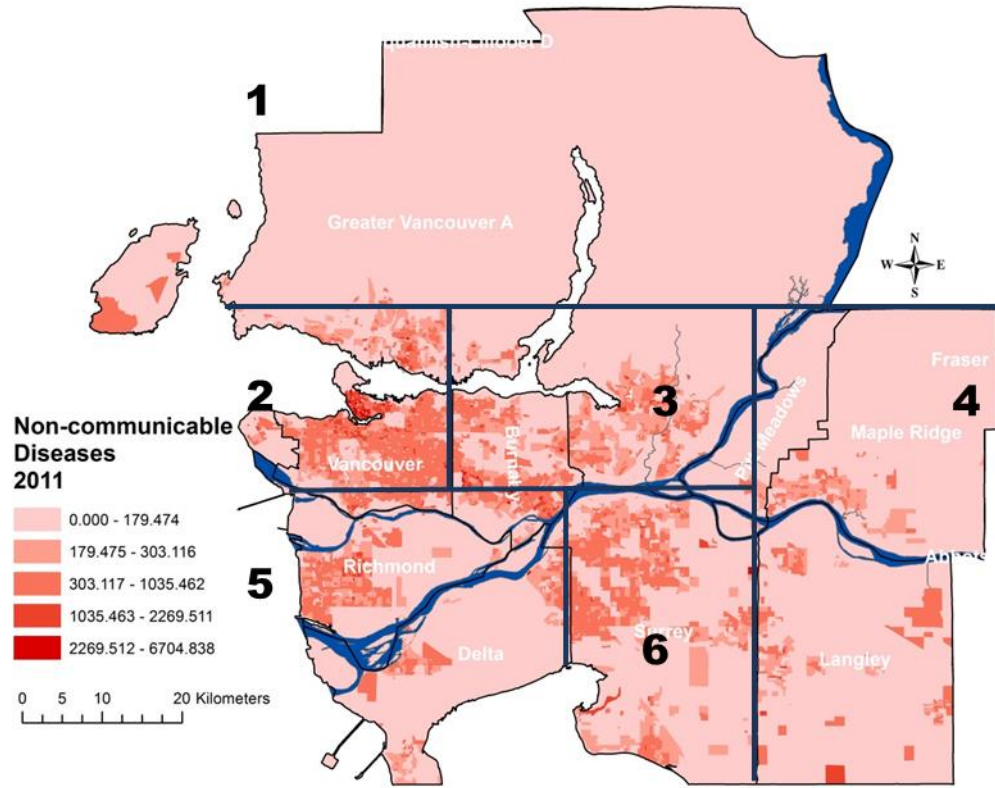


Figure 44 Calculated normalized densities of non-communicable diseases for Metro Vancouver for 2011 (number of non-communicable diseases per square kilometer).

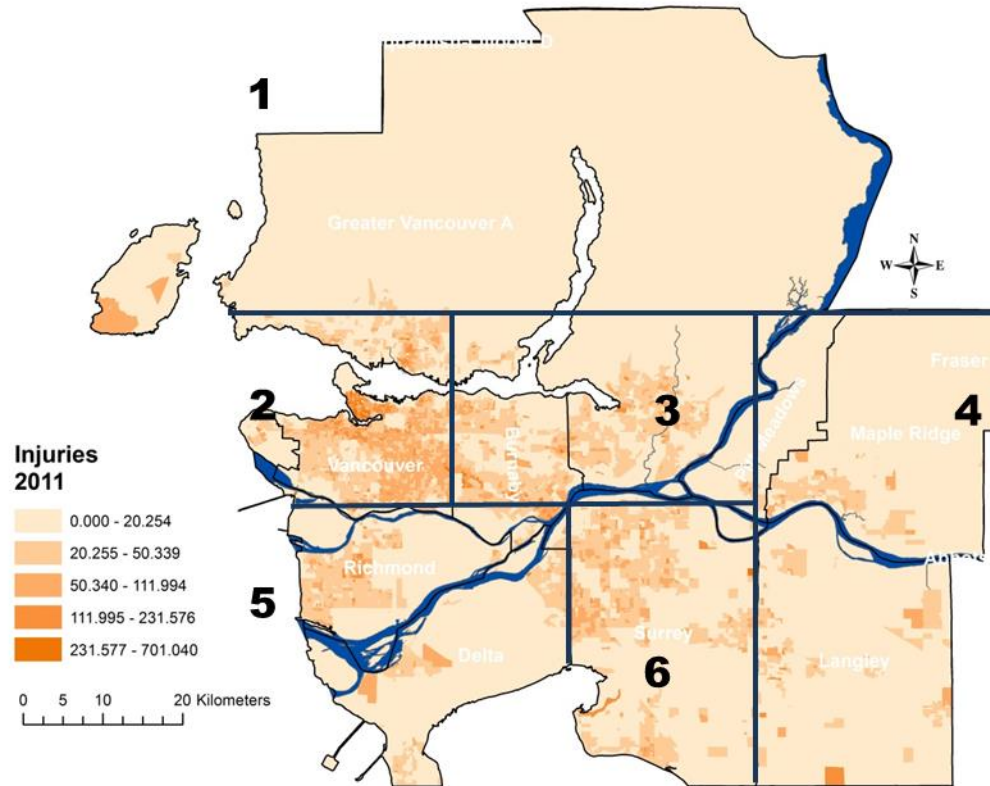


Figure 45 Calculated normalized densities of injuries for Metro Vancouver for 2011 (number of injuries per square kilometer).

5.3.3 Demographic assessment

5.3.3.1 Total population

Metro Vancouver has experienced changing development patterns, economic conditions and social characteristics as a result of the growing population. Social, economic and built-environment changes have altered the population vulnerability in many ways. Over the last several decades, Metro Vancouver has achieved a significant level of socioeconomic development. In that period, Metro Vancouver's economic expansion was greater than the national average (Statistics Canada 2012). As a consequence, employment in Metro Vancouver reached 1.1 million in 2006, representing the fastest pace of job growth among Canada's three largest metropolitan areas of Toronto, Vancouver and Montreal (Turcotte and Schellenberg, 2006).

Rapid socioeconomic development has followed the parallel trends of considerable population growth and rapid urbanization. In 2011, Metro Vancouver had a population of 2,476,328 people distributed over a land area of about 2,883 km² for a population density of 856.2 people/km² (Statistics Canada, 2012). In contrast, Metro Vancouver's population in the year 1981 was 1,169,831. This shows an increase of more than 100 percent over three decades (Statistics Canada, 2012).

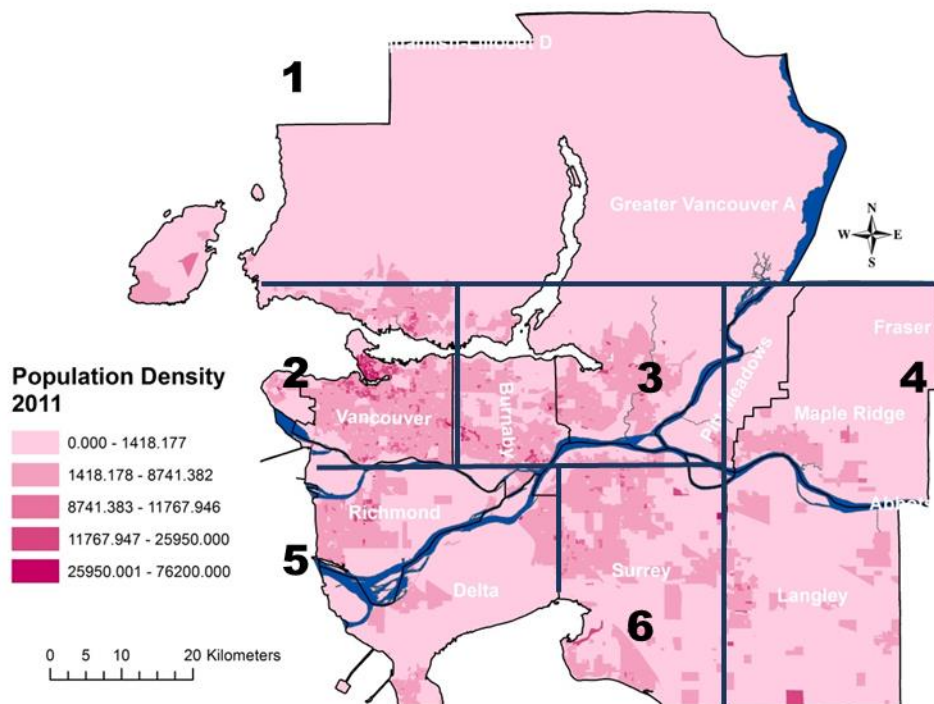


Figure 46 Calculated normalized population density for Metro Vancouver for 2011 (population per square kilometer).

It is essential to identify the variability in the vulnerability of populations exposed to hazards in order to develop adaptation strategies and improve the response to potential climate change-related disasters. Figure 46 shows the normalized population density distribution over Metro Vancouver for 2011. This map is based on dissemination areas and classified into 5 different population density groups which present the number of people per square kilometer. Regions with a higher population density are more vulnerable in terms of public health. The darker pink regions show that the areas with the highest density are mostly located in the City of Vancouver, Burnaby and Richmond, with pockets of more densely populated areas in

Surrey and Delta. Zone 5 (which includes the cities of Richmond and Delta) has some moderate to densely populated areas which may be particularly vulnerable due to their location in the flood plain, as discussed in Section 5.2. Zones 1 and 4 are not as densely populated and therefore more focus should be directed to zones 2, 3, 5 and 6. Research has indicated that high population density neighborhoods urban centers may experience greater difficulty in terms of obtaining necessary health services following disaster events. For example, damage to transportation infrastructure may prevent provision of health services for many people (Dilley 2005). Consequently, future development decisions should take into consideration the uneven spatial population densities which may have a significant impact on the level of health risks and impacts resulting from climate related weather extremes. The set of maps representing population densities for the years 1981, 1986, 1991, 1996, 2001, and 2006 can be accessed in Appendix C.

5.3.3.2 Senior population

Figure 47 represents the normalized population density distribution of seniors (number of persons 65 years and older per square kilometer) in Metro Vancouver for 2011. It is also based on dissemination areas and is classified into 5 different population density groups which present the number of people per square kilometer. The population varies between 0 and 790 people per dissemination area for 2011. The density value is normalized (between 0 and 11500). Numbers closer to 11500 represent a higher density. Dark purple areas with higher senior population densities are easily identified as areas with higher needs for medical care and higher levels of risk. The Cities of Richmond, Vancouver, and Burnaby have higher senior population densities as shown in the 2011 map (zones 2, 3, and 5). Also in zone 6, where Surrey is located, there are some areas that have a high density of seniors within the northern and southern portions. The southern parts of Surrey and Richmond are both highly vulnerable to flooding and sea level rise.

Future development decisions should be informed by the spatial distribution of healthcare facilities for seniors in these municipalities. Providing sufficient and accessible healthcare facilities for this subpopulation is already an important issue but as the whole region

experiences a further increase in senior population density, there will be an increase in the level of risk carried by the existing senior health care delivery system. For the final health impact assessment, the same set of maps for senior population density have been assembled for the years 1981, 1986, 1991, 1996, 2001, and 2006 and can be found in Appendix C.

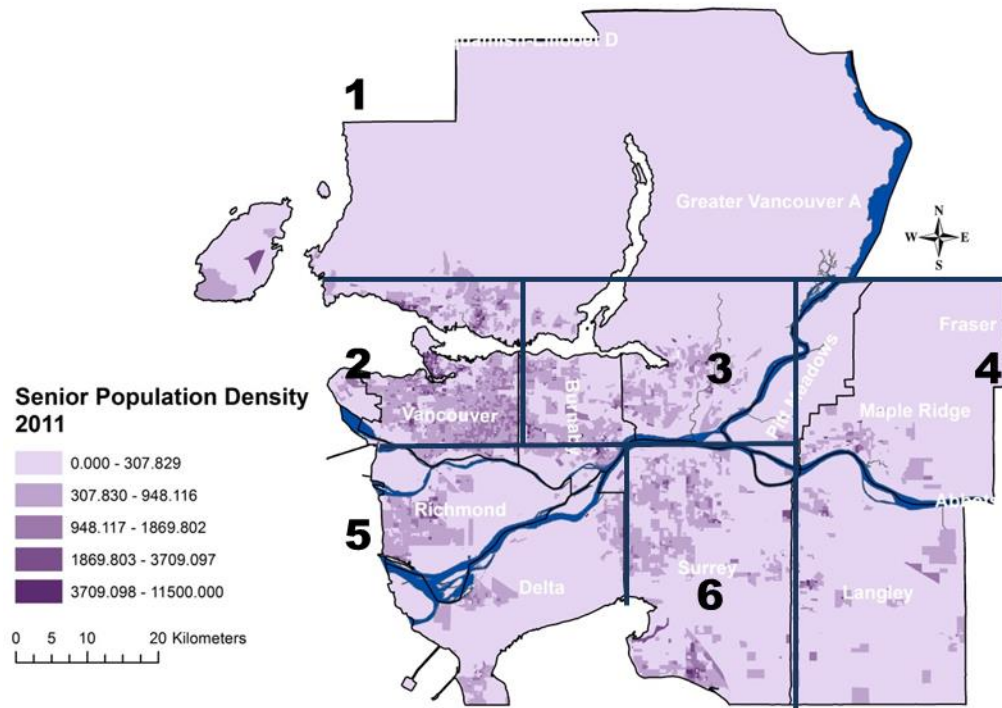


Figure 47 Calculated normalized senior population density for Metro Vancouver for 2011 (number of seniors per square kilometer).

5.3.3.3 Children population

Children under age 4 are recognized as a population group of increased vulnerability because of climate change-related health risks. As such, it is important to consider them in the assessment of human health impacts of climate change. Figure 48 presents the distribution of population densities (number of children per square kilometer) for children four years of age and younger in Metro Vancouver for 2011. The population density has been normalized

(between 0 and 5500 per square kilometer). Numbers that are closer to 5500 are the areas with the higher density of children and hence have an increased human health risk from climate change-related hazards. The cities of North Vancouver, Vancouver, Burnaby and Surrey (Zones 2, 3, and 6) have the higher rate of child populations per dissemination area. Similarly in zone 4 there is a higher rate of child population in comparison to the senior population, which may be a result of the affordability of these newly developed regions for younger families (Property value is lower in these regions in comparison with the downtown area). For the final health impact assessment, the same set of maps for children's population density have been assembled for the years 1981,1986, 1991, 1996, 2001, and 2006 (see Appendix C).

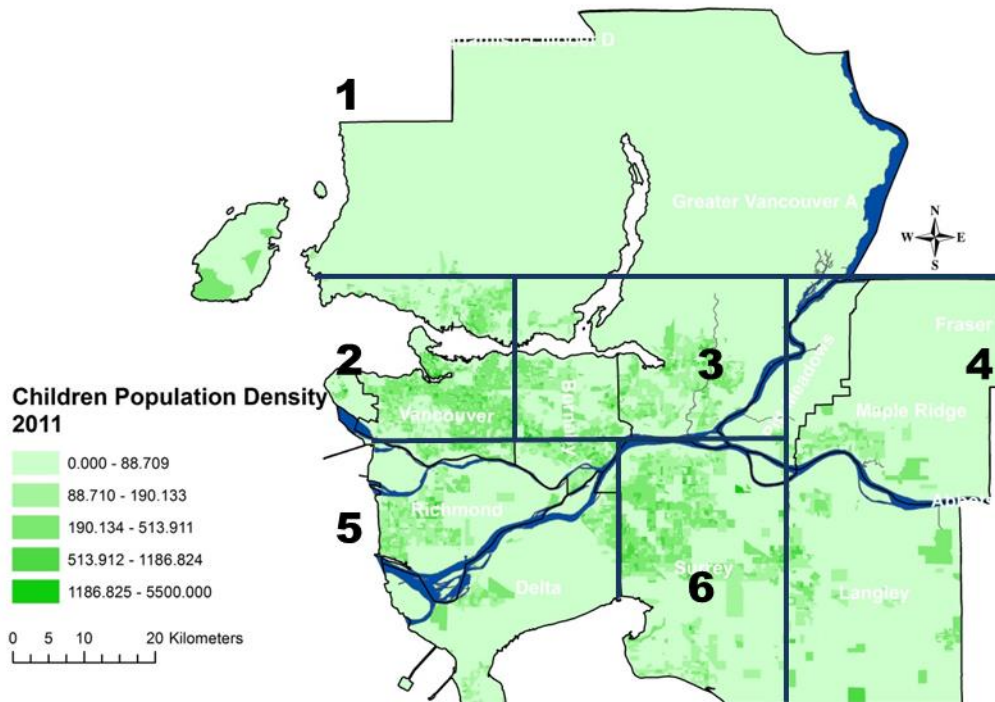


Figure 48 Calculated normalized children population density for Metro Vancouver for 2011 (number of children per square kilometer).

5.4 Mapping climate change-related health risks for an integrated city resilience model

Land use change analysis, topography, and flood inundation mapping have considered (see Equation 4) physical inputs and total population density, senior population density, and children population density have been considered as nonphysical inputs. Also different categories of burden of disease are grouped under a general measure and constitute the nonphysical health inputs to the assessment. The main objective of this methodology is to establish a composite measure of human health in the form of a human health impact map, which contains various values of health impacts in time and space. The output of this mapping exercise provides an integrated view of public health that can be used in development of targeted, adaptive and risk reducing strategies to improve the resilience of Metro Vancouver. This methodology has been applied using 7 years of spatial data in order to facilitate dynamic modelling of health impacts using a resilience simulator. The research demonstrates how composite health impact maps can be used as an input for resilience modeling, as well as for a stand-alone product.

5.4.1 Nonphysical health impact map (NPHIM)

The normalized health and social conditions presented in separate maps have been integrated into one single map. The resulting map helps in identification of Metro Vancouver regions which are vulnerable based on nonphysical conditions for the last 7 census years. Figure 49 shows the nonphysical impact map that integrates total population density, senior population density, children population density, communicable diseases, non-communicable diseases and injuries for 2011. This map is also normalized and rasterized. The same set of maps for NPHIM are assembled for the years 1981, 1986, 1991, 1996, 2001, and 2006 and can be accessed in Appendix C.

In 1981 the population of Metro Vancouver was 1,169,831 people and most of the people lived in the cities of Vancouver (414,281), Surrey (147,135), Burnaby (136,494), Richmond (96,154), and Delta (74,692). In 2011 (based on Canada Census data) this population has increased to 2,476,328 for the metropolitan area. The majority of the population lives in Vancouver (603,502), Surrey (513,322), Burnaby (223,218), Richmond (205,262), and Delta

(99,863). Detailed population changes are presented in Figure 50. This drastic increase in the city's population is the main source for potential nonphysical health impacts and it is highly correlated to the rates for burden of disease. The cities of Vancouver, Richmond, Delta, Burnaby and Surrey are shown to be the regions with the greatest vulnerability in terms of nonphysical health impact.

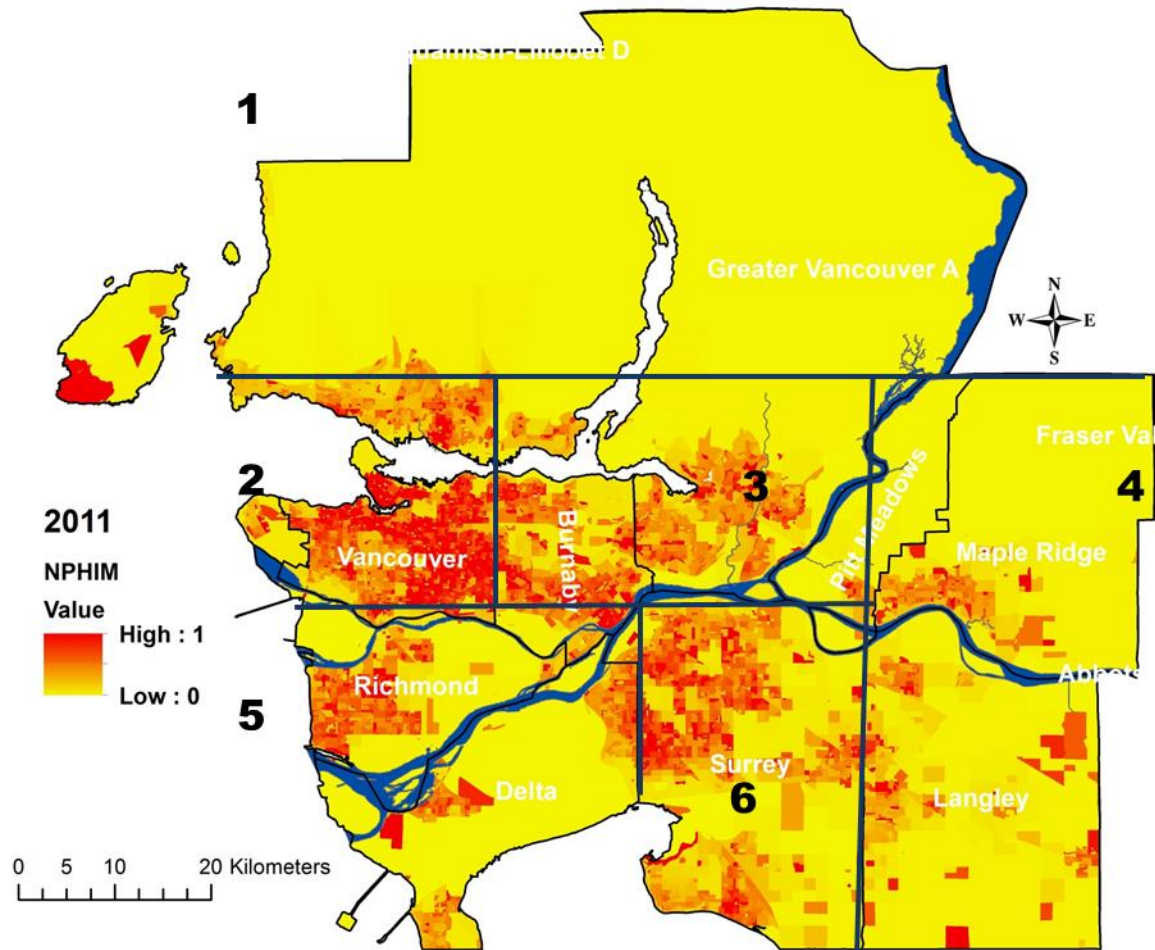


Figure 49 Nonphysical health impact map (NPHIM) generated for Metro Vancouver for 2011.

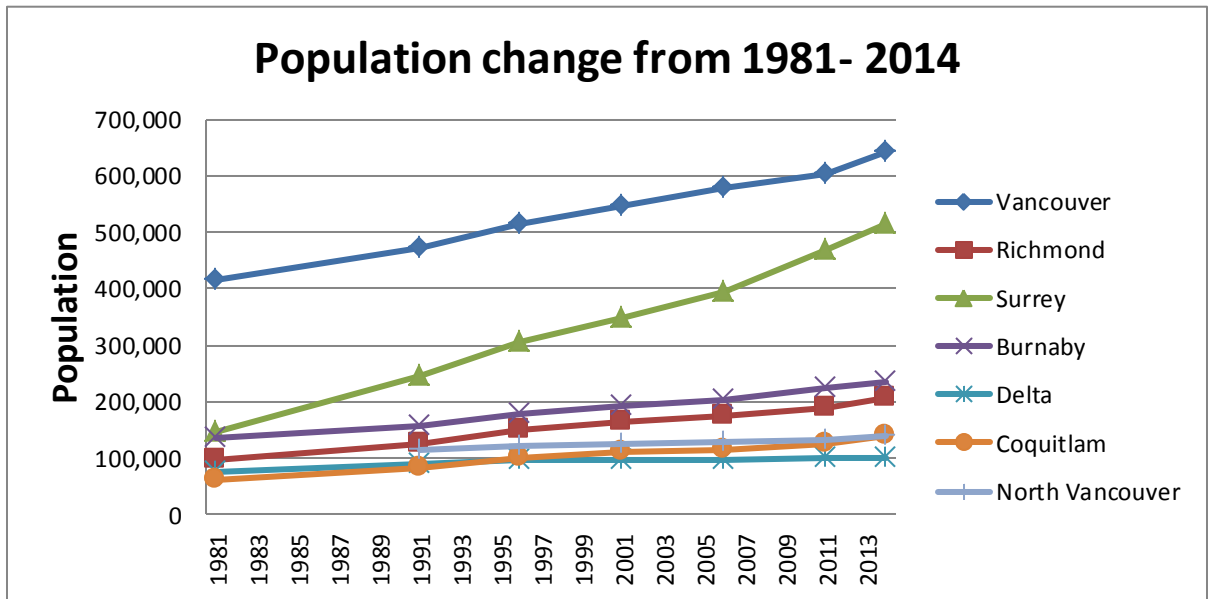


Figure 50 Population change for major municipalities in Metro Vancouver from 1981 to 2014.

Figure 51 contains a comparison of nonphysical health impact maps for Metro Vancouver between 1981 and 2011. It is clear that this significant increase in human population directly contributes to the corresponding increase in vulnerability across most parts of the city. The greatest change has occurred in zone 6, where Surrey is located. This significant increase in the potential for nonphysical health impacts in a city with close proximity to the sea and river makes it increasingly vulnerable to climate change-related hazards such as sea level rise and flooding. The population in Surrey has increased by more than three times since 1981. Other municipalities including Burnaby, Richmond, Delta, North Vancouver, and Langley have also experienced significant population growth.

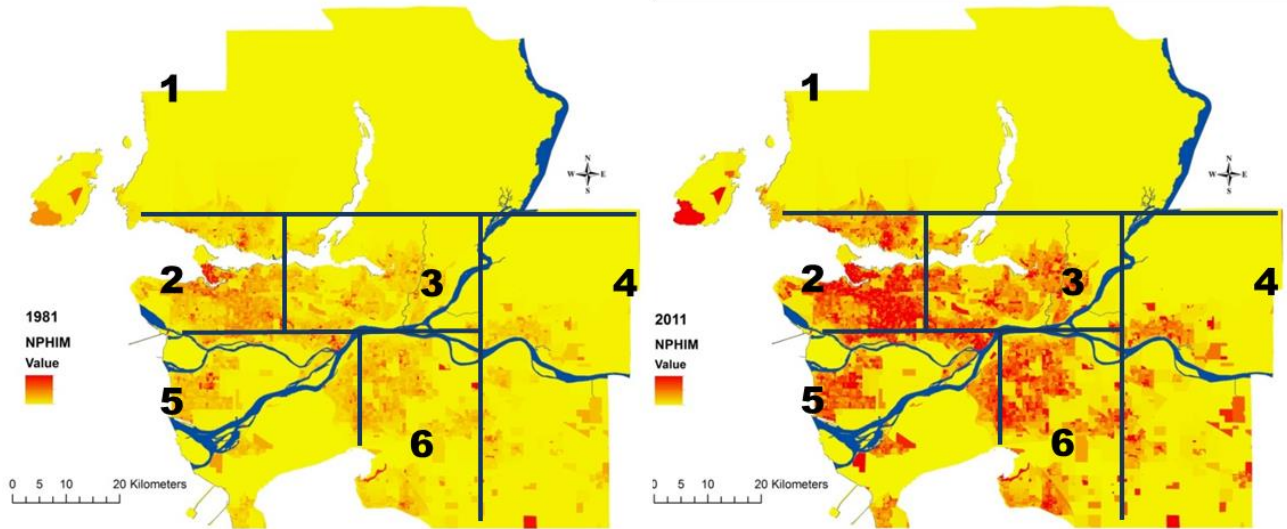


Figure 51 Comparison of nonphysical health impact map generated for Metro Vancouver between the years 1981 and 2011.

5.4.2 Integration of physical and nonphysical impacts of climate change on human health

Integration of the physical and nonphysical impacts maps is performed in two phases. First, nonphysical impacts have been integrated into a single map for each year and then the results are integrated with the physical conditions of flood inundation hazard, topography and vegetation. At this point (and prior to any integration) all maps are standardized between 0 and 1 using Equations 10 and 11. A value of 0 represents the least potential climate change impact to human health and 1 represents the highest impact for the particular element considered in each map. When all the spatial data inputs have been standardized between 0 and 1, the general integration Equation 19 is used to develop the final health impact maps for each year.

Weights play an important role in this proposed methodology as they allow the user to put emphasis on specific inputs to the final health impact. If an expert thinks that a specific element (e.g. population) has more influence on the vulnerability of the entire city or a small part of the city, then a specific weight may be applied to that element in that location with the results shown spatially. In this way, it is possible to produce a map that reflects priorities or concerns either in specific locations or across the entire city.

The methodology for generation of the health impact map (HIM) is presented in Section 3.4. The value to be mapped is calculated using Equation 19 which applies the weighting scheme chosen by the expert. In this equation α_1 and α_2 play an important role in differentiating between the priority of physical versus nonphysical inputs in the assessment. Some data cannot change significantly (e.g. topography) and therefore the implementation of the same procedure for different cities will face with the same results.

Compare, as a thought experiment, flat, riverine Winnipeg with the varied terrain of Metro Vancouver. By adjusting α factors, it is possible to address the unique physical and nonphysical conditions of each study area. This adds flexibility in the methodology. Local conditions and specific issues can be dealt with using weight to rank their importance.

5.4.3 Health impact map (HIM)

The next step in the methodology is to combine the physical outputs (sections 5.1 and 5.2) including land use change analysis, topography and the flood inundation map, with the nonphysical health impact map using Equation 20. The weights used for this integration are assumed to be the same. Figures 52 and 53 show the final health impact maps for 1981 and 2011, which have been rescaled between 0 and 1 for all seven years. These seven maps have been normalized together to allow for the comparison of human health impacts over time (including future extrapolations). The resulting maps demonstrate clearly that Vancouver, Richmond, Delta and Surrey are more vulnerable compared to other municipalities in the region in terms of climate change-related flooding and sea level rise and the corresponding impacts of these events on human health. For the final health impact assessment, HIMs have been assembled for the years 1986, 1991, 1996, 2001, and 2006 these can be accessed in Appendix C.

In 1981 the population of the Metropolitan area was significantly less than what it is today. As a consequence of this, the land-use and vegetation cover has changed dramatically. Vancouver's dramatic population increases over the last thirty years have been a result of increased immigration to the city rather than the birth rate. The increasing population has resulted in increased land use leading to increased imperviousness to rainfall and therefore increased runoff. Factor in rising sea levels and adverse effects of climate change become

increasingly likely. The highest rate of vegetation decrease and population growth has occurred in zone 6 (in which the city of Surrey is located). Zone 5, which includes the cities of Richmond and Delta, has also experienced dramatic population growth in the last 30 years. An important characteristic that is common to each of these three municipalities is that they are located in highly vulnerable flood zones. Vancouver and Burnaby (zones 2 and 3 respectively) have the highest population density, therefore the rate of the nonphysical health impact is higher than for the rest of municipalities.

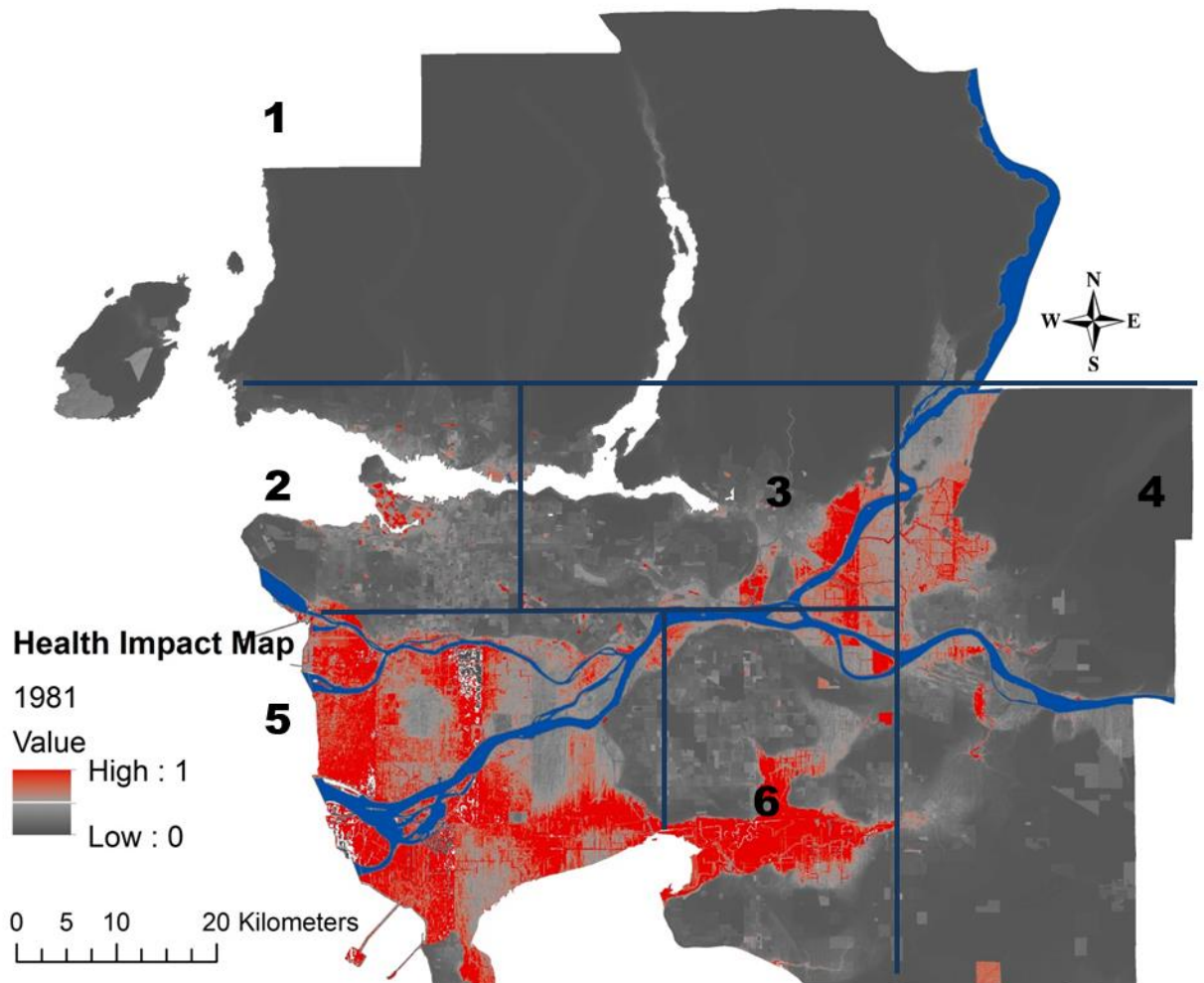


Figure 52 Human health impact map generated for Metro Vancouver for 1981.

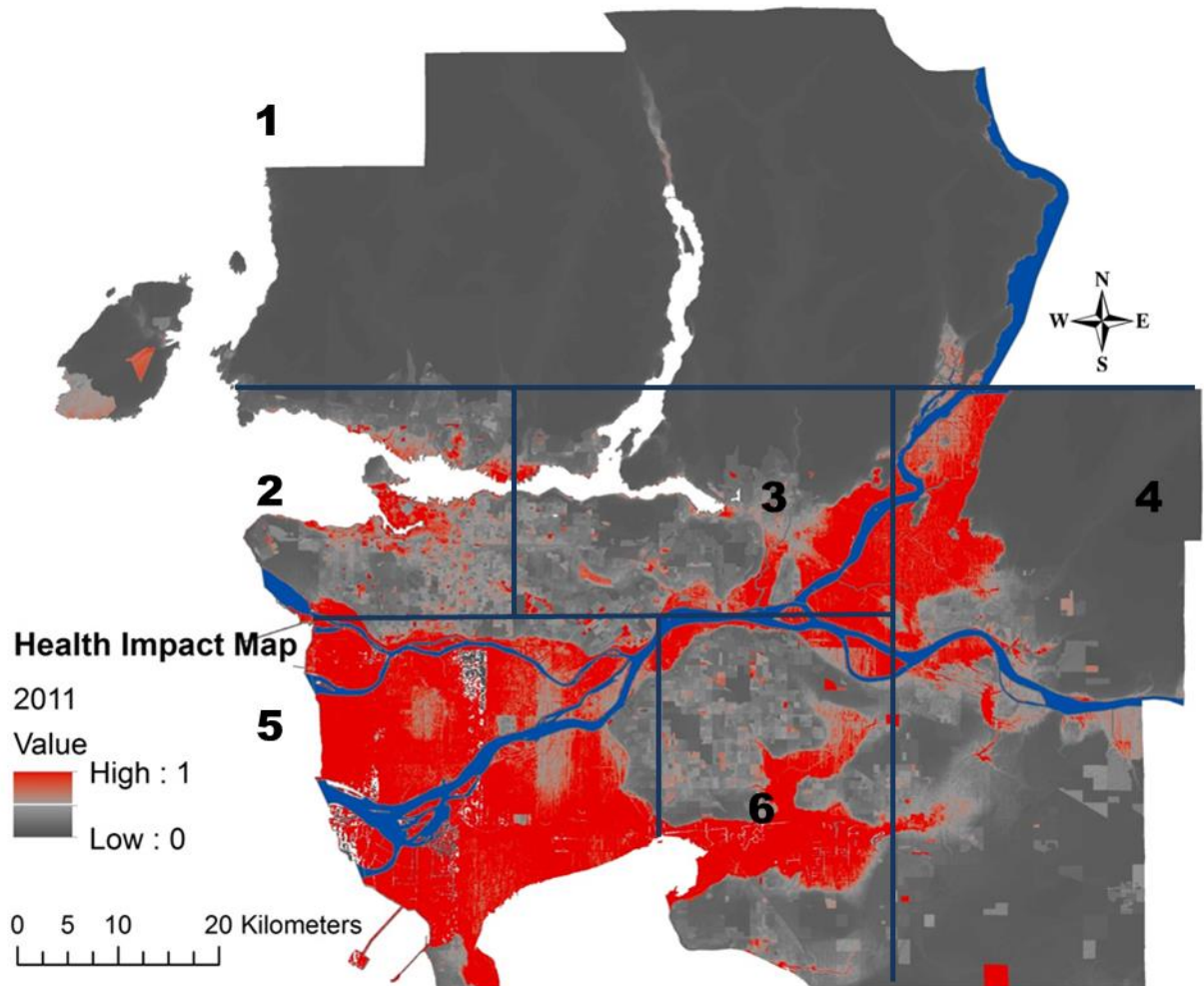


Figure 53 Human health impact map generated for Metro Vancouver for 2011.

The linear spatio-temporal extrapolation and auto regressive spatio-temporal extrapolation models presented in Section 3.5. 2 were applied to generate a future health impact map for 2050. Most of the sea level rise projections are focused on 2100 and 2050. Because there was a limited amount of historical spatial data for long term spatio-temporal extrapolation, the method was applied to project the year 2050 and the results are presented in Figures 54 and 55. The main sources of vulnerability include significant population increases in combination with land-use changes and the region's topography. One exception is in zone one, which remains sparsely populated and has a generally higher elevation. Disaster in the

long run is likely across most of Vancouver as the population continues to rise. Zone 5 is particularly vulnerable because of the significant degree human presence squarely in the midst of a floodplain.

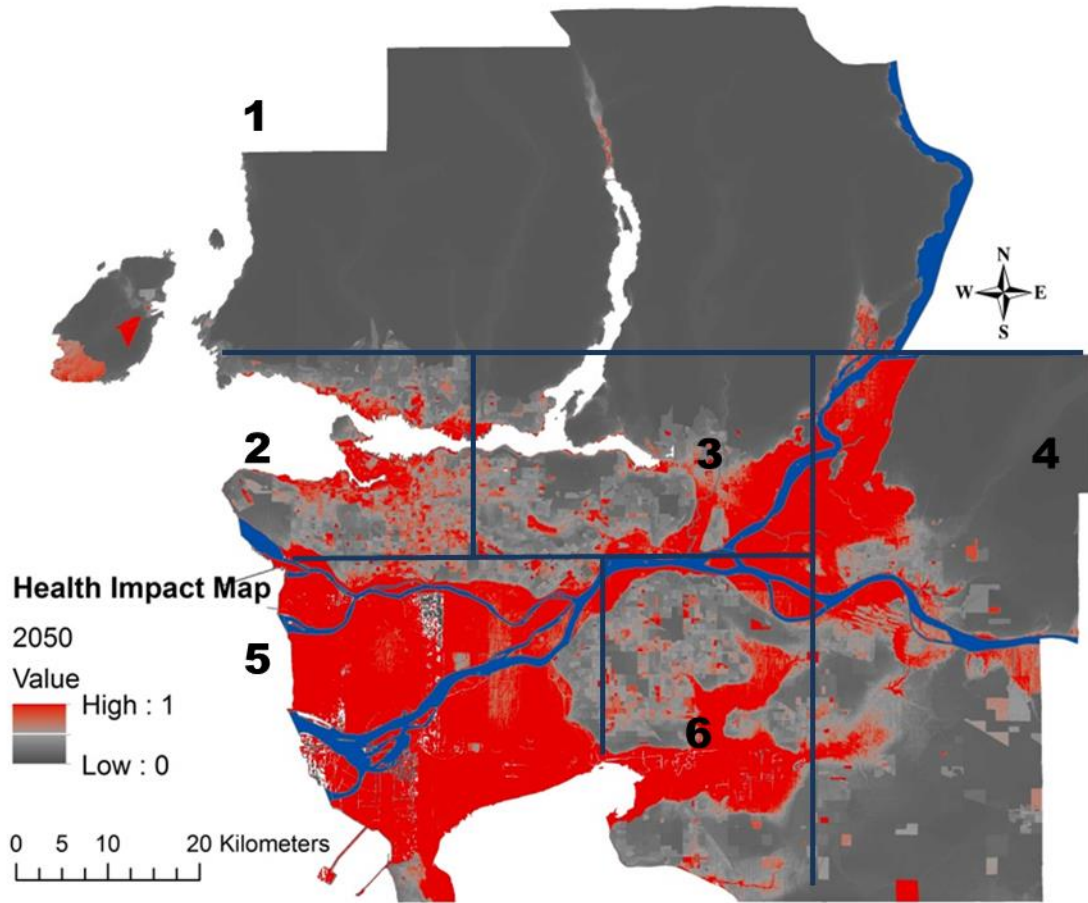


Figure 54 Human health impact map generated for Metro Vancouver for 2050 using linear spatio-temporal extrapolation.

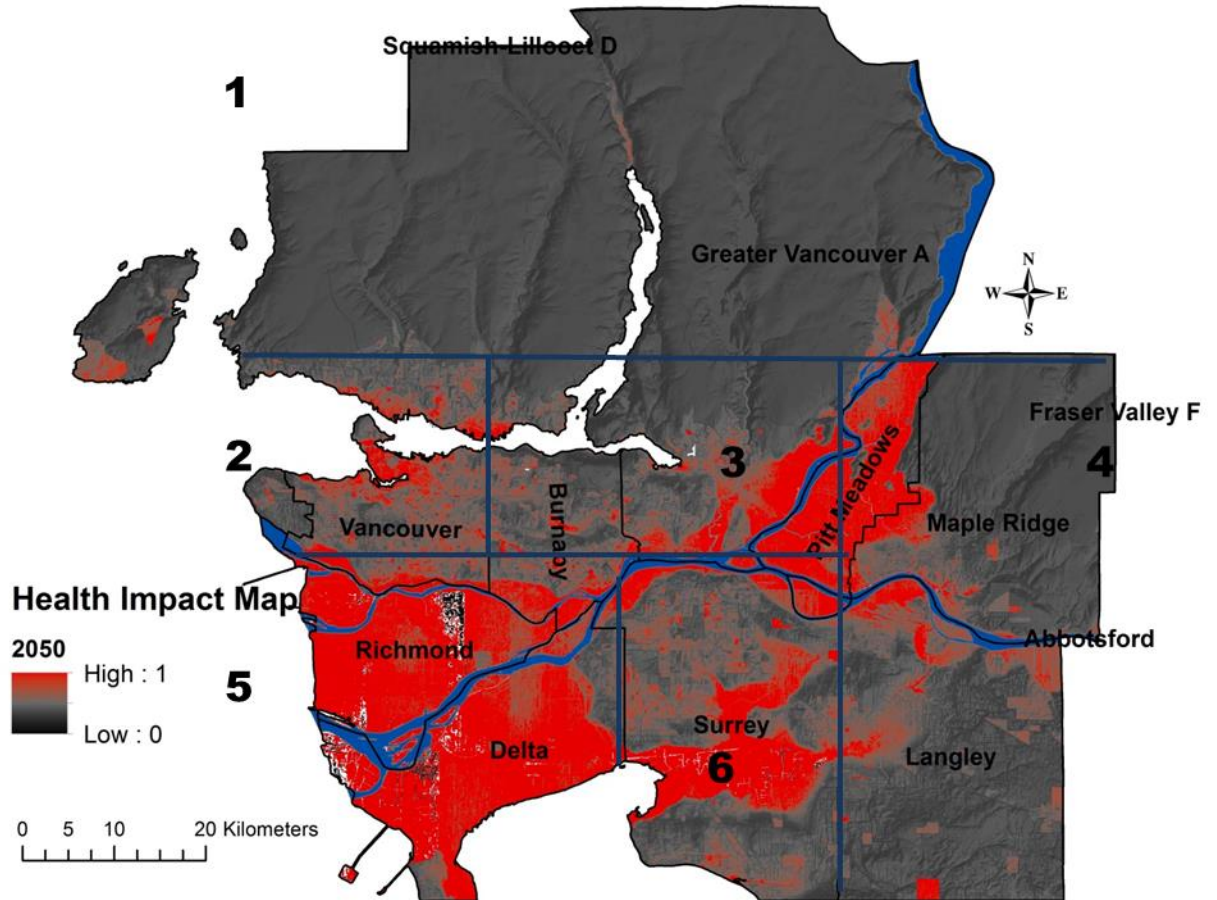


Figure 55 Human health impact map generated for Metro Vancouver for 2050 using auto regressive spatio-temporal extrapolation.

The next two figures provide a visual comparison for researchers and policy makers. A comparison of 1981 to 2011 is presented in Figure 56. It is clear that urbanization, associated with a significant increase in population and decrease in vegetation cover, is the main cause of the dramatic change in the extent of the vulnerable areas. Figure 57 compares the health impact maps between 2011 and the linear spatio-temporal extrapolations for 2050. It is notable that land-use planning and demographic distribution management two of the most important tasks that should be considered for near-term risk reduction planning.

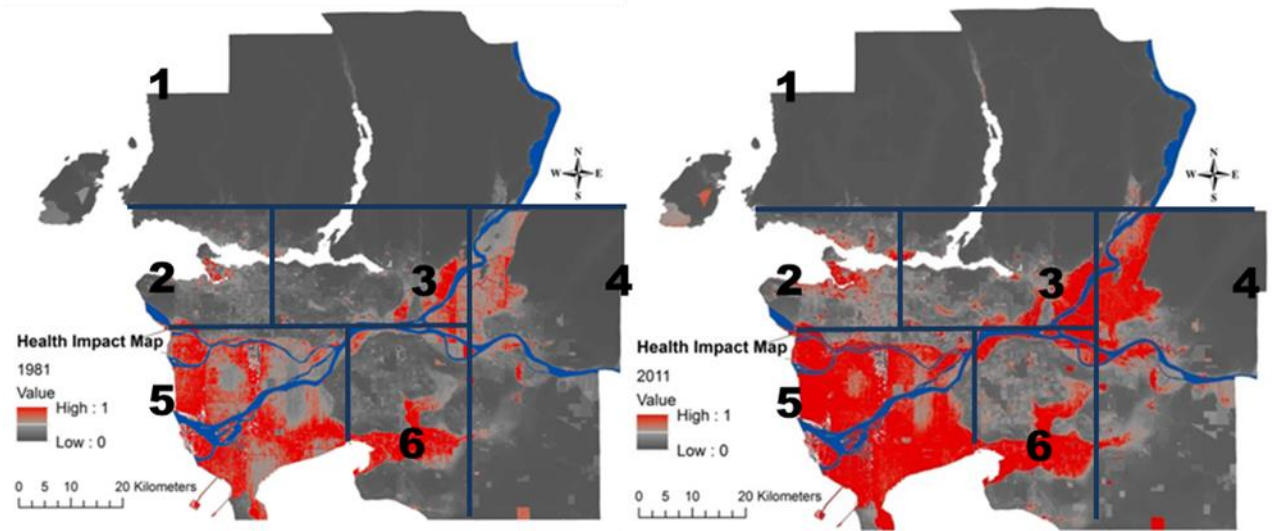


Figure 56 Comparison of the human health impact map between 1981 and 2011.

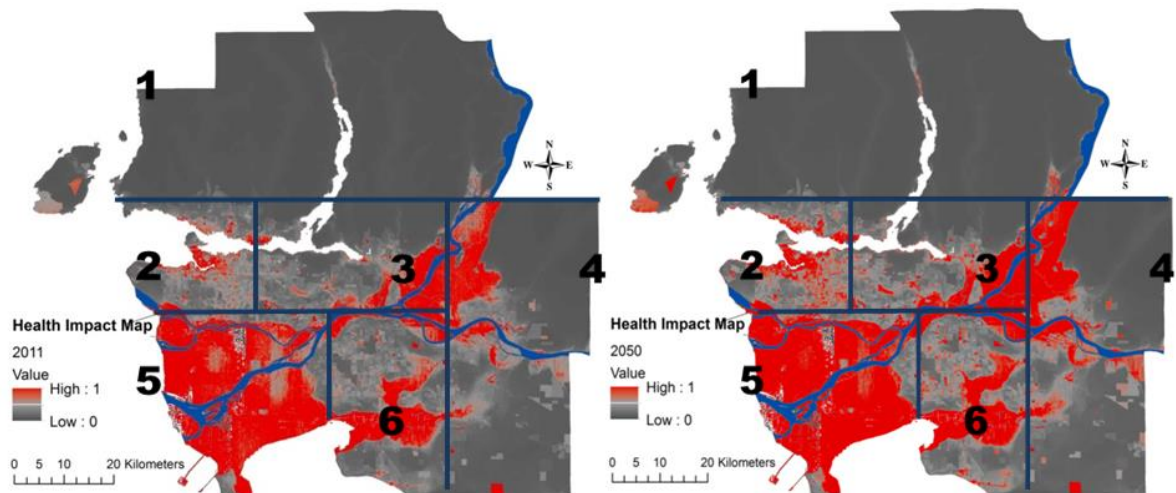


Figure 57 Comparison of the human health impact map between 2011 and 2050.

Figure 58 presents a comparison between the two final health impact map spatio-temporal extrapolations. Figures 59, 60, and 61 present detailed comparisons in different municipalities across the metropolitan area. The resolutions of each of these maps are 25 m^2 . In the linear extrapolations (left), the extent of the high risk areas (red regions) is greater than in comparison with the auto-regressive extrapolations (right). In these comparisons, it is clear that there is a notable increase in the extent of vulnerable regions in the overall projected health impacts when linear extrapolation is used. The use of a linear extrapolation provides

less reliable and detailed projections than the auto regressive model. Results for zones 2 and 3 are shown in Figure 59; the maps show an increase in potential climate related health impacts, mainly due to nonphysical health factors such as population density. Figure 60 contains the assessment of zone 5's floodplain. It should be noted that neither projection is significantly different from the one made for 2011. The main reason for this is that the topography of the region is not changing with time, and the areas are already prone to flooding and sea level rise. Figure 61 focuses on zones 3, 4, and 6, where nonphysical elements play a notable role and changes in potential health impacts over time can be seen as a result of population growth. The spatio-temporal extrapolation procedures provide researchers and policy makers with a methodology that facilitates the investigation of potential climate change-related impacts in time and space.

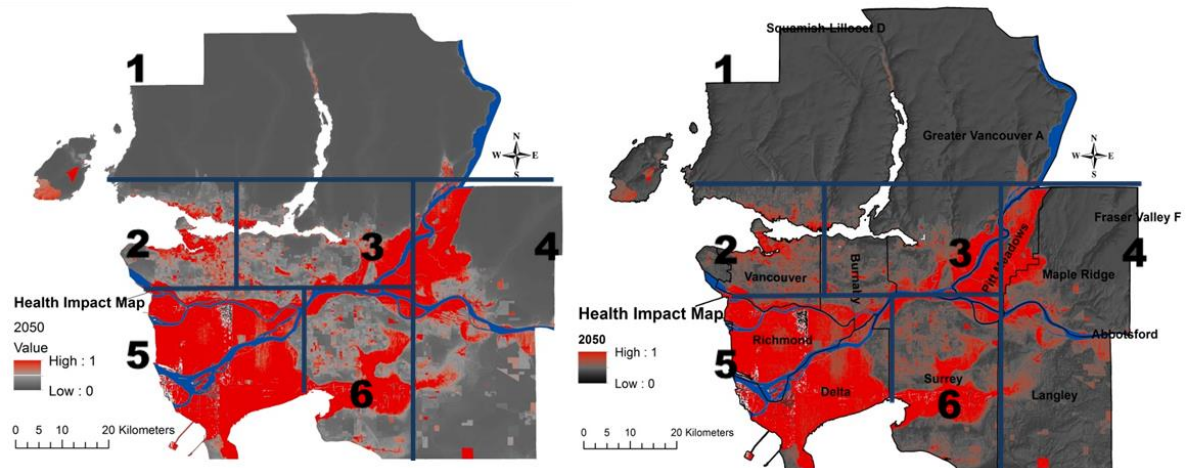


Figure 58 Comparison between linear spatio-temporal extrapolation (left) and auto regressive spatio-temporal extrapolation (right) for Metro Vancouver.

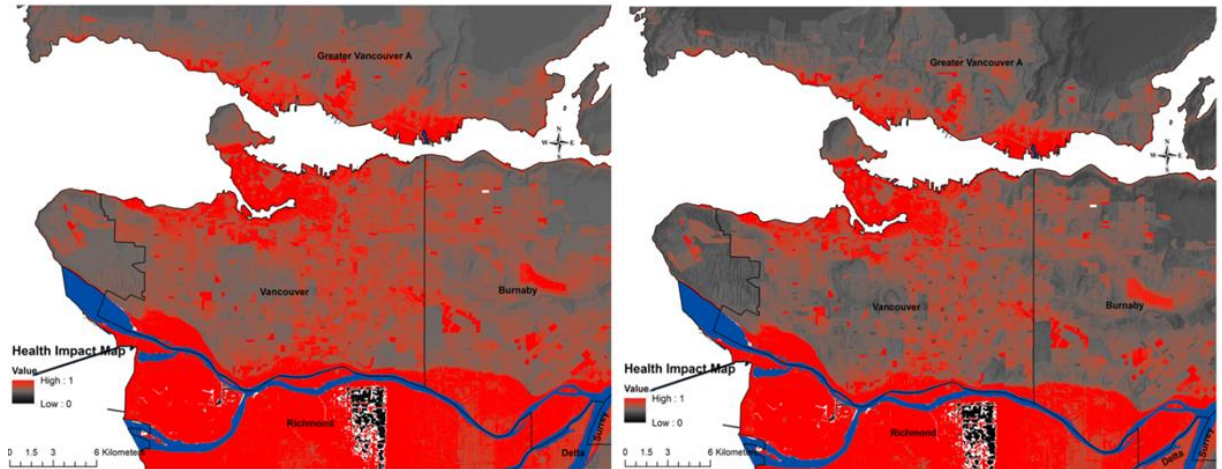


Figure 59 Comparison between linear spatio-temporal extrapolation (left) and autoregressive spatio-temporal extrapolation (right) for the cities of Vancouver, North Vancouver, West Vancouver and Burnaby.

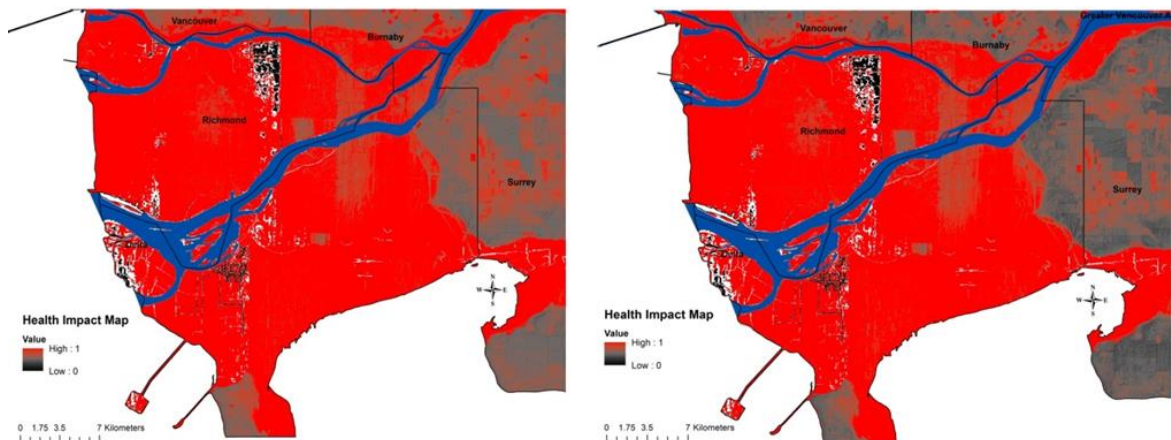


Figure 60 Comparison between linear spatio-temporal extrapolation (left) and autoregressive spatio-temporal extrapolation (right) for the Cities of Richmond and Delta.

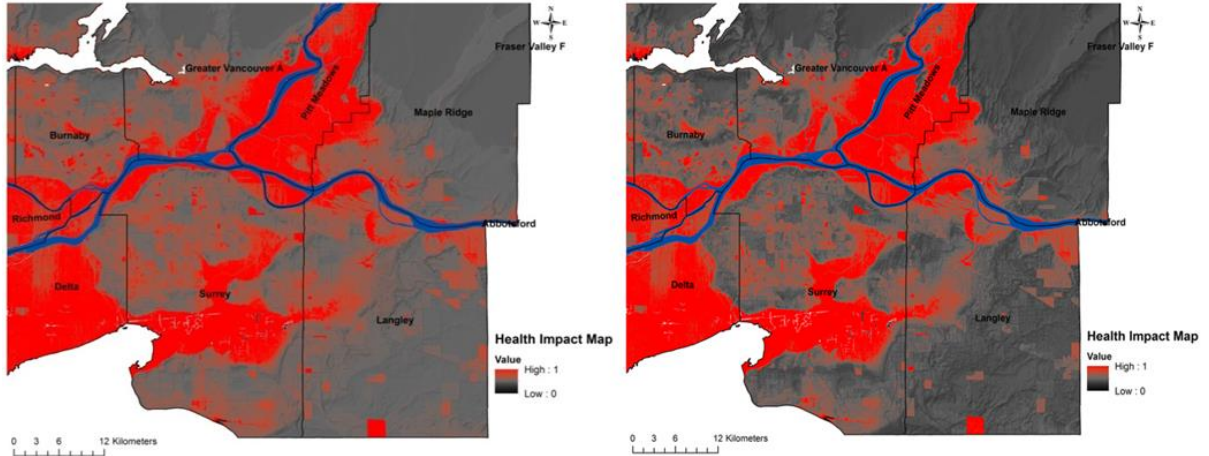


Figure 61 Comparison between linear spatio-temporal extrapolation (left) and autoregressive spatio-temporal extrapolation (right) for the Cities of Surrey, Langley, Pitt Meadows, Burnaby, and Maple Ridge.

Health impact maps can be used as a stand-alone measure for future climate change-related adaptation policies and to explore which adaptation measures might have the greatest impact during the course of a disaster. These maps are provided in high resolution format for detailed urban planning and decision making. One way for engineers and decision makers to utilize these maps is to overlay essential infrastructures that are either existing or planned in order to determine an efficient and optimal layout that addresses different sources of vulnerability. Essential infrastructures to be considered include health care facilities, major roads, major pipelines, educational facilities, and hydraulic infrastructure.

There are very few investigations relating to the potential impacts of climate change on health facilities. It is partly because accurate epidemiological data regarding which facilities cater to which health care services are often incomplete or out dated even though, it is essential to have some understanding of the health consequences associated with the potential impacts of climate change (e.g. flooding). The World Health Organization’s “Hospitals Safe in Emergencies” and the United Nations International Strategy for Disaster Reduction (UN/ISDR) initiative “Safer Hospitals” are both campaigns that focus on protection of health infrastructures and hospitals.

Figure 62 shows an overlay of the available healthcare facilities including hospitals, long-term care centers, nursing stations, outpatient clinics and community health centers across

Metro Vancouver (Blue circles). Black lines represent all of the major roadways and highways in Metro Vancouver. Both have been overlaid on the 2011 health impact map. This procedure provides a good indication about where some of the more vulnerable infrastructure assets are located. The roads along the Fraser River in Richmond or Delta including Vancouver Blaine highway, highway 17 (SFPR), East West connector, and Marine Drive are highly vulnerable in terms flooding and it is clear that a few of these roads provide the main access route for several of the area's major healthcare facilities. There are also two main roads including Pacific Highway and 152nd street connecting Surrey's northern and southern sections which cross major floodplains.

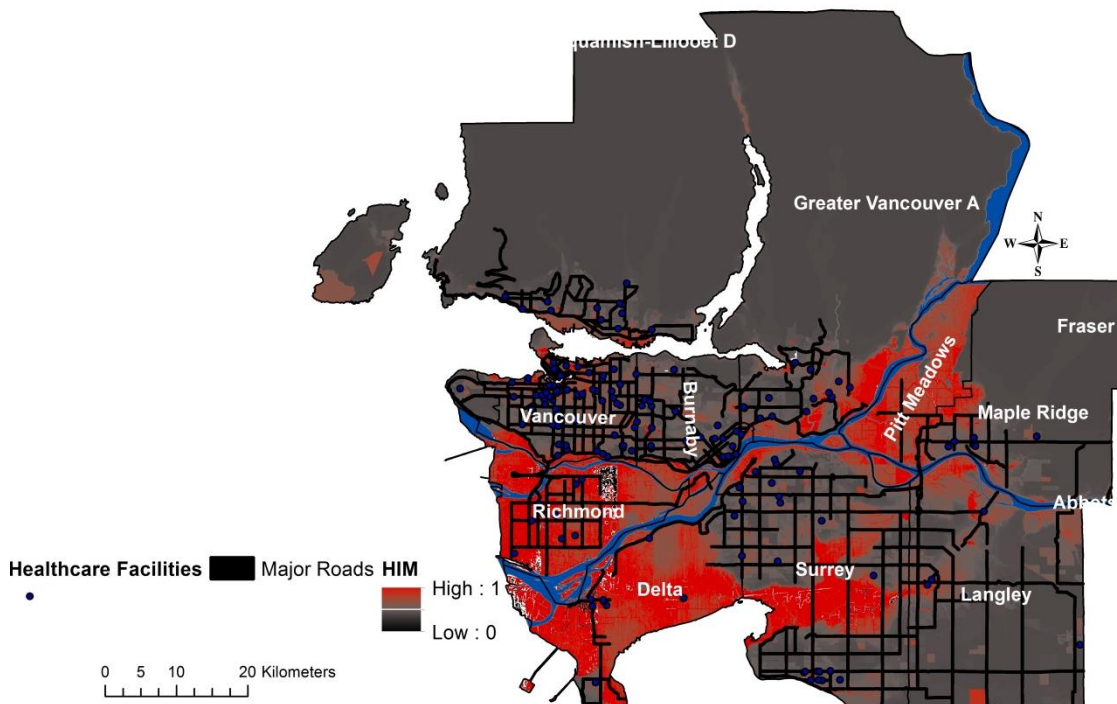


Figure 62 Healthcare facilities, major roads and highways overlaid onto the health impact map for 2011.

An important land-use planning issue involves the use of building footprints. A building footprint is a polygon that represents the rooftop of a detached building and includes features such as city hall, fire stations, schools, churches or police stations. Figure 63 presents existing building footprints across the metropolitan area which are overlaid on top of the

2011 health impact map. It is clear from the map that there are a significant number of residential buildings along the Fraser River and in floodplain areas. It is important that a significant effort be made to educate people about the increased probability of flood events due to climate change. In the northern part of Richmond there are a significant number of residential areas located close to the river bank which are highly vulnerable to flooding. There is a similar situation in northern part of Delta and the southern part of Burnaby. In zone two in particular the Vancouver downtown area, the building footprints indicate the size of the impervious area. Thoughtful planning, design and monitoring of urban drainage and flood control systems should be considered for this high density residential area.

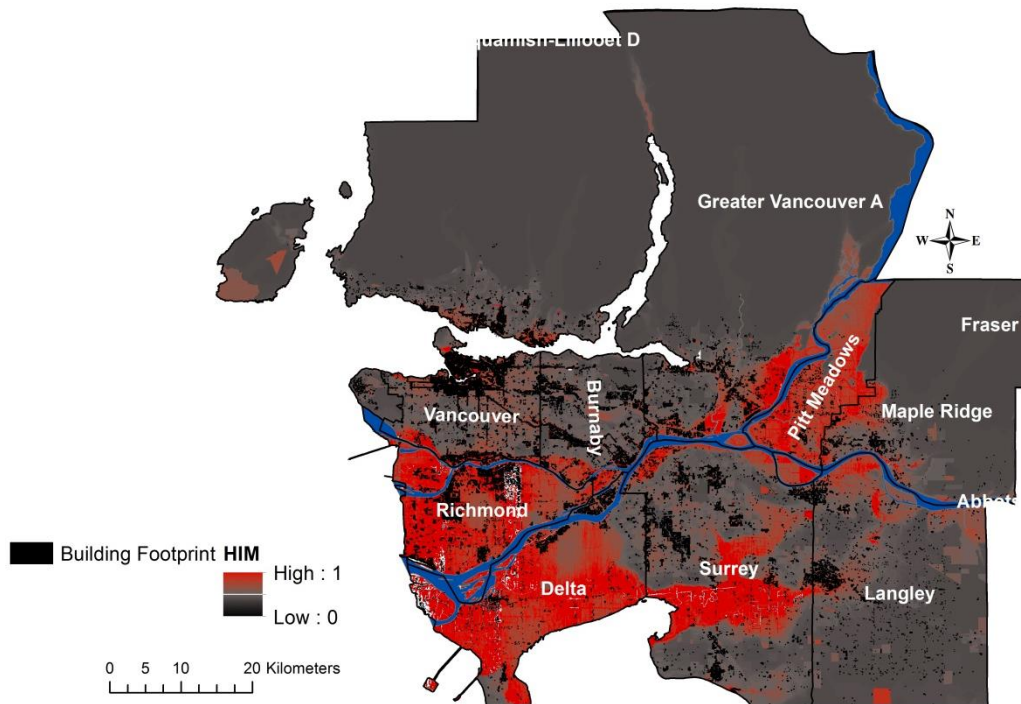


Figure 63 Building footprints and health impact map for 2011.

The education layer contains elementary schools, high schools (secondary schools), universities, and colleges. During catastrophes, schools can play an important role as they may be used to provide shelter, gathering areas, and places for food distribution. For resilience planning, safe and less vulnerable schools should be identified and be equipped, in terms of providing services during extreme events. Figure 64 presents the location of various

schools across the Metropolitan area overlaid on the health impact map for 2011. The city of Surrey, which has had the highest rate of population growth in the last 30 years has wisely located educational facilities at higher elevations and in less vulnerable areas as compared to Delta and Richmond.

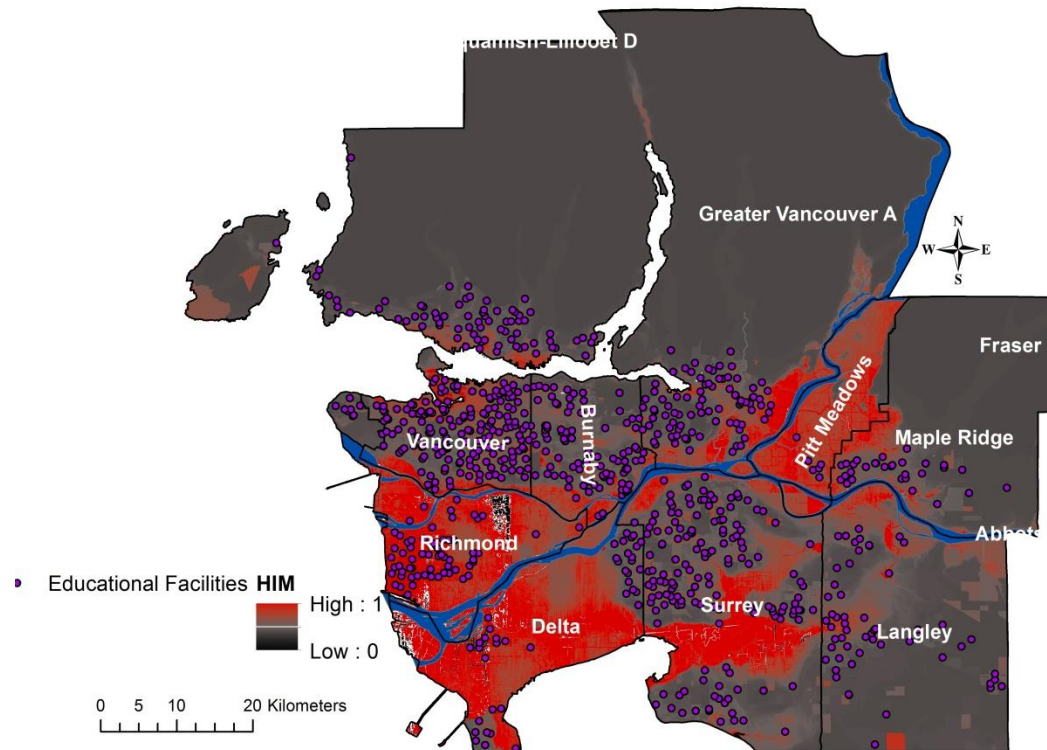


Figure 64 Elementary Schools, High Schools (secondary schools), Universities, Colleges and the health impact map for 2011.

Other important types of infrastructure in terms of flooding and sea level rise are structures that provide flood and hydraulic control. Hydraulic infrastructure is classified as any feature relating to the surface water (except the waterbodies and rivers themselves), for example dams, dykes, reservoirs, seawalls and wharfs. Figure 65 presents the location of these infrastructures based on 2011 Metro Vancouver data. Because the flood inundation map does not provide any information regarding the flow depth, it is not possible to provide any detailed recommendations about the performance of each structure; a detailed high resolution hydraulic model would be required to perform this task.

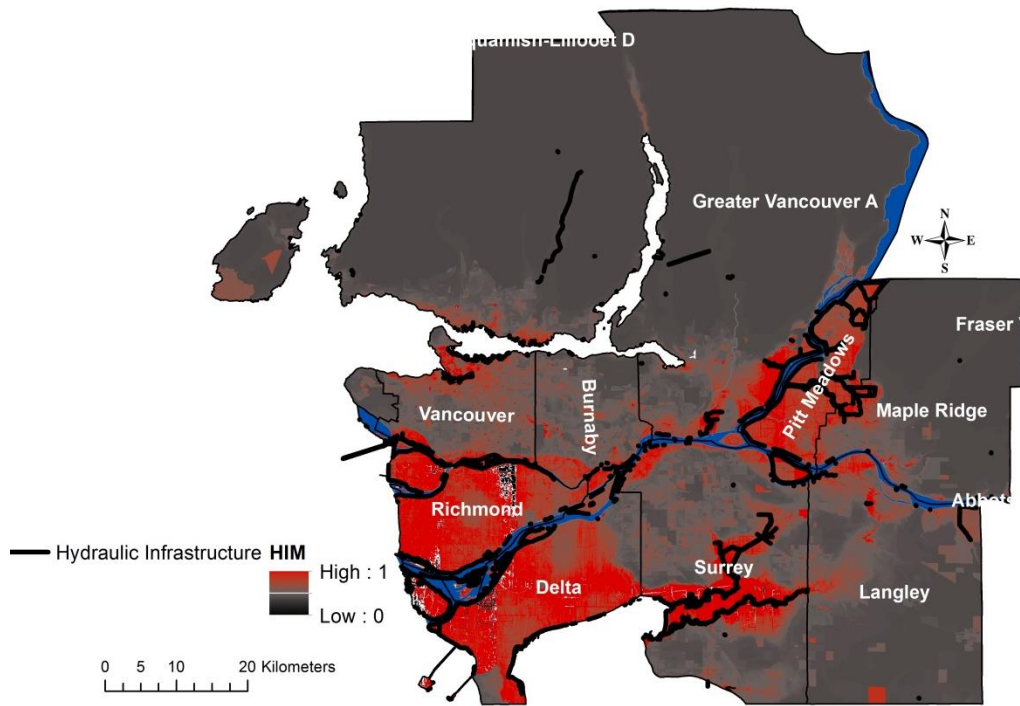


Figure 65 Hydrographic structures and health impact map for 2011.

Vegetation cover is one of the main ways to decelerate flood velocity and reduce damages. Based on the available spatial information on existing parks and recreation areas, it is clear that Richmond and Delta (which are the most vulnerable municipalities) have the smallest proportion of vegetated area (Figure 66). Vancouver and Burnaby have a better balance of residential areas versus parks and recreational areas.

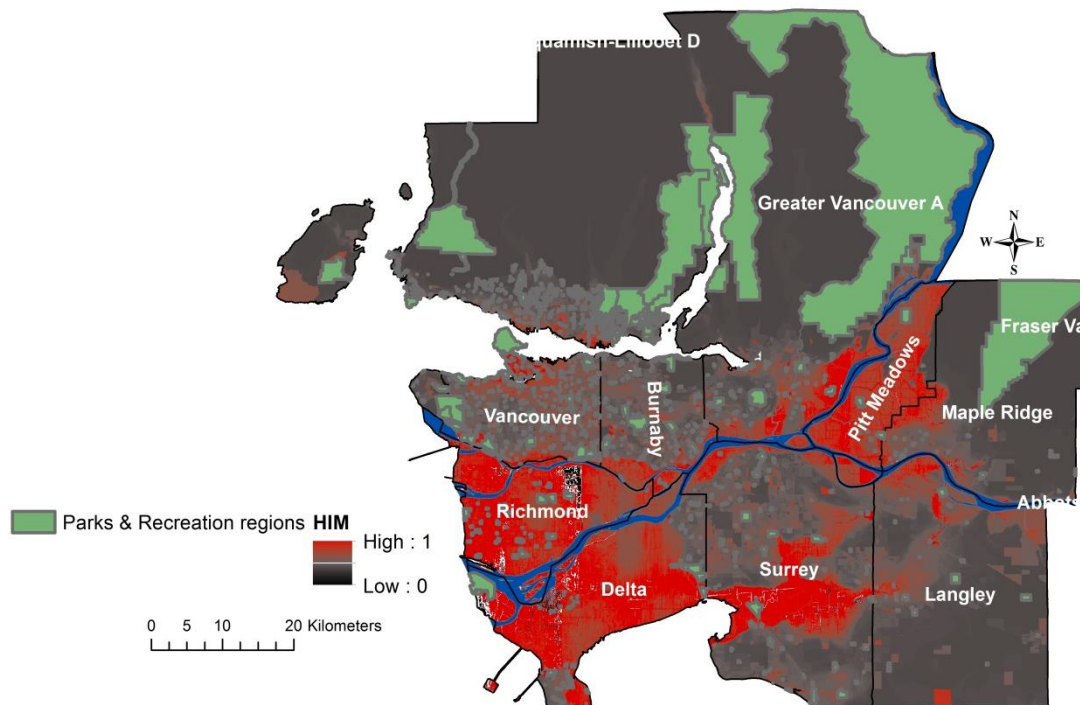


Figure 66 Parks & Recreation regions and health impact map for 2011.

Water and electricity are two essential needs of people living in cities. Therefore the location, direction and the size of each major pipeline, cable and power transmission line need to be taken into consideration, and emergency substitute supports should be considered in order to supply resources following a disaster. Figure 67 provides the location of the main water pipelines and power transmission facilities, overlaid on the health impact map for 2011. The northernmost yellow lines are major water pipelines which bring the water from three main reservoirs (Capilano, Seymour, and Coquitlam). There are also other major pipelines and

electrical transmission lines that cross over the Fraser River in Delta and Richmond which are located in the floodplain.

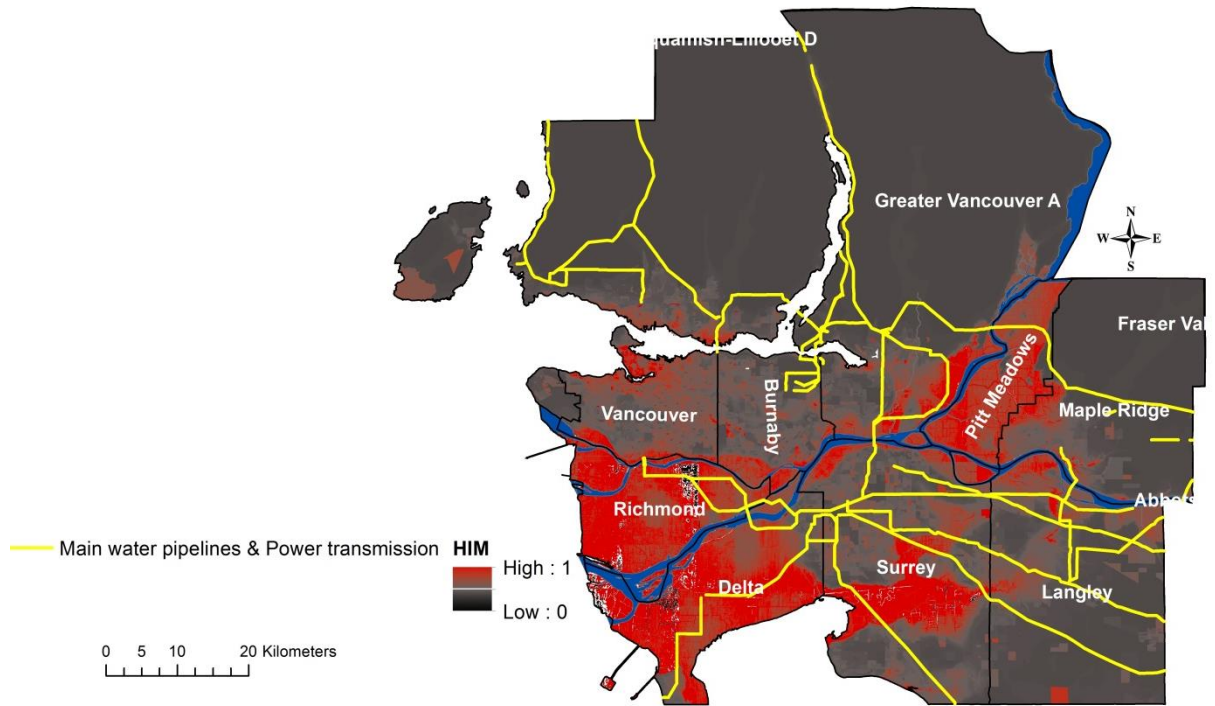


Figure 67 Water pipelines and power transmission and health impact map for 2011.

Chapter 6

6. Conclusions

This chapter addresses the three research questions and provides a list of recommendations for future work.

6.1 Lessons learned in the shift from qualitative to quantitative climate change-related health impact assessment for city resilience studies

The need to move from primarily qualitative data to more quantifiable inputs as they relate to health, economics, and other sociological conditions is becoming ever more apparent as urban planners make preparations for climate change and the impacts these are going to have on urban communities is becoming well accepted. Using the concept of resilience, which is of use in such plans, requires the use of quantitative inputs. This research is a first attempt at trying to establish a methodology that will fit the needs for quantifying data in order to allow for the more holistic modeling that is becoming available. Much of the difficulty lies in being able to find data sets such as census data and burden of disease, in a standardized fashion that is widely available and able to be applied to other urban settings.

The important question is how to address or adapt different mitigation and adaptation strategies to a different hazards using various sources of spatio-temporal quantitative data. Various physical and non-physical spatio-temporal data related to various hazards have different units and values. Therefore, normalization and re-standardization needs to be applied before integration and assessment can be performed. The same approach of spatial normalization and re-standardization could be implemented for all relevant impacts. Then the generic impact assessment approach can be implemented using dimensionless input data. .

For Vancouver the census data is relatively robust, as is the burden of disease and although the estimates still have a degree of uncertainty associated with them they are useable in this context. The same may not be true for other coastal mega-cities where even accurate population data is hard to come by let alone being able to convert the data to spatial dispersion and provide these same data over a reasonable number of time frames to allow for

a more dynamic appreciation of the issues. The development of tools to assist disaster planners and policy makers in selection of mitigation and adaptation measures is becoming more and more of a priority as climatic conditions continues to change and urban populations continue to grow. Assessment of climate change impacts on human health in urban environments is a complex procedure. There are limited data sources and consequently, limited final outcomes. The initial research assumptions made are very important and have a direct impact on final outcomes. Climate change impacts human health and the determinants of health in a very complex way. It is essential to cover all of the potential sources of climate change-related impacts on human health in urban environments for a comprehensive health impacts assessment. A spatio-temporal health impact assessment is required to ensure consideration of important space and time aspects of the problem.

Currently, resilience is an important concept related to urban disasters and risk management. The resilience approach is designed to integrate physical, economic, health, social and organizational impacts of climate change in urban environments. This spatio-temporal health impact assessment is itself resilient enough to fit into a broad array of city resilience planning activities. One of the key research objectives of this study has been to investigate how to deploy spatio-temporal health impact assessments across a comprehensive city resilience simulation model (Simonovic and Peck, 2013). This model scrutinizes climate change adaptation options and considers mechanisms for the integration of various impacts of climate change-related disasters.

The spatio-temporal assessment presented in Chapter 3 demonstrates that the output of the assessment takes into account important characteristics such as the total population density, senior population density, children population density, burden of diseases conditions and the potential physical impacts. It considers historical and existing physical and nonphysical elements in an appropriate manner. Through the use of spatio-temporal extrapolation methods, the future behavior of the same key spatial variables can be projected.

The spatio-temporal assessment presented in chapter 3 has been implemented for Metro Vancouver, British Columbia, Canada. The output of this study provides a more fully integrated view of population health to allow for the development of more targeted strategies that deal with adaptation and risk reduction at a local level for Metro Vancouver. This

methodology has been applied using spatial and temporal data for 7 years, 1981, 1986, 1991, 1996, 2001, 2006 and 2011 in order to give a dynamic simulation of health impacts. The final maps indicate that the Richmond and Delta districts of Metro Vancouver are the most vulnerable to climate change-related sea level rise and flooding in comparison to the other municipalities. This research also demonstrates how composite health impact maps can be used both as an input for resilience modeling, as well as for stand-alone product that can be utilized in the assessment and development of health related mitigation and adaptation strategies for different cities.

6.2 Types of spatio-temporal data required for quantitative assessment

The focus of this research also deals with the selection of appropriate sources of spatio-temporal data to be utilized in this complex quantitative approach and the integration of these various data sources. For answering this comprehensive question the following two important tasks need to be focused:

- Consider the prioritization of different spatio-temporal data sources and how their selection may impact the final assessment results.
- Application of different types of spatio-temporal data with different units and resolutions.

Different sources of physical and nonphysical data have been used for this spatio-temporal health impact assessment. Land-use changes, topography characteristics and flood inundation maps are the main sources for interpreting potential physical impacts. Total population density, senior population density, children population density, and burden of diseases condition including communicable diseases, non-communicable diseases and injuries have been considered as the potential nonphysical impacts. The wide range of spatio-temporal data used in the methodology provides researchers with an opportunity to increase the accuracy of resilience planning at the city level by taking more factors into consideration.

Over the last three decades, urbanization has occurred at a rapid pace worldwide and deforestation of newly urbanized areas is common. From a conservation point of view, urban

planning is essential in the development of urban areas to ensure appropriate measures are taken to reduce the negative effects of urbanization on people and the environment. Due to an increase in impermeable areas, precipitation moves more quickly into stream beds, reducing the time to peak and producing higher peak flows in the drainage channels.

Developing a time series vegetation condition map is an essential step for any specific land-use change analysis research. Remote sensing data and techniques give researchers a chance to extract different type of land-use features including alterations in vegetation coverage across the last three or four decades (depending on satellites function and availability). Detailed NDVI calculations presented in Chapter 3 have provided an approach that can be applied to different cities world-wide. Satellite image sources (NOAA-AVHRR and SPOT-VGT) that have been presented in this research are freely available so image noise reduction, comparison and replacement of the images are possible. This approach has been implemented in the Metro Vancouver area from 1984 to 2012. The results of the vegetation analysis show the significant changes in some part parts of the city, including Surrey and Burnaby, have occurred over the last 28 years. With the help of remote sensing technology, the Metro Vancouver area could be studied efficiently in less time than as compared to conventional methods. To update the land-use database in the region, more recent and higher-resolution satellite imagery will be required together with the land-use classification.

The case study is an example of how remote sensing technology can help in understanding the development patterns of an area and their effects on the flood regime. Therefore, this technology is useful for development of conservation policies dealing with land-use in urban areas. In summary, vegetation analysis and conservation are important factors that influence human health and flood emergency management in mega-cities. It is important to increase the capacity of mega-cities to successfully adapt and cope with risks posed by the effects of climate change.

In the case of any potential flooding or sea level rise, topographic characteristics and flood inundation maps are also playing an important role in identifying vulnerable areas in the urban environment. Mega-cities are dealing with a number of municipalities and sectors just as a burgeoning population adds its own challenges. Up-to-date flood inundation maps are increasingly important. Chapter three has suggested ameliorations for critical sectors of the

twenty-first-century mega-city: flood-prone areas identification and hazard grading from remotely sensed elevation datasets. In this method, 4 different available DEM data sources—SRTM, ASTER GDEM, USGS and CDED—have been presented. Flood inundation maps for different cities all over the world can be generated using the presented DEMs, open source GRASS software and *r.hazard.flood* add-on extension modules. Metro Vancouver is also facing the same challenge in maintenance of an up-to-date its flood inundation map. The methods outlined have been implemented the Metro Vancouver area using SRTM and CDED data. The results show that the cities of Richmond and Delta are highly vulnerable to flooding but there are also areas in Surrey, Pitt Meadows and North Vancouver that are highly vulnerable to inundation.

The case study is an example of how the proposed methods can help in understanding how the development of flood prone areas impact public health. Developing a flood inundation map is an essential step in development of a spatio-temporal human health assessment that can be used for flood emergency management in mega-cities.

For this holistic assessment it is important to consider spatial and temporal variations in conditions related to population distribution and burden of disease in the city. Therefore, total population density, senior population density, and children population density calculations presented in Chapter 3 can be implemented using small, comparatively stable geographic units (e.g. dissemination area and census tract data) in each city. All three potential social conditions have been implemented in Metro Vancouver for the seven census years 1981,1986,1991,1996, 2001, 2006, and 2011. The results show that Vancouver has the highest total population density and Surrey has the highest rate of population growth in the last 30 years.

The study develops a technique for the development of spatio-temporal health impact assessment for use with the city resilience system dynamics simulation model. The main focus of the methodology is in the application of DALY estimates as a measure of the baseline burden of disease and combing these results with potential physical and social health impacts. Flood related health risk can be defined as the exposure of the various segments of the population to three different health impacts of inundation (communicable and non-communicable diseases, and injuries) caused by climate change-related riverine flooding and

sea level rise. The major shortcoming of this definition may well be apparent: the DALY estimates are for the country as a whole and are not broken down for urban populations.

However, the majority of Canada's population now resides in urban environments. If some local knowledge is available that indicates disease rates are exceeding the national average in urban settings, this could be used to modify the input into the spatio-temporal process. The data are based on population numbers, and the accuracy of population estimates varies from city to city depending on the country. For example, the City of Vancouver has more accurate population data than Lagos, but the goal is to use the same method for calculation for the burden of disease in any city to allow for assessment of resilience in the future. The main advantages of this approach are that it is feasible and the basic data selected are available for most countries. The results provide an informative picture of the baseline burden of disease in three major disease categories for any selected case study.

After quantifying all physical and nonphysical elements and dealing with their different units and resolutions, the resultant maps have been rasterized, normalized, and standardized between 0 and 1. Once this has been accomplished integration is possible in two phases. First, nonphysical impacts can be integrated into one map for each year. The presented approach provides an opportunity for engineers and policy makers to apply different weights to different elements based on the perceived priority and importance of each element. The generated nonphysical health impact map can then be integrated with the physical conditions including flood inundation areas, topography and vegetation cover, all of which are also standardized between 0 and 1 using Equations 10 and 11. When all the spatial data inputs have been rescaled between 0 and 1, then by general integration formula 3.19, the final health impact maps (HIM) for each year are created. Likewise, another set of weight coefficients are utilized to assign priority to the physical vs nonphysical inputs.

The detailed integration steps described in this work have been implemented for the spatial data collected for Metro Vancouver. The resulting health impact map (HIM) for each year presents areas which have higher population densities and shows where lower elevations along the floodplains and coast are more vulnerable compared to other parts of the city.

6.3 Use of the final outcomes of this approach in the comparison of short and long term climate change adaptation policies

This research presents a methodology using spatial and temporal analysis to generate a health impact map. This tool has significant potential for selection of appropriate adaptation strategies to address climate change-related natural disasters in different cities. Application of the physical, health and social vulnerability assessment to climate change-related flooding using remote sensing, GIS, and mapping techniques have enabled a quantitative assessment of the health risks of each sector and each district for Metro Vancouver, Canada.

The human health impact map can be used as a stand-alone product to determine which regions might experience the greatest impact during a flooding-related disaster. By overlaying different infrastructure onto the health impact map, identifying the more vulnerable infrastructure components which are located in highly vulnerable areas is possible. The methodology has enabled quantitative assessment of vulnerable areas using available spatial data for Metro Vancouver for the seven years 1981,1986,1991,1996, 2001, 2006, and 2011. After generating a set of temporal health impact maps, the extrapolation of health impact maps for the near future is possible using different spatio-temporal extrapolation techniques. For this, linear and auto-regressive spatio-temporal models have been employed to develop Metro Vancouver 2050's health impact map. The purpose of this tool is to assist mega-cities in development of risk maps that can help in developing more targeted adaptation and risk reduction strategies at a local level. The methodology is flexible and allows cities to select the relevant data and change the weighting of each data input based on local concerns. The integrated health impact mapping approach is shown to be a useful tool to guide long-term sustainable development in coastal mega-cities.

6.4 Recommendations and future works

The recommendations in this section focus on how the outcomes of this assessment can be improved. In both physical and nonphysical sections of the presented spatio-temporal assessment, potential areas for improvement include:

- Using higher resolution satellite images like Landsat and ASTER for developing land-use change maps. The square-kilometer resolution from NOAA-AVHRR and SPOT-VGT images is fairly coarse for assessment of land-use change in urban environments, however they are the only freely available source (and have been globally available for about thirty years).
- Developing a complete hydrologic and hydraulic model for identifying vulnerable flood prone areas to develop more accurate flood inundation maps. The outcome of a hydraulic mapping procedure could help determine both the extent of flooding and the potential depth of flooding in different regions.
- DALY numbers are based on national data for different countries. Finding local burden of disease information for cities could significantly help improve the final outcomes of the assessment.
- Census tract and dissemination areas are at fairly coarse resolutions in terms of monitoring demographic assessments. Therefore the use of more detailed spatial population data could help improve the accuracy of the final health impact map and would give policy makers a better indication of population related issues.
- To increase the accuracy of the spatio-temporal extrapolation of the final health impact map, it is essential to collect as much accurate historical spatial data as possible. The more robust and historically informed the data set, the greater the certainty of the projected outcome.
- This approach deals only with hydro-meteorological components of climate change (sea-level rise and flooding). To develop a more accurate assessment of climate change related health risks, some consideration of temperatures should be made. Heat waves are another important source of climate-related health impacts that have not been considered in this assessment.

References

- Abaya, S. W., Mandere, N., & Ewald, G. (2009). Floods and health in Gambella region, Ethiopia: a qualitative assessment of the strengths and weaknesses of coping mechanisms. *Global health action*, 2.
- Achard, F., & D'Souza, G. (1994). *Collection and pre-processing of NOAA-AVHRR 1km resolution data for tropical forest resource assessment*. European Commission.
- Adelekan, I. O. (2010). Vulnerability of poor urban coastal communities to flooding in Lagos, Nigeria. *Environment and Urbanization*, 22(2), 433-450.
- Agam, N.(2014). "Development Of Inundation Maps For The Vancouver Coastline Incorporating the Effects of Sea Level Rise and Extreme." *University of Western Ontario - Electronic Thesis and Dissertation Repository*. Paper 2613. <http://ir.lib.uwo.ca/etd/2613>
- Ahern, M., Kovats, R. S., Wilkinson, P., Few, R., & Matthies, F. (2005). Global health impacts of floods: epidemiologic evidence. *Epidemiologic reviews*, 27(1), 36-46.
- Akter, T., & Simonovic, S. P. (2005). Aggregation of fuzzy views of a large number of stakeholders for multi-objective flood management decision-making. *Journal of Environmental Management*, 77(2), 133-143.
- Alderman, K., Turner, L. R., & Tong, S. (2012). Floods and human health: a systematic review. *Environment international*, 47, 37-47.
- Allan, R. P., & Soden, B. J. (2008). Atmospheric warming and the amplification of precipitation extremes. *Science*, 321(5895), 1481-1484.
- Arkema, K. K., Guannel, G., Verutes, G., Wood, S. A., Guerry, A., Ruckelshaus, M., ... & Silver, J. M. (2013). Coastal habitats shield people and property from sea-level rise and storms. *Nature Climate Change*, 3(10), 913-918.
- Arnell, N. W. (2004). Climate change and global water resources: SRES emissions and socio-economic scenarios. *Global environmental change*, 14(1), 31-52.

- Arrieta, M. I., Foreman, R. D., Crook, E. D., & Icenogle, M. L. (2009). Providing continuity of care for chronic diseases in the aftermath of Katrina: from field experience to policy recommendations. *Disaster medicine and public health preparedness*, 3(03), 174-182.
- Balica, S. F., Wright, N. G., & Van der Meulen, F. (2012). A flood vulnerability index for coastal cities and its use in assessing climate change impacts. *Natural hazards*, 64(1), 73-105.
- BC Flood Safety Section. 2014. *Simulating the Effects of Sea Level Rise and Climate Change on Fraser River Flood Scenarios*. BC Ministry of Forests, Lands and Natural Resource Operations.
- BC Stats, 2010. Greater Vancouver Regional District: Community Facts (BC Stats: 250-387-0327). BC Government Ministry of Citizens Services, Victoria BC. <http://www.bcstats.gov.bc.ca/pubs/qrs/rd15.pdf> (Accessed Oct 2012).
- Berelowitz, L. (2010). *Dream city: Vancouver and the global imagination*. Douglas & McIntyre.
- Berkes, F., Folke, C., & Colding, J. (Eds.). (2000). *Linking social and ecological systems: management practices and social mechanisms for building resilience*. Cambridge University Press.
- Bezirtzoglou, C., Dekas, K., & Charvalos, E. (2011). Climate changes, environment and infection: facts, scenarios and growing awareness from the public health community within Europe. *Anaerobe*, 17(6), 337-340.
- Bivand, R. S., Pebesma, E. J., Gómez-Rubio, V., & Pebesma, E. J. (2008). *Applied spatial data analysis with R* (Vol. 747248717). New York: Springer.
- Bivand, R., Altman, M., Anselin, L., Assunção, R., Berke, O., Bernat, A., ... & Carvalho, M. (2015). Package 'spdep'.
- Bronstert, A. (2003). Floods and climate change: interactions and impacts. *Risk Analysis*, 23(3), 545-557.

- Brown, L., & Murray, V. (2013). Examining the relationship between infectious diseases and flooding in Europe: A systematic literature review and summary of possible public health interventions. *Disaster Health, 1*(2), 117-127.
- Campbell, J. B. (2002). *Introduction to remote sensing*. CRC Press.
- Canadian Digital Elevation Data (CDED) (2013)
<http://www.geobase.ca/geobase/en/about/index.html>. (Accessed Sep 2013)
- Cannings, R. J., & Cannings, S. G. (1996). *British Columbia: a natural history*. Greystone Books.
- Chalabi, Z., & Kovats, S. (2014). Tools for developing adaptation policy to protect human health. *Mitigation and Adaptation Strategies for Global Change, 19*(3), 309-330.
- Cheng, C. S., Li, G., Li, Q., Auld, H., & MacIver, D. (2007). Climate Change and Extreme Rainfall-related Flooding and Surface Runoff Risks in Ontario. Plain Language Summary Report, Climate Change Impacts and Adaptation Program. A901. *Toronto, Ontario: Environment Canada*.
- Chow, V. T. (1964). Handbook of applied hidrology: a compendium of water-resources technology. In *Handbook of applied hidrology: a compendium of water-resources technology*. McGraw-Hill.
- Christensen, J. H., & Christensen, O. B. (2003). Climate modelling: severe summertime flooding in Europe. *Nature, 421*(6925), 805-806.
- Church, J. A., Monselesan, D., Gregory, J. M., & Marzeion, B. (2013). Evaluating the ability of process based models to project sea-level change. *Environmental Research Letters, 8*(1), 014051.
- Commonwealth Health Minister's Update. Commonwealth Secretariat, Pro-Book Publishing: Suffolk, UK, (2009). Available online:
http://www.thecommonwealth.org/files/210353/FileName/CHMU2009_ebook2.pdf
 (Accessed Feb 2015).

- Consultants, N. H. (2008). Comprehensive review of Fraser River at Hope, flood hydrology and flows—Scoping study, Northwest hydraulic consultants, North Vancouver, BC, Canada.
- Cressie, N., & Wikle, C. K. (2011). *Statistics for spatio-temporal data*. John Wiley & Sons.
- Cunderlik, J. M., & Ouarda, T. B. (2009). Trends in the timing and magnitude of floods in Canada. *Journal of Hydrology*, 375(3), 471-480.
- Davison, J. (2013). Is Extreme Weather the New Normal? CBC News. August 8, 2013. Accessed from <http://www.cbc.ca/news/canada/is-extreme-weather-the-newnormal-1.1321493>. (Accessed Nov 2013)
- de Espindolaa, G. M., Pebesmab, E., & Câmara, G. (2014). Spatio-Temporal Regression Models for Deforestation in the Brazilian Amazon. National institute for space research (INPE), Brazil.
- DeFries, R. S., Asner, G. P., & Houghton, R. A. (2004). Ecosystems and land use change. *Washington DC American Geophysical Union Geophysical Monograph Series*, 153.
- Degiorgis, M., Gnecco, G., Gorni, S., Roth, G., Sanguineti, M., & Taramasso, A. C. (2012). Classifiers for the detection of flood-prone areas using remote sensed elevation data. *Journal of Hydrology*, 470, 302-315.
- Del Ninno, C., & Lundberg, M. (2005). Treading water: the long-term impact of the 1998 flood on nutrition in Bangladesh. *Economics & Human Biology*, 3(1), 67-96.
- DESA, U. (2009). Population Division of the Department of Economic and Social Affairs of the United Nations Secretariat, World Population Prospects: The 2008 Revision.
- Diaz, J. H. (2003). The public health impact of hurricanes and major flooding. *The Journal of the Louisiana State Medical Society: official organ of the Louisiana State Medical Society*, 156(3), 145-150.
- Dilley, M. (2005). *Natural disaster hotspots: a global risk analysis* (Vol. 5). World Bank Publications.

- Dodman, D., Bicknell, J., & Satterthwaite, D. (Eds.). (2012). *Adapting Cities to Climate Change: Understanding and addressing the development challenges*. Routledge.
- Duchemin, É. (2000). Hydroelectricity and greenhouse gases: Emission evaluation and identification of biogeochemical processes responsible for their production. *Dissertation, Université du Québec à Montréal, Montréal (Québec), Canada, 321*.
- EEA (2004), Signals 2004, “A European Environment Agency update on selected issues”, Office for Official Publications of the European Communities, Luxembourg.
- EM-DAT, C. R. E. D. (2010). The OFDA/CRED international disaster database. Université catholique.
- Eum, H. I., Simonovic, S. P., & Kim, Y. O. (2010). Climate change impact assessment using k-nearest neighbor weather generator: case study of the Nakdong River basin in Korea. *Journal of Hydrologic Engineering, 15*(10), 772-785.
- ESRI, (2014), <http://www.esri.com/> , (Accessed Sep 2014).
- ESRI, (2015), <http://www.esri.com/> , (Accessed Mar 2015).
- Evans, E. (2004). Foresight: future flooding: scientific summary: volume II: managing future risks. London: Dept. of Trade and Industry.
- Few, R., Ahern, M., Matthies, F., & Kovats, S. (2004). *Floods, health and climate change: a strategic review*. Norwich: Tyndall Centre for Climate Change Research.
- Foley, J. A., DeFries, R., Asner, G. P., Barford, C., Bonan, G., Carpenter, S. R., ... & Snyder, P. K. (2005). Global consequences of land use. *science, 309*(5734), 570-574.
- Forseth, P. (2012). *Adaptation to sea level rise in Metro Vancouver: a review of literature for historical sea level flooding and projected sea level rise in Metro Vancouver*. Adaptation to Climate Change Team.
- Fraser Basin Council (2013). *A Business Plan – Advancing a Collaborative, Regional Approach to Flood Management in British Columbia’s Lower Mainland*.

- Frei, C. (2003). Camouflage, bluff, or real? Statistical uncertainty of trends in catastrophic extremes.
- Friel, S., Bowen, K., Campbell-Lendrum, D., Frumkin, H., McMichael, A. J., & Rasanathan, K. (2011). Climate change, noncommunicable diseases, and development: the relationships and common policy opportunities. *Annual review of public health*, 32(1), 133-147.
- Fundter, D. Q., Jonkman, B., Beerman, S., Goemans, C. L., Briggs, R., Coumans, F., ... & Bierens, J. (2008). Health impacts of large-scale floods: governmental decision-making and resilience of the citizens. *Prehospital and disaster medicine*, 23(S2), s70-s73.
- Genovese, E. (2006). A methodological approach to land use-based flood damage assessment in urban areas: Prague case study. *Technical EUR Reports, EUR*, 22497.
- Goodess, C. M., Osborn, C. T., & Hulme, M. (2003). *The identification and evaluation of suitable scenario development methods for the estimation of future probabilities of extreme weather events*. Tyndall Centre for Climate Change Research.
- GRASS (2013a) Geographic Resources Analysis Support System (GRASS) GIS. URL: <http://grass.osgeo.org/> (Accessed Jan 2014).
- GRASS (2013b) r.watershed: Calculates hydrological parameters and RUSLE factors. Geographic Resources Analysis Support System. URL: <http://grass.osgeo.org/grass70/manuals/r.watershed.html>. (Accessed Jan 2014).
- GRASS (2012) r.slope.aspect: Generates raster maps of slope, aspect, curvatures and partial derivatives from a elevation raster map. Geographic Resources Analysis Support System. URL: <http://grass.osgeo.org/grass70/manuals/r.slope.aspect> (Accessed Jan 2014)
- Green, A. (2014). Impacts on Flood Risk from Land Use Strategies for Coping with Climate Change—An Assessment using the Time-Area Method.
- Griggs, D. J., & Noguera, M. (2002). Climate change 2001: the scientific basis. Contribution of working group I to the third assessment report of the intergovernmental panel on climate change. *Weather*, 57(8), 267-269.

- GVTA (Greater Vancouver Transportation Authority) (2002). Program Plan Summary and Budget. Draft. March 25. TransLink, Burnaby BC. <http://www.translink.ca/site-info/search-results.aspx> (Accessed Dec 2013). Metro Vancouver, 2008a. Metro Vancouver Corporate 2005 Greenhouse Gas Emission Inventory, Backcast and Forecast. Metro Vancouver, Burnaby BC.
- Hallegatte, S., Green, C., Nicholls, R. J., & Corfee-Morlot, J. (2013). Future flood losses in major coastal cities. *Nature climate change*, 3(9), 802-806.
- Hanson, S., Nicholls, R., Ranger, N., Hallegatte, S., Corfee-Morlot, J., Herweijer, C., & Chateau, J. (2011). A global ranking of port cities with high exposure to climate extremes. *Climatic change*, 104(1), 89-111.
- Hoeke, R. K., McInnes, K., Kruger, J., McNaught, R., Hunter, J., & Smithers, S. G. (2013). Widespread inundation of Pacific Islands by distant-source wind-waves. *Glob. Planet. Chang*, 108, 1-11.
- Holben, B. N. (1986). Characteristics of maximum-value composite images from temporal AVHRR data. *International journal of remote sensing*, 7(11), 1417-1434.
- Holmgren, P. (1994). Multiple flow direction algorithms for runoff modelling in grid based elevation models: an empirical evaluation. *Hydrological processes*, 8(4), 327-334.
- Hopkins, T. S., Bailly, D., Elmgren, R., Glegg, G., Sandberg, A., & Støttrup, J. G. (2012). A systems approach framework for the transition to sustainable development: potential value based on coastal experiments. *Ecology and Society*, 17(3).
- Hunt, J. C. R. (2002). Floods in a changing climate: a review. *Philosophical Transactions of the Royal Society of London A: Mathematical, Physical and Engineering Sciences*, 360(1796), 1531-1543.
- Hunter, J. (2012). A simple technique for estimating an allowance for uncertain sea-level rise. *Climatic Change*, 113(2), 239-252.

- Hunter, P. R. (2003). Climate change and waterborne and vector-borne disease. *Journal of applied microbiology*, 94(s1), 37-46.
- IFRC (2003). World disasters report: focus on ethics in aid International Federation of Red Cross and Red Crescent Societies, Geneva.
- International Organization for Migration (IOM) (2008). Migration and Climate Change, IOM Report 37, Geneva, 64 pp.
- International Strategy for Disaster Reduction. (2004). *Living with risk: a global review of disaster reduction initiatives* (Vol. 1). United Nations Publications. UNITED NATIONS, Geneva, Switzerland, 429 p. ISBN 9211010640.
- IPCC, (2013a). Climate Change 2013: The Physical Science Basis. Contribution of Working Group I to the Fifth Assessment Report of the Intergovernmental Panel on Climate Change [Stocker, T.F., D. Qin, G.-K. Plattner, M. Tignor, S.K. Allen, J. Boschung, A. Nauels, Y. Xia, V. Bex and P.M. Midgley (eds.)]. Cambridge University Press, Cambridge, United Kingdom and New York, NY, USA, 1535 pp.
- IPCC, (2013b). Summary for policy makers. In: Climate Change 2013: The Physical Science Basis. Contribution of Working Group I to the Fifth Assessment Report of the Intergovernmental Panel on Climate Change [Stocker, T.F., D. Qin, G.-K. Plattner, M. Tignor, S. K. Allen, J. Boschung, A. Nauels, Y. Xia, V. Bex, and P.M. Midgley (eds.)]. Cambridge University Press, Cambridge, UK and New York, NY, USA, pp. 1-36.
- ISDR, (2005). <http://www.unisdr.org/eng/library/isdr-publication/flood-guidelines/isdr-publicationfloods.htm> (Accessed July 2013)
- Ivers, L. C., & Ryan, E. T. (2006). Infectious diseases of severe weather-related and flood-related natural disasters. *Current opinion in infectious diseases*, 19(5), 408-414.
- Jakob, M., Holm, K., Lazarte, E., & Church, M. (2014). A flood risk assessment for the City of Chilliwack on the Fraser River, British Columbia, Canada. *International Journal of River Basin Management*, (ahead-of-print), 1-8.

- Jiang, T., Kundzewicz, Z. W., & Su, B. (2008). Changes in monthly precipitation and flood hazard in the Yangtze River Basin, China. *International Journal of Climatology*, 28(11), 1471-1481.
- Kalkstein, L. S., & Smoyer, K. E. (1992). *The impact of climate on Canadian mortality: Present relationships and future scenarios*. Center for Climate Research, Department of Geography, University of Delaware.
- Kang, M. G., Jeong, H. S., Lee, J. H., & Kang, B. S. (2013). Assessing national flood management using a sustainable flood management framework. *Water Policy*, 15(3), 418-434.
- King, Leanna M., "Application of a K-Nearest Neighbour weather generator for simulation of historical and future climate variables in the Upper Thames River basin" (2012). University of Western Ontario - Electronic Thesis and Dissertation Repository. Paper 673.
- King, L. M., Irwin, S., Sarwar, R., McLeod, A. I. A., & Simonovic, S. P. (2012). The effects of climate change on extreme precipitation events in the Upper Thames River Basin: a comparison of downscaling approaches. *Canadian Water Resources Journal*, 37(3), 253-274.
- Konrad, C.P., and Booth, D.B., (2002), Hydrologic trends associated with urban development for selected streams in western Washington: U.S. Geological Survey Water-Resources Investigations Report 02-4040, 40 p., <http://water.usgs.gov/pubs/wri/wri024040>. (Accessed July 2013)
- Konrad C. P. (2003). "Effects of Urban Development on Flood", U.S. Department of the Interior, U.S. Geological Survey, USGS Fact Sheet FS-076-03.
- Kottek, M., Grieser, J., Beck, C., Rudolf, B., & Rubel, F. (2006). World map of the Köppen-Geiger climate classification updated. *Meteorologische Zeitschrift*, 15(3), 259-263.
- Kovats, R.S. et al. (1999). *El Niño and Health*: World Health Organization.
- Krige, Danie G. (1951). "A statistical approach to some basic mine valuation problems on the Witwatersrand". *J. of the Chem., Metal. and Mining Soc. of South Africa* 52 (6): 119–139.

- Kulkarni, A. T., Mohanty, J., Eldho, T. I., Rao, E. P., & Mohan, B. K. (2014). A web GIS based integrated flood assessment modeling tool for coastal urban watersheds. *Computers & Geosciences*, *64*, 7-14.
- Kundzewicz, Z. W., & Kaczmarek, Z. (2000). Coping with hydrological extremes. *Water International*, *25*(1), 66-75.
- Lanfredi, M., Lasaponara, R., Simoniello, T., Cuomo, V., & Macchiato, M. (2003). Multiresolution spatial characterization of land degradation phenomena in southern Italy from 1985 to 1999 using NOAA-AVHRR NDVI data. *Geophysical Research Letters*, *30*(2).
- Lankao, P. R. (2007). Are we missing the point? Particularities of urbanization, sustainability and carbon emissions in Latin American cities. *Environment and Urbanization*, *19*(1), 159-175.
- Li, X., Tan, H., Li, S., Zhou, J., Liu, A., Yang, T., ... & Sun, Z. (2007). Years of potential life lost in residents affected by floods in Hunan, China. *Transactions of the Royal Society of Tropical Medicine and Hygiene*, *101*(3), 299-304.
- Ligon, B. L. (2006). Infectious diseases that pose specific challenges after natural disasters: a review. In *Seminars in pediatric infectious diseases* (Vol. 17, No. 1, pp. 36-45). WB Saunders.
- Lillesand, T. M., Kiefer, R. W., & Chipman, J. W. (1994). Remote sensing and image interpretation Wiley. *New York*.
- Lim, S. S., Vos, T., Flaxman, A. D., Danaei, G., Shibuya, K., Adair-Rohani, H., ... & Davis, A. (2013). A comparative risk assessment of burden of disease and injury attributable to 67 risk factors and risk factor clusters in 21 regions, 1990–2010: a systematic analysis for the Global Burden of Disease Study 2010. *The lancet*, *380*(9859), 2224-2260.
- Maibach, E. W., Chadwick, A., McBride, D., Chuk, M., Ebi, K. L., & Balbus, J. (2008). Climate change and local public health in the United States: preparedness, programs and perceptions of local public health department directors. *PLoS One*, *3*(7), e2838.

- Malakooti, M. A., Biomndo, K., & Shanks, G. D. (1998). Reemergence of epidemic malaria in the highlands of western Kenya. *Emerging infectious diseases*, 4(4), 671.
- Malczewski, J., Pazner, M., & Zaliwska, M. (1997). Visualization of multicriteria location analysis using raster GIS: a case study. *Cartography and Geographic Information Systems*, 24(2), 80-90.
- Manfreda, S., Di Leo, M., & Sole, A. (2011). Detection of flood-prone areas using digital elevation models. *Journal of Hydrologic Engineering*, 16(10), 781-790.
- Massam, B. H. (1988). Multi-criteria decision making (MCDM) techniques in planning. *Progress in planning*, 30, 1-84.
- McBean, G. (2014). The grand challenges of integrated research on disaster risk. *Extreme Natural Hazards, Disaster Risks and Societal Implications*, 1, 15.
- McCarthy, J. J. (Ed.). (2001). *Climate change 2001: impacts, adaptation, and vulnerability: contribution of Working Group II to the third assessment report of the Intergovernmental Panel on Climate Change*. Cambridge University Press.
- McGranahan, G., Balk, D., & Anderson, B. (2007). The rising tide: assessing the risks of climate change and human settlements in low elevation coastal zones. *Environment and urbanization*, 19(1), 17-37.
- McMichael, A. J., Campbell-Lendrum, D. H., Corvalán, C. F., Ebi, K. L., Githeko, A. K., Scheraga, J. D., & Woodward, A. (2003). *Climate change and human health: risks and responses*. World Health Organization.
- McMichael, A. J., Woodruff, R. E., & Hales, S. (2006). Climate change and human health: present and future risks. *The Lancet*, 367(9513), 859-869.
- Milly, P. C. D., Wetherald, R., Dunne, K. A., & Delworth, T. L. (2002). Increasing risk of great floods in a changing climate. *Nature*, 415(6871), 514-517.
- Min, S. K., Zhang, X., Zwiers, F. W., & Hegerl, G. C. (2011). Human contribution to more-intense precipitation extremes. *Nature*, 470(7334), 378-381.

- Mirza, M. M. Q. (2002). Global warming and changes in the probability of occurrence of floods in Bangladesh and implications. *Global environmental change*, 12(2), 127-138.
- MMM (MMM Group Ltd.) (2014). National Floodplain Mapping Assessment. Ottawa: Public Safety Canada. 68 pages.
- Monfreda, C., Ramankutty, N., & Foley, J. A. (2008). Farming the planet: 2. Geographic distribution of crop areas, yields, physiological types, and net primary production in the year 2000. *Global biogeochemical cycles*, 22(1).
- Montz, B. E. (2000). The generation of flood hazards and disasters by urban development of floodplains. *Floods*, 1, 116-127.
- Mooney, H. A., Cropper, A., Capistrano, D., Carpenter, S. R., Chopra, K., Dasgupta, P., ... & Shidong, Z. (2005). Ecosystems and human well-being: synthesis, Millenium Ecosystem Assessment.
- Morshed, M. G., Scott, J. D., Fernando, K., Beati, L., Mazerolle, D. F., Geddes, G., & Durden, L. A. (2005). Migratory songbirds disperse ticks across Canada, and first isolation of the Lyme disease spirochete, *Borrelia burgdorferi*, from the avian tick, *Ixodes auritulus*. *Journal of Parasitology*, 91(4), 780-790.
- Mouchet, J. E. A. N., Manguin, S., Sircoulon, J. A. C. Q. U. E. S., Laventure, S. T. E. P. H. A. N. E., Faye, O. U. S. M. A. N. E., Onapa, A. W., ... & Fontenille, D. (1998). Evolution of malaria in Africa for the past 40 years: impact of climatic and human factors. *Journal of the American Mosquito Control Association*, 14(2), 121-130.
- Mudelsee, M., Börngen, M., Tetzlaff, G., & Grünewald, U. (2003). No upward trends in the occurrence of extreme floods in central Europe. *Nature*, 425(6954), 166-169.
- Nardi, F., Grimaldi, S., Santini, M., Petroselli, A., & Ubertini, L. (2008). Hydrogeomorphic properties of simulated drainage patterns using digital elevation models: the flat area issue/Propriétés hydro-géomorphologiques de réseaux de drainage simulés à partir de modèles numériques de terrain: la question des zones planes. *Hydrological sciences journal*, 53(6), 1176-1193.

- Nardi, F., Vivoni, E. R., & Grimaldi, S. (2006). Investigating a floodplain scaling relation using a hydrogeomorphic delineation method. *Water Resources Research*, 42(9).
- Nicholls, R.J., et al., (2007a). Coastal systems and low-lying areas. *Climate Change 2007: Impacts, Adaptation and Vulnerability. Contribution of Working Group II to the Fourth Assessment Report of the Intergovernmental Panel on Climate Change*, M.L. Parry, et al., Eds., Cambridge University Press, Cambridge, UK, 315-356.
- Nicholls, R.J., et al., (2007b). OECD Environment Working Paper: "Screening Study: Ranking Port Cities with High Exposure and Vulnerability to Climate Extremes. Interim Analysis: Exposure Estimates", ENV/WKP(2007)1, OECD 2007. www.oecd.org/env/workingpapers/
- Nicholls, R. J. (2004). Coastal flooding and wetland loss in the 21st century: changes under the SRES climate and socio-economic scenarios. *Global Environmental Change*, 14(1), 69-86.
- Nicholls, R. J., Hoozemans, F. M., & Marchand, M. (1999). Increasing flood risk and wetland losses due to global sea-level rise: regional and global analyses. *Global Environmental Change*, 9, S69-S87.
- Nirupama N, Simonovic SP (2007). Increase of flood risk due to urbanisation: a Canadian example. *Nat Hazards* 40:25–41. doi:10.1007/s11069-006-0003-0
- OECD, (2012). Economic surveys Canada. June 2012, OECD Publishing <http://www.oecd.org/newsroom/future-flood-losses-in-major-coastal-cities.htm> (Accessed June 2014)
- OECD. Publishing. (2008). *OECD Environmental Outlook to 2030*. Organisation for Economic Co-operation and Development.
- OFDA/CRED. EM-DAT: The international disaster database. <http://www.cred.be/emdat> (Accessed Dec 2011).
- OFDA/CRED. EM-DAT (2001). The International Disaster Database. Brussels, Belgium, Université Catholique de Louvain, www.cred.be/emdat.

- Oliver, M. A., & Webster, R. (1990). Kriging: a method of interpolation for geographical information systems. *International Journal of Geographical Information System*, 4(3), 313-332.
- Osborn, Liz. (2015) "[Canada's Rainiest Cities](#)". CurrentResults.com. (Accessed May, 2015).
- Owranji, A. M., Lannigan, R., & Simonovic, S. P. (2015). Mapping climate change-caused health risk for integrated city resilience modeling. *Natural Hazards*, 1-22.
- Owranji, A. M., Lannigan, R., & Simonovic, S. P. (2014). Interaction between land-use change, flooding and human health in Metro Vancouver, Canada. *Natural hazards*, 72(2), 1219-1230.
- Pall, P., Aina, T., Stone, D. A., Stott, P. A., Nozawa, T., Hilberts, A. G., ... & Allen, M. R. (2011). Anthropogenic greenhouse gas contribution to flood risk in England and Wales in autumn 2000. *Nature*, 470(7334), 382-385.
- Palmer, T. N., & Räisänen, J. (2002). Quantifying the risk of extreme seasonal precipitation events in a changing climate. *Nature*, 415(6871), 512-514.
- Parker D.J., (2000). Floods. Routledge, ISBN-13: 978-0415172387
- Parry, M. L. (Ed.). (2007). *Climate Change 2007: impacts, adaptation and vulnerability: contribution of Working Group II to the fourth assessment report of the Intergovernmental Panel on Climate Change* (Vol. 4). Cambridge University Press.
- Patz, J. A., McGeehin, M. A., Bernard, S. M., Ebi, K. L., Epstein, P. R., Grambsch, A., ... & Trtanj, J. (2000). The potential health impacts of climate variability and change for the United States: executive summary of the report of the health sector of the US National Assessment. *Environmental health perspectives*, 108(4), 367.
- Pavri, F. (2010). Urban Expansion and Sea-Level Rise Related Flood Vulnerability for Mumbai (Bombay), India Using Remotely Sensed Data. In *Geospatial techniques in urban hazard and disaster analysis* (pp. 31-49). Springer Netherlands.
- Peck, A., Bowering, E., & Simonovic, S. P. (2011). City of London: Vulnerability of infrastructure to climate change final report.

- Peck, A., & Simonovic, S. P. (2013). Coastal cities at risk (CCaR): generic system dynamics simulation models for use with city resilience simulator. *Water Resources Research Report*, (083).
- Pilkey, O. H., & Cooper, J. A. G. (2004). Society and sea level rise. *Science*, 303(5665), 1781-1782.
- Poff, N. L. (2002). Ecological response to and management of increased flooding caused by climate change. *Philosophical Transactions of the Royal Society of London. Series A: Mathematical, Physical and Engineering Sciences*, 360(1796), 1497-1510.
- Prüss-Ustün, A., Mathers, C., Corvalán, C., & Woodward, A. (2003). *Introduction and methods: assessing the environmental burden of disease at national and local levels* (Vol. 1). OMS.
- PSC (Public Safety Canada). (2014). *Canadian Disaster Database*. Accessed from <http://www.publicsafety.gc.ca/cnt/rsrscs/cndn-dsstr-dtbs/index-eng.aspx> (Accessed Sep 2014)
- Raheja, N. (2003). GIS-based software applications for environmental risk management. In *Map India Conference* (p. 9).
- Rahmstorf, S., Cazenave, A., Church, J. A., Hansen, J. E., Keeling, R. F., Parker, D. E., & Somerville, R. C. (2007). Recent climate observations compared to projections. *Science*, 316(5825), 709-709.
- Ramin, B. M., & McMichael, A. J. (2009). Climate change and health in sub-Saharan Africa: a case-based perspective. *EcoHealth*, 6(1), 52-57.
- Reacher, M., McKenzie, K., Lane, C., Nichols, T., Kedge, I., Iversen, A., ... & Simpson, J. (2004). Health impacts of flooding in Lewes: a comparison of reported gastrointestinal and other illness and mental health in flooded and non-flooded households. *Communicable disease and public health/PHLS*, 7(1), 39-46.
- Rees, W. E. (2009). The ecological crisis and self-delusion: implications for the building sector. *Building Research & Information*, 37(3), 300-311.
- Revi, A., D.E. Satterthwaite, F. Aragón-Durand, J. Corfee-Morlot, R.B.R. Kiunsi, M. Pelling, D.C. Roberts, and W. Solecki, (2014). Urban areas. In: *Climate Change 2014: Impacts,*

- Adaptation, and Vulnerability. Part A: Global and Sectoral Aspects. Contribution of Working Group II to the Fifth Assessment Report of the Intergovernmental Panel on Climate Change [Field, C.B., V.R. Barros, D.J. Dokken, K.J. Mach, M.D. Mastrandrea, T.E. Bilir, M. Chatterjee, K.L. Ebi, Y.O. Estrada, R.C. Genova, B. Girma, E.S. Kissel, A.N. Levy, S. MacCracken, P.R. Mastrandrea, and L.L.White (eds.)]. Cambridge University Press, Cambridge, United Kingdom and New York, NY, USA, pp. 535-612.
- Rosenzweig, C., Solecki, W. D., Hammer, S. A., & Mehrotra, S. (Eds.). (2011). *Climate change and cities: first assessment report of the Urban Climate Change Research Network*. Cambridge University Press.
- Sallenger Jr, A. H., Doran, K. S., & Howd, P. A. (2012). Hotspot of accelerated sea-level rise on the Atlantic coast of North America. *Nature Climate Change*, 2(12), 884-888.
- Sandwell, A. (2011). *Climate Change Adaptation Guidelines for Sea Dikes and Coastal Flood Hazard Land Use*. Draft Policy Discussion Paper.
- Schaefer, D.G. (1979b). Meteorological developments contributing to the Terrace area flood of early November 1978. Atmos. Environ. Serv. Scientific Serv., Vancouver, B.C. 7 p.
- Schwartz, B. S., Harris, J. B., Khan, A. I., Larocque, R. C., Sack, D. A., Malek, M. A., ... & Ryan, E. T. (2006). Diarrheal epidemics in Dhaka, Bangladesh, during three consecutive floods: 1988, 1998, and 2004. *The American journal of tropical medicine and hygiene*, 74(6), 1067-1073.
- Schwartz, R., & McConnell, A. (2009). Do crises help remedy regulatory failure? A comparative study of the Walkerton water and Jerusalem banquet hall disasters. *Canadian Public Administration*, 52(1), 91-112.
- Septer, D. (2007). Flooding and landslide events northern British Columbia 1820–2006. *Victoria: BC Ministry of Environment*.
- Shalaby, A., & Tateishi, R. (2007). Remote sensing and GIS for mapping and monitoring land cover and land-use changes in the Northwestern coastal zone of Egypt. *Applied Geography*, 27(1), 28-41.

- Sharma, A. J., Weiss, E. C., Young, S. L., Stephens, K., Ratard, R., Straif-Bourgeois, S., ... & Rubin, C. H. (2008). Chronic disease and related conditions at emergency treatment facilities in the New Orleans area after Hurricane Katrina. *Disaster medicine and public health preparedness*, 2(01), 27-32.
- Shepard, C. C., Agostini, V. N., Gilmer, B., Allen, T., Stone, J., Brooks, W., & Beck, M. W. (2012). Assessing future risk: quantifying the effects of sea level rise on storm surge risk for the southern shores of Long Island, New York. *Natural Hazards*, 60(2), 727-745.
- Simonovic, S. P., & Ahmad, S. S. (2007). A New Method for Spatial Analysis of Risk in Water Resources Engineering Management. *Open Civil Engineering Journal*, 1, 1-12.
- Simonovic, S. P., & Peck, A. (2013). Dynamic resilience to climate change caused natural disasters in coastal megacities quantification framework. *British Journal of Environment and Climate Change*, 3(3), 378-401.
- Simonović, S. P. (2012). *Floods in a changing climate: risk management*. Cambridge University Press. Cambridge, United Kingdom and New York, NY, USA, 276 p, ISBN: 9781107018747.
- Simonovic, S. P. (2011). *Systems approach to management of disasters: methods and applications*. John Wiley & Sons.
- Singh, R. B., Hales, S., de Wet, N., Raj, R., Hearnden, M., & Weinstein, P. (2001). The influence of climate variation and change on diarrheal disease in the Pacific Islands. *Environmental health perspectives*, 109(2), 155.
- Solomon, S. (Ed.). (2007). *Climate change 2007-the physical science basis: Working group I contribution to the fourth assessment report of the IPCC* (Vol. 4). Cambridge University Press.
- Spot Vegetation Programme. (2011). <http://www.vgt.vito.be/> (Accessed Mar 2013)
- Stachel, B., Gtz, R., Herrmann, T., Krger, F., Knoth, W., Ppke, O., ... & Uhlig, S. (2004). The Elbe flood in August 2002-occurrence of polychlorinated dibenzo-p-dioxins, polychlorinated

- dibenzofurans (PCDD/F) and dioxin-like PCB in suspended particulate matter (SPM), sediment and fish. *Water Science & Technology*, 50(5), 309-316.
- Statistics Canada, (2012). Greater Vancouver, British Columbia (Code 5915) and British Columbia (Code 59). Census Profile. Statistics Canada Catalogue no. 98-316-XWE. Ottawa
- Statistics Canada, (2006). Census Data: Population, Urban and Rural, by Province and by Territory. <http://www.statcan.gc.ca/tables-tableaux/sum-som/l01/cst01/demo62a-eng.htm>. (Accessed Jan 2013)
- Stephens, K. U., Grew, D., Chin, K., Kadetz, P., Greenough, P. G., Burkle, F. M., ... & Franklin, E. R. (2007). Excess mortality in the aftermath of Hurricane Katrina: a preliminary report. *Disaster medicine and public health preparedness*, 1(01), 15-20.
- Strauss, B. H., Ziemiński, R., Weiss, J. L., & Overpeck, J. T. (2012). Tidally adjusted estimates of topographic vulnerability to sea level rise and flooding for the contiguous United States. *Environmental Research Letters*, 7(1), 014033.
- Sullivent, E. E., West, C. A., Noe, R. S., Thomas, K. E., Wallace, L. D., & Leeb, R. T. (2006). Nonfatal injuries following Hurricane Katrina—New Orleans, Louisiana, 2005. *Journal of safety research*, 37(2), 213-217.
- Taubenböck, H., Esch, T., Felbier, A., Wiesner, M., Roth, A., & Dech, S. (2012). Monitoring urbanization in mega cities from space. *Remote sensing of Environment*, 117, 162-176.
- Tebaldi, C., Strauss, B. H., & Zervas, C. E. (2012). Modelling sea level rise impacts on storm surges along US coasts. *Environmental Research Letters*, 7(1), 014032.
- Telesca, L., & Lasaponara, R. (2006). Pre-and post-fire behavioral trends revealed in satellite NDVI time series. *Geophysical research letters*, 33(14).
- Temmerman, S., Meire, P., Bouma, T. J., Herman, P. M., Ysebaert, T., & De Vriend, H. J. (2013). Ecosystem-based coastal defence in the face of global change. *Nature*, 504(7478), 79-83.
- The Arlington Group Planning and Architecture Inc., EBA, a Tetra Tech Company, DE Jardine Consulting, Sustainability Solutions Group. (2013). Sea Level Rise Adaptation Primer A

- Toolkit To Build Adaptive Capacity On Canada's South Coasts. BC Ministry of Environment.
- Tomio, J., Sato, H., & Mizumura, H. (2010). Interruption of medication among outpatients with chronic conditions after a flood. *Prehospital and disaster medicine*, 25(01), 42-50.
- Turcotte M. and Schellenberg M. (2006). A Portrait of Seniors in Canada. Published by authority of the Minister responsible for Statistics Canada, Catalogue no. 89-519-XIE ISBN 978-0-662-45047-4
- United Nations International Strategy for Disaster Reduction. (2010). The Economic and Social Commission for Asia and the Pacific. Protecting Development Gains, Reducing Disaster Vulnerability and Building Resilience in Asia and the Pacific - The Asia Pacific Disaster Report 2010. Bangkok, Thailand.
http://www.unisdr.org/preventionweb/files/16132_asiapacificdisasterreport20101.pdf
 (Accessed Feb 2013)
- United Nations, (2013). World Population Prospects: The 2012 Revision, Highlights and Advance Tables (Working Paper No. ESA/P/WP. 228). Working Paper No. ESA/P/WP.228.
- UNPD (United Nations Department of Economics and Social Affairs, Population Division). (2009). World Urbanization Prospects: the 2009 Revision: File 2: Percentage of Population Residing in Urban Areas by Major Area, Region and Country, 1950e2050.
<http://esa.un.org/unpd/wup/index.htm>. (Accessed Mar 2014)
- Vancouver, M. (2006). Census Bulletin# 2: Census of Agriculture. *Burnaby, BC: The Sustainable Region Initiative, Metro Vancouver, 11*.
- Vanneuville, W. (2011). Strengthening European Research for Flood Risk Management: CRUE ERA-Net main activities and outcomes.
- Walker, I.J. and Sydneysmith, R. (2007). British Columbia; in From Impacts to Adaptation: Canada in a Changing Climate 2007, edited by D.S. Lemmen, F.J. Warren, J. Lacroix, and E. Bush. Government of Canada, Ottawa, ON, pp. 329–386.

- Ward, R. C. (1978). *Floods- a geographical perspective*. *Publ. by: Macmillan*.
- Watson, J. T., Gayer, M., & Connolly, M. A. (2007). Epidemics after natural disasters. *Emerging infectious diseases*, 13(1), 1.
- Webster, R., & Oliver, M. A. (2007). *Geostatistics for environmental scientists*. John Wiley & Sons.
- WMO. (2011) Greenhouse Gases Reach Record Levels WMO Highlights Concerns about Global Warming and Methane. Press Release No. 903. In. Geneva: World Meteorological Organization; http://www.wmo.int/pages/mediacentre/press_releases/pr_903_en.html. (Accessed Feb 2014).
- World Bank. (2009). Water and climate change: understanding the risks and making climate-smart investment decisions. Alavian, V., Qaddumi, H. M., Dickson, E., Diez, S. M., Danilenko, A. V., Hirji, R. F., ... & Blankespoor, B. *World Bank: Washington, DC*.
- World Health Organization. (2014). http://www.who.int/hac/techguidance/ems/flood_cds/en/ (Accessed Oct 2014)
- World Health Organization. (2011). Flooding and Communicable Diseases Fact Sheet., from http://www.who.int/hac/techguidance/ems/flood_cds/en/. (Accessed Jan 2014).
- World Health Organization. (2008). Protecting Health from Climate Change - World Health Day. Geneva.. http://www.who.int/world-health-day/toolkit/report_web.pdf. (Accessed Jan 2013).
- World Health Organization (2010). Global status report on noncommunicable diseases. A. Alwan A, editor. Available at http://whqlibdoc.who.int/publications/2011/9789240686458_eng.pdf. (Accessed Feb 2014).
- Wong, P.P., I.J. Losada, J.-P. Gattuso, J. Hinkel, A. Khattabi, K.L. McInnes, Y. Saito, and A. Sallenger. (2014). Coastal systems and low-lying areas. In: *Climate Change 2014: Impacts, Adaptation, and Vulnerability. Part A: Global and Sectoral Aspects. Contribution of Working Group II to the Fifth Assessment Report of the Intergovernmental Panel on Climate Change* [Field, C.B., V.R. Barros, D.J. Dokken, K.J. Mach, M.D. Mastrandrea, T.E. Bilir, M. Chatterjee, K.L. Ebi, Y.O. Estrada, R.C. Genova, B. Girma, E.S. Kissel, A.N. Levy,

- Yevjevich, V. Luis da Cunha, & Evan Vlachos (eds.). (1983). *Coping with Droughts*. Littleton, Colorado: Water Resources Publications.
- Yin, Y. (2001). *Designing an Integrated Approach for Evaluating Adaptation Options to Reduce Climate Change Vulnerability in the Georgia Basin: Final Report*. University of British Columbia, Sustainable Development Research Institute.
- Zhang, X., Vincent, L. A., Hogg, W. D., & Niitsoo, A. (2000). Temperature and precipitation trends in Canada during the 20th century. *Atmosphere-ocean*,38(3), 395-429.

Appendices

Appendix A Python code for flood inundation mapping

Python is a programming language that lets us work quickly and integrate systems more effectively. This software can be accessed through <https://www.python.org/downloads/> (Last Access May 2015).

GRASS GIS, commonly referred to as GRASS (Geographic Resources Analysis Support System), is a free and open source Geographic Information System (GIS) software suite used for image processing, graphics, geospatial data management and analysis, and maps production, spatial modeling, and visualization. <http://grass.osgeo.org/> (Last Access March 2015). Also, GRASS is capable to read Python code.

Implemented *r.hazard.flood.py* module developed in 2010 by Margherita Di Leo, can be used for Metro Vancouver DEM files using Python and GRASS.

```
#####
##

#% module

#% description: Fast procedure to detect flood prone areas

#% keywords: raster

#% end

#% option

#% key: map

#% type: string

#% gisprompt: old,cell,raster

#% key_desc: elevation
```

```
## description: Name of elevation raster map

## required: yes

##end

##option

## key: flood

## type: string

## gisprompt: new,cell,raster

## key_desc: flood

## description: Name of output flood raster map

## required: yes

##end

##option

## key: mti

## type: string

## gisprompt: new,cell,raster

## key_desc: MTI

## description: Name of output MTI raster map

## required: yes

##END

import sys
```



```
import os

try:

import grass.script as grass

except:

try:

from grass.script import core as grass

except:

sys.exit("grass.script can't be imported.")

if not os.environ.has_key("GISBASE"):

print "You must be in GRASS GIS to run this program."

sys.exit(1)

def main():

##### check if we have the r.area addon

if not grass.find_program('r.area', ['help']):

grass.fatal_("The 'r.area' module was not found, install it first:" +

"\n" +

"g.extension r.area")
```

```
r_elevation = options['map'].split('@')[0]

mapname = options['map'].replace("@", " ")

mapname = mapname.split()

mapname[0] = mapname[0].replace(".", "_")

r_flood_map = options['flood']

r_mti = options['mti']

# Detect cellsize of the DEM

info_region = grass.read_command('g.region', flags = 'p', rast = '%s' % (r_elevation))

dict_region = grass.parse_key_val(info_region, ':')

print(dict_region['nsres'])

print(dict_region['ewres'])

#resolution = (float(dict_region['nsres']) + float(dict_region['ewres']))/2

resolution = float(90)

grass.message("Cellsize : %s " % resolution)

# Flow accumulation map MFD

grass.run_command('r.watershed', elevation = r_elevation , accumulation = 'r_accumulation' ,
convergence = 5, flags = 'fa')

grass.message("Flow accumulation done. ")
```

```
# Slope map

grass.run_command('r.slope.aspect', elevation = r_elevation , slope = 'r_slope' )

grass.message("Slope map done. ")

# n exponent

n = 0.016 * (resolution ** 0.46)

grass.message("Exponent : %s " % n)

# MTI threshold

mti_th = 10.89 * n + 2.282

grass.message("MTI threshold : %s " % mti_th)

# MTI map

grass.message("Calculating MTI raster map.. ")

grass.mapcalc("$r_mti = log((exp(((rast1+1)*resolution) , $n)) / (tan(rast2+0.001)))",

r_mti = r_mti,

rast1 = 'r_accumulation',

resolution = resolution,

rast2 = 'r_slope',

n = n)
```

```
# Cleaning up

grass.message("Cleaning up.. ")

grass.run_command('g.remove', quiet = True, rast = 'r_accumulation')

grass.run_command('g.remove', quiet = True, rast = 'r_slope')

# flood map

grass.message("Calculating flood raster map.. ")

grass.mapcalc("r_flood = if($rast1 > $mti_th, 1, 0)",

rast1 = r_mti,

mti_th = mti_th)

### # Deleting isolated pixels

# Recategorizes data in a raster map by grouping cells that form physically discrete areas into
unique categories (preliminar to r.area)

grass.message("Running r.clump.. ")

grass.run_command('r.clump', input = 'r_flood',

output = 'r_clump',

overwrite = 'True')

# Delete areas of less than a threshold of cells (corresponding to 1 square kilometer)

# Calculating threshold

th = int(1000000 / resolution**2)
```

```
grass.message("Deleting areas of less than %s cells.. " % th)

grass.run_command('r.area', input = 'r_clump', output = 'r_flood_th', treshold = th, flags = 'b')

# New flood map

grass.mapcalc("$r_flood_map = $rast1 / $rast1", r_flood_map = r_flood_map, rast1 =
'r_flood_th')

# Cleaning up

grass.message("Cleaning up.. ")

grass.run_command('g.remove', rast = 'r_clump')

grass.run_command('g.remove', rast = 'r_flood_th')

grass.run_command('g.remove', rast = 'r_flood')

grass.message(_('Done.'))

if __name__ == "__main__":

options, flags = grass.parser()

sys.exit(main())
```

Appendix B DALY calculation

The unit proposed for all cities is the Disability Adjusted Life Year (DALY) which is available for all cities in several parameters. The table that can be used by all cities is the age standardized DALY table. This is in keeping with the population data which is not age stratified either. It might be possible for some cities to refine the data at a later stage but for developing the baseline resilience this crude estimate can be used. The following steps should be followed to get the appropriate DALY table:

- a) Age standardized DALY can be found at the WHO website

(http://www.who.int/healthinfo/global_burden_disease/estimates_country/ Last Accessed Mar 2014).

- b) This opens a page with the World Health Organization, logo. The subcategory heading is Health Statistics and Health Information Systems. A subheading just below this heading is Disease and Country Estimates, Burden of Disease. Under the category, Death and DALY estimates for 2004 by Cause for WHO member states, the first download tab is “Persons all ages”. This will download an Excel spreadsheet. By clicking on the tab “Age-std DALY rates” it will open the appropriate data set.

The data is organized by Country, and into a number of disease categories. The three broad categories listed on the left hand side of the table are:

I. Communicable, maternal, perinatal and nutritional conditions.


II. Non-communicable diseases.

III. Injuries.

- c) Next to these headings (the next column under each country) is a Total DALY’s per 100,000 populations for each Category. So under Afghanistan category I the number is 33,092 DALY’s. It is the total number under each category I, II and III that should be

used to determine the numbers of DALY's in each area of the city. So if the area has a population of 200,000 the number of DALY's in Category I would be 2x whatever the category total is.

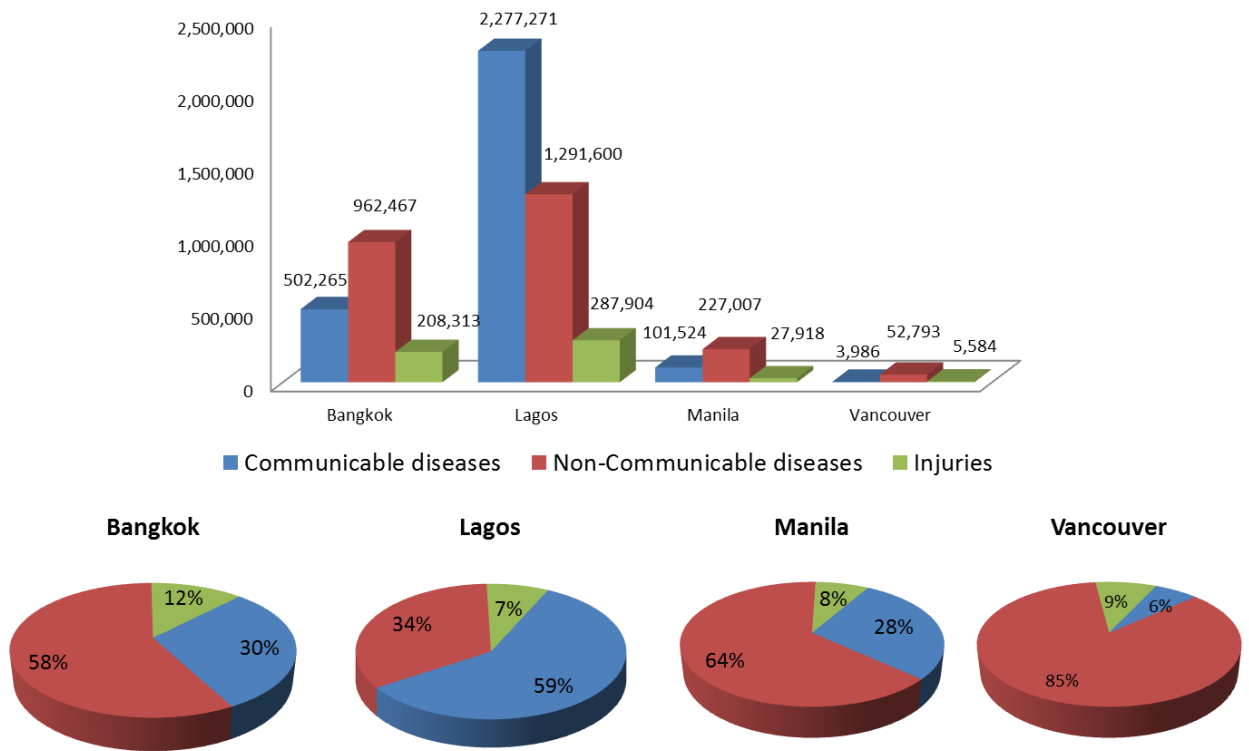
WHO Age-standardized DALYs per 100,000 by cause, and Member State, 2004.

	A	B	C	D	E	F	G	H	I	
1			World Health Organization Organisation Mondiale de la Santé Department of Measurement and Health Information February 2009				Table 6. Age-standard			
2										
3										
4										
5										
6										
7		GBD code	GBD cause (b)				WHO Country code	Afghanistan	Albania	
8							3010	4005		
9			<i>Data sources - level of evidence</i>							
10			All cause mortality (c)				Level 4b	Level 2b		
11			Cause-specific mortality (d)				Level 4	Level 2b		
12			Incidence, prevalence, severity, duration (n)				Level 4	Level 3		
13										
14										
15			<i>Population ('000) (e)</i>				<i>24,076</i>	<i>3,134</i>		
16										
17		W000	All Causes				61,622	16,106		
18		W001	I. Communicable, maternal, perinatal and nutritional conditions				33,032	2,034		

Demonstrates a calculation of the number of DALYs for all three disease categories for Metro Vancouver.

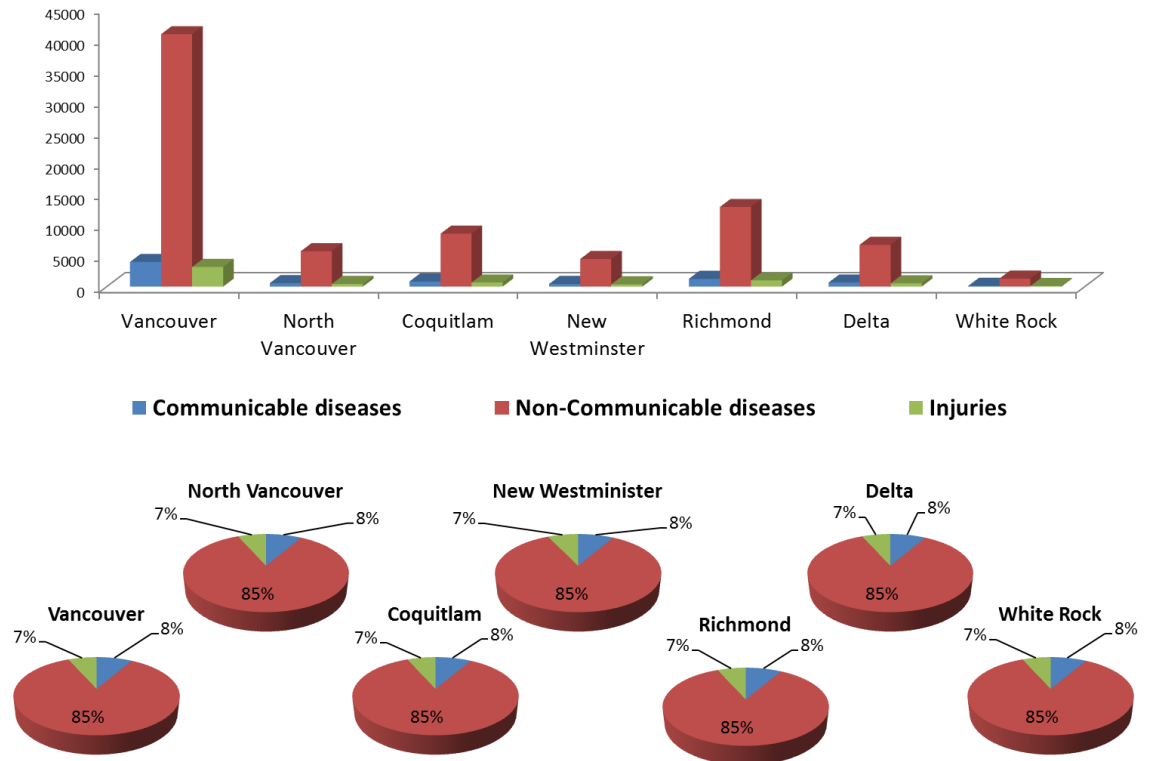
City	Population 2011	Communicable	Non- Communicable	Injuries	Total DALYS
Vancouver	603,503	3989	40766	3174	47929
North Vancouver	84,412	558	5718	444	6720
Coquitlam	126,456	836	8545	665	10046
New Westminster	65,976	436	4458	347	5241
Richmond	190,473	1259	12868	1002	15129
Delta	99,863	661	6755	526	7942
White Rock	19,339	126	1283	100	1508

The following figure presents the number of potential DALYs base on four cities' populations. It is clear that cities in developed countries face fewer DALYs compared to the circumstances faced in developing countries. Vancouver has almost 8 times less population compared to the other cities in our sample and the rate of different categories of burden of diseases is much less compared to the other cities. Lagos in western Africa has the highest proportion of communicable diseases among these four cities and Vancouver has the lowest.



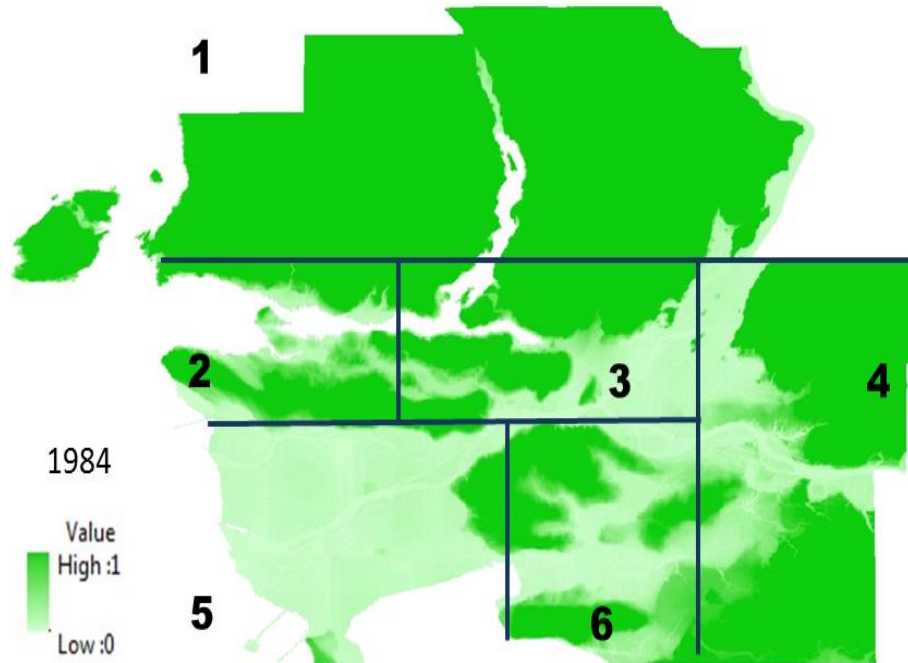
Number of DALYs base on four different cities population.

Using the DALY calculation method presented in Section 3.3, three different categories of communicable diseases, non-communicable diseases and injuries have been quantified. Results are shown graphically in following figure. In each of these municipalities, non-communicable diseases have the highest proportion.

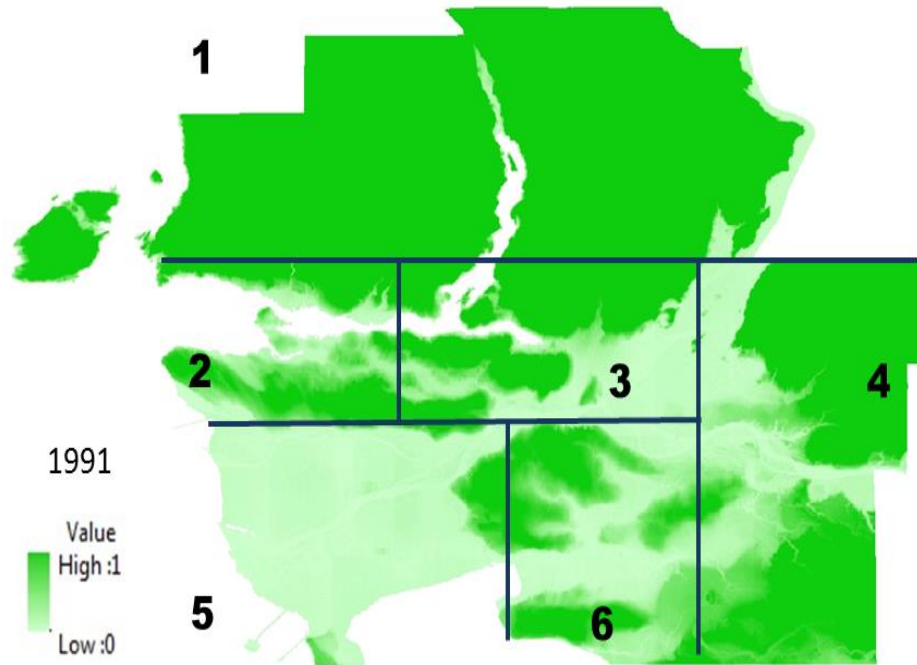


Number of DALYs for seven major municipalities in Metro Vancouver based on 2011 population census data.

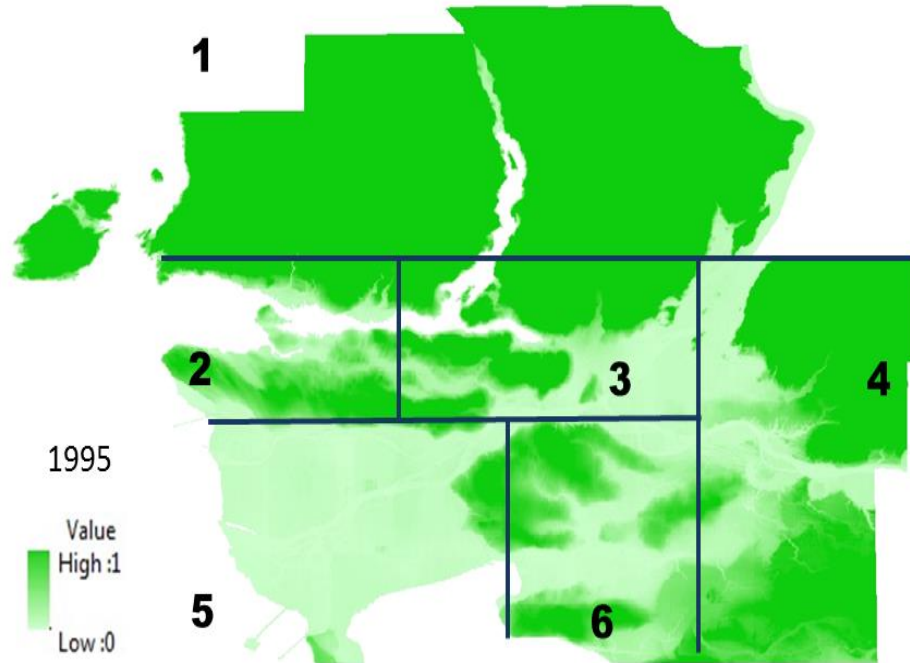
Appendix C Developed maps for different physical and nonphysical variables of the composite health impacts measure for Metro Vancouver



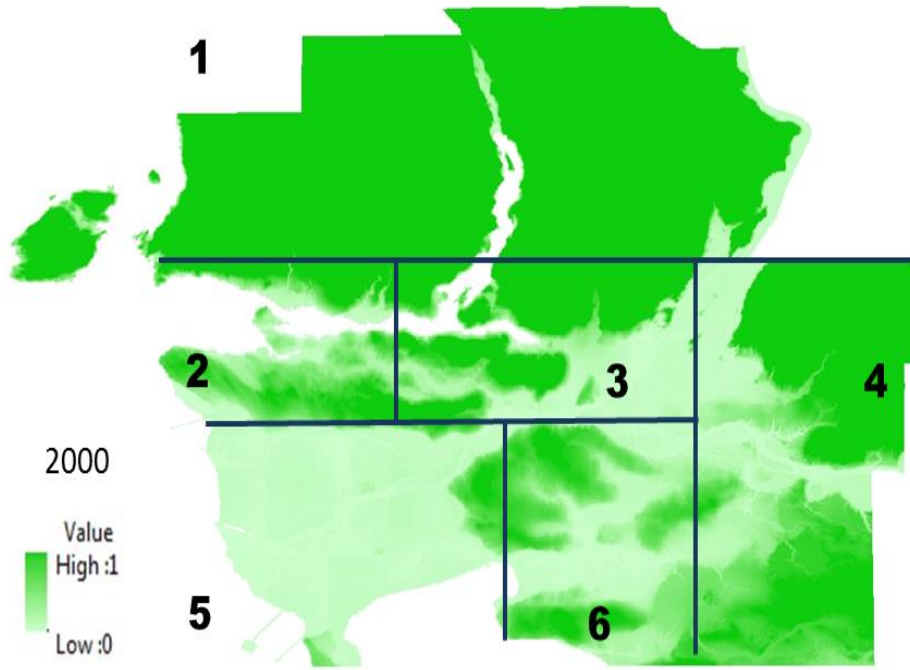
The vegetation condition for Metro Vancouver for 1984



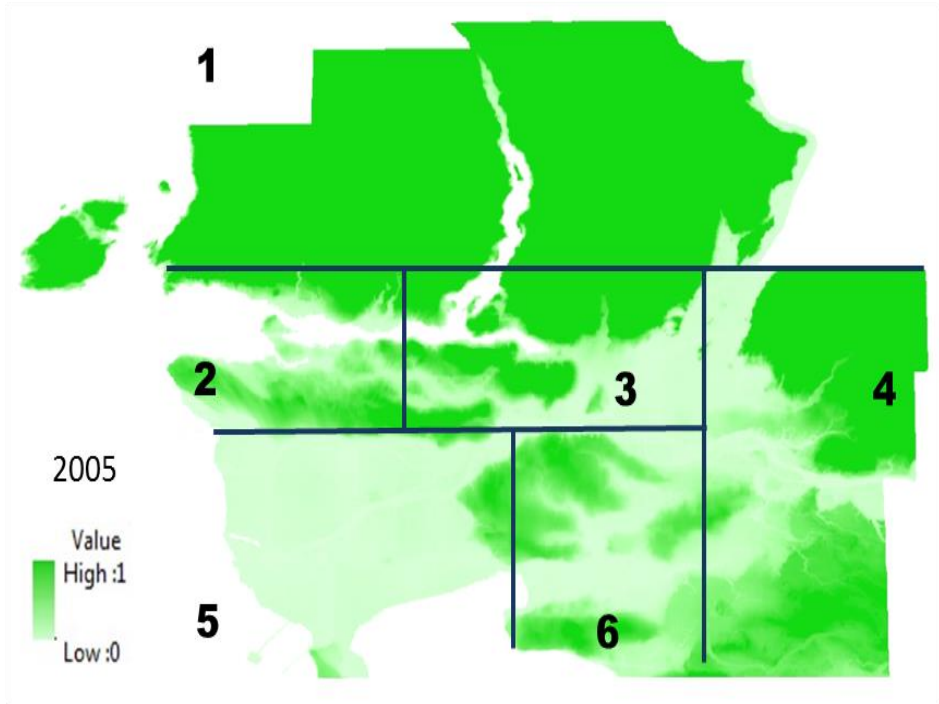
The vegetation condition for Metro Vancouver for 1991



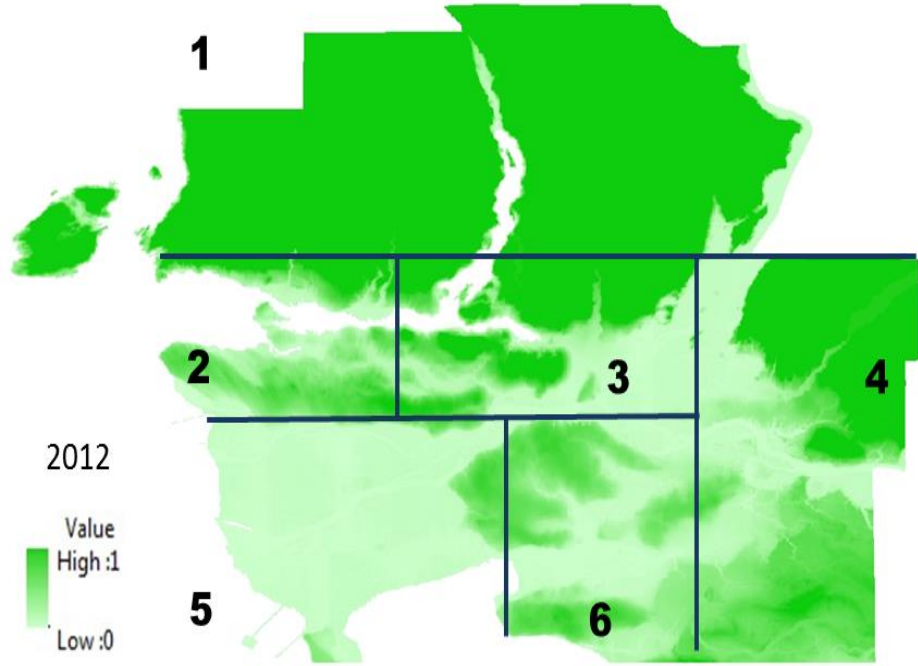
The vegetation condition for Metro Vancouver for 1991



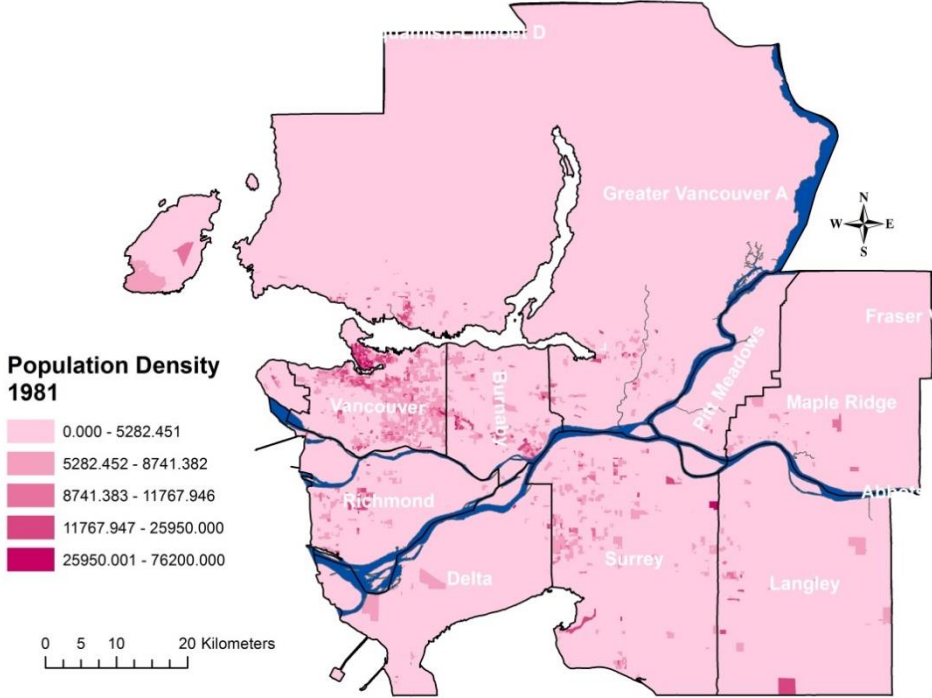
The vegetation condition for Metro Vancouver for 2000



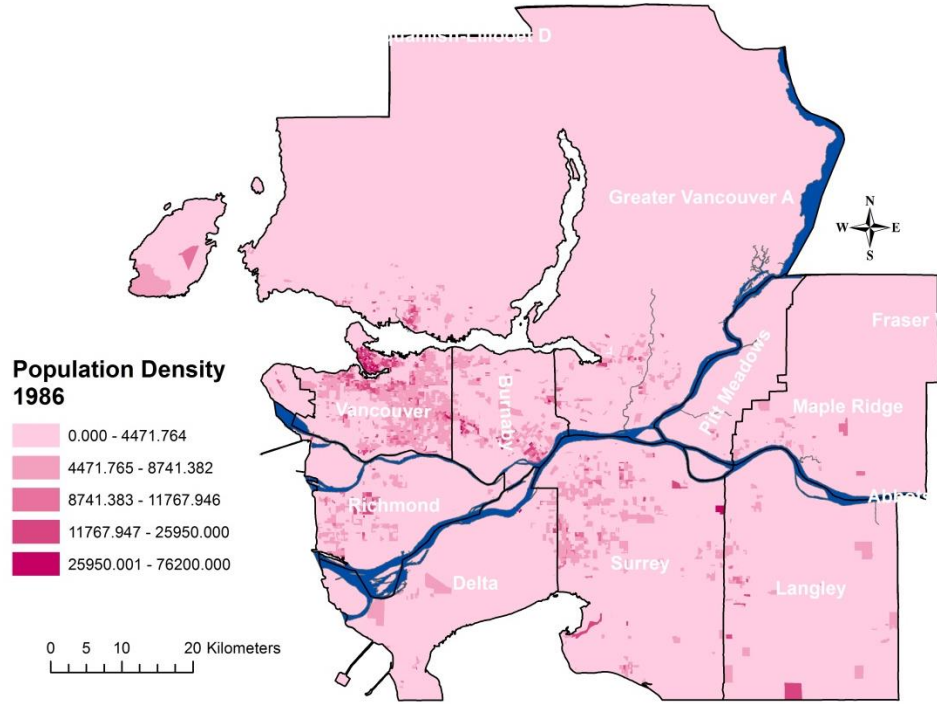
The vegetation condition for Metro Vancouver for 2005



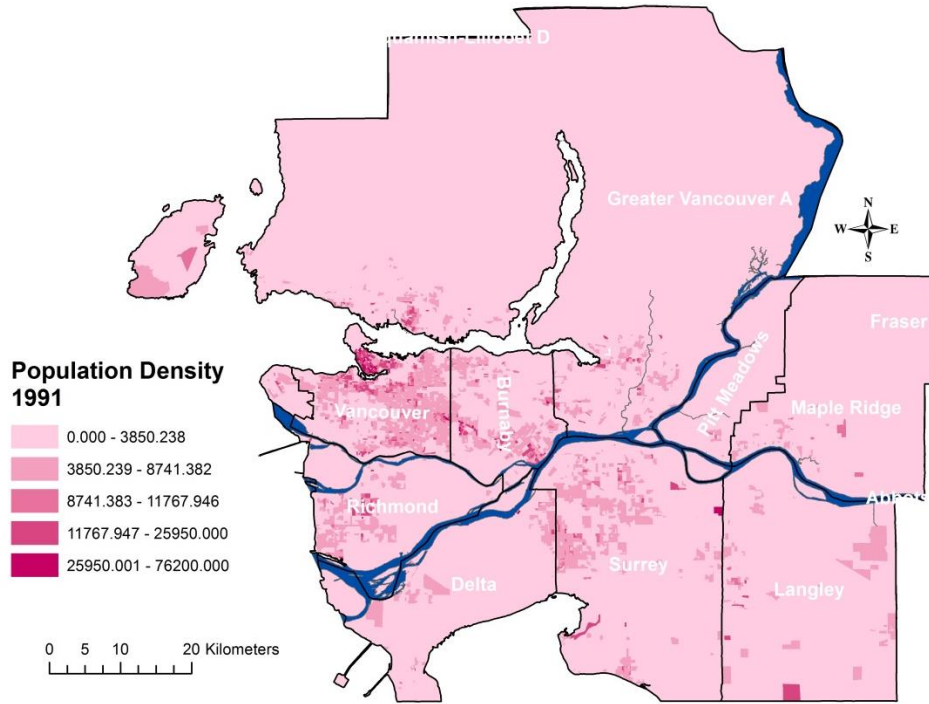
The vegetation condition for Metro Vancouver for 2012



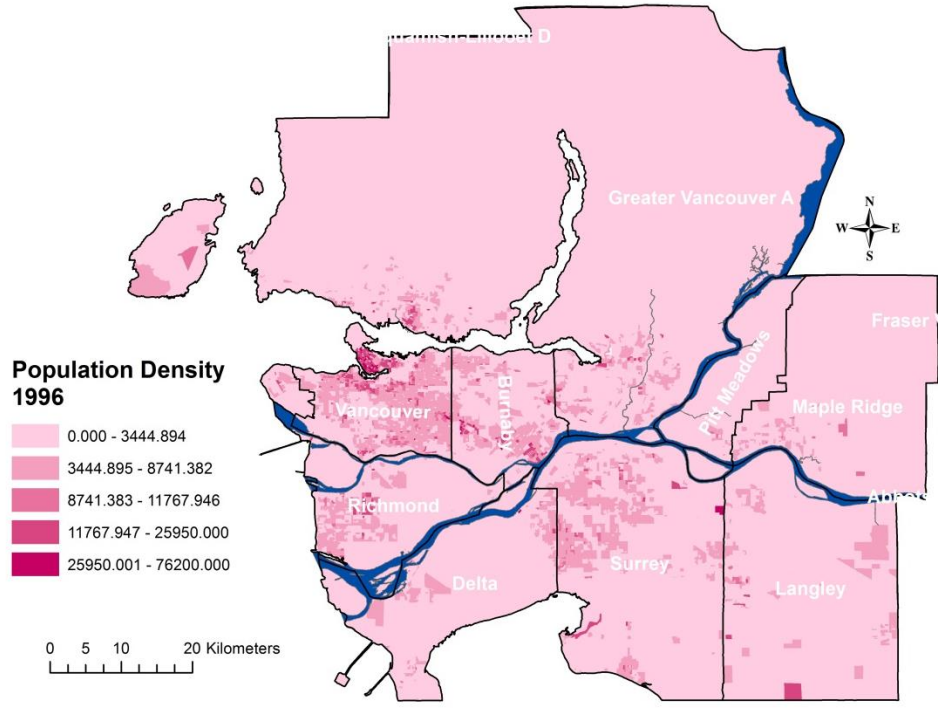
Calculated normalized population density for Metro Vancouver for 1981 (population per square kilometer).



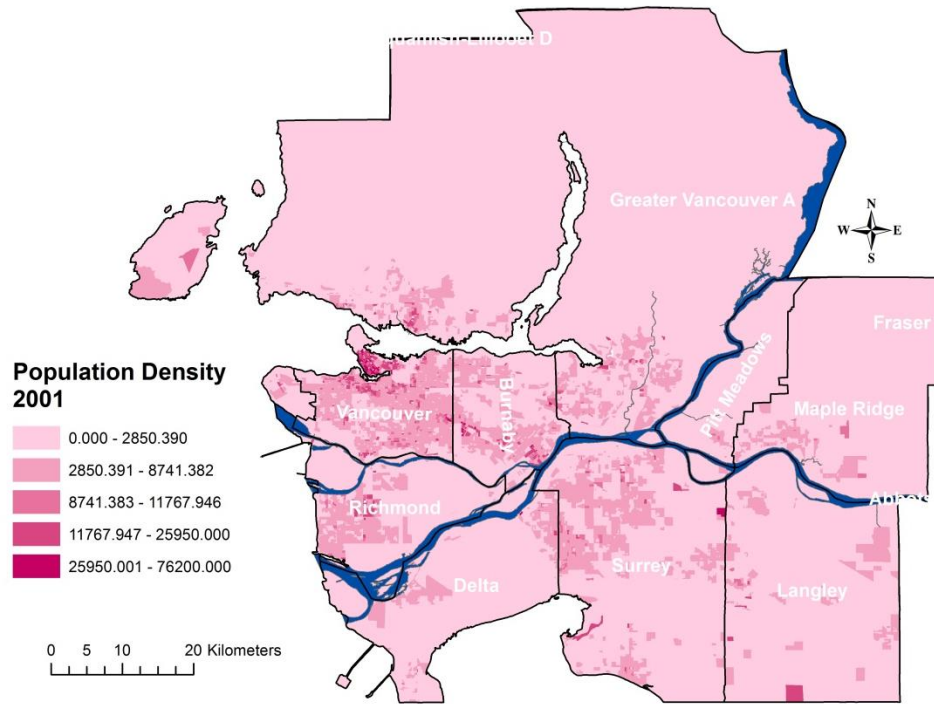
Calculated normalized population density for Metro Vancouver for 1986 (population per square kilometer).



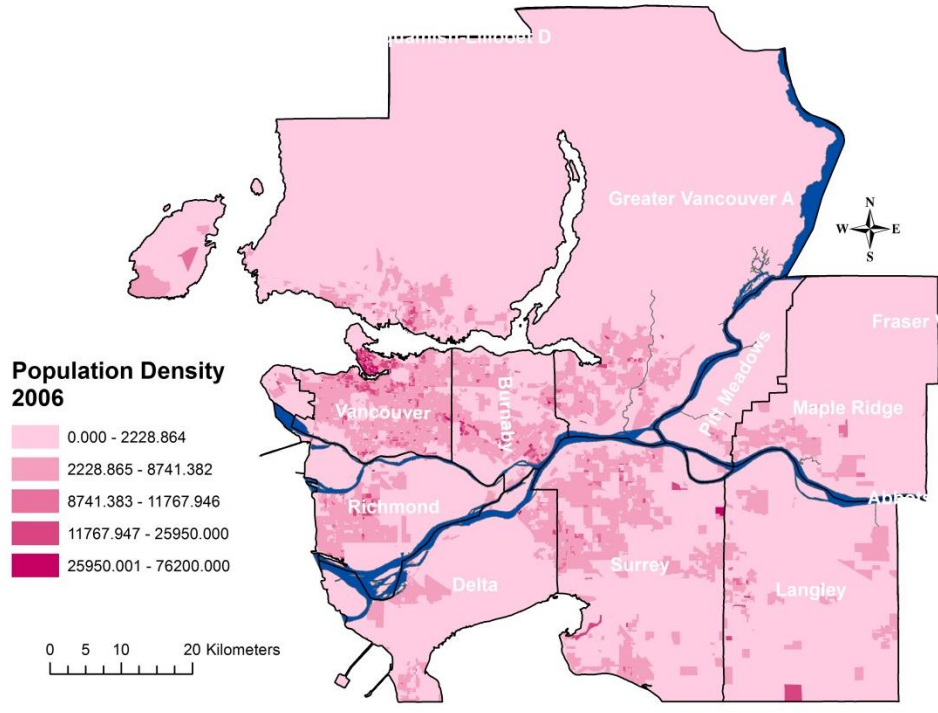
Calculated normalized population density for Metro Vancouver for 1991 (population per square kilometer).



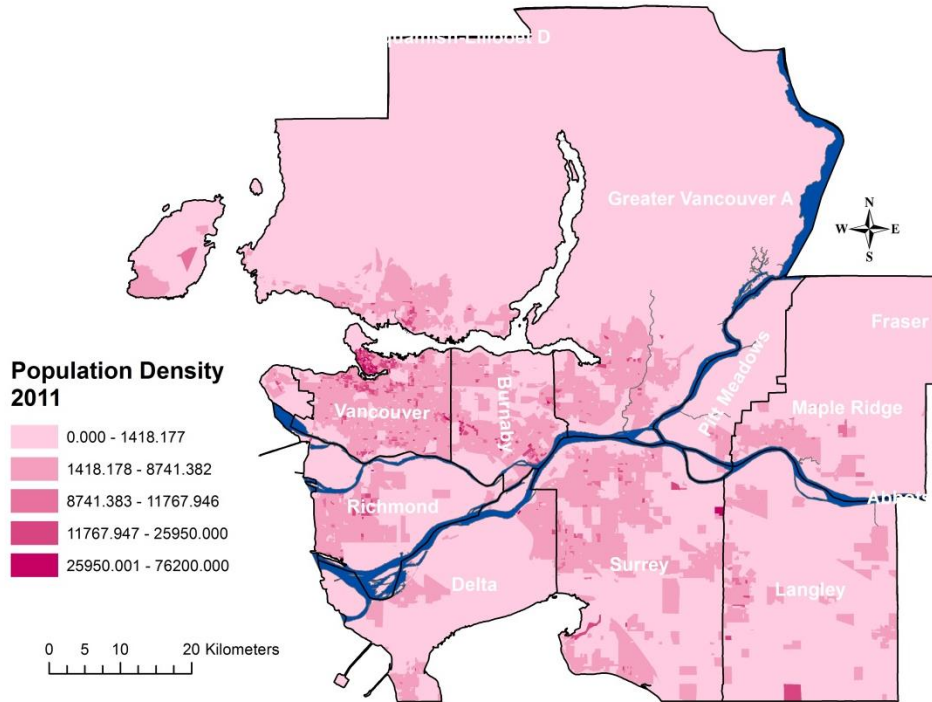
Calculated normalized population density for Metro Vancouver for 1996 (population per square kilometer).



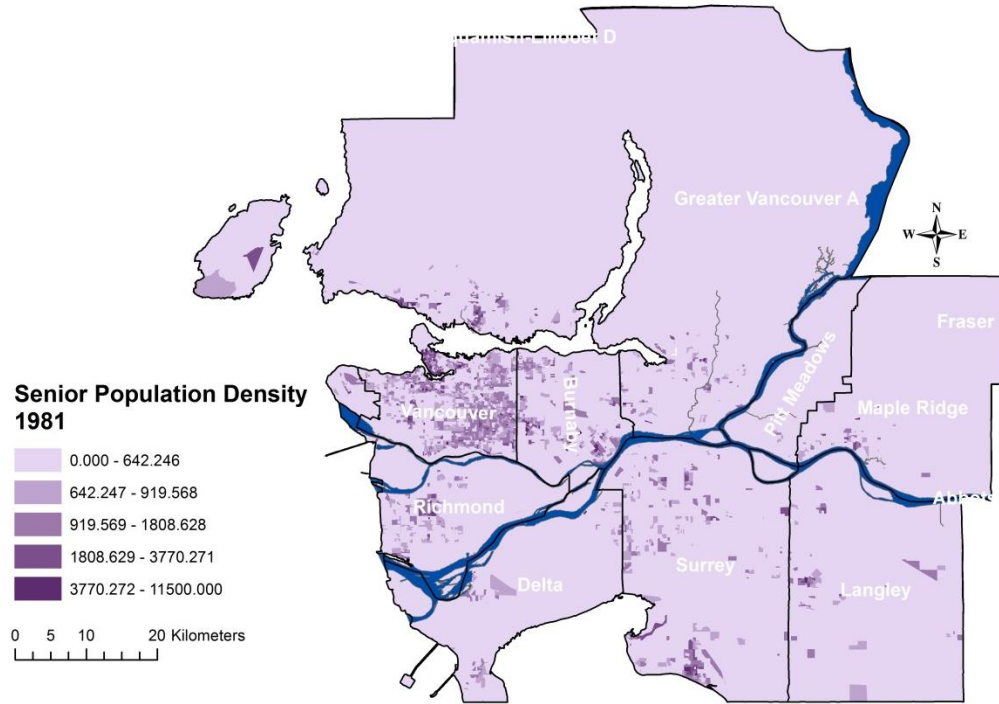
Calculated normalized population density for Metro Vancouver for 2001 (population per square kilometer).



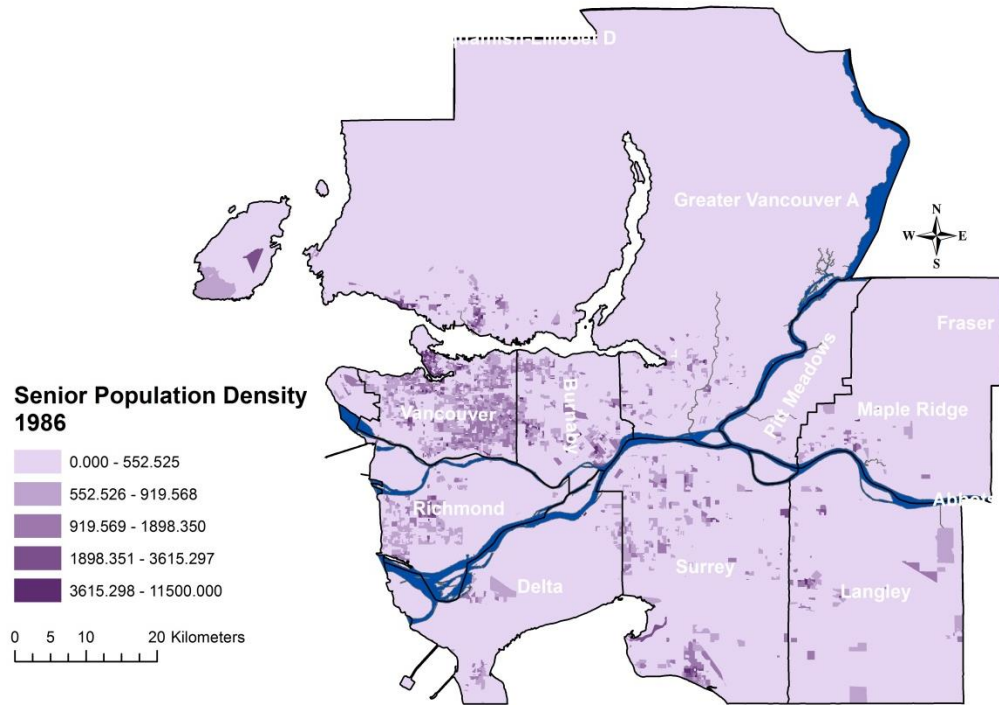
Calculated normalized population density for Metro Vancouver for 2006 (population per square kilometer).



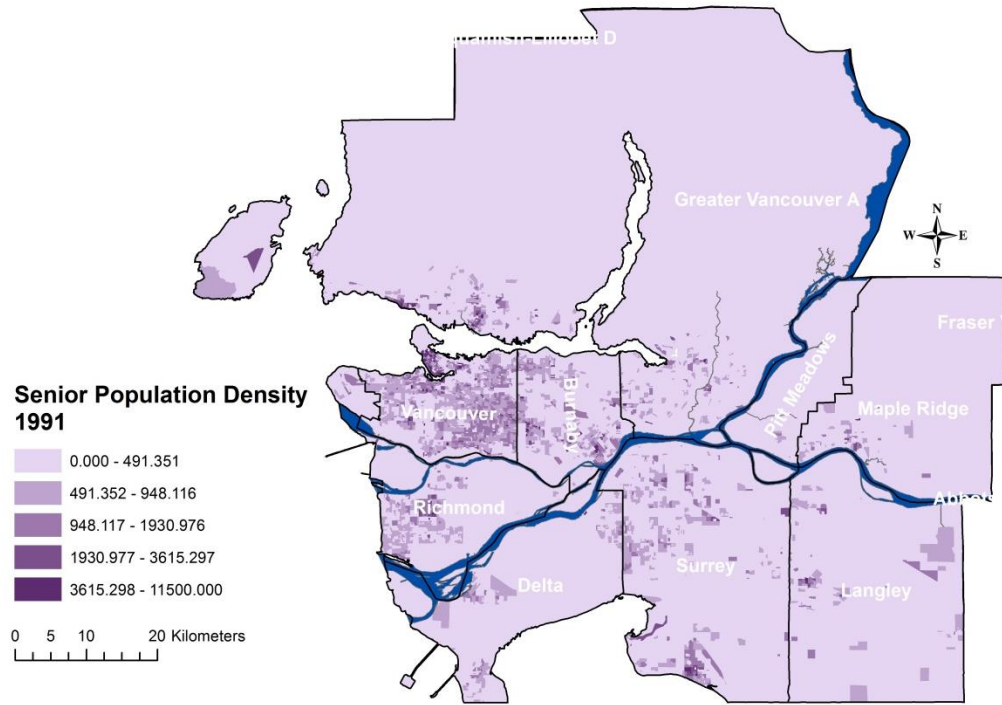
Calculated normalized population density for Metro Vancouver for 2011 (population per square kilometer).



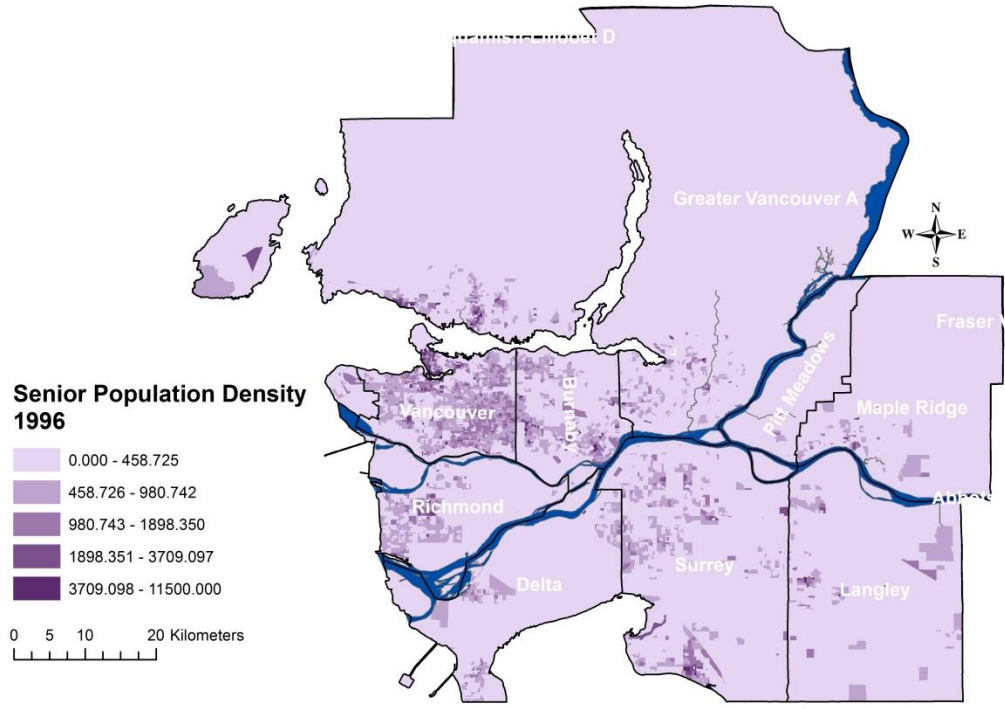
**Calculated normalized senior population density for Metro Vancouver for 1981
(number of seniors per square kilometer).**



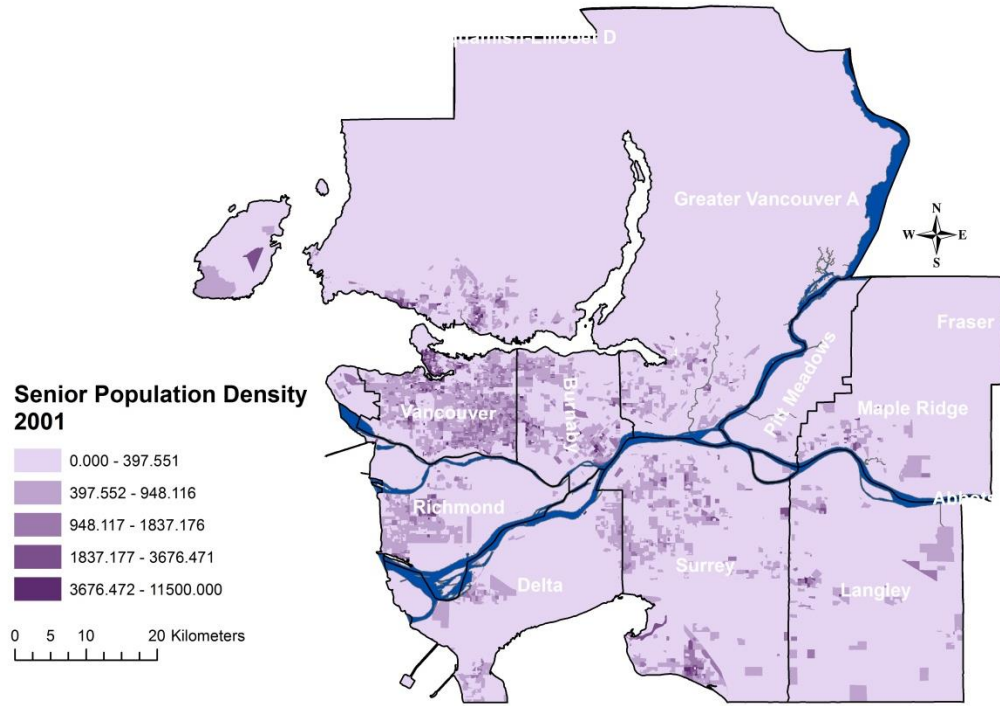
**Calculated normalized senior population density for Metro Vancouver for 1986
(number of seniors per square kilometer).**



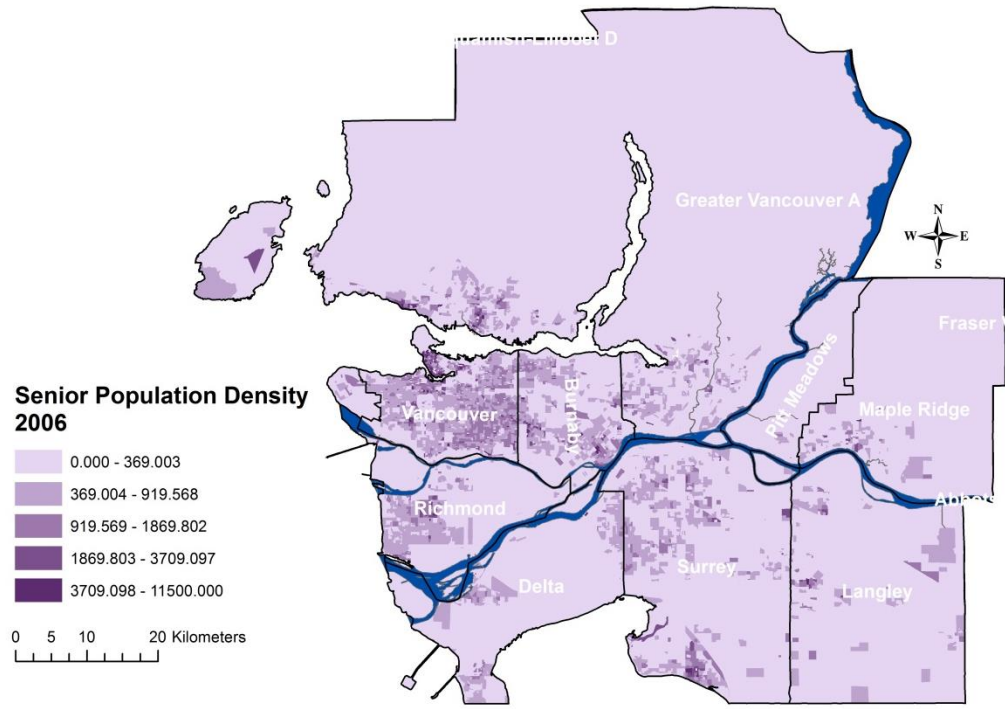
**Calculated normalized senior population density for Metro Vancouver for 1991
(number of seniors per square kilometer).**



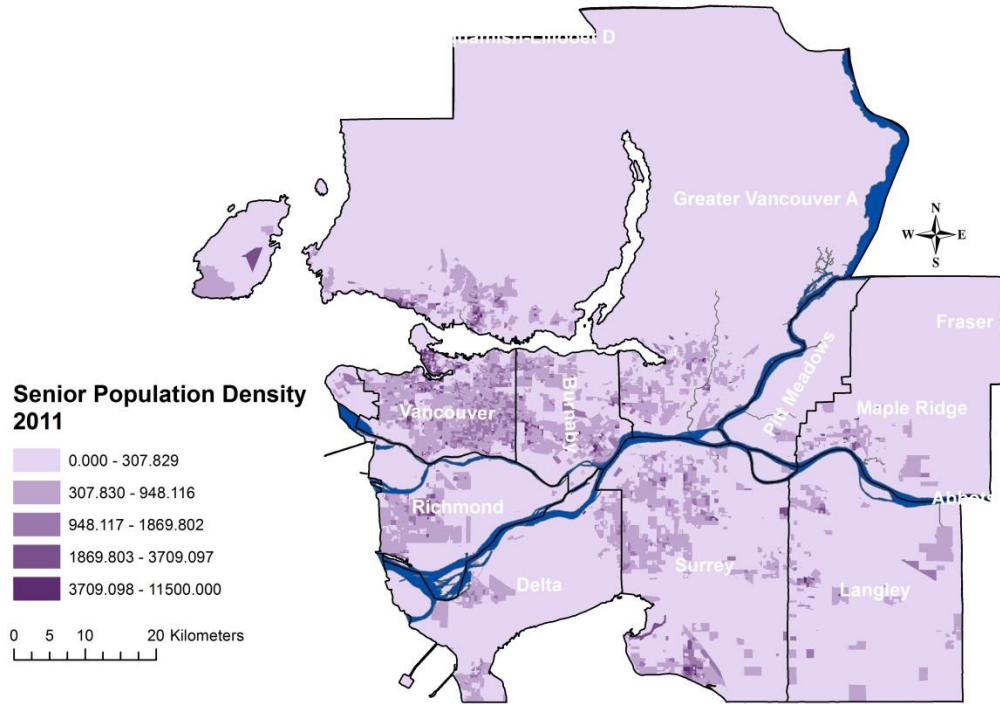
**Calculated normalized senior population density for Metro Vancouver for 1996
(number of seniors per square kilometer).**



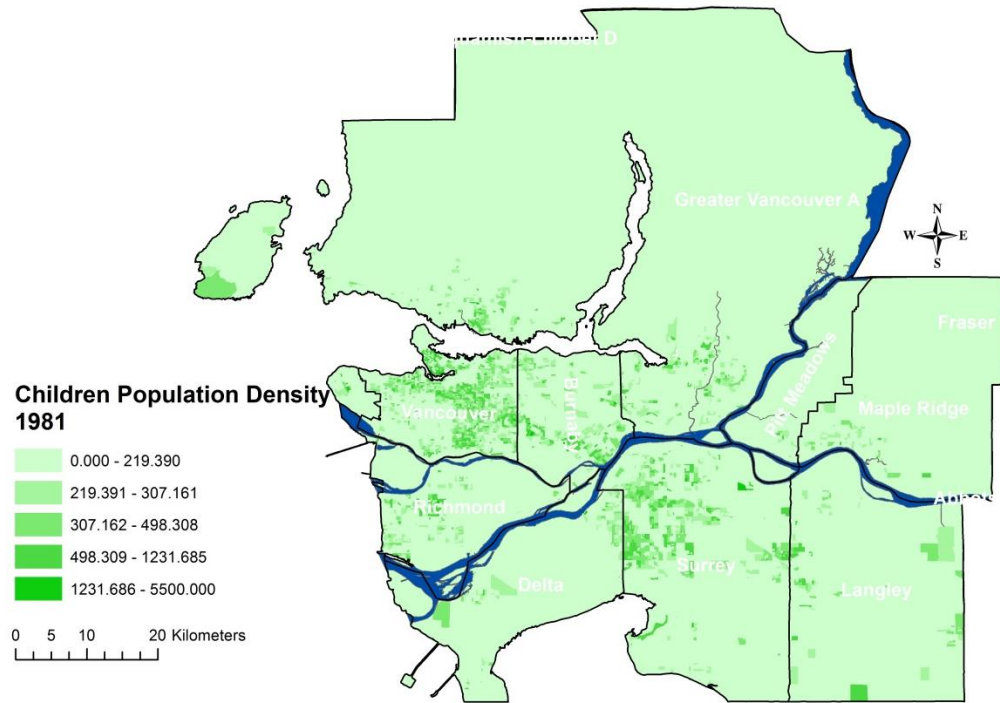
**Calculated normalized senior population density for Metro Vancouver for 2001
(number of seniors per square kilometer).**



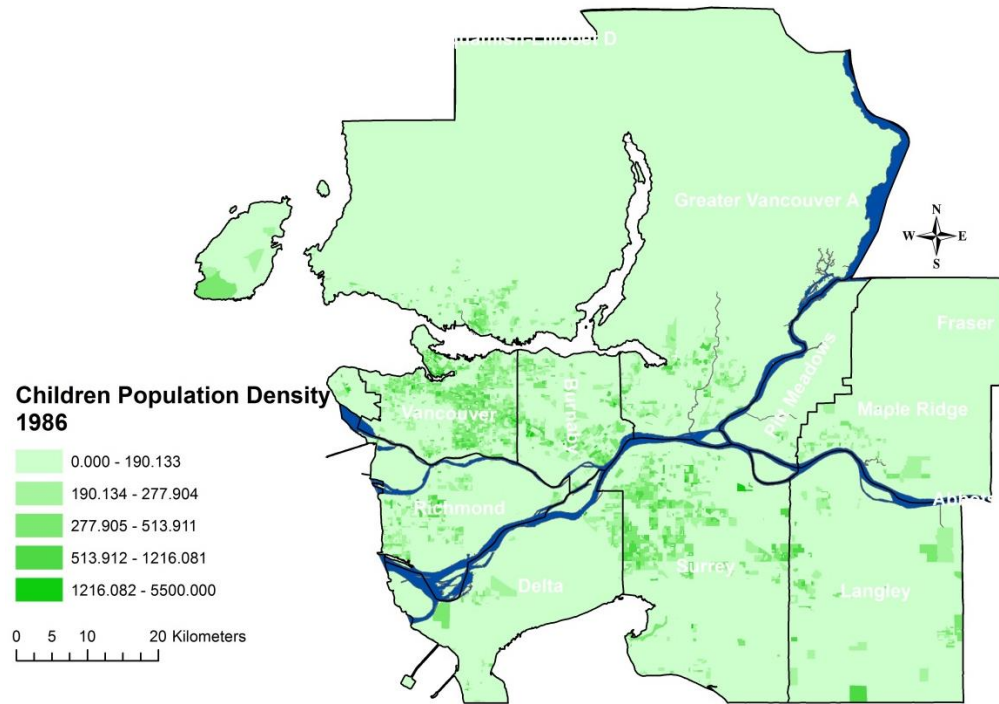
**Calculated normalized senior population density for Metro Vancouver for 2006
(number of seniors per square kilometer).**



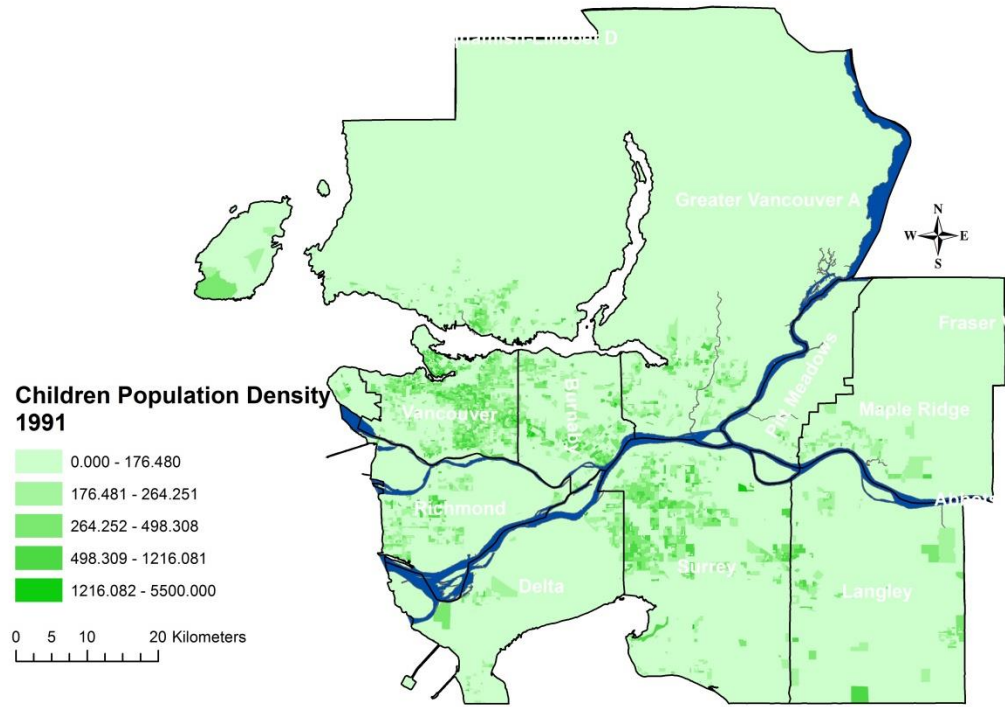
**Calculated normalized senior population density for Metro Vancouver for 2011
(number of seniors per square kilometer).**



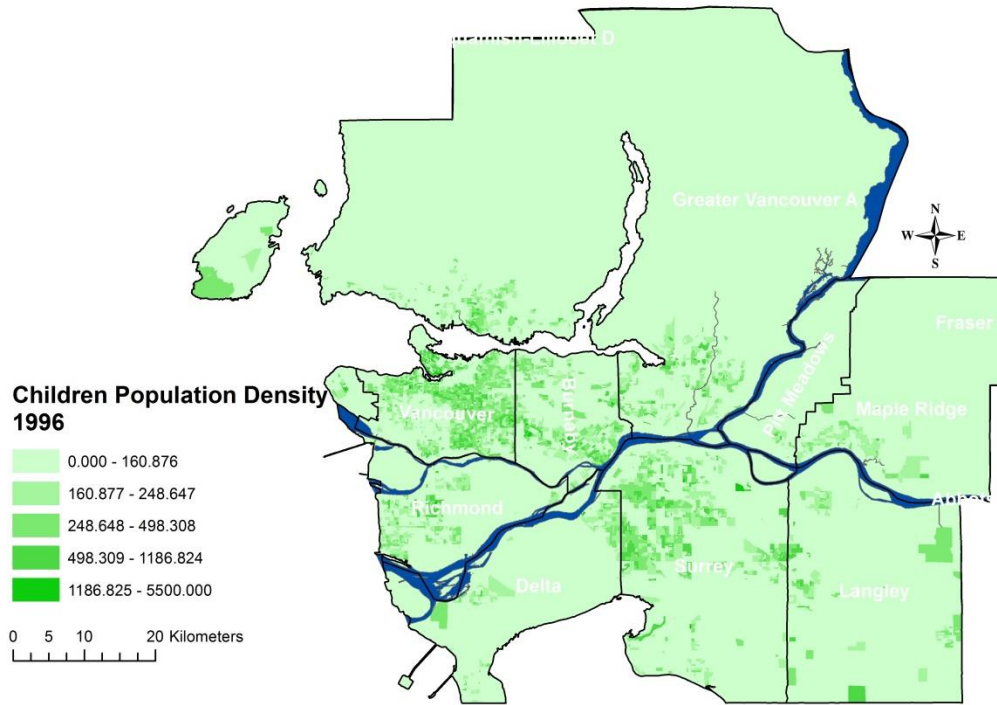
Calculated normalized children population density for Metro Vancouver for 1981 (number of children per square kilometer).



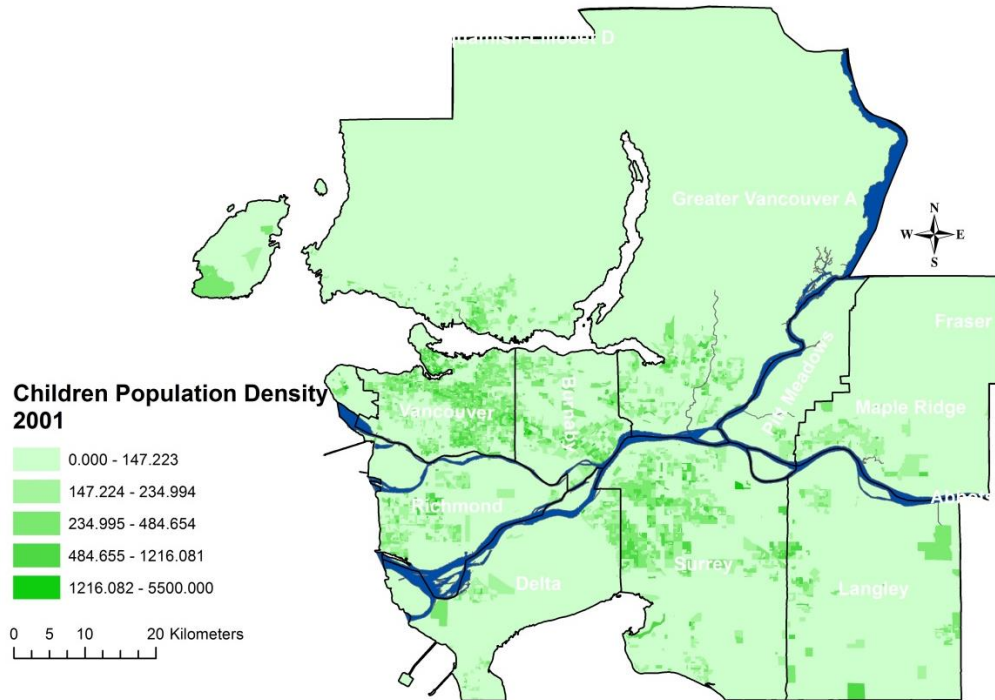
Calculated normalized children population density for Metro Vancouver for 1986 (number of children per square kilometer).



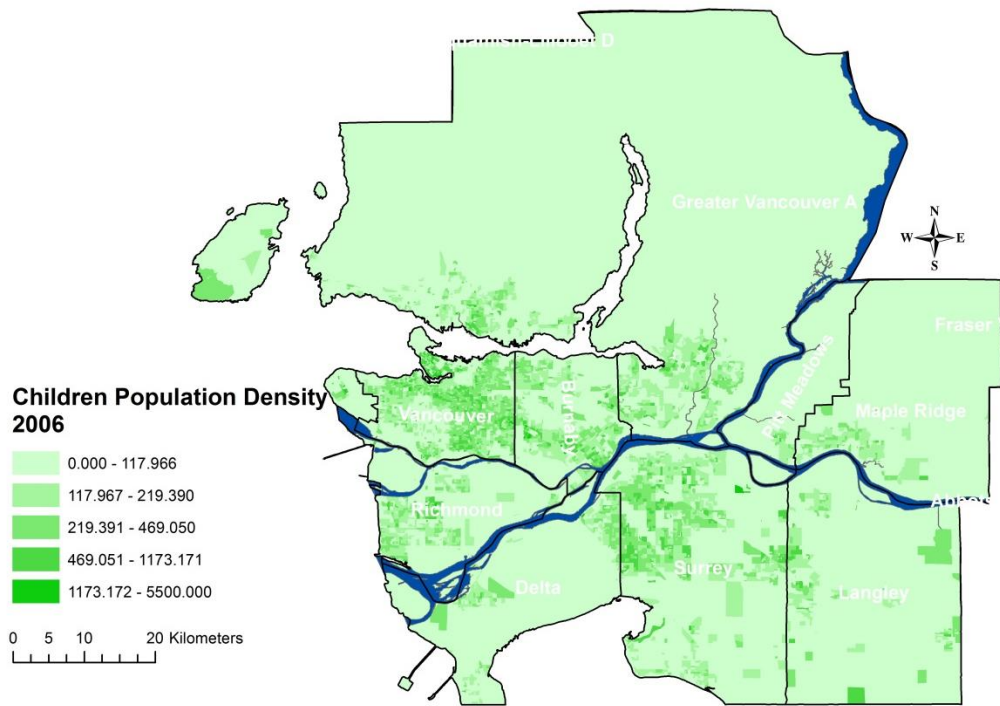
Calculated normalized children population density for Metro Vancouver for 1991 (number of children per square kilometer).



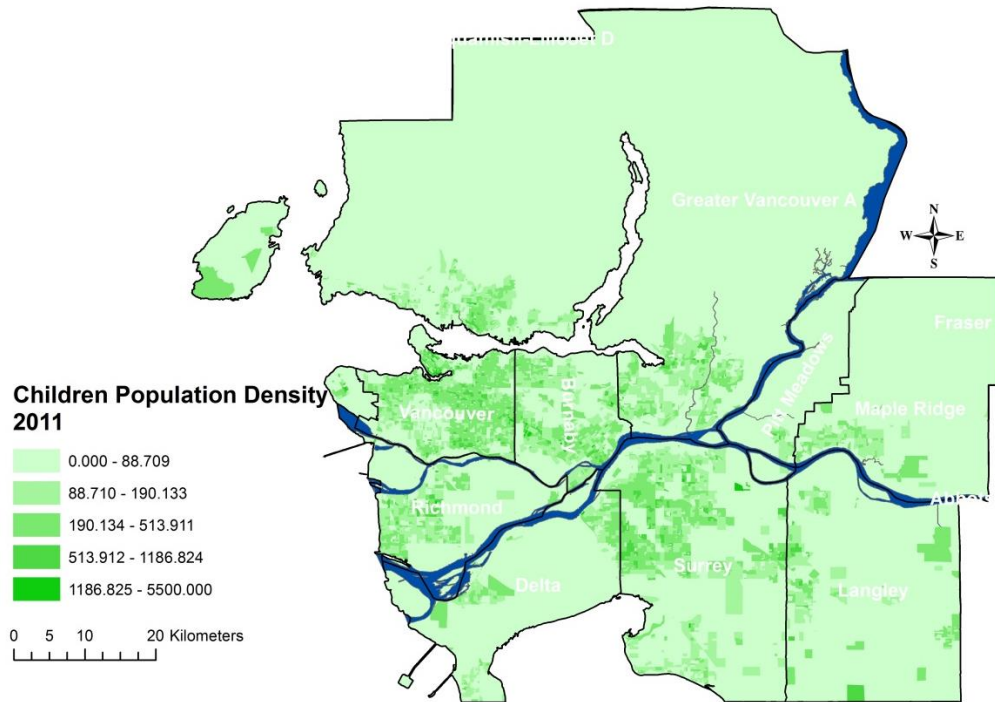
Calculated normalized children population density for Metro Vancouver for 1996 (number of children per square kilometer).



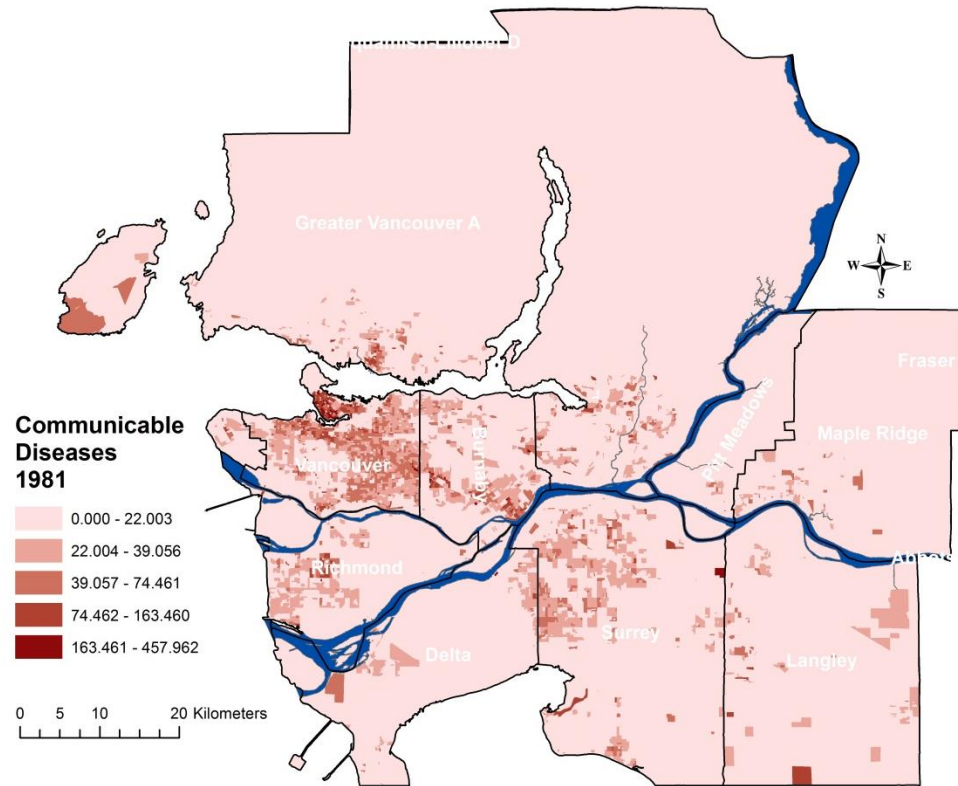
**Calculated normalized children population density for Metro Vancouver for 2001
(number of children per square kilometer).**



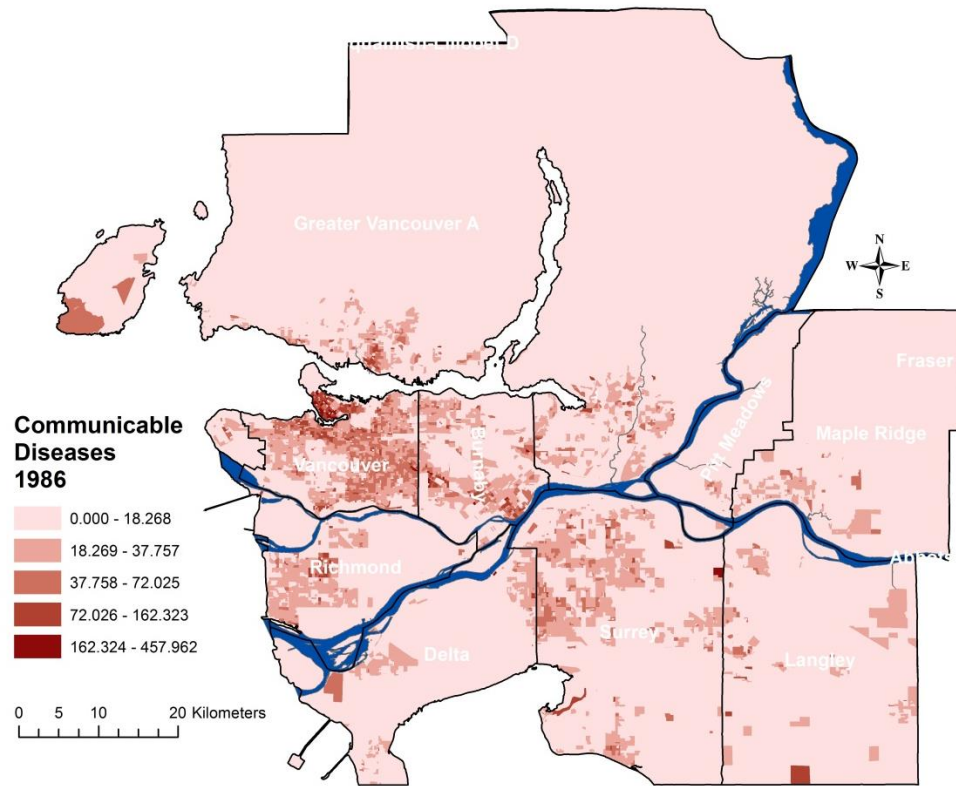
**Calculated normalized children population density for Metro Vancouver for 2006
(number of children per square kilometer).**



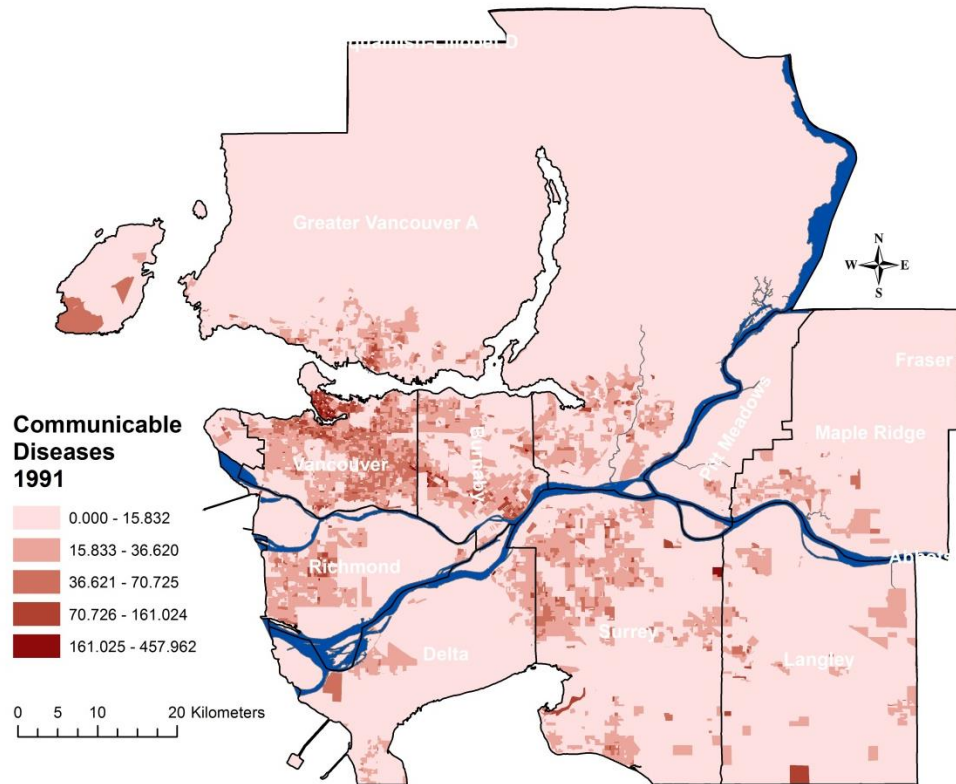
**Calculated normalized children population density for Metro Vancouver for 2011
(number of children per square kilometer).**



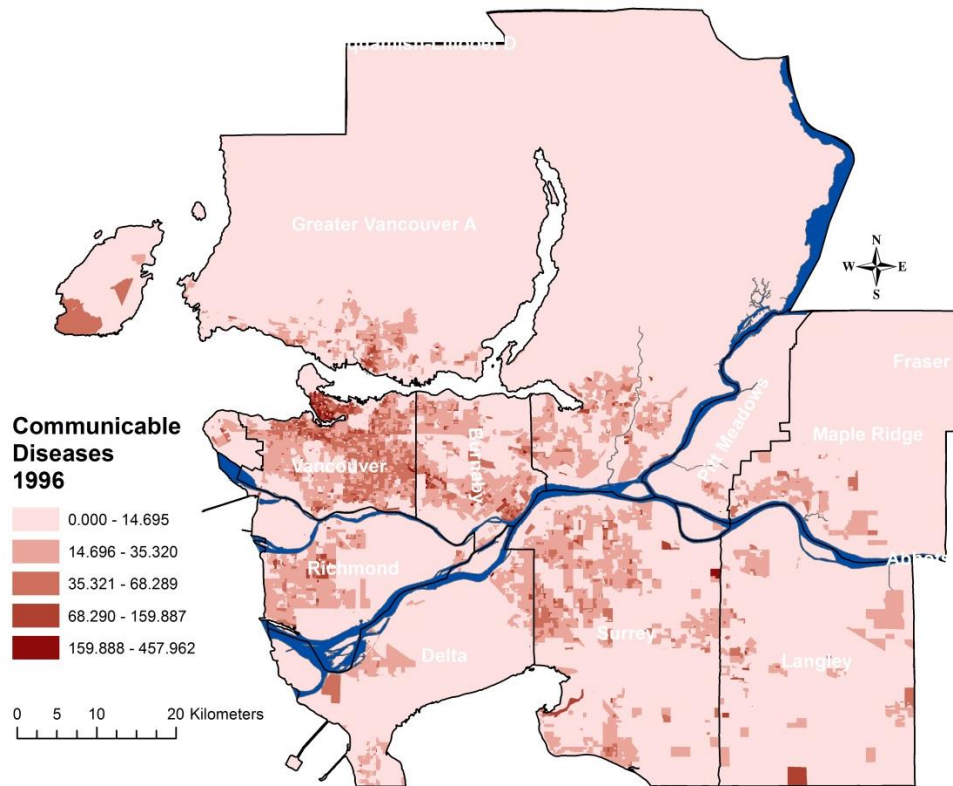
Calculated normalized densities of communicable diseases for Metro Vancouver for 1981 (number of communicable diseases per square kilometer).



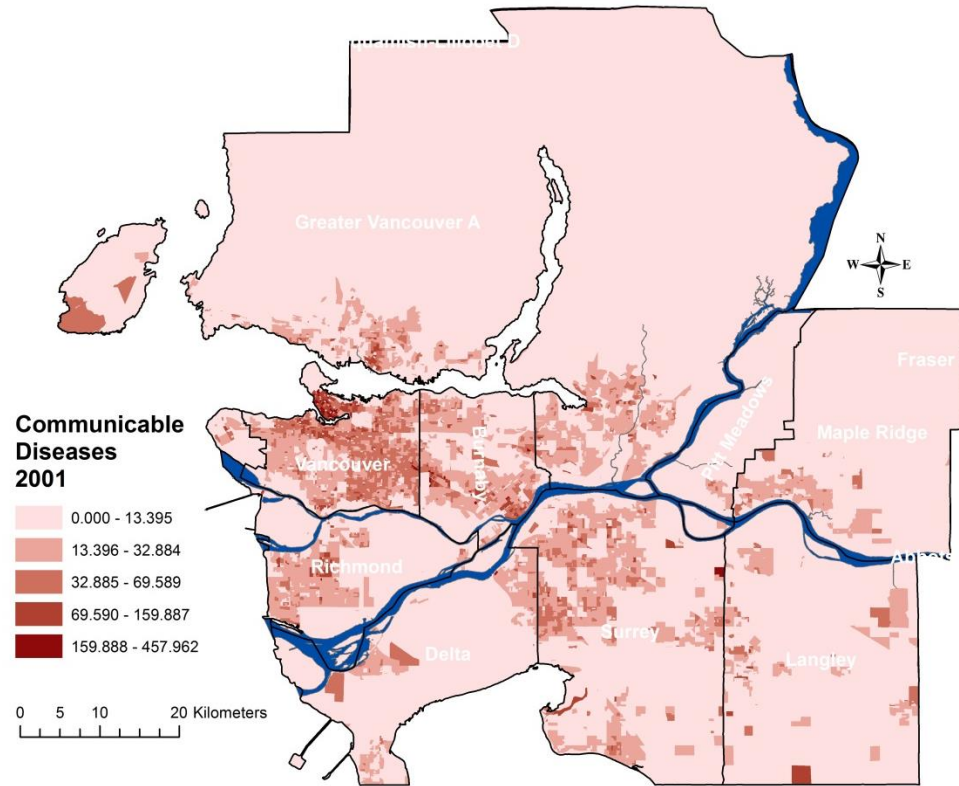
Calculated normalized densities of communicable diseases for Metro Vancouver for 1986 (number of communicable diseases per square kilometer).



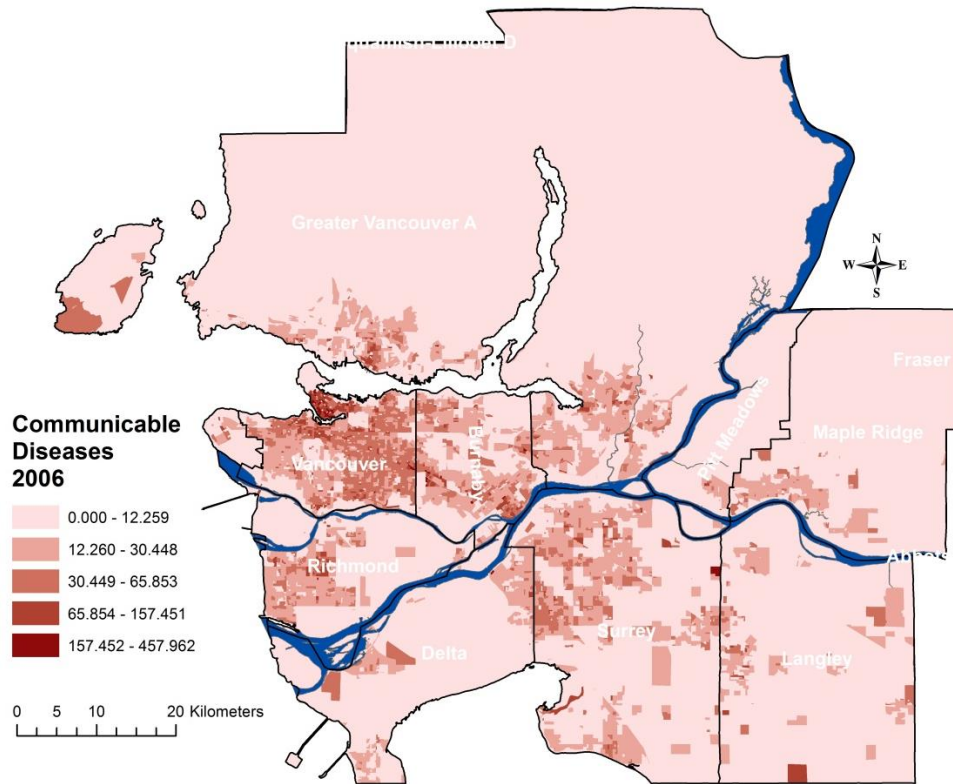
Calculated normalized densities of communicable diseases for Metro Vancouver for 1991 (number of communicable diseases per square kilometer).



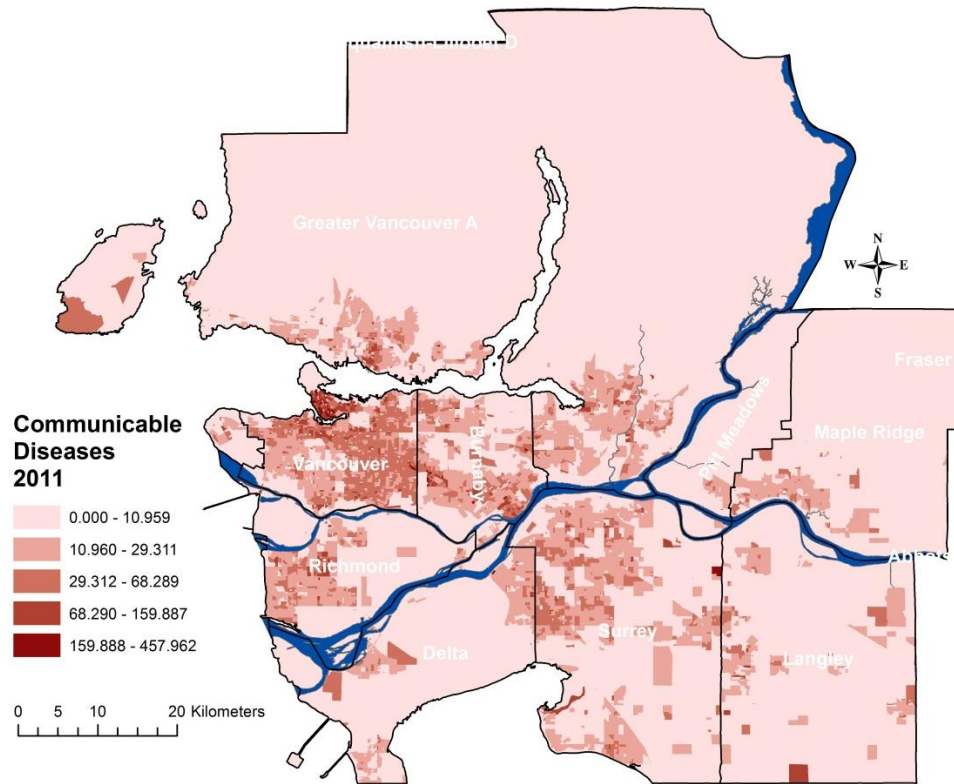
Calculated normalized densities of communicable diseases for Metro Vancouver for 1996 (number of communicable diseases per square kilometer).



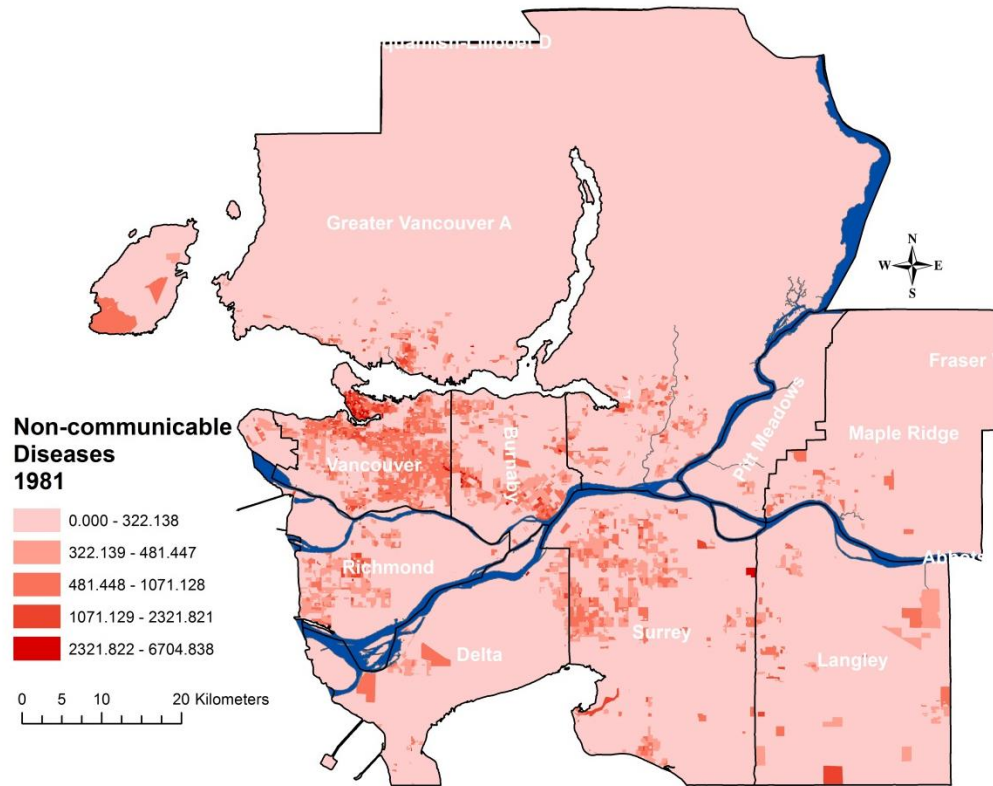
Calculated normalized densities of communicable diseases for Metro Vancouver for 2001 (number of communicable diseases per square kilometer).



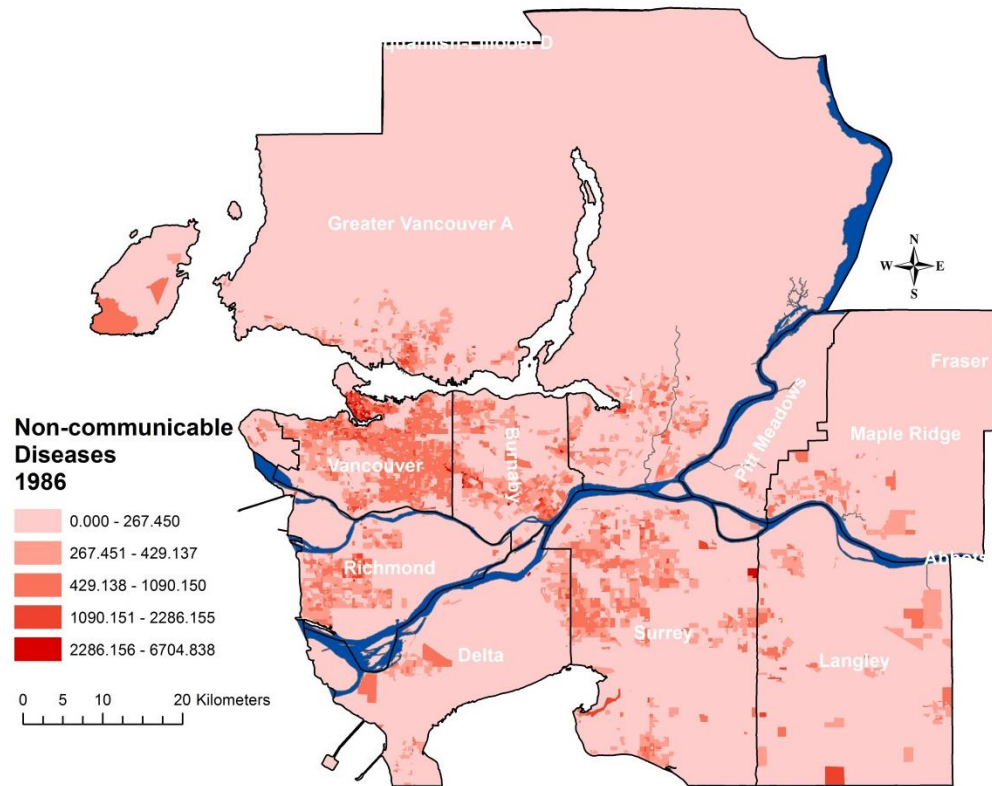
Calculated normalized densities of communicable diseases for Metro Vancouver for 2006 (number of communicable diseases per square kilometer).



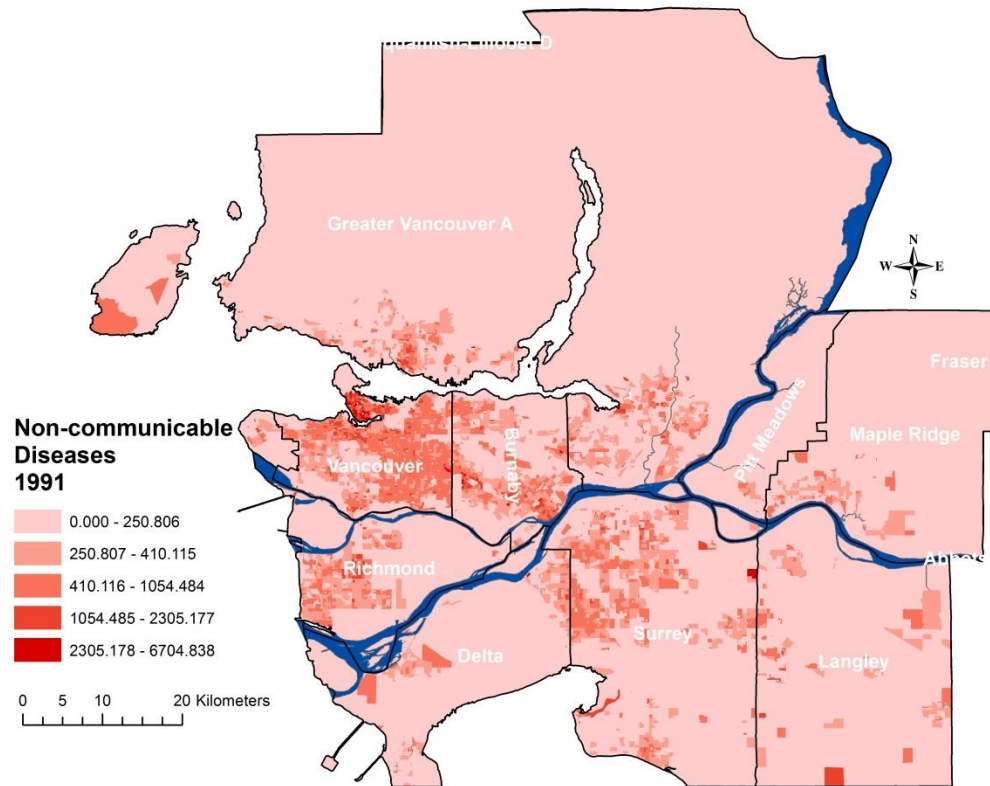
Calculated normalized densities of communicable diseases for Metro Vancouver for 2011 (number of communicable diseases per square kilometer).



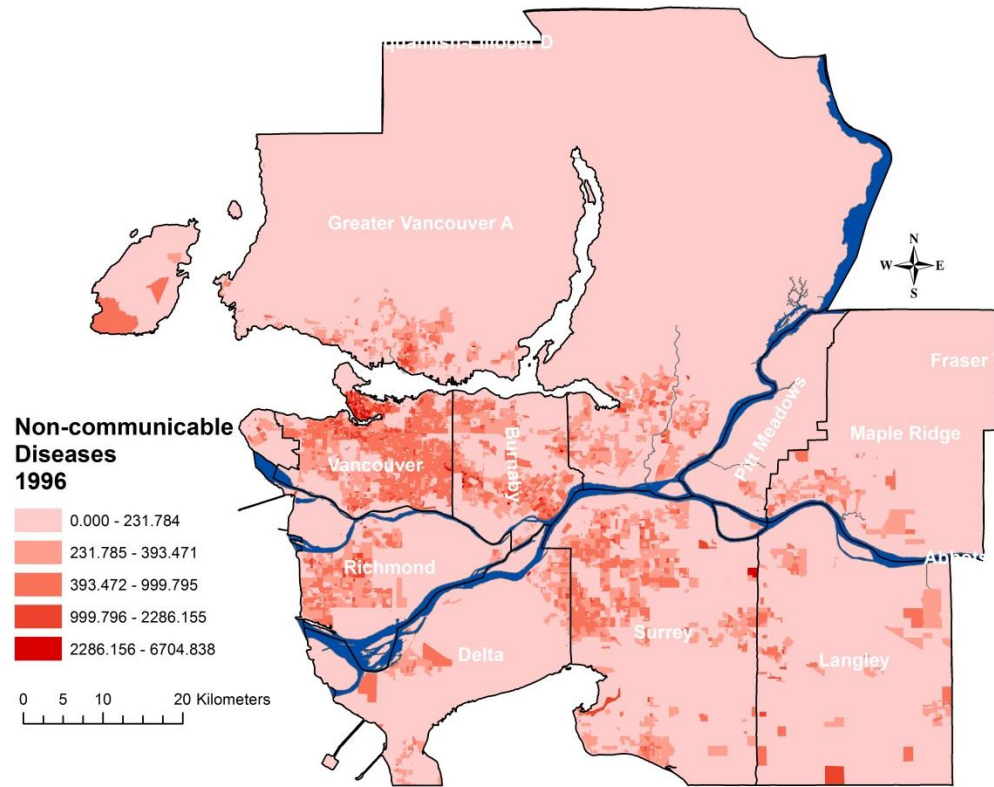
Calculated normalized densities of non-communicable diseases for Metro Vancouver for 1981 (number of non-communicable diseases per square kilometer).



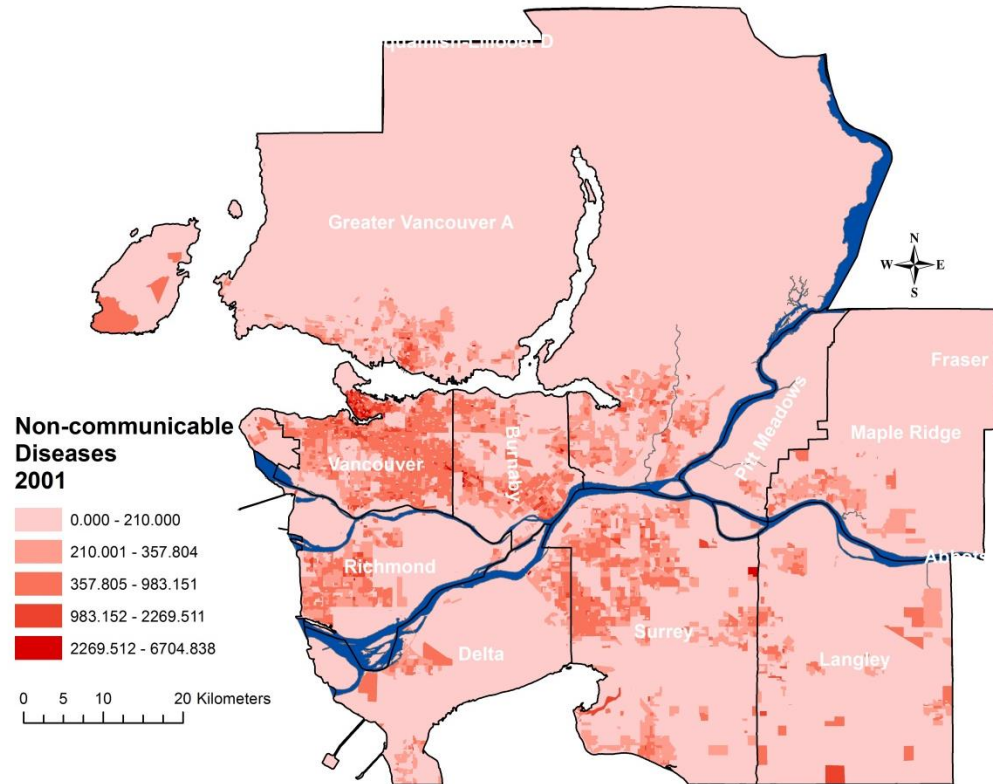
Calculated normalized densities of non-communicable diseases for Metro Vancouver for 1986 (number of non-communicable diseases per square kilometer).



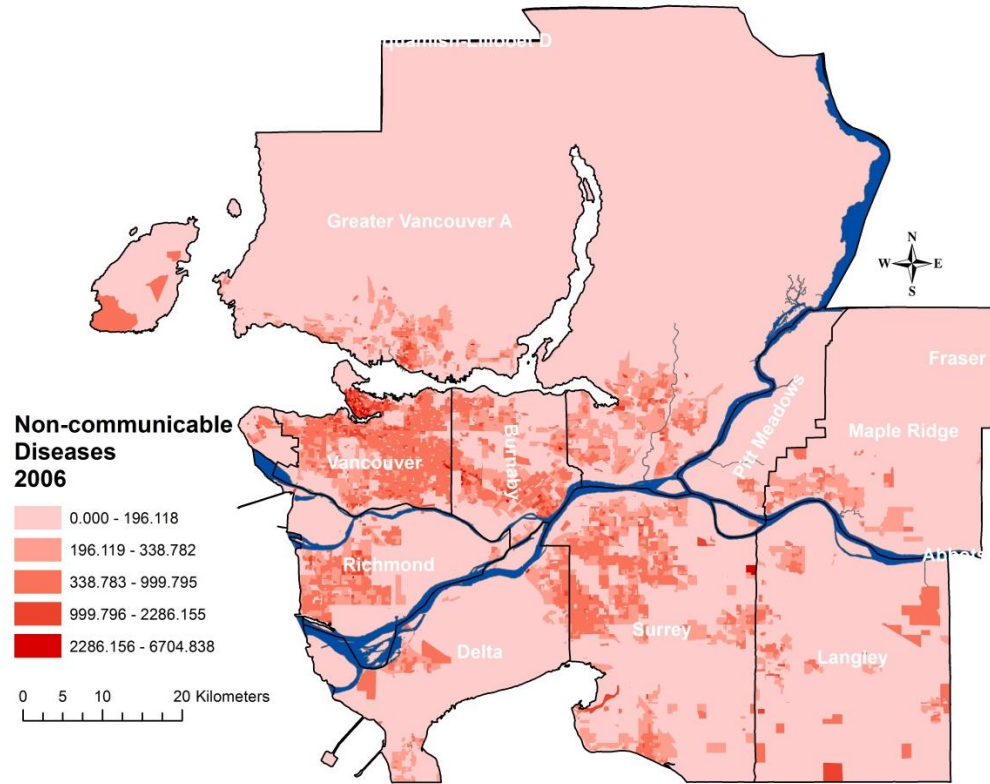
Calculated normalized densities of non-communicable diseases for Metro Vancouver for 1991 (number of non-communicable diseases per square kilometer).



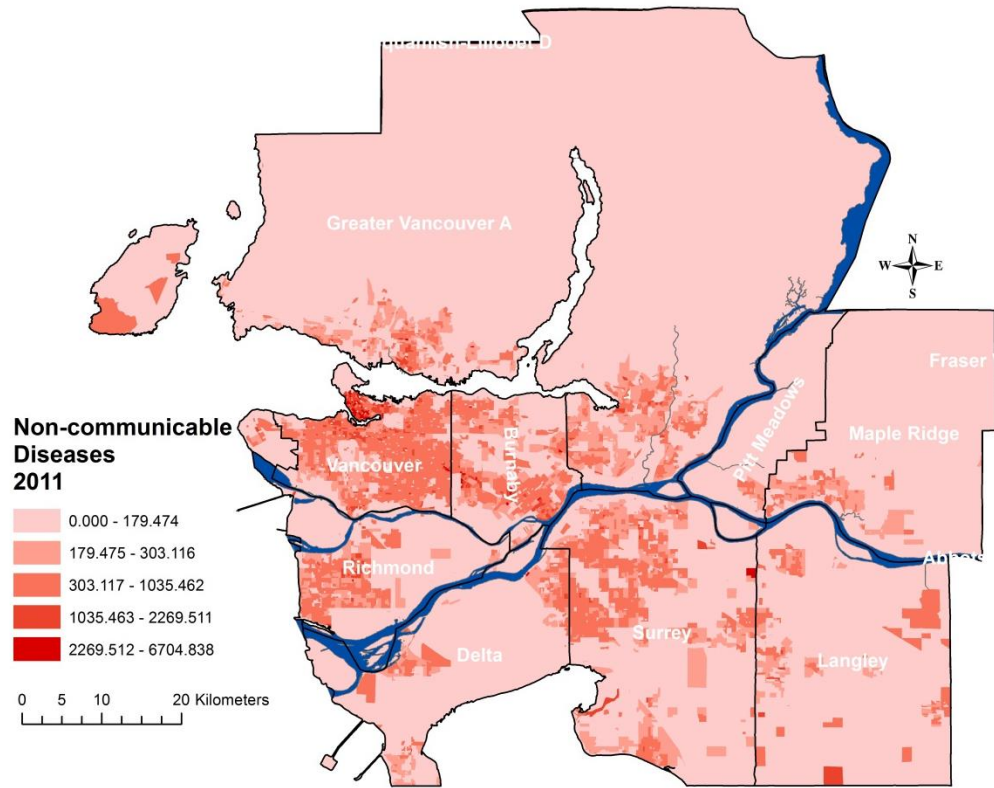
Calculated normalized densities of non-communicable diseases for Metro Vancouver for 1996 (number of non-communicable diseases per square kilometer).



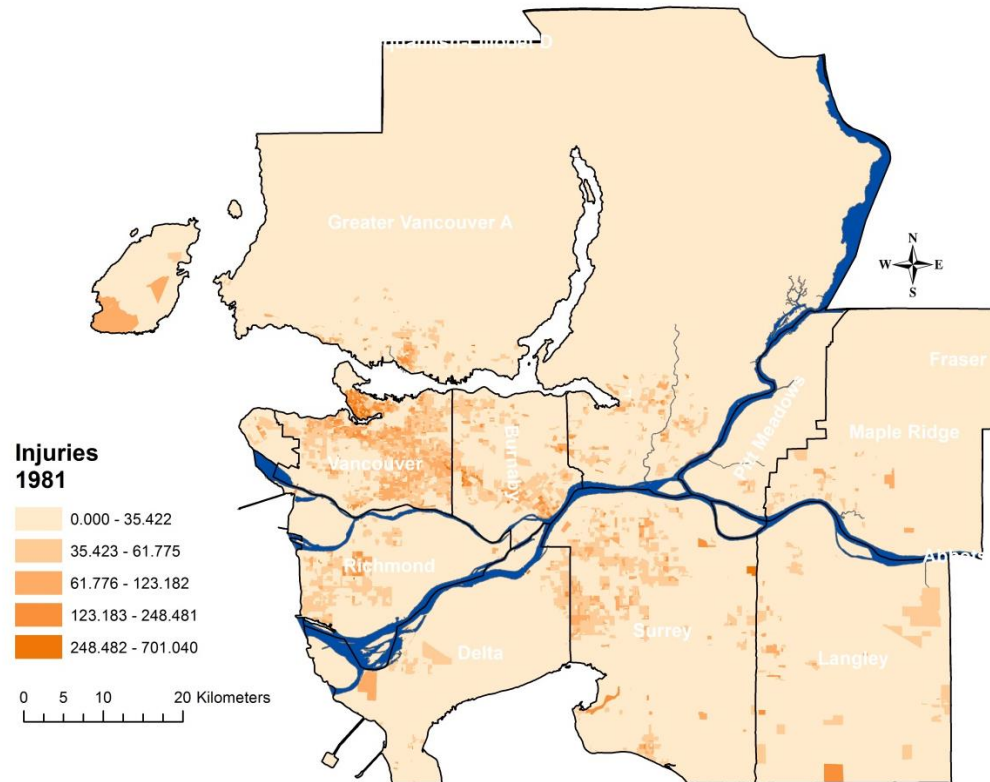
Calculated normalized densities of non-communicable diseases for Metro Vancouver for 2001 (number of non-communicable diseases per square kilometer).



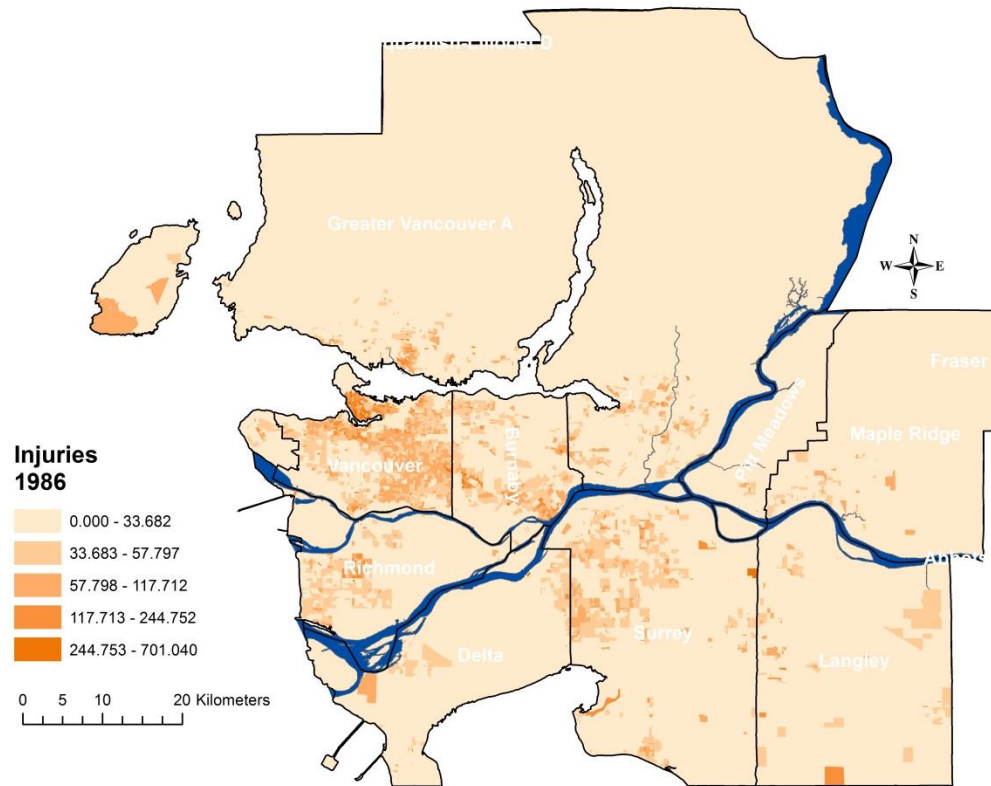
Calculated normalized densities of non-communicable diseases for Metro Vancouver for 2006 (number of non-communicable diseases per square kilometer).



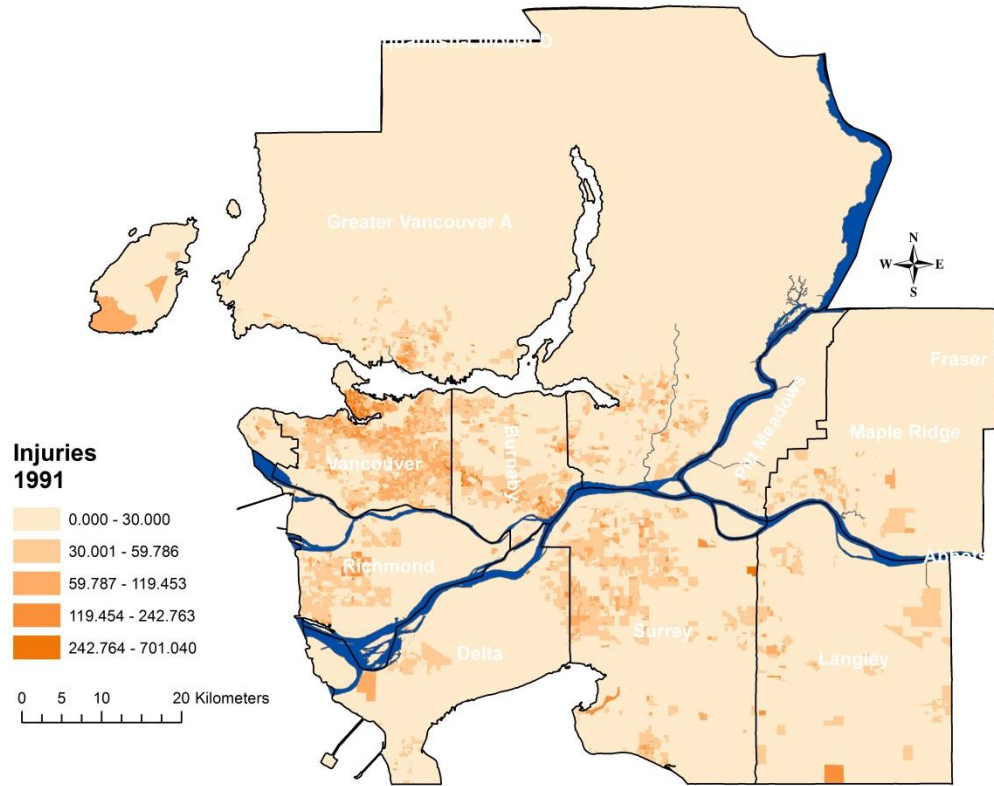
Calculated normalized densities of non-communicable diseases for Metro Vancouver for 2011 (number of non-communicable diseases per square kilometer).



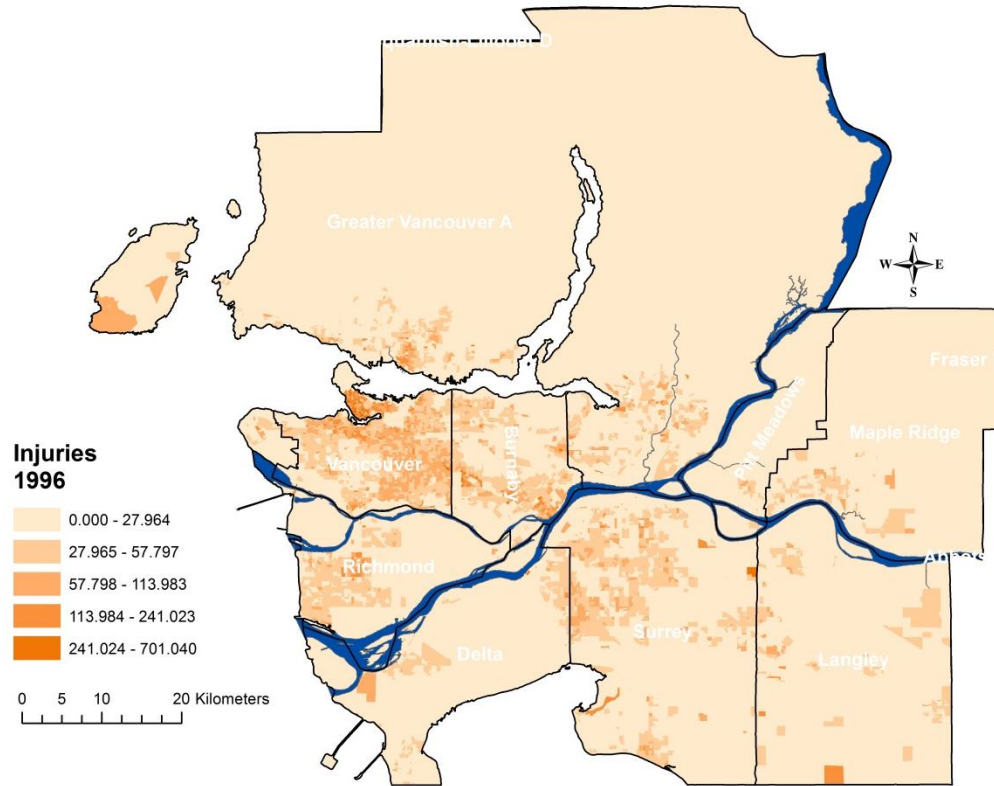
Calculated normalized densities of injuries for Metro Vancouver for 1981 (number of injuries per square kilometer).



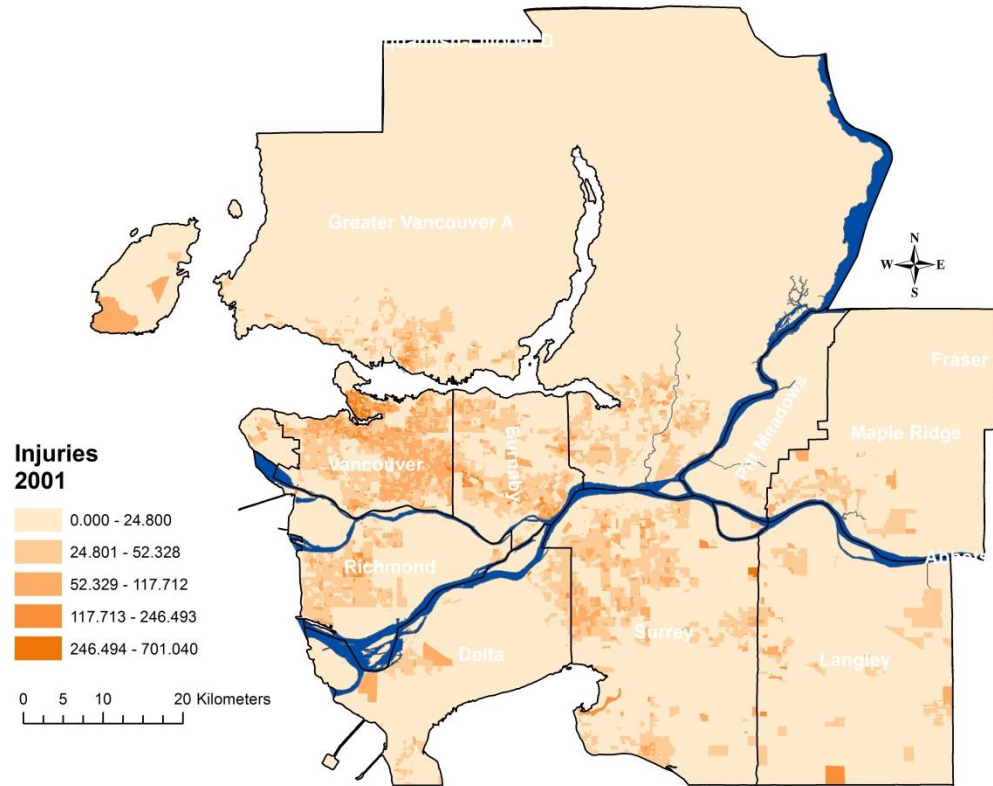
Calculated normalized densities of injuries for Metro Vancouver for 1986 (number of injuries per square kilometer).



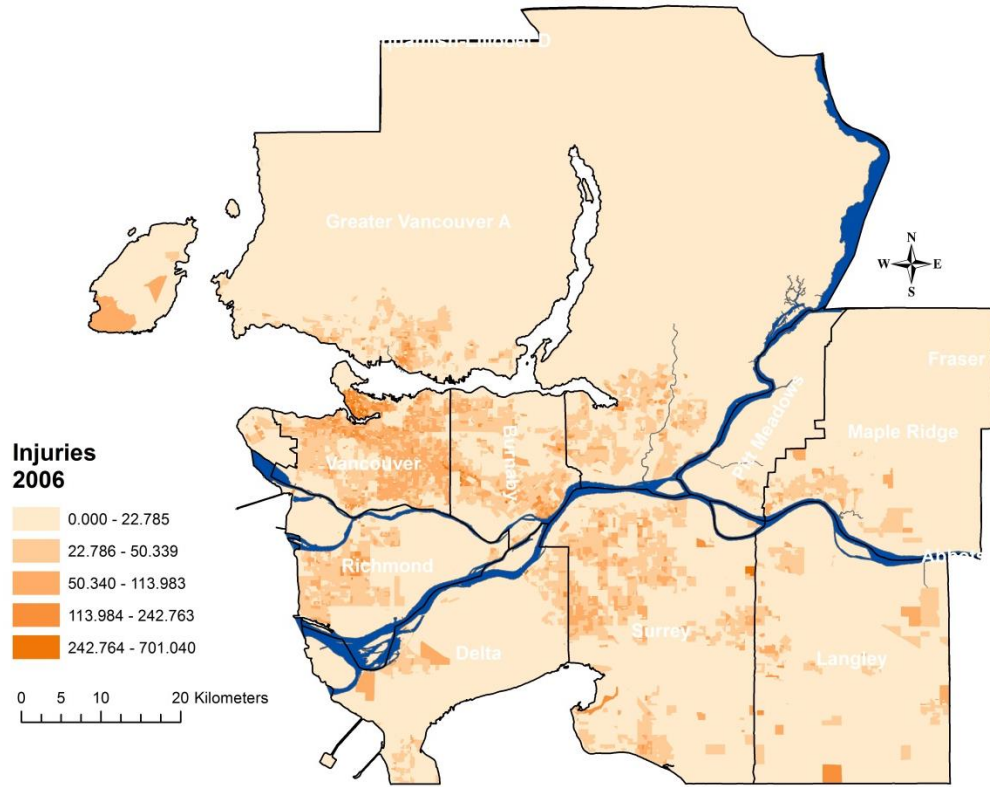
Calculated normalized densities of injuries for Metro Vancouver for 1991 (number of injuries per square kilometer).



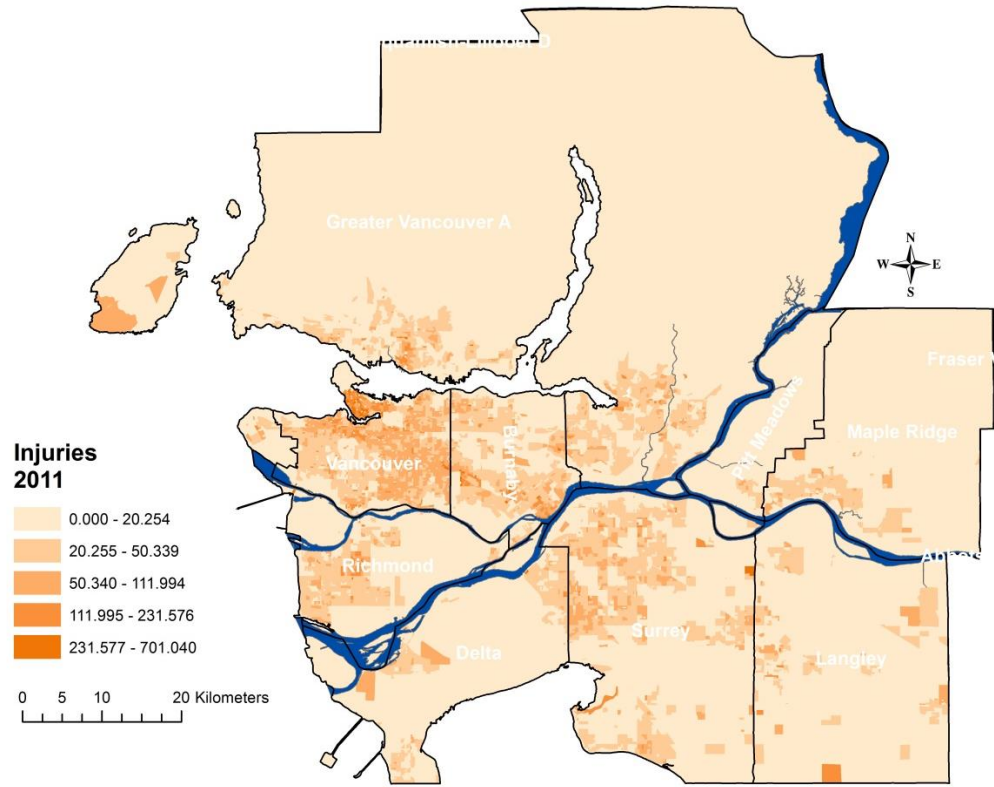
Calculated normalized densities of injuries for Metro Vancouver for 1996 (number of injuries per square kilometer).



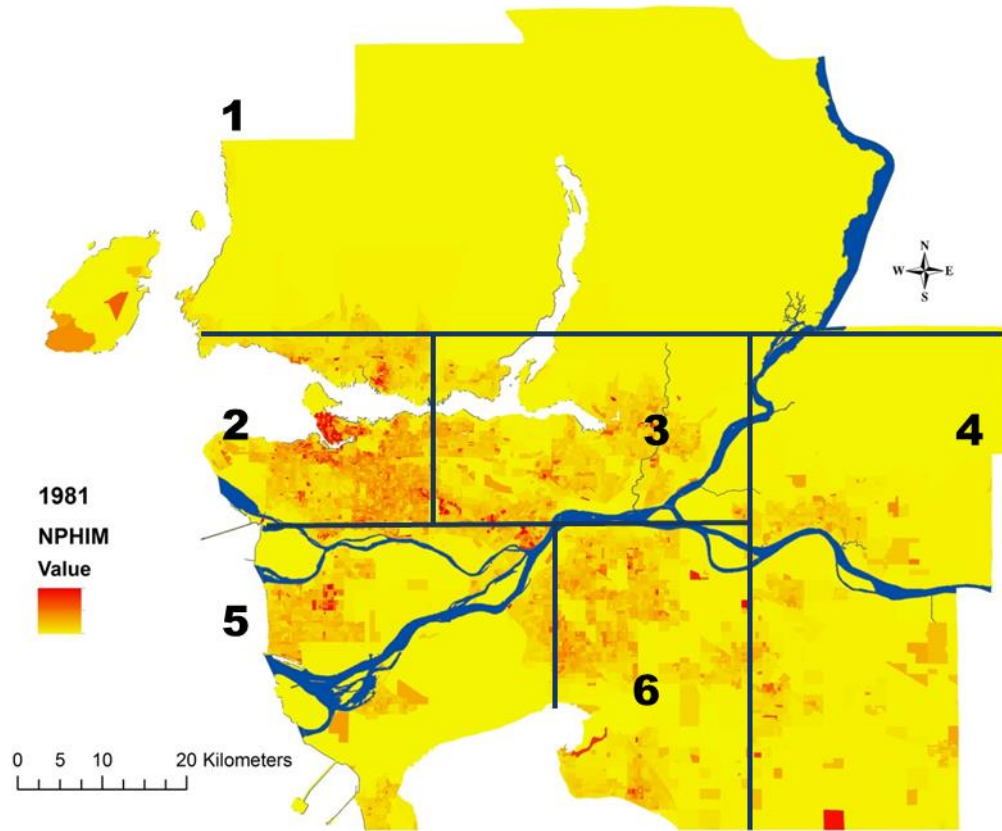
Calculated normalized densities of injuries for Metro Vancouver for 2001 (number of injuries per square kilometer).



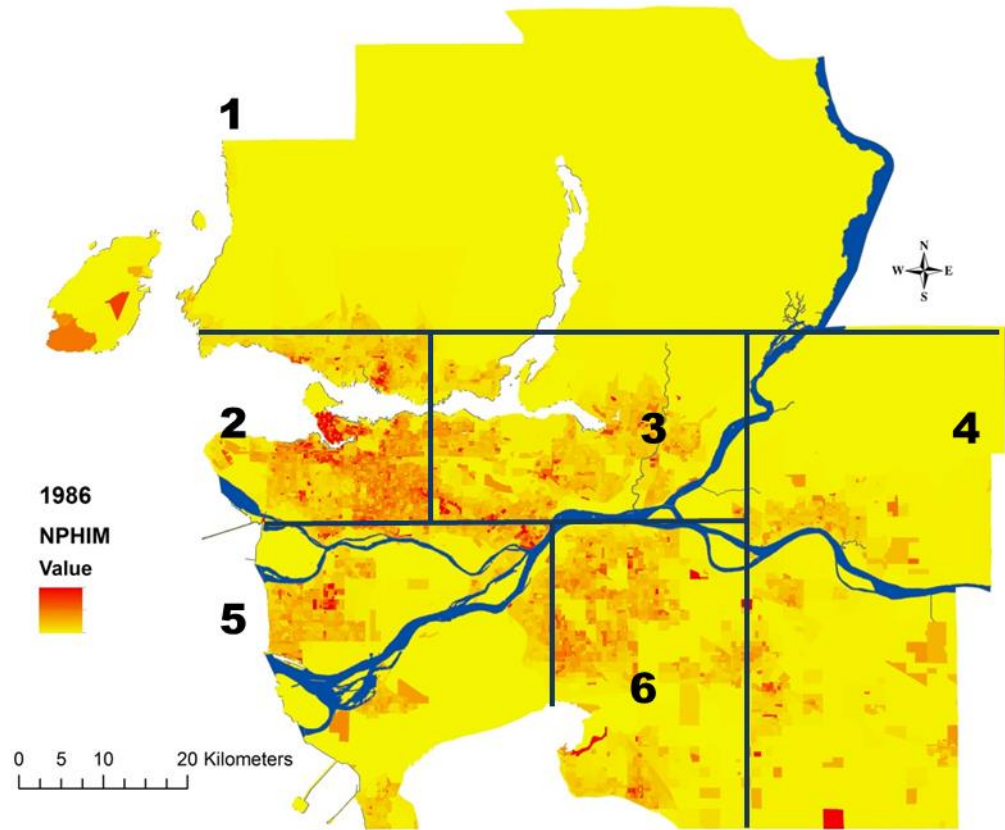
Calculated normalized densities of injuries for Metro Vancouver for 2006 (number of injuries per square kilometer).



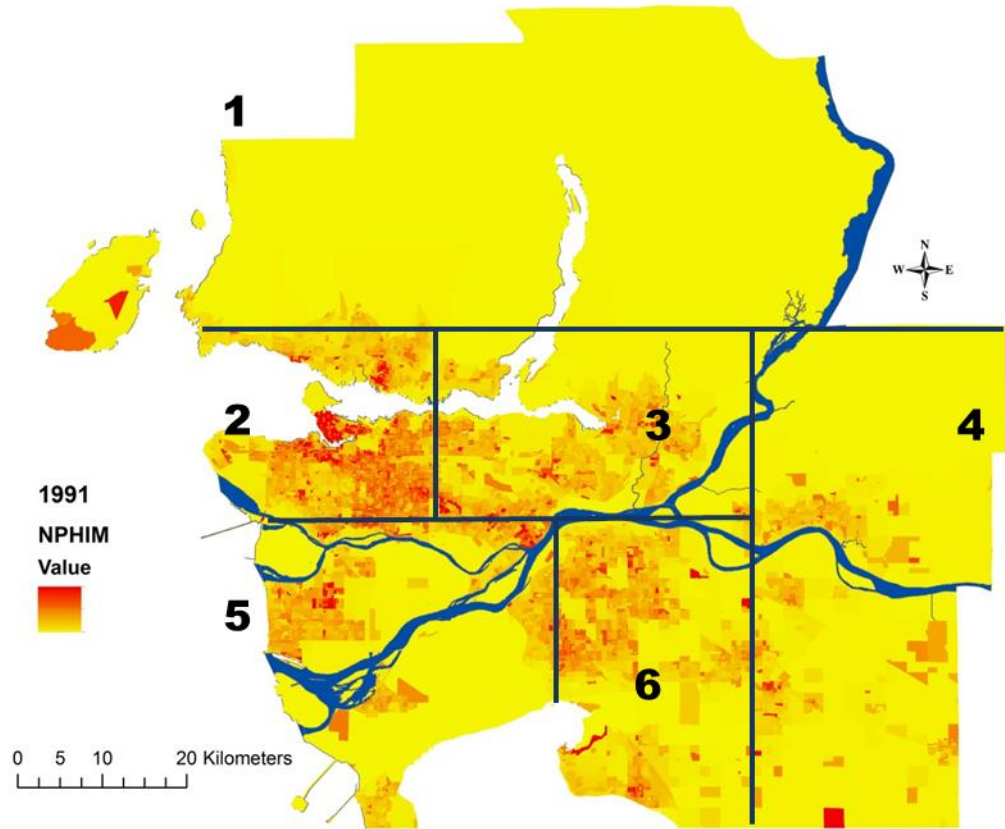
Calculated normalized densities of injuries for Metro Vancouver for 2011 (number of injuries per square kilometer).



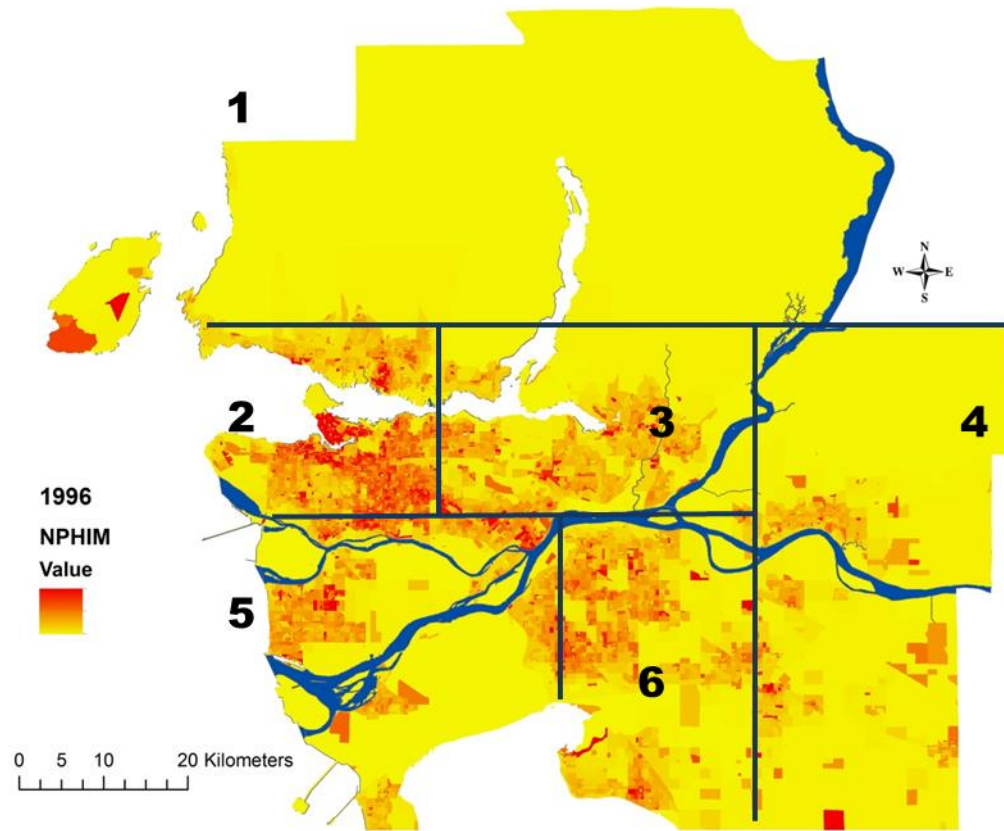
Nonphysical health impact map generated for Metro Vancouver for 1981.



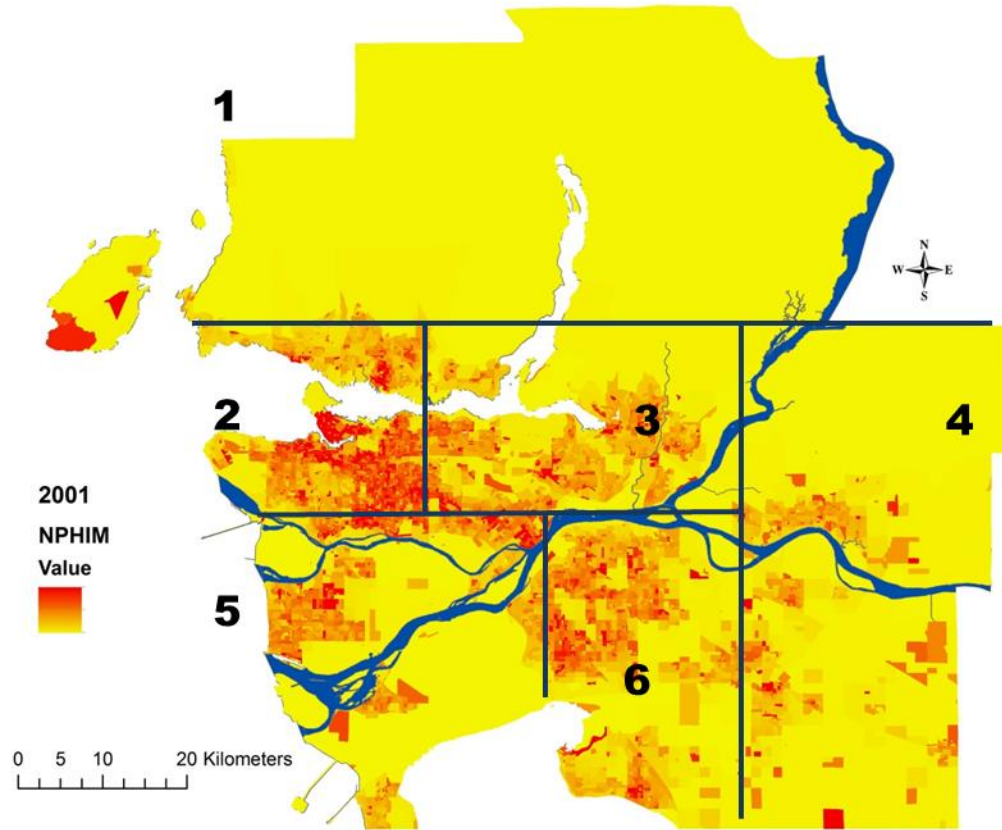
Nonphysical health impact map generated for Metro Vancouver for 1986.



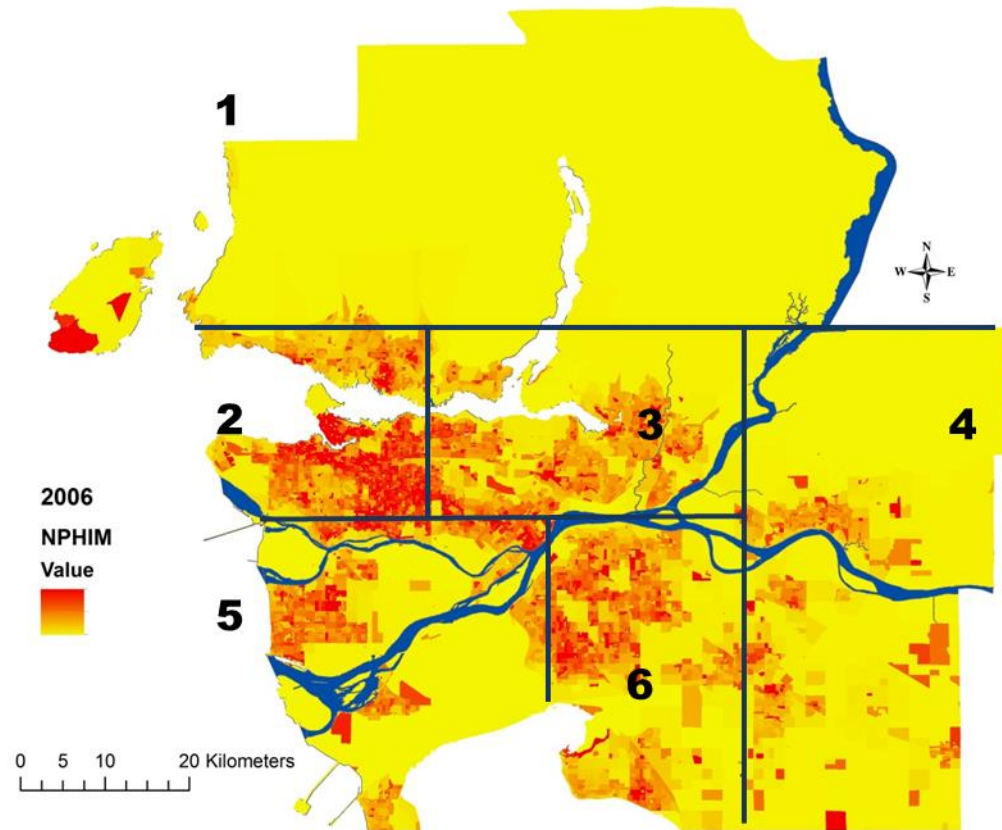
Nonphysical health impact map generated for Metro Vancouver for 1991.



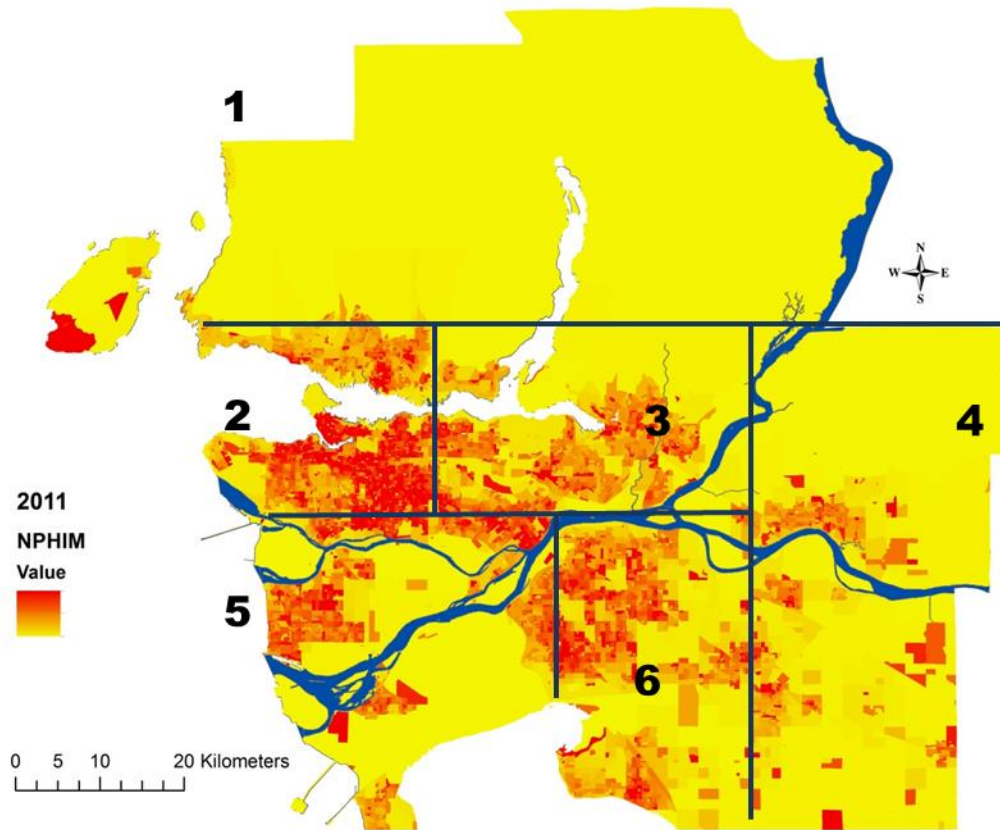
Nonphysical health impact map generated for Metro Vancouver for 1996.



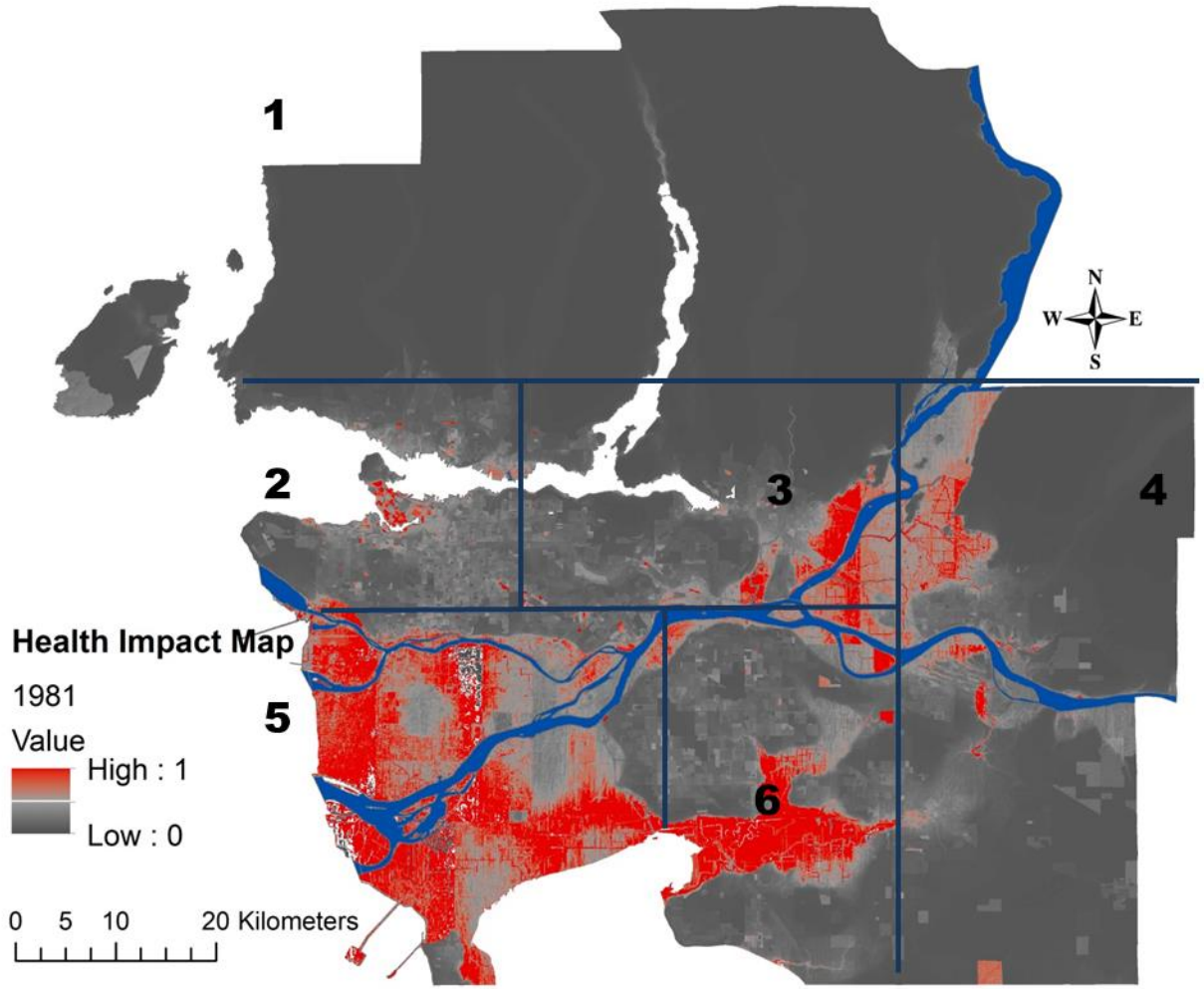
Nonphysical health impact map generated for Metro Vancouver for 2001.



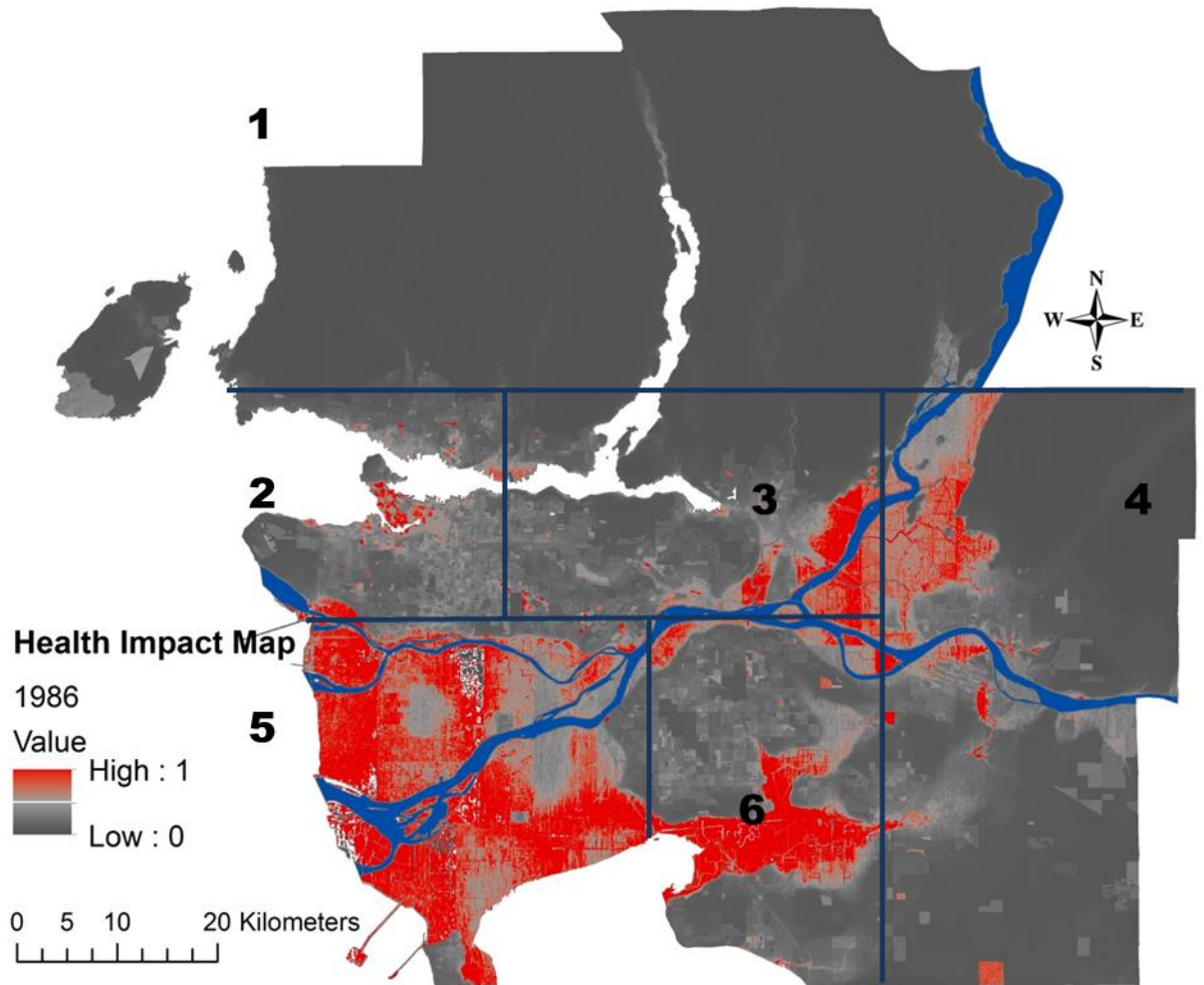
Nonphysical health impact map generated for Metro Vancouver for 2006.



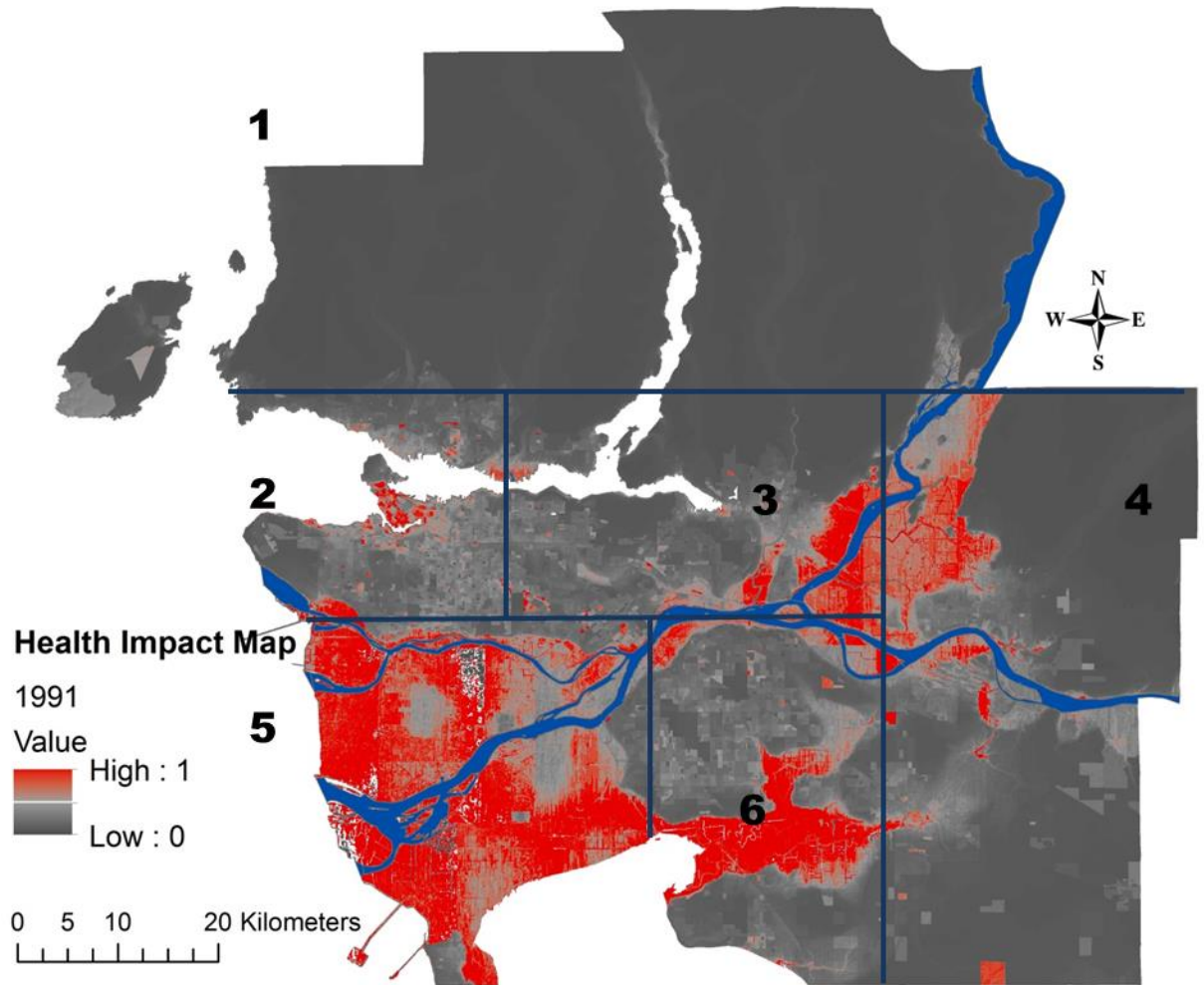
Nonphysical health impact map generated for Metro Vancouver for 2011.



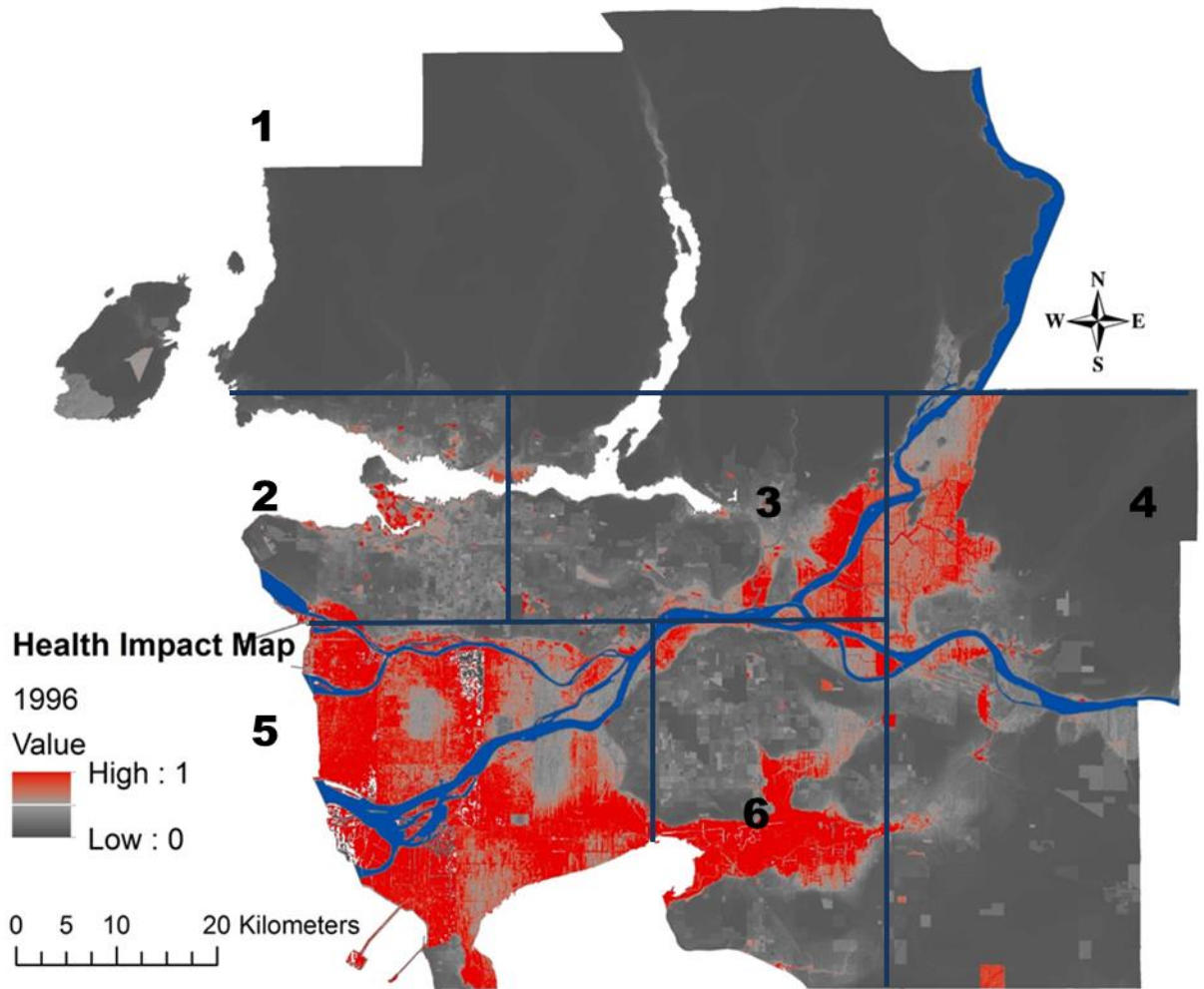
Health impact map generated for Metro Vancouver for 1981.



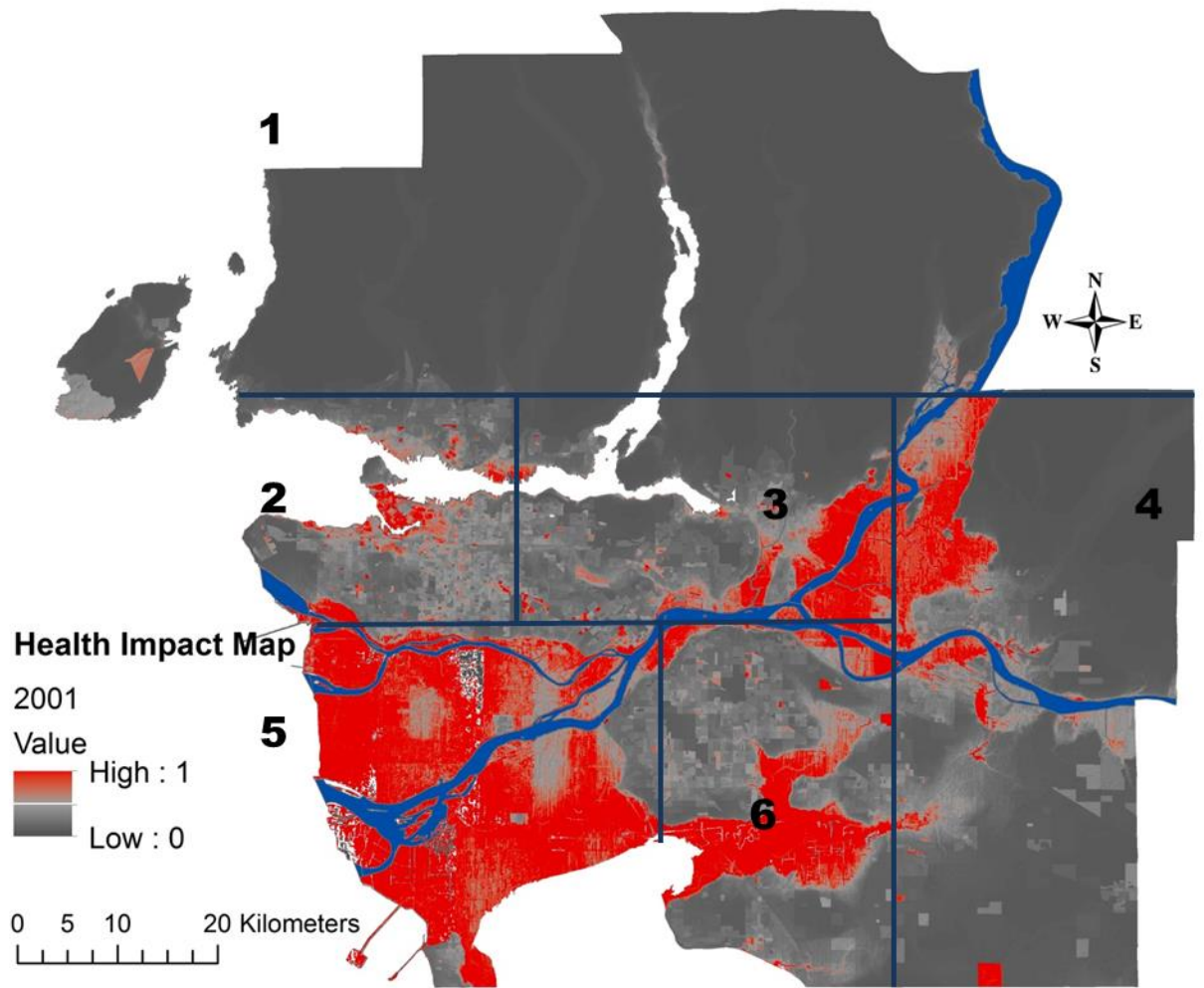
Health impact map generated for Metro Vancouver for 1986.



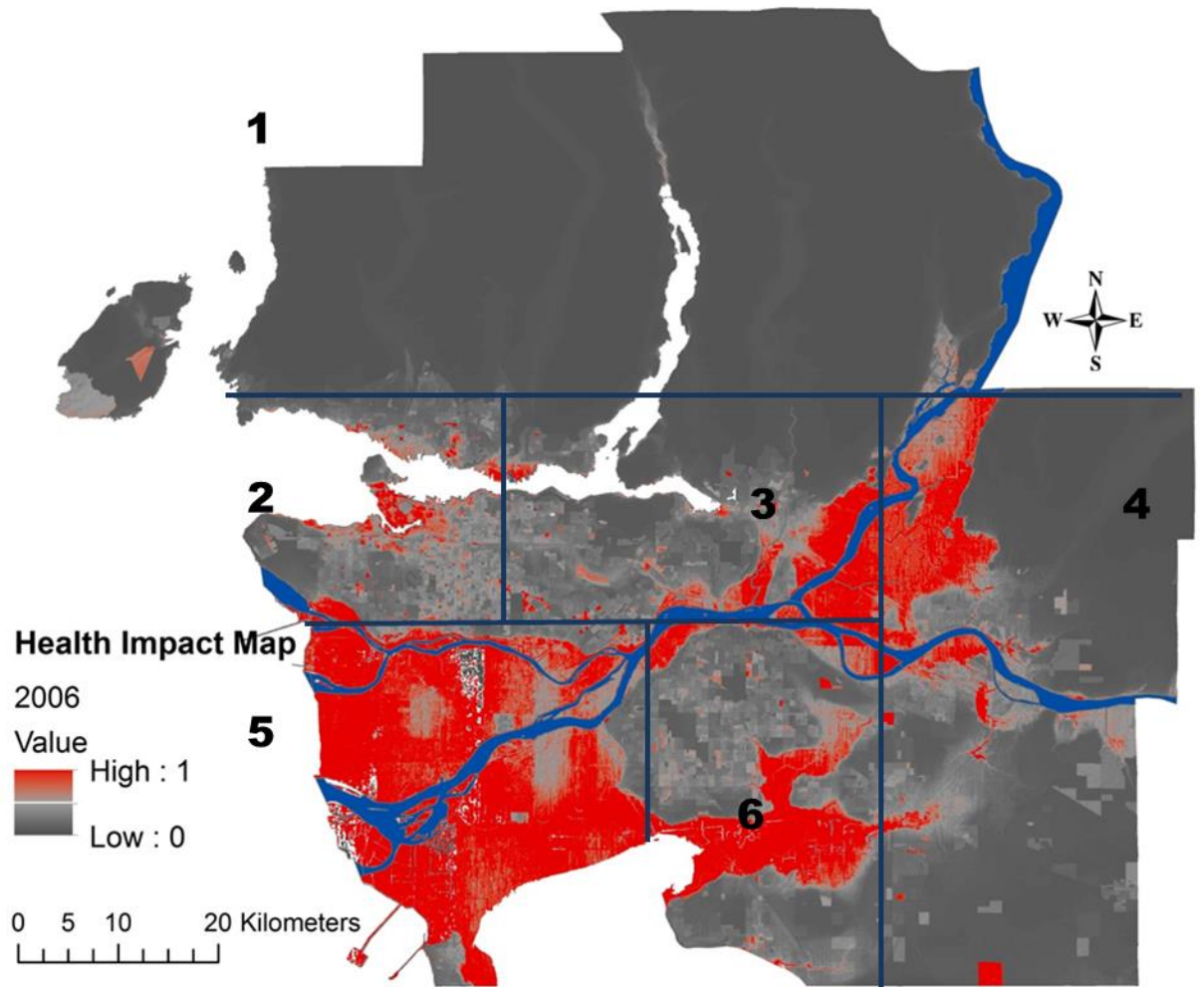
Health impact map generated for Metro Vancouver for 1991.



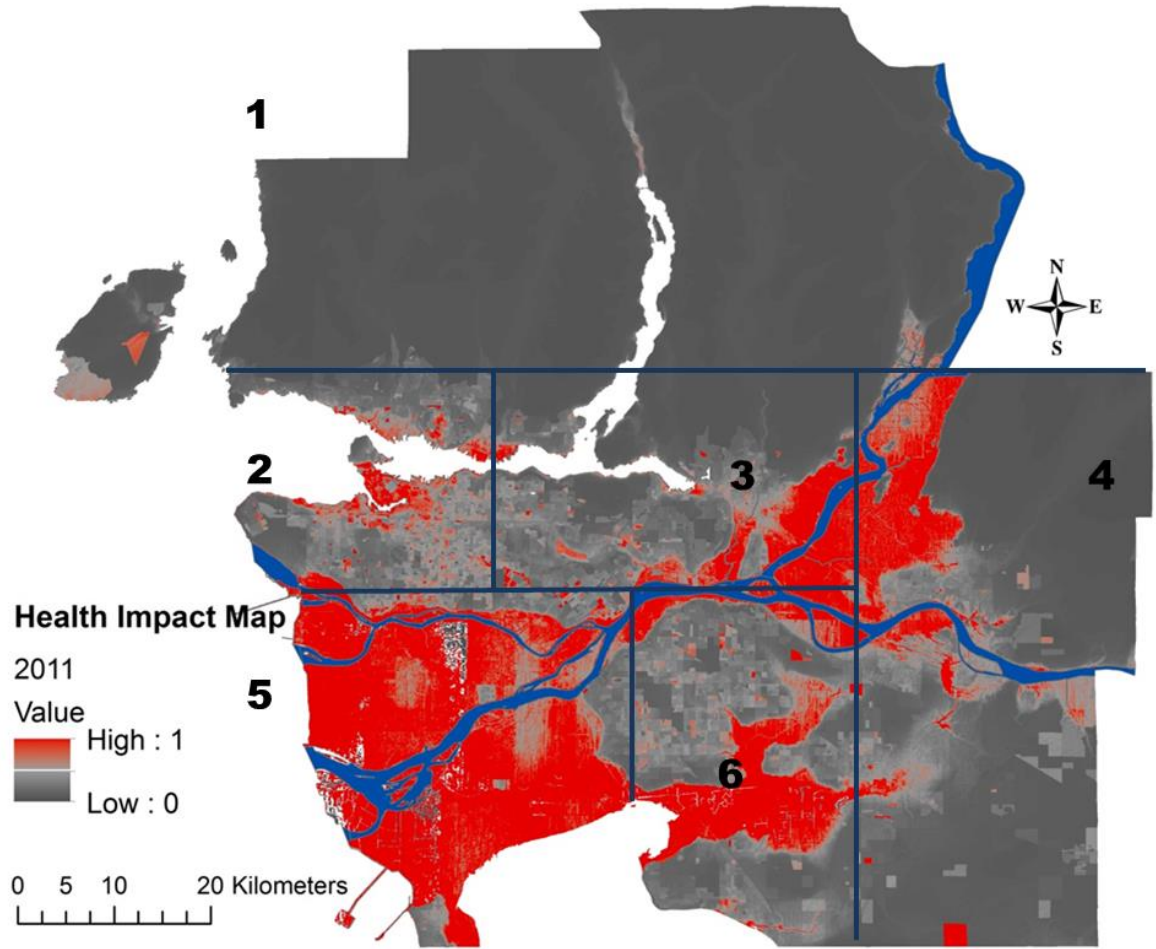
Health impact map generated for Metro Vancouver for 1996.



Health impact map generated for Metro Vancouver for 2001.



Health impact map generated for Metro Vancouver for 2006.



Health impact map generated for Metro Vancouver for 2011.

Appendix D Detailed information how to access shapefile boundaries for Metro Vancouver

This section is providing the detailed information how to access shapefile boundaries and data for Metro Vancouver. The shapefile format was created in the 1990s, and it uses the dBase-III format to store geometric location and attributes information of geographic features (ESRI, 2014). In a shapefile, geographic features are points, lines or polygons. Also, a shapefile includes dBASE tables that can store a number of additional attributes that can be related to a shapefile's features (ESRI, 2014).

Population density, senior population density, and children population density are three main categories of demographic information in urban environments that need to be considered for developing the method for this assessment. Different countries provide different formats of spatial population data and there is no one single source for accessing the population data for different cities all over the world. Statistics Canada is responsible for collecting, archiving and disseminating the population data Canada.

A dissemination area (DA) is a small, comparatively stable geographic unit composed of one or more adjacent dissemination blocks. It is the smallest standard geographic area for which all census data are disseminated. DAs cover all the territory of Canada (Statistics Canada, 2012).

Statistics Canada provides few rules for developing dissemination areas. Dissemination areas respect several description criteria designed to maximize their practicality for data analysis and to meet working constraints (Statistics Canada, 2012).

1. Dissemination area (DA) boundaries respect the boundaries of census subdivisions and census tracts. DAs therefore remain stable over time, to the extent that census subdivisions and census tracts do.
2. Dissemination area boundaries follow roads. DA boundaries may follow other features (such as railways, water features, power transmission lines), where these features form part of the boundaries of census subdivisions or census tracts.

3. Dissemination areas are uniform in terms of population size, which is targeted from 400 to 700 persons to avoid data suppression. DAs with lower population counts (including zero population) may result in order to respect the boundaries of census subdivisions and census tracts. DAs with higher population counts may also occur.
4. Dissemination areas are delineated based on block population counts from the previous census due to operational constraints.
5. Dissemination areas are compact in shape, to the extent possible while respecting the above criteria.
6. The number of dissemination blocks that are included in a dissemination area is limited to 99 due to operational constraints.

The census years that Statistics Canada provides spatial data for dissemination area are 2001, 2006, and 2011 and can be downloaded through equinox website (<http://equinox2.uwo.ca/> Last access Mar 2015).

The population data in dissemination area can be accessed for the 2001, 2006, and 2011 Census of Canada through the Canadian Census Analyzer website (<http://datacenter.chass.utoronto.ca/census/2011/index.html> Last Access Mar 2015).

[Census tracts](#) are small, relatively stable geographic areas that usually have a population of 2,500 to 8,000. They are identified using seven-character numeric 'names' (e.g., 0005.00) and are located in census metropolitan areas (CMAs) (Statistics Canada, 2012). For census the years 1981, 1991, and 1996 census tract boundaries can be accessed through different sources.

1981

<http://maps.library.utoronto.ca/cgi-bin/files.pl?idnum=491> (Last Access Feb 2015)

1991

<http://equinox2.uwo.ca/EN/DataRequest/ProcessBinaryDataRequest.asp?secgroup=DLI&file>

[path=dli\maps\1991Census\c1991-ct-cmaca933-dcf.zip](#) (Last Access Jan 2015)

1996

<http://equinox2.uwo.ca/EN/DataRequest/ProcessBinaryDataRequest.asp?secgroup=DMTI&filepath=DMTI\Census1996\arcview\boundary\CANct.zip> (Last Access Jan 2015)

The population data for these years can be downloaded from the [Canadian Census Analyzer](#). For 1981, 1986, 1991, and 1996, the population counts are broken down by age and gender. <http://datacenter.chass.utoronto.ca/census/2011/index.html> (Last Access Oct 2014)

Appendix E Access to the satellite images used in this study

In order to study the land-use cover in Metro Vancouver, 10-day composite NDVI data are derived from the sensor VEGETATION on board the SPOT satellite platform which was assimilated from “Vlaamse Instelling Voor Technologisch Onderzoek” (SPOT-VGT 2011) for 1998–2012. NOAA-AVHRR images have been used for 1984–1997. The SPOT-VGT S10 (10-day composite) NDVI composites have a spatial resolution of 1 km² and are derived from primary SPOT-VGT products; the composites were corrected for reflectance, scattering, water vapor, ozone and other gas absorption using the procedures described by Achard et al. (1994) and Duchemin (2000) in the ENVI environment.

NOAA-AVHRR images have been taken by the local area coverage AVHRR (LAC AVHRR) aboard the NOAA 14–16 satellite. This was preprocessed using ENVI. ENVI software is a software application used to process and analyze geospatial imagery. It is commonly used by remote sensing professionals and image analysts.

For temporal analysis, a 28-year period was chosen in order to study the long-term effects of urbanization on the vegetation cover. This research was limited to 28 years due to the unavailability of data records prior to 1984. A preliminary examination of AVHRR data collected from the NOAA satellite database (NOAA 2013) shows that a number of images have severe cloud contamination and/or missing passes. Of the 130 images collected during 1984–1997 (April–September), 14 raw AVHRR images were selected. The downloaded images are available on FIDS external drive (due to size of the material).

Appendix F *spautolm* Spatial conditional autoregression modeling code

spautolm Spatial conditional and simultaneous autoregression model estimation

Description: Function taking family and weights arguments for spatial autoregression model estimation by Maximum Likelihood, using dense matrix methods.

Author: Roger Bivand (2015)

Value

A list object of class *spautolm*:

- ✓ `fit` a list, with items:
 - *coefficients* ML coefficient estimates
 - *SSE* ML sum of squared errors
 - *s2* ML residual variance
 - *imat* ML coefficient covariance matrix (before multiplying by *s2*)
 - *signal_trend* non-spatial component of fitted.values
 - *signal_stochastic* spatial component of fitted.values
 - *fitted.values* sum of non-spatial and spatial components of fitted.values
 - *residuals* difference between observed and fitted values

- ✓ `lambda` ML autoregressive coefficient
- ✓ `LL` log likelihood for fitted model
- ✓ `LL0` log likelihood for model with `lambda=0`
- ✓ `call` the call used to create this object
- ✓ `parameters` number of parameters estimated
- ✓ `aliased` if not NULL, details of aliased variables
- ✓ `method` Jacobian method chosen
- ✓ `weights` case weights used
- ✓ `interval` the line search interval used
- ✓ `timings` processing timings
- ✓ `na.action` (possibly) named vector of excluded or omitted observations if non-default `na.action` argument used
- ✓ `llprof` if not NULL, a list with components `lambda` and `ll` of equal length
- ✓ `lambda.se` Numerical Hessian-based standard error of `lambda`
- ✓ `fdHess` Numerical Hessian-based variance-covariance matrix

Code

```
lm0 <- lm(Z ~ PEXPOSURE + PCTAGE65P + PCTOWNHOME, data=nydata)

summary(lm0)

lm0w <- lm(Z ~ PEXPOSURE + PCTAGE65P + PCTOWNHOME, data=nydata,
weights=POP8)

summary(lm0w)

esar0 <- errorsarlm(Z ~ PEXPOSURE + PCTAGE65P + PCTOWNHOME, data=nydata,
listw=listw_NY)

summary(esar0)

system.time(esar1f <- spautolm(Z ~ PEXPOSURE + PCTAGE65P + PCTOWNHOME,
data=nydata, listw=listw_NY, family="SAR", method="eigen", verbose=TRUE))

res <- summary(esar1f)

print(res)

sqrt(diag(res$resvar))

sqrt(diag(esar1f$fit$imat)*esar1f$fit$s2)

sqrt(diag(esar1f$fdHess))

system.time(esar1M <- spautolm(Z ~ PEXPOSURE + PCTAGE65P + PCTOWNHOME,
data=nydata, listw=listw_NY, family="SAR", method="Matrix", verbose=TRUE))

summary(esar1M)

## Not run:

system.time(esar1M <- spautolm(Z ~ PEXPOSURE + PCTAGE65P + PCTOWNHOME,
data=nydata, listw=listw_NY, family="SAR", method="Matrix", verbose=TRUE,
control=list(super=TRUE)))

summary(esar1M)
```

```

esar1wf <- spautolm(Z ~ PEXPOSURE + PCTAGE65P + PCTOWNHOME, data=nydata,
listw=listw_NY, weights=POP8, family="SAR", method="eigen")
summary(esar1wf)

system.time(esar1wM <- spautolm(Z ~ PEXPOSURE + PCTAGE65P + PCTOWNHOME,
data=nydata, listw=listw_NY, weights=POP8, family="SAR", method="Matrix"))
summary(esar1wM)

esar1wlu <- spautolm(Z ~ PEXPOSURE + PCTAGE65P + PCTOWNHOME, data=nydata,
listw=listw_NY, weights=POP8, family="SAR", method="LU")
summary(esar1wlu)

esar1wch <- spautolm(Z ~ PEXPOSURE + PCTAGE65P + PCTOWNHOME, data=nydata,
listw=listw_NY, weights=POP8, family="SAR", method="Chebyshev")
summary(esar1wch)

ecar1f <- spautolm(Z ~ PEXPOSURE + PCTAGE65P + PCTOWNHOME, data=nydata,
listw=listw_NY, family="CAR", method="eigen")
summary(ecar1f)

system.time(ecar1M <- spautolm(Z ~ PEXPOSURE + PCTAGE65P + PCTOWNHOME,
data=nydata, listw=listw_NY, family="CAR", method="Matrix"))
summary(ecar1M)

ecar1wf <- spautolm(Z ~ PEXPOSURE + PCTAGE65P + PCTOWNHOME, data=nydata,
listw=listw_NY, weights=nydata$POP8, family="CAR", method="eigen")
summary(ecar1wf)

system.time(ecar1wM <- spautolm(Z ~ PEXPOSURE + PCTAGE65P + PCTOWNHOME,
data=nydata, listw=listw_NY, weights=POP8, family="CAR", method="Matrix"))
summary(ecar1wM)

example(nc.sids)

```

```

ft.SID74 <- sqrt(1000)*(sqrt(nc.sids$SID74/nc.sids$BIR74) +
sqrt((nc.sids$SID74+1)/nc.sids$BIR74))

lm_nc <- lm(ft.SID74 ~ 1)

sids.nhbr30 <- dnearneigh(cbind(nc.sids$east, nc.sids$north), 0, 30,
row.names=row.names(nc.sids))

sids.nhbr30.dist <- nbdists(sids.nhbr30, cbind(nc.sids$east, nc.sids$north))

sids.nhbr <- listw2sn(nb2listw(sids.nhbr30, glist=sids.nhbr30.dist, style="B",
zero.policy=TRUE))

dij <- sids.nhbr[,3]

n <- nc.sids$BIR74

e11 <- min(dij)/dij

e12 <- sqrt(n[sids.nhbr$to]/n[sids.nhbr$from])

sids.nhbr$weights <- e11*e12

sids.nhbr.listw <- sn2listw(sids.nhbr)

both <- factor(paste(nc.sids$L_id, nc.sids$M_id, sep=":"))

ft.NWBIR74 <- sqrt(1000)*(sqrt(nc.sids$NWBIR74/nc.sids$BIR74) +
sqrt((nc.sids$NWBIR74+1)/nc.sids$BIR74))

mdata <- data.frame(both, ft.NWBIR74, ft.SID74, BIR74=nc.sids$BIR74)

outl <- which.max(rstandard(lm_nc))

as.character(nc.sids$names[outl])

mdata.4 <- mdata[-outl,]

W <- listw2mat(sids.nhbr.listw)

W.4 <- W[-outl, -outl]

sids.nhbr.listw.4 <- mat2listw(W.4)

esarI <- errorsarlm(ft.SID74 ~ 1, data=mdata, listw=sids.nhbr.listw,
zero.policy=TRUE)

```



```

summary(esarI)

esarIa <- spautolm(ft.SID74 ~ 1, data=mdata, listw=sids.nhbr.listw,
family="SAR")

summary(esarIa)

esarIV <- errorsarlm(ft.SID74 ~ ft.NWBIR74, data=mdata, listw=sids.nhbr.listw,
zero.policy=TRUE)

summary(esarIV)

esarIVa <- spautolm(ft.SID74 ~ ft.NWBIR74, data=mdata, listw=sids.nhbr.listw,
family="SAR")

summary(esarIVa)

esarIaw <- spautolm(ft.SID74 ~ 1, data=mdata, listw=sids.nhbr.listw,
weights=BIR74, family="SAR")

summary(esarIaw)

esarIIaw <- spautolm(ft.SID74 ~ both - 1, data=mdata, listw=sids.nhbr.listw,
weights=BIR74, family="SAR")

summary(esarIIaw)

esarIVaw <- spautolm(ft.SID74 ~ ft.NWBIR74, data=mdata,
listw=sids.nhbr.listw, weights=BIR74, family="SAR")

summary(esarIVaw)

ecarIaw <- spautolm(ft.SID74 ~ 1, data=mdata.4, listw=sids.nhbr.listw.4,
weights=BIR74, family="CAR")

summary(ecarIaw)

ecarIIaw <- spautolm(ft.SID74 ~ both - 1, data=mdata.4,
listw=sids.nhbr.listw.4, weights=BIR74, family="CAR")

summary(ecarIIaw)

```

```
ecarIVaw <- spautolm(ft.SID74 ~ ft.NWBIR74, data=mdata.4,  
listw=sids.nhbr.listw.4, weights=BIR74, family="CAR")  
summary(ecarIVaw)  
nc.sids$fitIV <- append(fitted.values(ecarIVaw), NA, outl-1)  
spplot(nc.sids, c("fitIV"), cuts=12) # Cressie 1993, p. 565  
data(oldcol)  
COL.errW.eig <- errorsarlm(CRIME ~ INC + HOVAL, data=COL.OLD,  
nb2listw(COL.nb, style="W"))  
summary(COL.errW.eig)  
COL.errW.sar <- spautolm(CRIME ~ INC + HOVAL, data=COL.OLD,  
nb2listw(COL.nb, style="W"))  
summary(COL.errW.sar)  
## End(Not run)
```

Curriculum Vitae

Name: Amin OWRANGI

EDUCATION

- | | |
|------------|---|
| 2011- 2015 | Department of Civil and Environmental Engineering,
The University of Western Ontario, London, Ontario, Canada
PhD |
| 2007-2009 | Department of Water Resources Engineering
Shiraz Azad University, Shiraz, Iran
MSc |
| 2000-2004 | Department of Irrigation Engineering
Shiraz Azad University, Shiraz, Iran
BSc |

PUBLICATIONS

Published

1. Amin M.Owrangi, Robert Lannigan, Slobodan P. Simonovic, "Mapping climate change-caused health risk for integrated city resilience modelling" *Journal of Natural Hazards, Springer*. DOI: 10.1007/s11069-014-1582-9.
2. Amin M.Owrangi, Robert Lannigan, Slobodan P. Simonovic, "Interaction between Land Use Change, Flooding and Human Health in Metro Vancouver, Canada." *Journal of Natural Hazards, Springer*. DOI: 10.1007/s11069-014-1064-0.
3. Amin M.Owrangi, Adamowski, J., Rahnamae, M., Mohammadzadeh, A., Sharifan, R.A., "Drought monitoring methodology based on AVHRR images and SPOT vegetation maps" *Journal of water resource and protection*, Vol. 3,No.5, 2011, pp. 325-334, DOI: 10.4236/jwarp.2011.35041.
4. Robert Lannigan, Amin M.Owrangi, Slobodan P. Simonovic, "An approach to developing a composite measure for human health as an input to dynamic systems model for investigating city resilience.", *In Proceedings 6th International Conference on Flood Management, ICFM6 2014*, Sao Paul, Brazil, September 16-18, 2014.
5. Amin M.Owrangi, Robert Lannigan, Slobodan P. Simonovic, "Assessment of climate change health impacts for coastal megacities.", *In Proceedings CSCE 21st Canadian Hydrotechnical Conference*, Banff, Alberta, Canada, May 14 - 17 2013.

6. Amin M.Owrangi, Rahnamae, M., Mohammadzadeh, A., Sharifan, R.A.," Using SPOT-VEG based vegetation indices compared with AVHRR based vegetation indices for drought monitoring in south of Iran." *In Proceedings IAHS 352 Remote Sensing and Hydrology*, Jackson Hole, Wyoming, USA, 2012.

Conferences:

Oral Presentations

1. Owrangi, M.A.,Lannigan, R., Simonovic, S.P., "Mapping climate change-caused health risk for the city of Metro Vancouver", *Livable Cities Forum, ICLEI 2014*, Vancouver , April 2-4, 2014,
2. Owrangi, M.A.,Lannigan, R., Simonovic, S.P. "Assessment of climate change health impacts for coastal megacities", *CSCE 21st Canadian Hydrotechnical Conference*, Banff, Alberta, May 14-17, 2013.
3. Owrangi, M.A., Lannigan, R., Simonovic, S.P., McBean,G."Health impacts of Floods due to climate change in coastal cities", *Transcending Borders Global Health Conference*, London, Ontario, Canada, April 27-29, 2012.
4. Owrangi, M.A., Li, S.S., "Characteristics of the Vegetation Cover for the St. Francois Watershed in Southern Quebec from Remote Sensing data" *The 20th Canadian Hydro-technical Conference, CSCE Ottawa, Ontario, Canada, 2011.*
5. Owrangi M.A., Rahnamae M., Sharifan R.A., Mohammadzadeh A., "Monitoring Hydrological drought dynamic by using different indices based on remote sensing on SPOT-Vegetation images and ground data, case study : Marvdasht region, Fars province , Iran." *International Conference on Water Resource, ICWR Shahrood, Iran, 2009.*
6. Owrangi M.A, Shamseddini A. Liaghat A. "Nekah flood, from reasons of occurrence till renovation Experiences". *Urban floods management conference*, Shiraz, Iran, 2007.

Poster Presentations

1. Owrangi, M.A.,Lannigan, R., Simonovic, "Mapping climate change-caused health risk for the city of Metro Vancouver", *GIS day workshop*, University of Western Ontario, London, Canada, October 2013.
2. Owrangi, M.A., Rahnamae, M., Mohammadzadeh, A., Sharifan, R.A.," Using SPOT-VEG based vegetation indices compared with AVHRR based vegetation indices for

drought monitoring in south of Iran." *Remote Sensing and Hydrology Symposium*, Jackson Hole, Wyoming, USA, 2010.

3. Owrangi, M.A., Rahnamae, M., Mohammadzadeh, A., Sharifan, R.A., "Using AVHRR-based vegetation indices for drought monitoring in south of Iran." *10th International Symposium on Stochastic Hydraulics and the 5th International Conference on Water Resources and Environment*, Quebec City, Canada, 2010.
4. Owrangi, M.A., Mohammadzadeh, A., Shamseddini, A., Baligh, A., " Hydrologic drought monitoring and preparedness by using different indices based on remote sensing and ground data in south of Iran." *International Disaster and Risk Conference IDRC*, Davos, Switzerland, 2010.